STRIATAL NEUROMODULATION OF SEROTONIN TRANSMISSION IN HEALTH AND A MOUSE MODEL OF EARLY PARKINSONISM

Qinbo Qiao

Department of Physiology, Anatomy and Genetics

Medical Science Division

Christ Church College

University of Oxford

Thesis submitted for the degree of

Doctor of Philosophy

Michaelmas Term 2025

Table of Contents

Statement of Authorship

This thesis does not contain any material that has been accepted for the award of any other degree in any University or other institution. All data represented in this thesis are fully my own work, and where data has been contributed by others their contribution is stated below and in the main text.

The data included in Chapter 3, Section 3.3.2 was partially collected by Dr. Helen Collins, a postdoctoral researcher in the laboratory of Prof. Peter Magill. These data are included with Dr. Collins's full permission and are identified in the corresponding figure legends.

The data included in Chapter 3, Section 3.3.3 was partially collected by Wenhui Wu, a former research assistant in the laboratory of Prof. Stephanie Cragg. These data are included with Ms. Wu's full permission and are identified in the corresponding figure legends.

Conference abstracts

Qiao, Q., Collins, HM., Magill, PJ. & Cragg, SJ. Striatal neuromodulation of serotonin transmission in health and a mouse model of early parkinsonism. (2025 SfN, San Diego)

Qiao, Q., & Cragg, SJ. Reciprocal regulation of striatal DA and 5-HT release in healthy and parkinsonian mice. Science Communications World Wide. (2024 FENS, Vienna)

Qiao Q., Cragg SJ. Investigating striatal serotonin and dopamine release regulation via 5-HT_4Rs and D_1/D_2Rs using electrophysiology in Parkinson disease mice. (2023 MMiN, North Carolina)

Manuscript and publication

Qiao, Q., Wu, W., Cragg, SJ. 5-HT_4 receptor ligand RS67333 modulates striatal acetylcholine and dopamine release via inhibition of acetylcholinesterase. *Neuropsychopharmacology*. (2025, under review)

Zhang, YF., Luan, P., **Qiao, Q**. *et al.* An axonal brake on striatal dopamine output by cholinergic interneurons. *Nat Neurosci* **28**, 783–794 (2025). https://doi.org/10.1038/s41593-025-01906-5

Acknowledgements

Looking back on my PhD journey, there are many people I would like to thank from the bottom of my heart. Their support, kindness, and encouragement have made this experience possible and truly special. The past three years have been the most memorable and meaningful years of my life, and I feel deeply grateful to everyone who has been there for me.

First, I would like to express my sincere thanks to my supervisor, Prof. Stephanie Cragg. I am deeply grateful for the opportunity to work under her supervision, and for the guidance and inspiration she has provided. Her passion for science and constant encouragement throughout my PhD have been invaluable, and I greatly appreciate her trust and support in every decision I made during these years. I would also like to thank all the current and former members of the Cragg group. Their help, advice, and friendship have made my time in the lab super enjoyable. I am especially grateful to Dr. Kathryn Todd for her valuable feedback and review of this thesis, which greatly improved its quality.

Second, I am thankful to all of my friends for their encouragement and companionship throughout this journey. In particular, I want to express my heartfelt gratitude to my partner, Yuzhou Zhou, who has always been by my side in the most difficult moments. His patience, care, and unwavering support gave me the strength to keep moving forward, and I could not have made it this far without him.

Last, I am deeply grateful to my parents for their unconditional love and support. Their sacrifices, especially in providing me with financial stability during my PhD, have allowed me to focus on my study without hesitation. I am also truly proud of myself and deeply grateful to my younger self for the perseverance and unwavering pursuit over the past ten years, which have finally made my long-cherished dream of studying at Oxford a reality.

Abstract

The striatum receives dense dopaminergic (DA) input from the midbrain and sparser serotonergic (5-hydroxytryptamine, 5-HT) input from the raphe nuclei. While striatal 5-HT is known to interact with DA signalling and regulate striatal output, the mechanisms underlying 5-HT release regulation have remained poorly understood, in part due to technical limitations. In this thesis, I used a genetically encoded G-protein-coupled receptor sensor ($GRAB_{5\text{-}HT3.0}$; Deng et al., 2024) to investigate how striatal 5-HT release is modulated by dopaminergic, cholinergic, and GABAergic systems in acute *ex vivo* brain slices from both healthy and parkinsonian mice.

I firstly characterised evoked $GRAB_{5\text{-}HT}$ signals and validated their specificity for 5-HT in both the dorsolateral striatum (DLS) and nucleus accumbens core (NAcC). Evoked signals were greater and decayed faster in NAcC than DLS consistent with greater 5-HT axon innervation density in NAcC. For comparison, $GRAB_{5\text{-}HT}$ signals evoked in the substantia nigra pars reticulata (SNr), a region receiving some of the densest 5-HT innervation in the brain, were an order of magnitude larger, consistent with detection of 5-HT and not DA. Furthermore, striatal $GRAB_{5\text{-}HT}$ signals were significantly prolonged by the selective 5-HT uptake inhibitor citalopram, while unilateral 6-OHDA injections into the substantia nigra pars compacta (SNc) to lesion striatal DA innervation reduced DA release detected by fast-scan cyclic voltammetry (FCV), but did not alter $GRAB_{5\text{-}HT}$ signals in DLS. Together, these characteristics are consistent with detection of 5-HT rather than DA in the striatum.

I then investigated how local neurotransmitter systems regulate evoked 5-HT release. Activation of D_1 receptors enhanced 5-HT release, while D_2 receptor activation suppressed it; both effects were abolished by selective antagonists, confirming receptor specificity. I also found that 5-HT release is modulated by cholinergic inputs: blocking nicotinic ACh receptors (nAChRs) or activating muscarinic ACh receptors (mAChRs) altered 5-HT release in a region-specific

manner, and the mAChR effect required intact nAChRs, suggesting an indirect mechanism via ACh release. In addition, I found that simultaneous blockade of $GABA_A$ and $GABA_B$ receptors enhanced 5-HT release, indicating tonic GABAergic inhibition of serotonergic axons.

In a mouse model of early Parkinson's disease (PD) overexpressing human wild-type alpha-synuclein (*SNCA*-OVX), I observed a compensatory increase in evoked striatal 5-HT release in DLS. This increase varied depending on the background dopaminergic and GABAergic tone, suggesting that the compensatory mechanisms are dynamically regulated. Additionally, I found that D_2 receptor-mediated inhibition of 5-HT release was diminished, and SERT function was also reduced in the PD model. Moreover, under conditions of dopaminergic receptor blockade, GABAergic modulation of 5-HT release was enhanced, implying a shift in the balance of inhibitory control in the parkinsonian striatum.

In summary, this thesis reveals how striatal 5-HT release is tightly regulated by dopaminergic, cholinergic, and GABAergic circuits and shows that this regulatory balance is disrupted in early PD. By combining real-time 5-HT imaging with pharmacological manipulations, I demonstrate region-specific and disease-specific alterations in neuromodulatory control of 5-HT. These findings provide new insights into the functional reorganization of striatal networks in PD and offer potential targets for future therapeutic intervention.

Abbreviations

$[5\text{-HT}]_o$	Extracellular serotonin concentration
$[ACh]_o$	Extracellular acetylcholine concentration
$[Ca^{2+}]_o$	Extracellular Ca^{2+} concentration
$[DA]_o$	Extracellular dopamine concentration
1p	Single pulse
5-HT	5-hydroxytryptophan (serotonin)
5p	Train of five pulses
6-OHDA	6-hydroxydopamine
AAV	Adeno-associated virus
ACh	Acetylcholine
AChE	Acetylcholinesterase
aCSF	Artificial cerebrospinal fluid
AUC	Area under the curve
cAMP	Cyclic AMP adenosine monophosphate
CFM	Carbon fibre microelectrode
ChI	Cholinergic interneuron

CPu	Caudate-putamen
D_1R	D_1-like dopamine receptor
D_2R	D_2-like dopamine receptor
DA	Dopamine
DAT	Dopamine transporter
DBS	Deep brain stimulation
DHβE	Dihydro-β-erythroidine
DLS	Dorsolateral striatum
FCV	Fast-scan cyclic voltammetry
FSI	Fast-spiking interneuron
GABA	γ-aminobutyric acid
$GABA_AR$	γ-aminobutyric acid A receptor
$GABA_BR$	γ-aminobutyric acid B receptor
GABARs	γ-aminobutyric acid receptors
GAT	γ-aminobutyric acid transporter
GPCR	G protein-coupled receptor
GPe	External segment of the globus pallidus
GPi	Internal segment of the globus pallidus

GRAB	GPCR-activation-based sensor
L-DOPA	Levodopa
mAChR	Muscarinic acetylcholine receptor
MSNs	Medium spiny neurons
NAcC	Nucleus accumbens core
nAChR	Nicotinic acetylcholine receptor
NAcSh	Nucleus accumbens shell
PD	Parkinson’s disease
ROI	Region of interest
SEM	Standard error of the mean
SERT	Serotonin transporter
SNc	Substantia nigra pars compacta
Snca	Mouse α-synuclein gene
SNCA	Human α-synuclein gene
SNCA-OVX	Mouse model overexpressing human α-synuclein
SNr	Substantia nigra pars reticulata
SPN	Spiny projection neuron
SST	Somatostatin

STD	Short-term depression
STP	Short-term plasticity
SSRI	Selective serotonin reuptake inhibitor
TH	Tyrosine hydroxylase
THIN	TH-expressing interneuron
TTX	Tetrodotoxin
VGCC	Voltage-gated calcium channel
VTA	Ventral tegmental area
WT	Wild-type

Chapter 1.
Introduction

1.1 Thesis overview

The striatum integrates diverse neuromodulatory inputs to regulate motor control, motivation, and learning. While dopaminergic signalling has long been recognised as central to striatal function, increasing evidence suggests that serotonergic transmission also plays a critical role. However, the mechanisms underlying 5-HT release and its regulation within striatal circuits remain incompletely understood, particularly in relation to other modulatory systems such as dopamine (DA), acetylcholine (ACh), and γ-aminobutyric acid (GABA).

This thesis investigates how striatal 5-HT release is shaped by local neuromodulatory inputs and how these regulatory mechanisms are altered in Parkinson's disease (PD). To address this, I employed a genetically encoded fluorescent sensor ($GRAB_{5\text{-}HT}$) to characterise the spatiotemporal dynamics of 5-HT release across striatal subregions, enabling high-resolution analysis of its modulation under both healthy and disease-relevant conditions. Across four experimental chapters, I examined the interactions between serotonergic signalling and cholinergic, dopaminergic, and GABAergic circuits, as well as their dysregulation in PD mouse models. **Chapter 3** investigates the characteristics of $GRAB_{5\text{-}HT}$ signals in striatum and the influence of cholinergic and GABAergic signalling on striatal 5-HT release. **Chapter 4** examines how DA receptors and reuptake mechanisms affect 5-HT transmission. **Chapter 5** explores, in turn, the effects of $5\text{-}HT_4$ receptor ligands on ACh and DA signalling, with particular emphasis on the role of acetylcholinesterase (AChE). **Chapter 6** assesses the potential imbalances in striatal 5-HT release and its modulation in a mouse model of parkinsonism.

Together, the studies presented in this thesis provide a framework for understanding how striatal 5-HT signalling is integrated within broader neuromodulatory networks. This work contributes to identifying potential mechanisms through which serotonergic dysfunction may arise in disease and offers new perspectives on the regulation of 5-HT within basal ganglia circuits.

1.2 The basal ganglia and striatum

The basal ganglia comprise a group of subcortical nuclei deeply involved in the regulation of voluntary motor control, procedural learning, reward processing, and action selection (Graybiel, 1998; Lanciego et al., 2012). These structures include the striatum, globus pallidus (external segment, GPe; internal segment, GPi), subthalamic nucleus (STN), substantia nigra (pars compacta, SNc; pars reticulata, SNr), and the ventral tegmental area (VTA) (Bolam et al., 2000; Obeso et al., 2014; Rocha et al., 2023). The striatum, receiving extensive glutamatergic input from the cortex and thalamus, serves as the primary input nucleus of the basal ganglia (Crittenden & Graybiel, 2011) (**Fig 1.1**). Output from the basal ganglia is primarily relayed via the GPi and SNr to the thalamus and brainstem (Crittenden & Graybiel, 2011; Foster et al., 2021; Lanciego et al., 2012).

The connectivity within the basal ganglia is classically described by two parallel pathways: the direct and indirect pathways (Albin et al., 1989; DeLong, 1990; Y. Smith et al., 1998). The direct pathway facilitates movement by disinhibiting thalamocortical circuits, whereas the indirect pathway suppresses movement through a more circuitous inhibitory route involving the GPe and STN (Crittenden & Graybiel, 2011; Y. Smith et al., 1998). Dopaminergic input from the SNc modulates the activity of these pathways by acting on D_1- and D_2-type DA receptors located on distinct populations of striatal projection neurons of the direct and indirect pathway respectively (DeLong & Wichmann, 2007). These circuits are essential for balanced motor control and are critically imbalanced in movement disorders such as PD (DeLong & Wichmann, 2007; Wichmann & Dostrovsky, 2011).

Beyond motor regulation, the basal ganglia contribute to a range of cognitive and affective functions, including motivation (Mogenson et al., 1980; Wise, 2004), goal-directed learning (Balleine & Ostlund, 2007), and reinforcement processing (Robinson & Berridge, 1993).

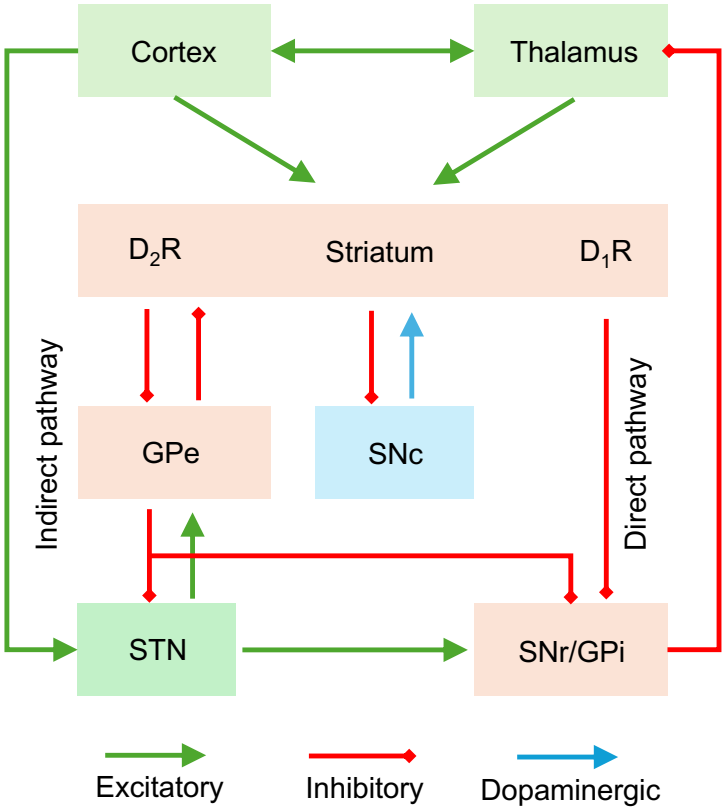

Figure 1.1. Simplified schematic of basal ganglia connectivity. A simplified schematic illustrating the main connections between the cortex, thalamus, and basal ganglia nuclei, with inhibitory GABAergic pathways shown in red, excitatory glutamatergic projections in green, and dopaminergic projections in light blue. GPi: internal segment of the globus pallidus; SNc: substantia nigra pars compacta; SNr: substantia nigra pars reticulata; STN: subthalamic nucleus; D_1R: DA D_1 receptor; D_2R: DA D_2 receptor.

Dysfunctions in basal ganglia circuitry have been associated with neurological and psychiatric disorders such as Huntington's disease, obsessive-compulsive disorder (OCD), and substance use disorders (Berke & Hyman, 2000; Ring & Serra-Mestres, 2002).

1.2.1 Anatomy and function of the striatum

The striatum derives its name from the striated appearance produced by interleaved grey and white matter fibres (Bamford & Bamford, 2019). In primates, the striatum is anatomically divided into the caudate nucleus and putamen, which are separated by the internal capsule. In rodents,

these structures are collectively referred to as the caudate-putamen (CPu) due to the lack of a prominent anatomical division (Voorn et al., 2004).

Functionally, the striatum can be subdivided along a dorsolateral to ventromedial gradient (**Fig 1.2**). The dorsolateral striatum (DLS) is involved in habitual and sensorimotor processes (Knowlton et al., 1996; Quinn et al., 2013; Yin et al., 2004), whereas the dorsomedial striatum (DMS) is implicated in goal-directed behaviours and cognitive flexibility (Burton et al., 2015; Voorn et al., 2004). The ventral striatum, which includes the nucleus accumbens core (NAcC) and shell (NAcSh), plays a critical role in motivation, reward learning, and affective processing (Burton et al., 2015; Carboni et al., 1989; Cardinal et al., 2002; Kalivas & McFarland, 2003; Kelley, 2004; Zahm, 1999).

In addition to regional segmentation, the striatum exhibits a compartmental architecture consisting of the striosome and matrix (Gerfen et al., 1987; Graybiel & Ragsdale, 1978). Striosomes account for approximately 15% of the striatal volume and are enriched in markers such as μ-opioid receptors (MOR), substance P, and D_1 receptors (D_1Rs) (Besson et al., 1988; Brimblecombe & Cragg, 2017; Crittenden & Graybiel, 2011; Pert et al., 1976). The matrix, by contrast, is enriched in calbindin, enkephalin (ENK), somatostatin (SST), and D_2 receptors (D_2Rs) (Brimblecombe & Cragg, 2017; Gerfen et al., 1987; Graybiel & Ragsdale, 1978). These compartments also differ in connectivity and function: striosomes preferentially receive input from limbic cortical areas, while the matrix is innervated by sensorimotor and associative cortices (Crittenden & Graybiel, 2011).

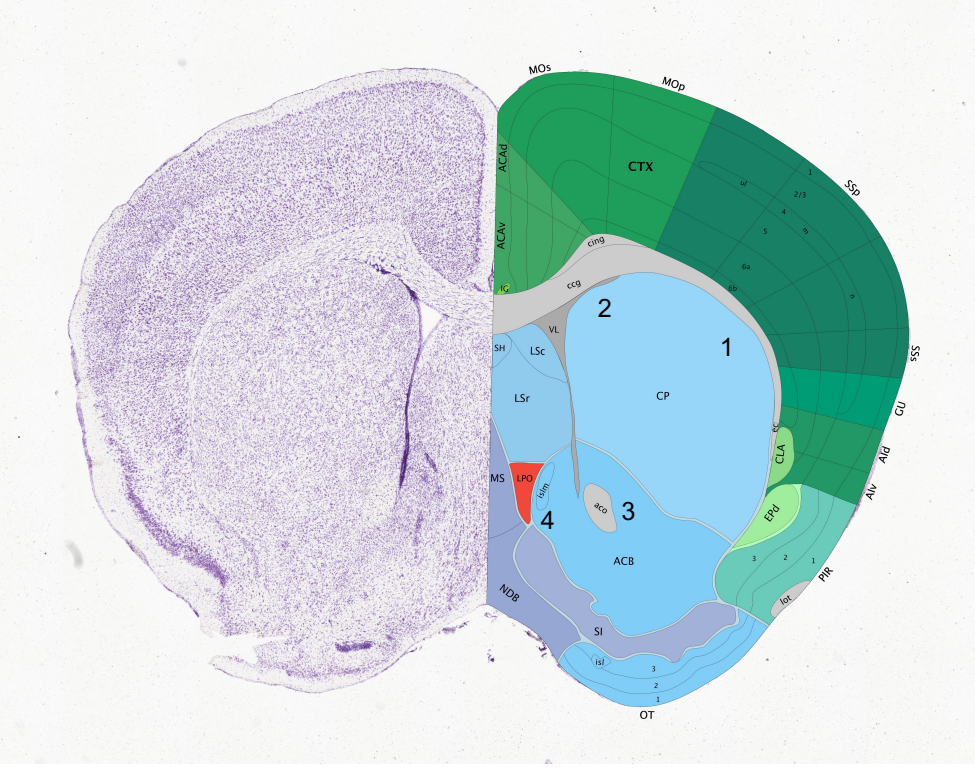

Figure 1.2. Nissl-stained coronal section of adult mouse brain with anatomical annotations. The dorsal striatum is labelled as the caudate putamen (CP), subdivided into the dorsolateral striatum (DLS, 1) and dorsomedial striatum (DMS, 2). The ventral striatum is labelled as the nucleus accumbens (ACB), comprising the nucleus accumbens core (NAcC, 3) and shell (NAcSh, 4). Image adapted from the Allen Mouse Brain Reference Atlas.

1.2.2 Neuronal composition of the striatum

The striatum comprises a highly specialised network of neuronal and non-neuronal cell types that together support its role as a central integrator within the basal ganglia. The predominant neuronal population in the striatum consists of projection neurons known as medium spiny neurons (MSNs), which account for approximately 95% of the total neuronal population in rodents (Graveland & DiFiglia, 1985; Tepper et al., 2010). These neurons primarily utilise GABA as their inhibitory neurotransmitter and are characterised by medium-sized somata and densely spiny dendritic arbors (Kawaguchi, 1993). MSNs receive glutamatergic inputs from the cortex and thalamus, as well as modulatory inputs from dopaminergic, serotonergic, and cholinergic afferents, and serve as the principal output neurons of the striatum, projecting to key basal

ganglia nuclei including the GP and SNr (Bolam et al., 2000; Kawaguchi et al., 1990; Lanciego et al., 2012). Based on their receptor expression and projection targets, MSNs are divided into two equally represented subtypes that give rise to the direct and indirect pathways. The direct pathway MSNs express dopamine D_1 receptors (D_1Rs) and project directly to the internal segment of the GPi and SNr, where their activation facilitates movement initiation (Bolam et al., 2000; Gerfen & Surmeier, 2011; Gittis & Kreitzer, 2012). Conversely, indirect pathway MSNs express dopamine D_2 receptors (D_2Rs) and send their axons to the external segment of the GPe, which connects to the STN and ultimately regulates output from the GPi/SNr to suppress inappropriate motor behaviours (Bolam et al., 2000; Cui et al., 2013; DeLong & Wichmann, 2007; Lanciego et al., 2012).

In addition to projection neurons, the striatum contains a diverse class of interneurons, which together constitute the remaining ~5% of the neuronal population (Kawaguchi, 1993; Tepper et al., 2010). Although fewer in number, these interneurons are highly heterogeneous in terms of their electrophysiological, morphological, and molecular characteristics, and they exert powerful local control over MSN excitability and synaptic integration (Assous & Tepper, 2019; Tepper et al., 2010). The majority of striatal interneurons are GABAergic and comprise several distinct subtypes, including fast-spiking interneurons (FSIs), low-threshold spiking interneurons (LTSIs) and tyrosine hydroxylase (TH)-expressing interneurons (THINs).

FSIs, which express parvalbumin (PV), are characterised by their narrow action potentials, short afterhyperpolarisations, and capacity for high-frequency firing (Gerfen, 1985; Kawaguchi, 1993; Tepper et al., 2010). FSIs form strong inhibitory synapses on MSNs, providing powerful feedforward inhibition that helps regulate the timing and synchronized MSN activity (Gittis et al., 2010; Koós & Tepper, 1999; Planert et al., 2010). Another major class is LTSIs, which express SST, nitric oxide synthase (NOS) and neuropeptide Y (NPY) (DiFiglia et al., 1982; Kawaguchi, 1993; Tepper et al., 2010; Vuillet et al., 1989). These interneurons display more slowly adapting

firing patterns and primarily target the distal dendrites of MSNs, contributing to more diffuse and integrative forms of inhibition (Ibáñez-Sandoval et al., 2011). Besides FSIs and LTSIs, THINs is another distinct class of GABAergic interneurons with diverse electrophysiological properties, which have been categorised into four subtypes based on firing patterns (Ibáñez-Sandoval et al., 2010). They receive excitatory input from both cortical and thalamic afferents and may also be influenced by dopaminergic projections (Assous et al., 2017; Ibáñez-Sandoval et al., 2010, 2015; Xenias et al., 2015). THINs target MSNs and SST-expressing interneurons, express nicotinic ACh receptors (nAChRs), and are involved in mediating polysynaptic inhibition between cholinergic interneurons (ChIs), suggesting a powerful role in shaping local microcircuit activity (Assous et al., 2017; Dorst et al., 2020; Ibáñez-Sandoval et al., 2010; Luo et al., 2013).

Additional to these GABAergic interneurons, ChIs represent small but functionally significant population that utilises ACh as their principal neurotransmitter and also co-release GABA (B. M. Roberts et al., 2021; Saunders et al., 2015). ChIs constitute approximately 1-2% of all striatal neurons and are easily identified by their large cell bodies (20-40 μm) and aspiny morphology (Bolam et al., 1984; Goldberg & Wilson, 2016; Phelps et al., 1985). They exhibit autonomous tonic firing at a rate of 2-10 Hz and release ACh continuously, exerting widespread modulatory influence via both muscarinic and nicotinic ACh receptors (Bennett & Wilson, 1999; Calabresi et al., 1998; Lee et al., 1998; Wilson et al., 1990; Yan & Surmeier, 1996). Despite their sparse numbers, ChIs have extensive axonal arborisations that allow them to influence widespread areas of the striatum. Their activity is shaped by excitatory input from the cortex and thalamus, and they play key roles in synaptic plasticity, reward-related learning, and modulation of dopaminergic and serotonergic transmission.

Alongside these neuronal populations, the striatum contains a network of glial cells, particularly astrocytes, which play a crucial role in maintaining homeostasis and regulating neuronal function (Hirrlinger & Nimmerjahn, 2022; Stedehouder et al., 2024). Astrocytes express

receptors and transporters for glutamate, GABA, ACh, and other monoamines, allowing them to sense changes in neuronal activity and modulate synaptic transmission through the release of gliotransmitters (De Ceglia et al., 2023; Liu et al., 2021; Ota et al., 2013; Paixão & Klein, 2010). They also regulate extracellular ion concentrations, clear neurotransmitters from the synaptic cleft, and participate in synapse formation and elimination (Allen, 2014; Araque, 2008; Benarroch, 2016; Chung et al., 2015; Haydon & Carmignoto, 2006). Emerging evidence highlights the involvement of astrocytic dysfunction in neurological disorders such as PD, emphasising their relevance not only as support cells but as active contributors to striatal signalling dynamics (Booth et al., 2017; Brandebura et al., 2023; Haydon & Carmignoto, 2006; Rossi & Volterra, 2009).

Together, the cellular composition of striatum - dominated by GABAergic MSNs and complemented by a diverse set of interneurons and glial elements - provides the anatomical and functional substrate for the complex integration of motor, cognitive, and motivational information within the basal ganglia.

1.2.3 FCV measurement in the striatum

While the previous section outlined the cellular architecture of the striatum, assessing neurotransmission dynamics requires temporally precise methods. FCV, developed and refined largely by Wightman and colleagues, has become a cornerstone technique for real-time monitoring of neurotransmitter release in the brain. Specifically, a carbon-fiber microelectrode rapidly scans voltage waveforms, allowing oxidation and reduction of electroactive species such as DA. The resulting faradaic currents are plotted against potential to yield cyclic voltammograms, whose characteristic redox peaks identify specific analytes (Wightman et al., 1988). Repeated scans at high frequency generate two-dimensional colour plots, where oxidation current changes are converted into concentration-time traces to visualize sub-second

neurotransmitter dynamics (Wightman et al., 1988). Wightman's group pioneered the application of FCV in the striatum, first demonstrating electrically evoked DA release and reuptake *in vivo* (Millar et al., 1985; Stamford et al., 1986; Wightman et al., 1988) and subsequently refining the technique through improved waveform control, data acquisition, and kinetic analysis (Garris & Wightman, 1994; Michael et al., 1999). They subsequently optimized waveform design and electrode conditioning to enhance selectivity and sensitivity, extending the method beyond DA to 5-HT through the use of "N-shaped" waveforms (Jackson et al., 1995). Later work from the same group quantified 5-HT release and uptake kinetics across striatal and midbrain regions and examined pharmacological modulation of transporter activity (Bunin & Wightman, 1998; Venton et al., 2003). Together, these studies established FCV as a powerful method to resolve spatially and temporally defined monoaminergic signals within the striatum.

1.3 Mesostriatal dopaminergic system

1.3.1 Mesostriatal dopaminergic projections and signalling

DA neurons projecting to the striatum are located predominantly in the SNc and the VTA, forming the nigrostriatal and mesolimbic pathways, respectively (Björklund & Dunnett, 2007; Molochnikov & Cohen, 2014). While SNc DA neurons mainly innervate the dorsal striatum, including the caudate and putamen, VTA DA neurons project more heavily to the ventral striatum, particularly the nucleus accumbens (NAc) (Björklund & Dunnett, 2007; Yetnikoff et al., 2014). These projections are not completely segregated and exhibit a degree of overlap, allowing for crosstalk between motor and motivational circuits (Björklund & Dunnett, 2007).

DA neurons display diverse firing patterns that directly influence the dynamics of DA release. *In vivo*, they can exhibit tonic low-frequency firing (~1-10 Hz), irregular single-spike patterns, or brief high-frequency bursts (20-40 Hz), particularly in response to salient stimuli (Freeman et al.,

1985; Grace & Bunney, 1984; Hyland et al., 2002). These patterns shape the mode and extent of DA transmission from their axon. Burst firing leads to larger phasic DA release events, while tonic firing supports baseline extracellular DA levels (Grace et al., 2007; Grace & Bunney, 1983, 1984).

Unlike classical synaptic transmission, striatal DA release predominantly operates through volume transmission, where DA diffuses to act on extrasynaptic receptors (Cragg & Rice, 2004; Rice, 2000; Rice & Cragg, 2008). Electron microscopy studies show that up to 70% of DA varicosities in the striatum lack postsynaptic densities, supporting a model of widespread, non-synaptic DA signalling (Descarries et al., 1996). DA uptake is mediated by DA transporters (DATs), which are largely localised extrasynaptically and restrict the spatial and temporal spread of extracellular DA (Cragg & Rice, 2004; Hersch et al., 1997; Nirenberg et al., 1997; Sesack et al., 1997).

1.3.2 Local striatal modulation of DA release

Although DA release is initiated by action potentials (AP) in midbrain cell bodies, axons in the striatum exhibit local mechanisms that dynamically modulate release. This local modulation allows DA output to be fine-tuned independently of somatic firing (Sulzer et al., 2016). Notably, DA axons form extensive, unmyelinated arbours that integrate signals from local neurotransmitter systems and neuromodulators, such as GABA, adenosine, 5-HT, nitric oxide (NO), hydrogen peroxide, and substance P (Aransay et al., 2015; Avshalumov et al., 2003; Brimblecombe & Cragg, 2015; Lopes et al., 2019; Matsuda et al., 2009; Navailles & De Deurwaerdère, 2011; Ng et al., 1999; Roberts et al., 2021).

One of the principal local modulators of striatal DA release is ACh, acting primarily through nAChRs and mAChRs located on DA axons (Rice & Cragg, 2004; Threlfell et al., 2010). Rather

than simply reflecting the firing patterns of midbrain DA neurons, striatal DA release is extensively shaped by cholinergic signalling within the striatum itself (Rice et al., 2011; Threlfell et al., 2012). These local mechanisms allow for activity-independent DA release and add a layer of control where striatal output can be modulated in real time.

Activation of β2-containing nAChRs on DA axons facilitates DA release evoked by single electrical pulses or low-frequency stimulation, in part by triggering a second, ACh-driven release event that merges with the directly evoked release (Wang et al., 2014). This cholinergic amplification enhances DA signalling under baseline conditions. However, following this facilitation, nAChR activation induces a short-term depression (STD) of DA release that limits subsequent phasic output. Notably, this depression is not due to vesicle depletion but instead reflects a release-independent mechanism, likely involving axonal depolarisation and reduced excitability (Zhang & Sulzer, 2004). As a result, when nAChR signalling is blocked or desensitised, the STD is alleviated, and DA release becomes more sensitive to the frequency of firing (Rice & Cragg, 2004; Threlfell & Cragg, 2011).

Importantly, ACh can directly trigger DA release in the striatum, even in the absence of somatic firing of DA neurons. This has been demonstrated by experiments where synchronous activation of ChIs led to local DA release via nAChRs, bypassing action potentials in DA soma (Brimblecombe et al., 2018; Cachope et al., 2012; Threlfell et al., 2012). Recent studies provide further support for this cholinergic-driven release mechanism. For instance, optogenetic stimulation of ChIs can evoke APs in distal DA axons, which are abolished by blocking β2-nAChRs (Liu et al., 2022). Moreover, ACh-mediated depolarisations resembling EPSPs have been recorded in DA axons following nicotinic stimulation, and their summation can lead to axonal firing and DA release (Kramer et al., 2022). Notably, this release is not a faithful readout of ChI firing patterns, suggesting that once initiated, the cholinergic influence on DA axons may be amplified locally (Shin et al., 2017; Threlfell et al., 2012).

In addition to nicotinic mechanisms, muscarinic ACh receptors also play a role in regulating the influence of ACh on DA output. Activation of M2 and M4 mAChRs on ChIs can inhibit their activity and reduce ACh release, thereby indirectly modulating nAChR-driven DA release and relieving STD (Threlfell et al., 2010). While M5 mAChRs are expressed in midbrain DA neurons (Vilaró et al., 1990; Weiner et al., 1990), their presence on axons remains uncertain, though they have been proposed to enhance DA release directly (Shin et al., 2015; Zhang et al., 2002).

Finally, ChIs act as integrative nodes for multiple neuromodulatory systems. Their activity can be influenced by glutamate, NO, opioids, and insulin, allowing these signals to shape striatal DA release via ACh (Britt & McGehee, 2008; Hartung et al., 2011; Kosillo et al., 2016; Stouffer et al., 2015). DA axons also express D_2-like auto receptors, which do not affect the initial pulse of release (when evoked in acute coronal slices) but limit subsequent release at inter-pulse intervals of a few hundred milliseconds (Condon et al., 2019). Beyond autoreceptors, striatal DA release is also shaped by other neuromodulators and by mechanisms intrinsic to DA axons. For instance, voltage-gated calcium channels (VGCCs) on DA axons mediate Ca^{2+} entry required for exocytosis, and distinct VGCC subtypes shape DA release probability and plasticity (Brimblecombe et al., 2024; Brimblecombe & Cragg, 2015). DATs not only transport DA but also influence release via regulation of axonal excitability and vesicle dynamics (Condon et al., 2019; Threlfell et al., 2021; Venton et al., 2006).

Additionally, several neurotransmitter systems modulate DA release locally. GABAergic input exerts both tonic and phasic inhibitory effects on DA axons, primarily via $GABA_A$ and $GABA_B$ receptors (Brodnik et al., 2019; Lopes et al., 2019; Pitman et al., 2014; Roberts et al., 2021). Adenosine, via A_1 receptors, inhibits DA release, while neuropeptides such as substance P may enhance it under certain conditions (Brimblecombe & Cragg, 2015; Roberts et al., 2022). These mechanisms highlight that DA release is not merely a reflection of DA neuron firing but is shaped extensively by the local striatal environment.

Beyond regulation by other neuromodulators, DA clearance itself is shaped by a diverse set of membrane transporters beyond DAT. While DAT remains the primary mechanism for high-affinity DA reuptake, a range of lower-affinity, higher-capacity transporters - including organic cation transporter 3 (OCT3) and plasma membrane monoamine transporter (PMAT) - also contribute to extracellular monoamine clearance (Daws, 2021; Gasser, 2019). These uptake-2 transporters are characterized by broader substrate selectivity and higher transport capacity, allowing them to compensate for impaired function of high-affinity systems such as DAT, SERT, or NET. In genetic or pharmacological models of transporter deficiency, both OCT3 and PMAT have been shown to be upregulated and capable of clearing monoamines from the extracellular space under conditions of elevated neurotransmitter levels or transporter blockade (Baganz et al., 2008; Li et al., 2013). Functionally, this compensatory mechanism has important implications for psychiatric pharmacology. Because uptake-2 transporters can clear monoamines even when DAT or SERT are blocked, they may reduce the effects of reuptake inhibitors used as antidepressant (Bacq et al., 2012; Daws, 2021; Daws et al., 2013; Horton et al., 2013).

In addition to these uptake-2 systems, high-affinity monoamine transporters can also display “promiscuous” substrate transport under certain physiological or compensatory conditions. When 5-HT transport via SERT is reduced - such as after SERT blockade, genetic deletion, or in serotonergic axons adjacent to DAergic regions - 5-HT can be taken up by DAT. In the striatum, 5-HT uptake has been shown to persist even in the absence of functional SERT, indicating that the DAT can mediate 5-HT reuptake under compensatory conditions (Zhou et al., 2002). Conversely, DA can also be transported via SERT. Larsen et al. (2011) demonstrated that human and rodent SERTs are capable of DA uptake *in vitro* and in forebrain synaptosomal preparations, although direct evidence in the striatum remains lacking. Using heterologous expression systems, they showed that SERT can transport DA through a mechanistically distinct mode of substrate translocation, characterized by lower affinity but higher maximal transport

velocity compared with 5-HT (Larsen et al., 2011). This atypical DA transport via SERT was sensitive to classical SERT inhibitors such as citalopram, confirming its transporter specificity (Larsen et al., 2011). These findings indicate that SERT can act as a secondary pathway for DA clearance under conditions of elevated extracellular DA or reduced DAT function.

In summary, this “promiscuous” transport properties of the monoamine uptake system allow for flexible and redundant mechanisms of extracellular monoamine clearance, which may become particularly relevant under pathophysiological or pharmacologically altered conditions.

1.3.3 DA modulation of striatal signalling

DA exerts its effects via two main receptor families: D_1-like (D_1 and D_5) and D_2-like (D_2, D_3, and D_4) receptors, all of which are GPCRs (Beaulieu et al., 2015; Kebabian & Calne, 1979; Martel & Gatti McArthur, 2020). D_1-like receptors couple to $G_{\alpha s/olf}$ proteins to stimulate adenylyl cyclase and increase cAMP, whereas D_2-like receptors couple to $G_{\alpha i/o}$ proteins and inhibit cAMP production (Beaulieu & Gainetdinov, 2011). D_1-like receptors have a lower affinity for DA and are preferentially activated under conditions of high extracellular DA, such as during phasic release, whereas D_2-like receptors can be engaged at lower DA concentrations due to their higher affinity (Martel & Gatti McArthur, 2020).

In the striatum, D_1Rs are primarily expressed on MSNs of the direct pathway and D_2Rs are expressed on MSNs of the indirect pathway (Gerfen & Surmeier, 2011). Activation of D_1Rs enhances excitability and synaptic strength in direct-pathway MSNs, while D_2Rs exert the opposite effect in indirect-pathway MSNs (Beaulieu et al., 2015; Beaulieu & Gainetdinov, 2011). This mechanism enables DA to regulate the balance between action facilitation and suppression.

Presynaptically, D_2-like auto receptors on DA axons serve as a feedback mechanism to limit further DA release. They do not influence the first pulse of evoked release but reduce subsequent release when the interval of stimuli is more than 0.5 s, providing a mechanism for temporal filtering of DA signals (Condon et al., 2019). DA also modulates the activity of striatal interneurons and afferent inputs, including cortico-striatal glutamatergic synapses, where D_1 and D_2 receptor activation can influence synaptic plasticity such as long-term potentiation and depression (Surmeier et al., 2007).

Moreover, DA receptors can form heteromers with other receptors, including adenosine and NMDA receptors, adding another layer of complexity to DA signalling. For instance, D_1-A_1 or D_2-A_2A receptor interactions allow crosstalk between DA and adenosine systems (Perreault et al., 2014), while D_1-NR_1 or D_2-NR_2B complexes integrate DA and glutamate signalling (Beaulieu et al., 2015).

1.3.4 Comparison of DA detection with voltammetry and photometry

Two widely used techniques for monitoring extracellular DA dynamics nowadays are voltammetry (i.e., FCV) and fluorescent DA sensors (e.g., dLight, $GRAB_{DA}$). These methods are slightly different in their detection principles, spatial and temporal resolution, and applicability across experimental contexts. Understanding their respective strengths and limitations is crucial for interpreting DA signals under both physiological and pharmacologically manipulated conditions. FCV offers high temporal resolution (sub-second) and quantitative insight into both release and reuptake kinetics of DA, since it measures direct extracellular DA near the electrode tip. However, it suffers from potential chemical cross-reactivity (e.g., with norepinephrine), and faces challenges in long-term or cell-type-specific recordings, particularly *in vivo*. In contrast, $GRAB_{DA}$ and similar sensors (e.g., dLight) detect DA through fluorescence changes in neurons that express the sensor. This optical approach captures DA dynamics integrated over a broader

spatial domain and is suitable for long-term recordings. Compared with FCV, $GRAB_{DA}$ signals are not influenced by electroactive molecules at the electrode surface, and the sensors can, in some cases, be expressed in specific cell types. However, it should be noted that both FCV and fluorescent sensors are sensitive to pH fluctuations, which can alter electrochemical currents in FCV and affect baseline fluorescence in optical recordings, thereby complicating data interpretation.

Salinas et al. (2023) performed a direct comparison between FCV and dLight in striatal slices and freely moving mice, highlighting both convergences and divergences between the two readouts. They observed that electrically evoked DA transients were comparable between methods in terms of sensitivity to presynaptic inhibition and excitability induced changed in DA release (Salinas et al., 2023). However, differences emerged after pharmacological manipulations. Upon application of cocaine or the selective DAT inhibitor Nomifensine, FCV detected a robust increase in peak amplitude, reflecting increased extracellular DA levels due to impaired reuptake and prolonged DA diffusion. However, dLight signals failed to show such peak enhancement, instead displaying little or no change in amplitude (Salinas et al., 2023). These differences are thought to arise from differences in how each method integrates DA dynamics: FCV is sensitive to local DA accumulation, while dLight signals are constrained by sensor saturation and receptor-like binding kinetics. In freely moving mice, dLight photometry enabled detection of behaviourally linked DA transients in DLS, a region where electrode-based measurements such as FCV are technically challenging (Salinas et al., 2023).

In summary, the two techniques are complementary: FCV provides high-resolution, quantitative assessment of extracellular DA dynamics and uptake kinetics within restricted sites, whereas genetically encoded sensors like dLight and $GRAB_{DA}$ allow broader spatial access and facilitate the analysis of circuit- and behaviour-associated DA signalling across brain regions.

1.3.5 Behavioural roles of mesostriatal DA

Mesostriatal DA plays a critical role in a wide range of behavioural functions, including movement, reinforcement learning, motivation, and reward. Seminal studies demonstrated that loss of nigrostriatal DA neurons underlies the motor deficits in PD (Ehringer & Hornykiewicz, 1960; Kish et al., 1988), while systemic L-DOPA administration restores DA levels and alleviates symptoms (Barbeau, 1969). DA neuron activity correlates with movement initiation, and burst firing seem closely coupled with transitions in motor states (Coddington & Dudman, 2019; Dodson et al., 2016; Schultz et al., 1983).

In reward-related contexts, DA neurons encode reward prediction-related events including errors, unpredicted rewards, and conditioned cues, wherein unexpected rewards and cues increase firing and DA release, whereas omission of expected rewards leads to suppression of DA activity (Schultz, 1997, 2013). This capacity to signal the mismatch between predicted and actual outcomes allows DA to guide adaptive learning and behavioural flexibility. Moreover, mesolimbic DA contributes to incentive salience, attributing motivational value to cues associated with rewards, and supports behavioural engagement (Mirenowicz & Schultz, 1996; Schultz, 2007).

Disruptions in DA signalling are implicated in a range of neuropsychiatric and neurodegenerative disorders. In addiction, repeated exposure to drugs of abuse hijacks DA circuits, leading to sensitisation of mesolimbic pathways and habit formation through nigrostriatal mechanisms (Poisson et al., 2021; Robinson & Berridge, 1993). In PD, progressive loss of nigrostriatal DA input leads to imbalance in basal ganglia output and motor impairments. Understanding how DA transmission contributes to these processes is essential for therapeutic strategies.

1.4 Striatal serotonergic system

Serotonergic afferents to the striatum primarily arise from the dorsal (and to a lesser extent, the median) raphe nuclei (DRN), projecting extensively across both dorsal and ventral regions of the striatum (Dorocic et al., 2014; Steinbusch, 1981). These projections form a modulatory layer that is essential to striatal function, despite there being no intrinsic serotonergic neurons within the striatum itself (Dorocic et al., 2014; Steinbusch, 1981). Importantly, descending modulation of raphe activity by basal ganglia outputs creates feedback loops that incorporate serotonergic tone into striatal information processing (Dorocic et al., 2014).

5-HT exerts its modulatory influence primarily by shaping synaptic integration among key neuronal populations, for example: ChIs, GABAergic MSNs, and local presynaptic terminals. Within this microcircuit, 5-HT acts at multiple sites. On ChIs, several 5-HTR subtypes regulate ACh release and ChI excitability (Blomeley & Bracci, 2005; Bonsi et al., 2011; Virk et al., 2016). In MSNs and presynaptic terminals, 5-HT influences synaptic transmission via distinct receptor classes and terminal innervation patterns (Brown & Molliver, 2000; Göthert, 1990; Shukla et al., 2014; Ward & Dorsa, 1996). By modulating afferent inputs from cortical and thalamic projections as well as local inhibitory and cholinergic networks, 5-HT fine-tunes synaptic integration and plasticity across striatal compartments. The complexity of serotonergic modulation is further reflected in the distinct distribution patterns of 5-HT receptor subtypes throughout the striatum, as described below.

1.4.1 5-HT receptors in striatum

The 5-HT receptor family includes seven principal classes - 5-HT_1 through 5-HT_7 - that together encompass up to 14 subtypes, including 5-HT_1 (5-HT_{1A}, 5-HT_{1B}, 5-$HT_{1D,}$ 5-HT_{1E}, and 5-HT_{1F}), 5-HT_2 (5-HT_{2A}, 5-HT_{2B} and 5-HT_{2C}), 5-HT_3, 5-HT_4, 5-HT_5 (5-HT_{5A} and 5-HT_{5B}), 5-HT_6 and 5-HT_7

(Filippo & Schmitz, 2024; Pithadia & Jain, 2009; Ślifirski et al., 2021). Within the striatum, at least eight of these subtypes - 5-HT_{1B}, 5-HT_{1D}, 5-HT_{2A}, 5-HT_{2C}, 5-HT_3, 5-HT_4, 5-HT_6 and 5-HT_7 - are robustly expressed, as demonstrated by autoradiography, *in situ* hybridization, and transcriptomic analyses (Filippo & Schmitz, 2024; Helboe et al., 2015; Ruat et al., 1993; Ward & Dorsa, 1996).

Evidence at the level of individual neuronal types reveals that ChIs within the striatum express multiple 5-HT receptor subtypes. These include 5-HT_{1A} and 5-HT_{1B}, which are particularly enriched in the ventral striatum, where they mediate inhibitory effects on ChI excitability (Blomeley & Bracci, 2005; Virk et al., 2016). In addition, 5-HT_{2C}, 5-HT_6 and 5-HT_7 receptors have also been identified on ChIs, as demonstrated by single-cell RT-PCR, electrophysiological depolarization assays, and recent transcriptomic analyses (Blomeley & Bracci, 2005; Bonsi et al., 2007; Rada et al., 1993; Virk et al., 2016). Immunohistochemical and autoradiographic studies further support this receptor distribution, showing relatively higher expression of 5-HT_7 in the dorsal striatum compare to the ventral striatum (Steinbusch, 1981; Virk et al., 2016). *In vivo* pharmacological data is consistent with this receptor topography: for instance, local infusion of 5-HT into the NAc reduces ACh release that is blocked by 5-HT_1 receptor antagonists, suggesting a presynaptic inhibitory mechanism (Rada et al., 1993).

Functionally, 5-HT exerts both excitatory and inhibitory influences on ChIs depending on the receptor subtype and anatomical region. In the dorsal striatum, bath application of 5-HT leads to depolarization and increased spontaneous firing of ChIs, an effect attributed to activation of 5-HT_2 receptors and blocked by selective antagonists (Blomeley & Bracci, 2005). Conversely, in the ventral striatum, 5-HT induces hyperpolarization of ChIs, likely via 5-HT_1 receptor signalling (Virk et al., 2016). These bidirectional effects highlight a region-dependent serotonergic modulation, where rapid fluctuations in extracellular 5-HT may dynamically adjust ChI firing and

cholinergic tone during behavioural events (Bonsi et al., 2007; Rada et al., 1993; Virk et al., 2016).

MSNs, encompassing both direct- and indirect-pathway cells, are thought to express 5-HT_{2A}, 5-HT_{2C}, and 5-HT_6 receptors at the mRNA level, with *in situ* hybridization indicating higher expression of 5-HT_{2C} in the patch compartments (Shukla et al., 2014; Ward & Dorsa, 1996). Functional studies further implicate 5-HT_6 receptors in shaping MSN excitability and influencing learning behaviours, through modulation of cAMP signalling downstream of G_s protein activation (Eskenazi et al., 2015) .

Presynaptically, 5-HT_{1B} and potentially 5-HT_{1D} autoreceptors are found in striatal axons, where they regulate neurotransmitter release by inhibiting 5-HT or glutamate release (Göthert, 1990; Guo & Rainnie, 2010; Hjorth et al., 2000; Moret & Briley, 2000; Nishijo et al., 2022). However, cell-type-specific expression of these receptors remains less well-defined. Certain subtypes - namely 5-HT_{1E}, 5-HT_{1F}, 5-HT_{2B}, and 5-$HT_{5A/B}$ - appear to be absent or expressed at very low levels in the striatum, as they are typically undetected in transcriptomic surveys and autoradiographic maps (Filippo & Schmitz, 2024; Nair et al., 2020; Pithadia & Jain, 2009).

In summary, striatal serotonergic modulation relies on the selective expression of receptor subtypes across neuronal types. The absence of several subtype expressions highlights the specificity of serotonergic signalling in the striatum, while the identified receptor distributions underscore the ability of 5-HT to tune striatal output through multiple cellular targets.

1.4.2 5-HT modulation of striatal DA transmission

5-HT exerts complex control over striatal DA transmission through diverse receptor mechanisms, resulting in both inhibitory and facilitatory modulation depending on receptor subtype and neural context. For example, activation of 5-HT_{2C} receptors located at presynaptic

sites within the dorsal striatum inhibits basal DA release, as shown by *in vivo* microdialysis studies using the inverse agonist SB206553, which enhances DA levels in a dose-dependent manner (Alex et al., 2005; Navailles et al., 2006). Conversely, systemic administration of the 5-HT_{2C} agonist mCPP suppresses striatal DA, further reinforcing the inhibitory role of 5-HT_{2C} on DA efflux (Alex et al., 2005; Navailles et al., 2006).

In addition to basal regulation, 5-HT_{2A} receptors modulate amphetamine-induced DA release *in vivo*: microdialysis studies in rats show that amphetamine-evoked DA release in the NAc and striatum is significantly attenuated by the selective 5-HT_{2A} antagonist SR46349B, without affecting basal DA levels (Porras et al., 2002). Conversely, morphine-induced DA release is enhanced when 5-HT_{2C} receptors are blocked using antagonists like SB206553, revealing contrasting roles for 5-HT_{2A} and 5-HT_{2C} in different stimulant contexts (De Deurwaerdère et al., 2004; Porras et al., 2002). Multiple studies have also demonstrated that activation of 5-HT_4 receptors facilitates striatal DA release via indirect, AP-dependent mechanisms. This effect has been consistently reported using *in vivo* and *ex vivo* models and is blocked by selective 5-HT_4 antagonists or TTX, indicating a circuit-mediated rather than terminal-specific action (Bonhomme et al., 1995; De Deurwaerdère et al., 1997; Steward et al., 1996).

Human and animal PET studies further support the concept that 5-HT receptor activity modulates dopaminergic transmission *in vivo*. In rodents, systemic pre-treatment with the 5-$HT_{2A/2C}$ antagonist ketanserin or the selective 5-HT_{2C} antagonist SB206553 significantly decreases striatal [^{11}C]raclopride binding, indicating increased DA release. Moreover, amphetamine-induced decreases in [^{11}C]raclopride binding are partially abolished by selective 5-HT_{2A} antagonism (Egerton et al., 2008). In humans, pharmacological increases in endogenous 5-HT - whether through SSRIs like citalopram or psychotropic drugs - consistently produce reductions in striatal D_2 receptor availability, suggesting elevated DA tone (Dewey et al., 1995; Smith et al., 1997; Vollenweider et al., 1999).

Beyond the well-characterised roles of 5-HT_{2A}, 5-HT_{2C}, and 5-HT_4 receptors, additional 5-HT receptor subtypes, including 5-HT_3, 5-HT_6, and 5-HT_7, have been implicated in modulating striatal DA release. *In vivo* microdialysis studies demonstrate that activation of 5-HT_3 receptors enhances extracellular DA levels in the striatum in a dose-dependent manner (Deurwaerdère et al., 1998; Imperato & Angelucci, 1989; Santiago et al., 1995). This effect is attenuated by 5-HT_3 antagonists and DAT blockers, indicating a facilitatory role of 5-HT_3 receptors on dopaminergic transmission (Deurwaerdère et al., 1998; Imperato & Angelucci, 1989; M. Santiago et al., 1995). 5-HT_6 receptors are G_s-coupled 5-HT receptors that stimulate intracellular cAMP accumulation upon activation, and are highly expressed in MSNs within the striatum, as shown by cloning, pharmacological binding and *in situ* hybridization (Grimaldi et al., 1998; Hirst et al., 2000; Roberts et al., 2002; Ruat, et al., 1993). However, current evidence does not support a direct role in modulating striatal DA release, but some evidence has suggested their ability to modulate striatal-based behaviours (Eskenazi et al., 2015; Ferguson et al., 2008; Hauser et al., 2015; Lopez et al., 2025; Mitchell et al., 2007). Autoradiography shows that 5-HT_7Rs are present in striatal regions, similar to their localization in hippocampus and thalamus (Bonaventure et al., 2002; Martín-Cora & Pazos, 2004; Ruat, et al., 1993). Electrophysiological studies further indicate that 5-HT-induced excitation of striatal ChIs is partly mediated by 5-HT_7Rs (Bonsi et al., 2007). Although direct behavioural evidence in the striatum is limited, 5-HT_7R-knockout mice display deficits in cognitive flexibility-based spatial tasks, suggesting an indirect role in striatal-dependent strategy switching (Sarkisyan et al., 2010). More broadly, 5-HT_7R contributes to neuronal development and plasticity across the brain, potentially influencing striatal circuit function (Volpicelli et al., 2014).

Besides receptor-mediated DA release, 5-HT also influences DA indirectly via modulation of local inhibitory circuits. For example, activation of 5-HT_{1B} receptors reduce lateral inhibition among MSNs, therefore altering the excitatory-inhibitory balance in striatal circuits and

potentially modifying DA-driven output patterns (Mathur et al., 2011; Pommer et al., 2021). Moreover, experimental evidence suggests that 5-HT can induce DA efflux in the striatum via reverse transport through DAT (Sershen et al., 2000). In striatal slices, exogenous 5-HT triggers DA release that is blocked by the DAT inhibitor GBR12909 and mimicked by cocaine, which blocks DAT (and also SERT), therefore preventing reuptake and promoting transporter-mediated efflux independent of vesicular mechanisms (Sershen et al., 2000).

Collectively, these lines of evidence highlight the complex regulatory role of 5-HT in modulating striatal DA release. The net outcome of serotonergic activity depends on the balance between inhibitory receptor subtypes and facilitating receptors, as well as local network interactions involving interneurons and transporters.

1.4.3 Behavioural roles of striatal 5-HT

The serotonergic system in the striatum plays a critical role in shaping a wide range of behaviours, including reward processing, motivation, emotional regulation, cognitive flexibility, and motor control (Bang et al., 2020; Eskenazi et al., 2015; Liu et al., 2025; Nair et al., 2020; Spring & Nautiyal, 2024). Striatal 5-HT modulates these behavioural outputs through coordinated actions of multiple receptor subtypes, as well as through its interactions with other neuromodulatory systems such as DA and ACh. Evidence from *in vivo* behavioural studies consistently supports the behavioural relevance of serotonergic signalling in the striatum. Serotonergic modulation critically shapes reward processing mechanisms: systemic elevation of 5-HT enhances DA release in the striatum, as shown in microdialysis studies, suggesting that 5-HT facilitates reward-related neural activity (Benloucif & Galloway, 1991). Beyond reward, serotonergic signalling in the striatum contributes to emotional process. For instance, reduced 5-HT levels in the ventral striatum have been associated with high anxiety-like behaviours in rodents, as shown by tissue analyses following elevated plus-maze performance (Schwarting et

al., 1998), highlighting the influence of striatal 5-HT tone on emotional regulation. Recent studies further emphasize the role of striatal 5-HT in adaptive cognitive behaviours. For example, human neuroimaging demonstrates that striatal 5-HT levels correlate with decision uncertainty, implicating 5-HT in the updating of behavioural confidence (Bang et al., 2020). Striatal 5-HT is also implicated in behavioural flexibility and goal-directed action. DRN serotonergic neurons exhibit tonic firing during delayed reward tasks, supporting behavioural persistence (Miyazaki et al., 2012). Separately, elevating 5-HT levels has been shown to improve flexibility in probabilistic reversal learning by reducing sensitivity to negative feedback, suggesting a role for 5-HT in behavioural updating based on outcome history (Bari et al., 2010). Finally, striatal 5-HT also modulates motor timing and motivational value. Under conditions of uncertainty or delayed reinforcement, 5-HT contributes to action restraint and persistence (Nair et al., 2020).

Importantly, the behavioural functions of 5-HT in the striatum are not restricted to serotonergic transmission alone but emerge from the dynamic interplay between 5-HT and other neuromodulators (Avery & Krichmar, 2017; Fischer & Ullsperger, 2017; Nair et al., 2020; Salvan et al., 2023). Additionally, *in vivo* studies show that serotonergic manipulation can alter DA-dependent measures of impulsivity. For example, systemic 5-HT_{1A} receptor agonism or global 5-HT depletion attenuates the ability of amphetamine to reduce impulsive choice, and the effect of amphetamine depends on intact DAergic circuitry within the NAc (Winstanley et al., 2003), highlighting that the behavioural impact of 5-HT requires functional DA pathways under certain circumstances. Meanwhile, 5-HT also has been reported to influence cholinergic level in a behaviourally relevant manner. Direct infusion of 5-HT or SSRI into the NAc significantly reduces extracellular ACh levels in freely moving rats, suggesting a suppressive 5-HT-ACh interaction that may shape motivational states or response inhibition (Rada et al., 1993). While

this demonstrated fundamental serotonergic control over ACh, it remains to be directly linked to behaviour through task-based paradigms.

In summary, striatal 5-HT has showed powerful influences on behaviour through both direct serotonergic mechanisms and interactions with other neuromodulatory systems. Independent 5-HT signalling regulates key behavioural functions, including reward valuation, decision-making, motor control, and emotional processing. These effects are mediated through diverse receptor subtypes and vary according to anatomical subregions, task demands, and temporal dynamics. In parallel, 5-HT modulates dopaminergic and cholinergic systems in a context-sensitive manner, shaping reward-seeking, impulsivity, and motivation. Together, these findings indicate that striatal 5-HT functions as a key coordinator within broader neurotransmitter networks that support adaptive behaviour.

1.4.4 5-HT measurement techniques and methodological advances

Accurate measurement of extracellular 5-HT is necessary for linking serotonergic neurochemistry to circuits, behaviours and diseases. Advances in 5-HT measurement have progressively enhanced temporal, spatial and chemical resolution, enabling finer dissection of 5-HT dynamics in the brain. Historically, microdialysis was commonly used to monitor extracellular 5-HT levels over time. Previous studies have shown that microdialysis can detect both basal and evoked 5-HT release. This has been demonstrated in raphe neuron graft experiments within the hippocampus and forebrain following pharmacological manipulations (Sharp & Foster, 1989; Sharp & Hjorth, 1990). These studies showed that extracellular 5-HT levels and their stimulus-evoked changes can be reliably measured in the brain, providing quantitative insight into serotonergic dynamics under physiological conditions. However, classical microdialysis suffers from limited temporal resolution and often fails to capture rapid phasic release events. To address this, Andrews's laboratory advanced fast microdialysis

protocols capable of sampling at 2 min intervals. For instance, Yang et al. (2013) reported that with enhanced temporal resolution, 5-HT overflow evoked by brief K^+ pulses could be resolved in the ventral striatum of mice (Yang et al., 2013). Their follow-up work further revealed sex- and SERT-mediated differences in stimulated 5-HT dynamics using this technique (Yang et al., 2015).

Despite these advances, sub-second measurements of 5-HT release and uptake were not possible until the development of FCV. Hashemi et al. (2009) first demonstrated *in vivo* detection of endogenous 5-HT using Nafion-coated carbon-fibre microelectrodes, overcoming electrode fouling and allowing simultaneous measurement of 5-HT and DA (Hashemi et al., 2009). Subsequent work refined this approach to permit reliable multi-analyte detection, including simultaneous measurement of 5-HT and histamine in the same recording site (Hashemi et al., 2011). Further analyses revealed distinct release and uptake kinetics between 5-HT and DA, reflecting their divergent regulatory mechanisms (Hashemi et al., 2012). Building on these developments, Dankoski and colleagues utilized FCV in behaving animals to monitor rapid monoamine signalling (Dankoski et al., 2014). Together, these studies established the basis for investigating fast serotonergic signalling.

Biosensor-based methods have greatly expanded the ability to detect 5-HT, and new techniques now enable precise tracking of its dynamics with high temporal and spatial resolution. Among these, $GRAB_{5\text{-}HT}$ sensors are genetically encoded fluorescent probes that use a modified 5-HT receptor linked to a circularly permuted GFP, allowing the direct visualization of transient serotonergic activity both *in vitro* and *in vivo* (Deng et al., 2024). In parallel, implantable aptamer–field-effect transistor (FET) neuroprobes have enabled continuous monitoring of 5-HT in head-fixed animals (Zhao et al., 2021). These technologies combine high chemical selectivity with spatial precision, complementing established approaches such as microdialysis and FCV for 5-HT detection.

In summary, advances from classical microdialysis to FCV and biosensor-based techniques have greatly enhanced our ability to study 5-HT dynamics, providing flexible tools to explore serotonergic function across physiological and pathological conditions.

1.5 Parkinson's disease

PD is a progressive neurodegenerative disorder that primarily affects the motor system but also cause a range of non-motor symptoms. First described by James Parkinson in 1817, PD is the second most prevalent neurodegenerative disease after Alzheimer's disease, affecting approximately 1% of individuals over the age of 60 (McGregor & Nelson, 2019; Poewe et al., 2017). The global number of patients with PD have been rising rapidly. Recent global estimates indicate that the number of individuals living with Parkinson's disease reached nearly 11.8 million in 2021, continuing the upward trend observed since 1990 (Dorsey et al., 2018; Li et al., 2025; Peng et al., 2025).

The clinical features of PD are heterogeneous, including both motor and non-motor symptoms. Classical motor symptoms include bradykinesia, rigidity, resting tremor, and postural instability, while non-motor symptoms range from sleep disturbances and depression to anosmia and cognitive decline (Jankovic & Tan, 2020; Poewe et al., 2017). Importantly, many non-motor symptoms appear during a long prodromal phase prior to clinical diagnosis, reflecting the widespread neurobiological alterations that occur early in the disease course (Jankovic & Tan, 2020). Despite the availability of symptomatic treatments, no current therapy halts or slows disease progression, representing a major unmet medical need (McGregor & Nelson, 2019; Peng et al., 2025; Poewe et al., 2017).

Although most PD cases have no known cause, rare familial forms have been linked to genetic mutations, including those in SNCA, LRRK2, PINK1, DJ-1 and PARK2 (Chartier-Harlin et al.,

2004; Cookson, 2012; Nuytemans et al., 2010; Singleton et al., 2003; Tran et al., 2020). In addition, environmental risk factors such as pesticide exposure and chronic disease comorbidities like diabetes have been associated with elevated PD risk, potentially due to shared pathogenic mechanisms like mitochondrial dysfunction and oxidative stress (Ascherio & Schwarzschild, 2016; De Pablo-Fernandez et al., 2018; Santiago & Potashkin, 2014).

1.5.1 Degeneration of DA neurons in PD

A pathological hallmark of PD is the selective degeneration of DA neurons in the SNc, which project to the dorsal striatum via the nigrostriatal pathway (Kish et al., 1988; Poewe et al., 2017). This leads to a marked reduction in striatal DA levels, disrupting the balance of activity across the basal ganglia circuitry and resulting in the characteristic motor deficits (Albin et al., 1989; DeLong, 1990; Poewe et al., 2017). Post-mortem studies show that the most vulnerable population comprises neuromelanin-positive and calbindin-negative DA neurons in the ventral tier of the SNc, which display large unmyelinated axonal arbors and high metabolic demand (Bolam & Pissadaki, 2012; Pissadaki & Bolam, 2013). These unique structural features make nigrostriatal DA neurons particularly susceptible to metabolic stress, oxidative damage, and mitochondrial dysfunction (Gonzalez-Rodriguez et al., 2020; Surmeier et al., 2017).

In PD, dopaminergic axons in the striatum often degenerate before the loss of SNc cell bodies, a pattern confirmed by post-mortem analyses, *in vivo* imaging, and transgenic animal models (Grosch et al., 2016; Koch et al., 2015; Koeglsperger et al., 2023). The resulting DA denervation of the striatum disrupts cortico-striatal integration and synaptic plasticity, affecting not only movement but also motivation and cognition (Obeso et al., 2017; Poewe et al., 2017).

Currently, the most widely used treatment for PD is Levodopa (L-DOPA), a DA precursor that restores DA synthesis. However, long-term use of L-DOPA is associated with complications

such as dyskinesia and motor fluctuations (Poewe et al., 2017). Other pharmacological approaches include DA receptor agonists and MAO-B inhibitors (Jankovic & Tan, 2020; Riederer & Müller, 2018; Schaeffer & Berg, 2017), while surgical treatments like deep brain stimulation (DBS) target the STN or GP to alleviate motor symptoms (Jankovic & Tan, 2020). Still, the underlying neurodegeneration remains unaddressed.

1.5.2 Alpha-synuclein in PD

Alongside DA neuron loss, PD is characterised by intracellular inclusions known as Lewy bodies, composed primarily of aggregated α-synuclein (Baba et al., 1998; Spillantini et al., 1998). Genetic studies have established that *SNCA* gene mutations, including point mutations and locus multiplications, can cause both familial and sporadic PD (Bekris et al., 2010; Singleton et al., 2003). Although the physiological function of α-synuclein is not fully understood, it is believed to play a role in synaptic vesicle trafficking, neurotransmitter release, and regulation of DA synthesis and reuptake (Burré, 2015; Cabin et al., 2002; Lautenschläger et al., 2018; Nemani et al., 2010; Threlfell et al., 2021).

Abnormal α-synuclein can oligomerise, form fibrils and aggregate, disrupting normal cell function and becoming toxic (Poewe et al., 2017; Taschenberger et al., 2012). These aggregates can impair mitochondrial function, inhibit lysosomal degradation, and interfere with intracellular trafficking, although the exact mechanisms of toxicity remain incompletely defined (Braak et al., 2003; Poewe et al., 2017; Schapira, 2015).

1.5.3 PD mouse models

To investigate PD mechanisms, a range of animal models have been developed, including neurotoxin and genetic models. Neurotoxin-based models using 6-hydroxydopamine (6-OHDA) or MPTP induce rapid DA neuron degeneration but lack progressive pathology and α-synuclein

aggregation (Perese et al., 1989; Sauer & Oertel, 1994). These models are widely used due to their reproducibility and mechanistic clarity but lack key pathological hallmarks of PD, including α-synuclein aggregation and progressive multisystem involvement. Conversely, genetic models targeting PD-associated genes better represent chronic disease progression and allow investigation of early synaptic dysfunction and compensatory changes prior to neuronal loss. For example, the MitoPark model represents mitochondrial dysfunction-induced neurodegeneration (Ekstrand & Galter, 2009). In this model, mitochondrial transcription factor A (Tfam) is selectively deleted in DAergic neurons. As a result, MitoPark mice exhibit gradual DAergic neuron loss and motor impairments, closely resembling key pathological and behavioural features of PD (Ekstrand & Galter, 2009). However, the MitoPark model often shows variable symptoms and a late onset, which makes it less suitable for studying early-stage changes.

Leveraging the strengths of both model types, the present study employs a synuclein-driven model that combines genetic specificity with a well-characterised DAergic background. This approach enables detailed characterisation of presynaptic pathology and neurotransmission deficits prior to overt neuronal loss, providing a tractable system for studying early mechanisms that may contribute to disease initiation. At the Oxford Parkinson's Disease Centre, a BAC-transgenic mouse model known as *SNCA*-OVX was developed to overexpress wild-type human α-synuclein on a mouse *Snca*-/- background (Janezic et al., 2013). This model mimics gene multiplication found in some familial PD and exhibits early impairments in evoked DA release within the dorsal striatum prior to cell body loss, followed by degeneration of SNc DA neurons and motor deficits (Dodson et al., 2016; Janezic et al., 2013; Roberts et al., 2020). Importantly, this model provides a valuable tool to study axon dysfunction, a process that may precede and even drive cell body loss in PD. More details about Parkinson's disease will be described in **Chapter 6**.

1.6 Thesis aims

Despite extensive research into striatal function, key questions remain regarding how 5-HT release is dynamically regulated and how it interacts with dopaminergic and cholinergic signalling under both physiological and pathological conditions. In particular, while DA transmission is well studied over the past decades, how striatal 5-HT release is regulated and interacts with other neurotransmitters is still not well understood. Addressing these gaps is critical for better understanding of how disturbances in monoamine system contributes to basal ganglia dysfunction in diseases. Altered DA and 5-HT signalling have been studied in a range of movement and psychiatric disorders, including PD, dystonia, depression, and addiction, yet the precise mechanisms by which serotonergic regulation influences striatal network activity remain poorly defined. A deeper understanding of these processes will not only refine our knowledge of striatal physiology but may also reveal novel targets for therapeutic intervention in disorders associated with imbalanced monoamine system.

Therefore, the main aim of this thesis was to investigate how striatal 5-HT release is dynamically regulated, particularly in relation to DA signalling, under both physiological and disease-relevant conditions. Two complementary techniques were employed to measure neurotransmitter release: fast-scan cyclic voltammetry for DA and the genetically encoded $GRAB_{5\text{-}HT}$ fluorescent sensor for 5-HT in striatal slices *ex vivo*. **Chapter 3** first validated the application of the $GRAB_{5\text{-}HT}$ sensor in the striatum. It is proposed that $GRAB_{5\text{-}HT}$ can retain high specificity for 5-HT over DA even in a DA-rich brain region - striatum, and thus reliably reports 5-HT dynamics. This chapter also investigated the modulation of striatal 5-HT release by local microcircuits, testing the hypothesis that both cholinergic and GABAergic systems shape the temporal and spatial dynamics of 5-HT release under physiological conditions. **Chapter 4** explores the dopaminergic regulation of striatal 5-HT release. It is hypothesised that D_1 and D_2

dopamine receptors, as well as DA reuptake system, exert modulatory control over 5-HT transmission. **Chapter 5** investigated the reciprocal modulation, focusing on how serotonergic signalling via 5-HT_4 receptors regulates DA and ACh release. This chapter characterised the impact of 5-HT_4R ligands on cholinergic and dopaminergic transmission, with a particular focus on the role of acetylcholinesterase. **Chapter 6** further examined alterations in serotonergic signalling in a transgenic mouse model of Parkinson's disease. This chapter aimed to test the hypothesis that the loss of striatal DA release leads to adaptive changes in 5-HT release and its regulation, potentially contributing to non-motor symptoms and therapeutic side effects.

Together, the studies presented in this thesis provide new mechanistic insights into how serotonergic, dopaminergic, and cholinergic systems interact to regulate striatal neurotransmission, and how these interactions are altered in Parkinson's disease.

Chapter 2.
General methods

2.1 Animal models for investigating striatal circuits

2.1.1 Ethical statement for the use of animals

The primary aim of this thesis is to investigate the mechanisms by which mammalian striatal 5-HT and DA release is regulated, with the ultimate goal of identifying novel targets for the treatment of human disorders involving dysfunctional serotonergic and dopaminergic neurotransmission. Although advances in computational modelling have enabled simulation of individual components of the mesostriatal pathway, the complete mapping of interacting regulatory circuits is not yet available, and experimental studies still require the use of biological tissue.

All experimental procedures were conducted in accordance with the UK Animals (Scientific Procedures) Act 1986 (PPL P9371BF54 and PP8860348), the University of Oxford ethical guidelines, and Home Office regulations. All mice were maintained on a C57BL/6 background and housed in the Biomedical Services Building, University of Oxford, in groups under controlled environmental conditions (temperature 22-24 °C; relative humidity 40-60%; 12 h light-dark cycle), with *ad libitum* access to food and water.

2.1.2 Investigating 5-HT and DA signalling in mouse acute brain slices

This thesis investigated 5-HT and DA signalling in the striatum using acute coronal *ex vivo* brain slices prepared from mice. Mice were selected due to their conserved neural architecture and close similarity to human brain organisation within mesostriatal and mesolimbic pathways, enabling the study of neurotransmission mechanisms with translational potential. The availability of numerous transgenic lines for targeted genetic manipulation allows for selective expression of fluorescent sensors and optogenetic tools in defined neuronal populations. Moreover, the

widespread use of mice in studies of striatal neurotransmission facilitates direct comparison of the present findings with an extensive body of literature.

Acute *ex vivo* slices containing dorsal and/or ventral striatum were used for all experiments monitoring real-time neurotransmitter release. This approach was chosen over primary *in vitro* cultures because slices preserve native striatal connectivity and neuronal spatial organisation, including the complex axonal arborisation of DA and 5-HT neurons (Matsuda et al., 2009). Compared with parasagittal sections, coronal slices isolate axons from their somatodendritic regions, enabling the investigation of axonal-specific mechanisms without confounding inputs from cell bodies.

An *ex vivo* preparation was preferred to *in vivo* approaches because it allows precise control of the extracellular environment, consistent bath application of pharmacological agents, and straightforward manipulation of ionic conditions, pH, and temperature. Additionally, multiple slices can be obtained from a single animal, increasing experimental throughput and reducing the total number of animals used in line with the principle of Reduction from the 3Rs framework. While *ex vivo* approaches cannot capture intact circuit-level or behavioural dynamics, they provide an optimal balance between experimental control and preservation of physiological striatal architecture for dissecting the mechanisms underlying neurotransmitter signalling.

To ensure that experimental findings were broadly applicable and not biased towards one sex, both male and female adult mice were included in all cohorts, with similar numbers of each sex whenever possible. Neuroscience research has historically shown a strong bias towards the exclusive use of male rodents, often justified by concerns that the oestrus cycle in females would introduce excessive variability (Beery, 2018; Perreault et al., 2014). However, comparative studies across behavioural, morphological, physiological, and molecular traits have demonstrated that variability in females is not greater than in males, and fluctuations across the

oestrus cycle are no larger than intrinsic variability observed in male animals (Beery, 2018; Perreault et al., 2014). Including both sexes therefore improves the relevance of preclinical research to the human population and supports the development of clinical studies with stronger translational validity (Clayton, 2016). Data from both sexes were combined unless sex-specific differences emerged.

2.1.3 Transgenic mouse lines

The majority of experiments described in Chapters 3, 4 and 5 used wild-type C57BL/6J mice (Charles River). In Chapter 6, striatal 5-HT signalling was studied in a genetic model of early PD - mice overexpressing human α-synuclein (*SNCA*-OVX, aged 3-4 months) at levels relevant to disease pathology (Janezic et al., 2013). These mice were generated by introducing a bacterial artificial chromosome (BAC) containing the complete human *SNCA* locus into C57BL/6 pronuclei, followed by backcrossing onto an α-synuclein-null (*Snca*-/-) background. Littermate *Snca*-/- mice served as controls, as they lack endogenous α-synuclein and therefore avoid confounding protein-protein interactions. Notably, *Snca*-/- animals exhibit normal DA storage and release compared with mice expressing moderate levels of human α-synuclein, indicating that functional deficits in *SNCA*-OVX mice arise from overexpression rather than α-synuclein expression itself (Janezic et al., 2013).

2.2 Fast-scan cyclic voltammetry for real-time detection of DA release

2.2.1 Rationale for the use of FCV

Fast-scan cyclic voltammetry (FCV) at carbon fibre microelectrodes (CFMs) was chosen in this work as the primary method to monitor DA release in the striatum due to its combination of high

temporal resolution, sensitivity, and chemical identification capabilities. FCV detects electroactive neurotransmitters by applying a triangular voltage waveform to the CFM, which induces oxidation and reduction reactions in molecules such as DA. The resulting faradaic current is proportional to the extracellular concentration of the analyte, and the shape of the cyclic voltammogram provides a unique chemical marker that can identify a specific molecule.

Compared with alternative approaches, FCV offers several advantages for the study of rapid DA signalling. Unlike microdialysis, which is limited to a temporal resolution of tens of seconds, FCV achieves sub-second sampling rates suitable for resolving release and uptake kinetics. In contrast to genetically encoded fluorescent DA indicators, which require viral delivery and report only relative changes in fluorescence, FCV can quantify absolute DA concentration changes through post-experiment calibration with known standards. It also avoids the lack of chemical specificity seen with constant-potential amperometry, which measures current at only one fixed voltage. Without scanning across a range of voltages, this method cannot capture the oxidation and reduction peaks needed to distinguish between different electroactive molecules with similar structures. These features make FCV particularly well suited for *ex vivo* slice experiments aimed at dissecting axonal-level mechanisms of DA regulation, while avoiding excessive invasiveness and preserving the physiological architecture of the striatum.

2.2.2 FCV for the detection of DA

FCV was implemented using CFMs positioned within the striatal recording site of acute *ex vivo* brain slices. This method exploits the electroactive nature of DA, which arises from its two hydroxyl groups that can be oxidised to dopamine-o-quinone and subsequently reduced back to DA. A triangular voltage waveform was applied between the working electrode and an Ag/AgCl reference electrode. During the positive-going phase of the sweep, DA was oxidised at approximately +0.6 V to form dopamine-o-quinone (**Fig. 2.1A**). During the negative-going

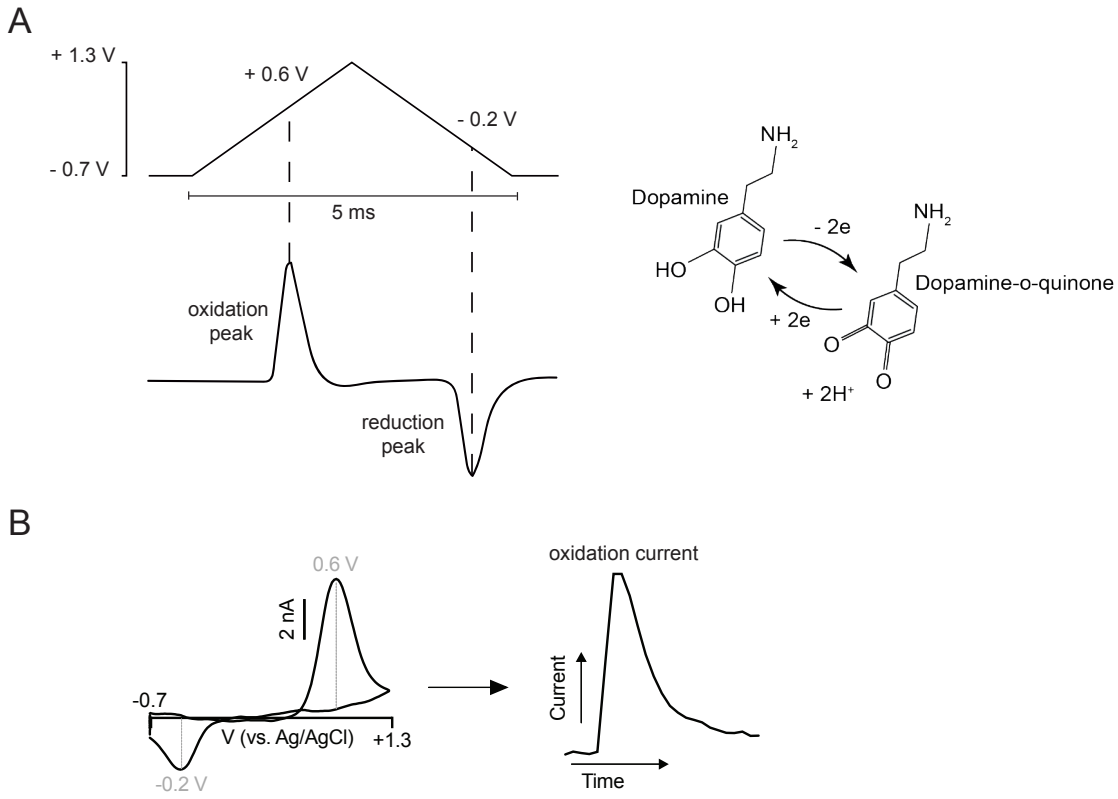

Figure 2.1. Fast-scan cyclic voltammetry for the detection of DA. **(A)** A triangular waveform is applied, ramping from -0.7 V to +1.3 V and back to -0.7 V, vs Ag/AgCl. In the background-subtracted voltammogram, DA is oxidised at 0.6 V to DA-o-quinone and reduced to DA at -0.2 V. **(B)** Current vs voltage plot showing background-subtracted cyclic voltammogram upon application of 2 μM DA. Current vs time plot, and an example of electrically-evoke DA transient.

phase, this product was reduced back to DA at approximately -0.2 V. The change in oxidation state involves the loss and gain of electrons, producing a faradaic current whose amplitude is directly proportional to the extracellular DA concentration at the electrode surface. A voltammogram where the potential applied is plotted against the current recorded is useful to identify the molecule of interest (**Fig. 2.1B**).

Each waveform scan lasted approximately five milliseconds and was repeated eight times per second (8 Hz), providing a sub-second sampling rate that is sufficient to resolve the rapid dynamics of DA release and uptake. A large, relatively stable background charging current, generated by capacitive effects at the electrode-tissue interface, was always present. This

background current was digitally subtracted in real time by a Millar voltammeter to isolate the faradaic component. In practice, the electrode was allowed to remain in the tissue for close to an hour before data acquisition commenced, ensuring that the local environment had stabilised and that slow fluctuations in the charging current had subsided.

To permit quantification, each recording electrode was calibrated at the end of the experiment with a known concentration of DA. This established a linear relationship between current amplitude and DA concentration over the physiological range observed in the slice preparation. When pharmacological agents were applied during recordings, calibrations were performed both in the presence and absence of these agents to verify that they did not alter electrode sensitivity, for example by interacting with the carbon fibre surface.

The recorded signals were identified as DA based on several lines of evidence. First, DA produces a characteristic cyclic voltammogram, with a peak oxidation potential around +0.6 V and a reduction peak near -0.2 V, which allows for clear differentiation from other electroactive molecules measurable with FCV, such as 5-HT, which exhibits a distinct voltammetric profile. During each experiment, voltammograms were compared with those obtained during end-of-day calibration using a known concentration of DA. Second, recordings were made in the striatum, where DA is far more abundant than other electroactive transmitters, making it the most likely source of the signal. Third, the application of pharmacological agents produced effects consistent with DA-specific mechanisms. For example, blocking the DA transporter with cocaine led to a slower decay of the evoked signal, as expected from inhibition of DA reuptake (Threlfell et al., 2021).

2.2.3 Fabrication of carbon fibre microelectrodes (CFMs)

Carbon fibre microelectrodes were fabricated in-house, and each electrode was used for a single day of recording. This ensured consistent sensitivity and response kinetics, as repeated exposure to DA and biological tissue can degrade electrode performance.

A single epoxy-free carbon fibre (7 µm diameter; Goodfellow Cambridge Ltd) was threaded through a borosilicate glass capillary tube (outer diameter 2.0 mm, inner diameter 1.6 mm; Multi Channel Systems, Harvard Bioscience Inc). The capillary was first filled with acetone to assist fibre insertion and cleaning, then dried thoroughly. The capillary tube was sealed tightly around the carbon fibre using a vertical electrode puller (PE-2, Narishige) with a high heat setting. This created a narrow glass tip and a strong seal around the fibre, which helps to minimise electrical noise during recordings. The seal was inspected under high magnification to ensure it was intact and free of cracks. The exposed fibre extending from the seal was then trimmed to a length between approximately 50-150 µm using a scalpel. This length provided a balance between signal sensitivity and noise levels. To complete the electrode, an insulated copper wire was partially stripped and coated with silver conductive paint (RS Components Ltd). This wire was inserted into the opposite end of the capillary tube until it made electrical contact with the carbon fibre. The wire was fixed in place using cyanoacrylate glue (Loctite).

Before use, each electrode was connected to the Millar voltammeter and assessed for stability and signal quality, ensuring the amplification factor (full signal gain) was ~3-12 mV/nA indicating an exposed fibre length of ~50-150 µm. The background charging current was examined, and electrodes showing abnormal noise or poor gain were discarded. Sensitivity was also checked, ensuring the electrode fell within an acceptable amplification range to provide reliable DA detection with sufficient signal-to-noise ratio.

2.2.4 Slice preparation

Acute coronal brain slices containing the striatum or SNr were prepared for all *ex vivo* recordings in this thesis. On the day of the experiment, mice were culled by cervical dislocation and the brain was removed and transferred to an ice-cold cutting solution, containing in mM: 194 sucrose, 30 NaCl, 4.5 KCl, 1 $MgCl_2$-$6H_2O$, 26 $NaHCO_3$, 1.2 NaH_2PO_4, 10 glucose, saturated with 95% O_2/5% CO_2. Coronal slices 300 µm-thick containing the striatum were cut using a vibratome (VT1200S, Leica Microsystems). Slices were immediately transferred to artificial cerebrospinal fluid (aCSF) containing in mM: 130 NaCl, 2.5 KCl, 26 $NaHCO_3$, 1.25 NaH_2PO_4, 2 $MgCl_2$-$6H_2O$, 2.5 $CaCl_2$ and 10 glucose, saturated with 95% O_2/5% CO_2. Sections were incubated at 34°C for 15 min before they were stored at room temperature (20-22°C) until recordings were performed. All recordings were obtained within 6 h of slicing.

2.2.5 FCV recording

Following incubation, individual slices were hemisected and transferred to a recording chamber perfused with aCSF at a flow rate of approximately 2 ml/min, maintained at 31-33°C and continuously bubbled with 95% O_2 / 5% CO_2. Slices were allowed to equilibrate in the bath for 30-40 minutes prior to recording. During this period, the CFM was inserted into the tissue with the voltammetric scan active, allowing the electrode surface to stabilise in the local environment and minimising baseline drift caused by interactions with endogenous electroactive molecules.

To begin recording, the CFM was positioned at a depth of 100-150 µm in the DLS or NAcC. Electrical stimulation is described in the following **Section 2.2.6**. Recording sites were excluded if stable release could not be achieved after multiple stimulations. At the end of each experimental day, electrodes were calibrated using 2 µM DA in aCSF. Calibration solutions were freshly prepared from a 2.5 or 5 mM DA stock in 0.1 M perchloric acid, stored at 4°C. In drug experiments, calibrations were repeated in the relevant drug-containing solution to assess any impact on electrode sensitivity.

Data were acquired using Axoscope software (version 10.7, Molecular Devices) and analysed with Python code written in-house. Peak DA oxidation current values were extracted from background-subtracted voltammograms, converted to concentration using the electrode-specific calibration factor, and plotted over time to produce DA transients.

2.2.6 Electrical stimulation and experimental design

To evoke DA release in striatal slices, local electrical stimulation was applied, as the coronal slices used in this study do not contain DA cell bodies and thus lack spontaneous dopaminergic activity. This approach enables selective investigation of presynaptic mechanisms regulating DA release without input from midbrain somatodendritic regions. However, it should be noted that electrical stimulation is not cell-type specific and may activate local non-dopaminergic elements.

Stimulation was delivered using a bipolar concentric Pt/Ir electrode (inner pole diameter approximately 25 µm; FHC Inc.), positioned on the tissue surface around 100 µm from the carbon fibre microelectrode. Stimulation pulses were 0.2 ms in duration and delivered at an amplitude of 0.6 mA.

Single-pulse and five-pulse stimulation protocols were used throughout, with stimulation delivered every 2.5 minutes to allow signal recovery and stable baseline measurements. Experiments involving drug application were initiated only once evoked DA release had stabilised, defined as no more than 10% variation across four consecutive recordings. Once stable, test compounds were applied for a period of 20-30 minutes (8-12 recordings), and their effects on evoked DA release were assessed. The single-pulse protocol was designed to reflect the low-frequency, tonic firing mode of DA neurons, typically ranging from 1 to 10 Hz under basal conditions. In contrast, DA neurons can switch to a burst firing mode in response to salient

stimuli, with average firing rates around 20-40 Hz, and in some cases reaching up to 100 Hz (Freeman et al., 1985; Grace & Bunney, 1984; Hyland et al., 2002).

2.3 GRAB sensor imaging

2.3.1 Stereotaxic intracranial injections

Stereotaxic intracranial injections were performed to deliver AAV-packaged GRAB sensors into the striatum of wild-type (C57BL/6J) or transgenic (*SNCA*-OVX and *Snca* -/-) mice (**Fig 2.2**). All surgical procedures were conducted under aseptic conditions and in accordance with the Project Licence approved by the UK Home Office.

Anaesthesia was induced using 4% isoflurane in an induction chamber and maintained at 1.5-2% throughout the procedure. Mice were placed in a stereotaxic frame (Kopf Instruments) and monitored for anaesthetic depth by the pedal withdrawal reflex. Eye ointment was applied, and core body temperature was maintained at 37°C using a rectal probe and heated mat. The incision site was shaved, cleaned with chlorhexidine gluconate (Chloraprep), and injected with bupivacaine hydrochloride (2 mg/kg, s.c.). Meloxicam (5 mg/kg, s.c.) and sterile saline (Vetivex) were also administered sub-cutaneously.

A midline scalp incision was made, and craniotomies were drilled at the target site: DLS (ML ±2.2 mm, AP +0.65 mm, DV -2.7 to -2.5 mm), NAcC (ML ±0.9 mm, AP +1.4 mm, DV -3.8 to -3.5 mm). Viral constructs were injected using a 32-gauge Hamilton syringe at 200 nL/min (1 µL per site), with the needle left in place for 5 minutes post-injection to allow diffusion. The injected constructs included AAV2/5-hSyn-5-HT3.0, AAV2/9-hSyn-5-HT3.0mut, AAV2/5-hSyn-ACh3.0 and AAV2/5-hSyn-DA3h/3m (BrainVTA), all at a titre of ≥ 2.00 x 10^{12} viral genome copies per ml.

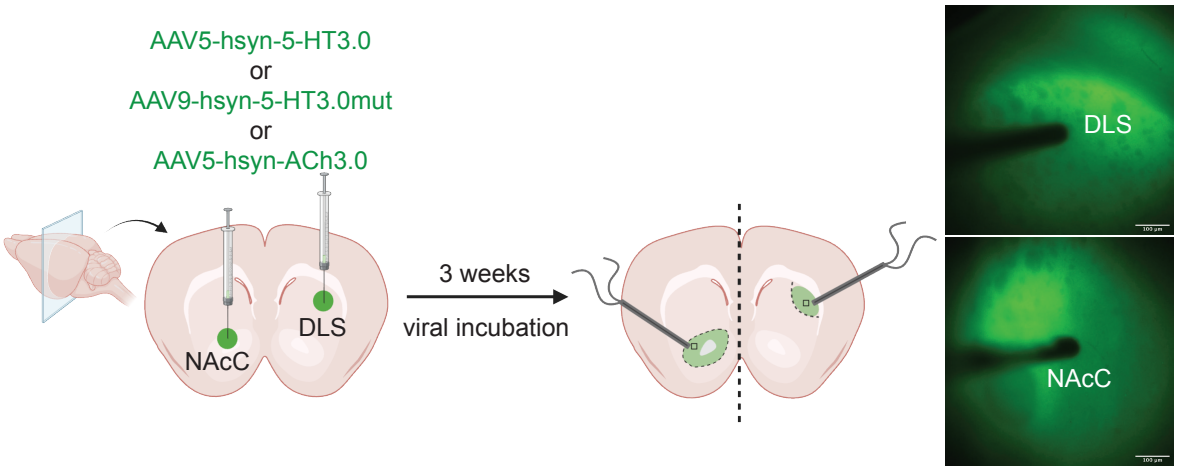

Figure 2.2. Schematic representation of the experimental procedure for GRAB sensor expression in mouse striatum. AAV-packaged $GRAB_{5\text{-}HT3.0}$ or $GRAB_{5\text{-}HT3.0mut}$ or $GRAB_{ACh3.0}$ sensors were bilaterally injected into the dorsal striatum (DLS) or ventral striatum (NAcC) of WT mice. After 3 weeks of expression, acute slices were prepared for recording. Representative fluorescence images show bright and uniform sensor expression in the targeted regions.

Following injection, the incision was closed with monofilament suture (Monocryl). Mice were placed in a temperature-controlled recovery cage until fully awake and monitored daily for 7 days post-surgery. Medicated jelly (Metacam) was provided on days 0-3 for analgesia. Mice were used for experiments 3-4 weeks after injection to allow time for sufficient viral expression.

2.3.2 GRAB imaging

Fluorescent GPCR-activation based sensors were used to monitor extracellular levels of 5-HT, ACh and DA in acute striatal brain slices. AAV2/5-hSyn-$GRAB_{5\text{-}HT3.0}$ sensors were used to detect 5-HT release, AAV2/5-hSyn-$GRAB_{ACh3.0}$ sensors for ACh, and AAV2/5-hSyn-$GRAB_{DA3h/3m}$ sensors for DA (all from BrainVTA).

All GRAB sensors were expressed under the control of the human synapsin 1 (hSyn) promoter, ensuring stable, neuron-specific expression at the injection site (Kügler et al., 2003). These constructs encode sensors based on modified human GPCRs, in which a circularly permutated GFP (cpGFP) is inserted into an intracellular loop of the receptor(Deng et al., 2024). Binding of

the relevant neurotransmitter triggers a conformational change in the receptor, leading to an increase in fluorescence.

2.3.3 Imaging acquisition

All imaging experiments were performed using the same recording setup and aCSF conditions as for FCV recordings, including temperature (~32 °C) and perfusion rate (~2 mL/min). Slices were placed in the recording chamber and held in place using silver pins. GRAB sensor expression was visualised using a 10x water immersion objective (Olympus) and a sCMOS camera (Teledyne Photometrics). The objective was lowered into the bath and an LED (470 nm, 4 mW, pE-300, CoolLED) was briefly switched on to visualise GFP expression to confirm expression, and to place the stimulating electrode in the desired expressing-region. For $GRAB_{5\text{-}HT}$, sampling rate was 10 Hz, exposure time 100 ms, field size was 665.6 µm x 665.6 µm and image sequences were recorded for 40 s with a 7 s pre-recording photo-bleaching time using Micro-Manager 2.0. For $GRAB_{ACh}$ and $GRAB_{DA}$, sampling rate was 100 Hz, exposure time 10 ms, field size was 665.6 µm x 665.6 µm and images sequences were recorded for 5 s with a 1 s pre-recording photo-bleaching time. Electrical stimulations were delivered every 2.5 minutes and the same stimulation parameters and protocols were used as in Section 2.2.6.

2.3.4 Data processing

Fluorescence data were extracted in ImageJ using a custom-written macro. For evoked release experiments, a square region of interest (ROI, 50 µm × 50 µm) was placed with its centre located 75 µm from the centre of the stimulating electrode (**Fig. 2.3A**), matching the spatial configuration used in FCV recordings.

The fluorescence values and corresponding frame numbers of the ROI were exported and analysed in MATLAB (R2023b, MathWorks) using a self-written code. Time was calculated from

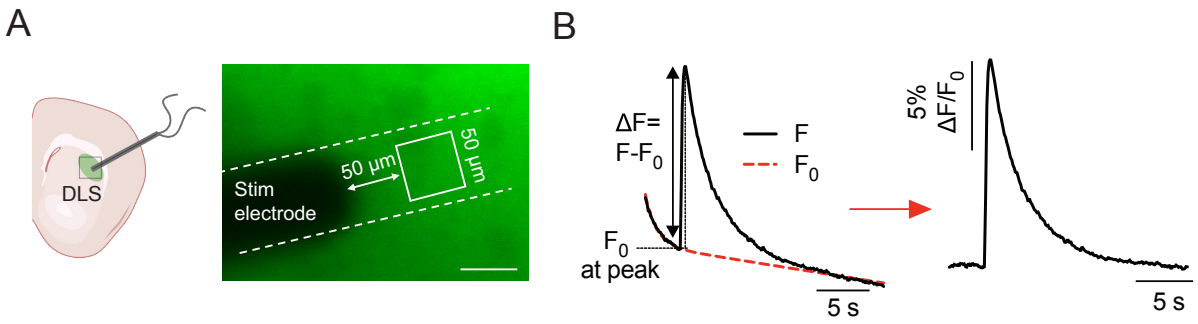

Figure 2.3. Data extraction and processing for imaging experiments with electrical stimulation. (A) Example recording window ($GRAB_{5\text{-}HT}$) and schematic of the recording configuration in the DLS. The stimulating electrode angle was measured, and a 50 µm × 50 µm square region of interest (ROI) was positioned with its centre 75 µm from the electrode tip. Scale var = 50 µm. **(B)** Example trace illustrating $\Delta F/F_0$ calculation. Raw fluorescence values (F) were fitted with an exponential decay function in MATLAB to determine baseline fluorescence (F_0). The fluorescence change ($\Delta F = F - F_0$) was then divided by F_0 to obtain $\Delta F/F_0$ values. The baseline fluorescence at the peak $\Delta F/F_0$ (F_0 at peak) was also extracted to monitor basal fluorescence changes over time and under different drug conditions.

frame numbers, and traces were generated by the signal from ROI. A 'exp2' MATLAB function, $f(x) = a^{bx} + c^{dx}$ was fit to the pre- and post-peak of the trace to estimate baseline fluorescence (F_0) in the absence of stimulation (**Fig. 2.3B**). Evoked responses were calculated as $\Delta F/F_0$, where $\Delta F = F - F_0$, and F is the raw fluorescence at the peak. In addition to measuring evoked transients, F_0 at the time of stimulation was also recorded as a proxy for tonic (non-evoked) neurotransmitter levels, to assess changes across time or in response to pharmacological manipulation.

2.4 AChE chemiluminescent assay

AChE activity was measured using a commercially available colorimetric assay kit (Abcam, ab138871), which utilizes 5,5′-dithiobis-(2-nitrobenzoic acid) (DTNB) to detect thiocholine (TCh), a product of acetylthiocholine (ATCh) hydrolysis catalyzed by AChE. The kit includes DTNB, assay buffer, ATCh, and AChE standards. Dorsal and ventral striatal tissue punches (1.2 mm diameter) were collected from 300 µm-thick acute coronal striatal slices, prepared using a

vibratome in ice-cold cutting solution as described above (**Section 2.2.4**). Each slice was bisected along the midline, with the left hemisphere incubated in aCSF as control and the right hemisphere treated with either 10 µM RS67333 or 10 µM BIMU8 for 1 hour at room temperature. Following treatment, tissue punches were lysed in PBS containing 0.5% IGEPAL CA-630 for 10 minutes, sonicated (10-15 s, 2-3 cycles), and centrifuged at 800 rpm for 5 minutes at 4 °C. The resulting supernatants were transferred to new Eppendorf tubes and diluted at a ratio of 1:5 in assay buffer for use in subsequent assays. To generate test mixtures with defined substrate concentrations (0%, 10%, 50%, 75%, and 100%), different proportions of ATCh-containing reaction mix (ATCh MIX) and control mix lacking substrate (Null MIX) were combined in a fixed total volume of 50 µL per well. The mixtures were loaded into the designated wells of a 96-well plate following addition of 50 µL of diluted sample to each well. After a 15-minute incubation at room temperature in the dark, absorbance was measured at 410 nm using a microplate reader. Saturation curves were generated based on the calculated enzyme activities. The test compounds (RS67333 or BIMU8) were present in the reaction buffer throughout the entire assay process. Michaelis constant (K_m) and maximum reaction velocity (V_{max}) were determined by fitting the data to the Michaelis–Menten equation using non-linear regression.

2.5 Statistical testing

Statistical analyses were performed using GraphPad Prism (version 10). Standard errors of the mean (SEMs) shown in figures were calculated based on slice-level replication, treating each slice as a statistical unit. For each dataset, SEM was then calculated as the standard deviation divided by the square root of the number of slices. This approach reflects the slice-level randomisation, handling, and recording protocols applied during the experiments. SEMs were not adjusted by the number of animals because the analysis was performed at the slice level. In

all cases, slices from different animals were appropriately balanced across treatment groups to avoid pseudo-replication and to maintain biological validity. Each slice was randomly allocated to a treatment group, independently handled, and recorded from a single site, fulfilling standard criteria for genuine biological replication. Additionally, all datasets were reviewed to ensure that no group-level effects or outliers were driven by data from a single animal or a specific sex, and no such biases were detected.

Statistical testing was applied to datasets with a minimum of four slices per group. In each case, the number of animals contributing to the dataset is reported, with a minimum of three animals per group unless otherwise stated.

Parametric tests were used in most cases, based on the assumption that evoked striatal neurotransmitter release follows a normal distribution with relatively consistent variance between slices and recording sites. Student's *t*-tests or two-way analysis of variance (ANOVA) were applied as appropriate, with Fisher's LSD post-*hoc* comparisons conducted where the main effect or interaction was significant. The threshold for statistical significance was set at $p < 0.05$. Significance levels are noted as: $*p < 0.05$, $**p < 0.01$, $***p < 0.001$. In the case of multiple comparisons, the absence of asterisks is taken to indicate no significant difference, unless explicitly stated that statistical testing was not performed. Detailed statistical results for each dataset are provided in the corresponding figure legends.

Chapter 3.

Exploring the modulation of striatal 5-HT transmission

3.1 Introduction

3.1.1 Serotonin in striatum

The striatum is a major target of ascending serotonergic input, receiving dense innervation from several midbrain raphe nuclei. In rodents, these inputs predominantly arise from the dorsal raphe nucleus (DRN), with additional projections from the median raphe (MRN) and supralemniscal nucleus (SLN) (Nair et al., 2020). These nuclei originate from distinct developmental rhombomeres and express divergent transcriptional profiles, which likely give rise to functionally heterogeneous serotonergic pathways (Okaty et al., 2015). Mapping studies using immunohistochemistry, retrograde and anterograde tracers, and genetic labelling approaches (e.g., GFP expression in 5-HT neurons) have helped delineate these distinct circuits (Doucet et al., 1986; Muzerelle et al., 2016; Vertes & Crane, 1997).

Importantly, the pattern of 5-HT innervation within the striatum is not uniform. The dorsal striatum receives inputs mainly from the DRN and SLN, while the ventral striatum, including the nucleus accumbens (NAc), receives converging projections from both the DRN and MRN (Kosofsky & Molliver, 1987). Comparative studies have shown that ventral striatal subregions exhibit denser serotonergic innervation than dorsal parts, particularly in the shell region of the NAc (Brown & Molliver, 2000). In primates and humans, these patterns are largely conserved, though with species-specific differences (Parent et al., 2011).

At the cellular and circuit level, 5-HT modulates the activity of both projection neurons and interneurons, thereby influencing striatal output across multiple behaviours- motor control, cognitive flexibility, inhibitory gating, and reward evaluation (Abg Abd Wahab et al., 2019; Carli & Invernizzi, 2014; Lesch & Waider, 2012; Matias et al., 2017). For example, 5-HT has been

shown to activate fast-spiking interneurons in the dorsal striatum, increasing local inhibitory tone (Blomeley & Bracci, 2009).

Finally, disruption of 5-HT signalling within the striatum is implicated in numerous neuropsychiatric and motor disorders, including PD, depression, and obsessive-compulsive disorder (OCD). Although many treatments aim to modulate serotonergic tone pharmacologically, there remains a lack of detailed understanding of how 5-HT operates within striatal microcircuits in real-time.

3.1.2 Evidence of striatal 5-HT regulation

Striatal 5-HT transmission is subject to modulation by multiple neurotransmitter systems, with DA exerting a strong influence. DA and 5-HT share a complex bidirectional relationship within the striatum. DA can suppress 5-HT release via D_2 receptor–mediated mechanisms and reciprocally, 5-HT modulates DA signalling through receptors such as 5-HT_{1B} and 5-HT_{2C}, forming a reciprocal regulatory loop (Di Giovanni et al., 2008; Di Matteo et al., 2008). This interplay helps fine-tune reward-related processes, action selection, and behavioural flexibility.

Recent advances in real-time imaging tools, particularly genetically encoded fluorescent sensors like $GRAB_{5\text{-HT}}$, have revealed that serotonergic release in the striatum is not simply a consequence of DRN activity. In an operant reward task, Liu et al. (2025) demonstrated that 5-HT levels in the dorsomedial striatum dynamically track reward-predictive cues and outcome values, and that these fluctuations occur independently of DRN firing (Liu et al., 2025). This indicates that 5-HT release is tightly regulated at the axonal level within striatal circuits, likely influenced by local modulators such as DA. These findings underscore the importance of local striatal mechanisms in shaping motivational and value-driven behaviours via serotonergic signalling.

Beyond dopaminergic modulation, accumulating evidence suggests that both cholinergic and GABAergic signalling pathways significantly contribute to the regulation of striatal 5-HT release. A recent study using optogenetic activation of ChIs found that synchronous firing of these neurons triggers robust local 5-HT release, and this mechanism is exaggerated in hypercholinergic states such as OCD-like conditions, implicating ChIs as key modulators of striatal serotonergic tone (Matityahu et al., 2024). GABAergic control of striatal monoamine release has also been well documented, particularly in the context of DA. Lopes et al. (2019) demonstrated that blocking $GABA_A$ and $GABA_B$ receptors significantly increased extracellular DA in the striatum, likely by removing tonic inhibitory control over DA axons (Lopes et al., 2019). Since DA influences 5-HT, GABAergic modulation may thus indirectly affect 5-HT release. Therefore, such findings collectively suggest that monoaminergic cross-regulation may represent a universal principle of neuromodulatory control within the striatum.

Additionally, 5-HT clearance is governed by monoamine transporters, primarily the serotonin transporter (SERT) and the DA transporter (DAT). Cocaine, a blocker of SERT, DAT, and NET, leads to increases in extracellular 5-HT levels, demonstrating the importance of transporter-mediated uptake in controlling 5-HT dynamics (Andrews & Lucki, 2001; Carey et al., 2001; Essman et al., 1994; Koe, 1976). Notably, studies have also reported that 5-HT can be taken up into dopaminergic axons via DAT and co-released with DA, further underscoring the functional coupling of these systems (F.-M. Zhou et al., 2005). These findings collectively support a model in which striatal 5-HT release is finely tuned by transporter activity and neuromodulatory inputs, and potentially co-released by DA systems, emphasizing the need to consider multisystem interactions when studying 5-HT function in the striatum.

Given the complex and highly interconnected regulatory landscape of striatal 5-HT signalling, further studies are required to more fully understand its release properties and modulation. This chapter aimed to investigate the local circuit mechanisms that modulate striatal 5-HT release,

using the genetically encoded fluorescent sensor $GRAB_{5\text{-}HT}$. The first hypothesis tested was that $GRAB_{5\text{-}HT}$ selectively reports extracellular 5-HT, rather than DA, in the striatum - a region with dense dopaminergic innervation over 5-HT. Establishing the specificity of this sensor in striatal tissue was essential for interpreting following experiments. Based on this, a second hypothesis was that striatal 5-HT release is dynamically regulated by local cholinergic and GABAergic signalling. Together, these studies define the key local modulatory influences that govern 5-HT signalling in the striatum and provide a validated new approach for monitoring 5-HT release *ex vivo*.

3.2 Methods

3.2.1 Animals and slice preparation

Wild-type C57BL/6J mice (6 - 8 weeks old, mixed sex) were injected with either AAV5-hSyn-5-HT3.0 or AAV9-hSyn-5-HT3.0mut (Brain VTA), as described in Chapter 2, Section 2.3.1. Mice were sacrificed 3 - 4 weeks after injection, and acute *ex vivo* coronal brain slices containing both dorsal and ventral striatum as well as SNr, were prepared as previously described in Section 2.2.2.

3.2.2 Stereotaxic intracranial injections

Mice were allowed to acclimate for at least 7 days prior to surgery. Post-operative supportive care included familiarization with recovery food, provision of soft bedding, and single housing to facilitate health monitoring.

For intracranial virus injections, AAV5-hSyn-GRAB5-HT3.0 (Brain VTA, PT-4724) was diluted by mixing 0.75 µL of virus with 3.25 µL of sterile saline on ice. 6-hydroxydopamine (6-OHDA;

Sigma-Aldrich) lesions were freshly prepared by dissolving 3 mg of powder in 1 mL of ice-cold ascorbic acid solution (3 mg/mL, made from 15 mL sterile saline with 3 mg L-ascorbic acid; Sigma). Desipramine hydrochloride (25 mg/mL in saline; Merck, D3900) was diluted 1:10 prior to intraperitoneal injection. All reagents were kept on ice and protected from light during preparation and use.

Mice were anesthetized with isoflurane (4 - 5% for induction and 1.5 - 2% for maintenance) and placed in a stereotaxic frame. $GRAB_{5\text{-}HT3.0}$ virus was injected bilaterally into the DLS at 240 nL per site using the following coordinates: AP -0.3 mm, ML ±2.5 mm, DV -2.1 mm. For SNc injections, 200 nL of either 6-OHDA (3 µg in 1 µL of ascorbic acid) or ascorbic acid alone was injected unilaterally at AP -3.2 mm, ML ±1.4 mm, DV -4.0 mm. Injections were performed slowly and followed by a 10-minute diffusion period before pipette withdrawal. To protect noradrenergic axons, desipramine (25 mg/kg; 0.3 mL i.p. for a 30 g mouse) was administered 45–60 minutes prior to 6-OHDA injection on the lesion side.

Following surgery, mice received 0.3 mL of Glucosaline subcutaneously. They were placed on a heating mat and monitored until ambulatory. Post-operative care included provision of soft food and hydration sources placed on the cage floor to support recovery. Mice were weighed and assessed twice daily for the first 3 days and then daily for at least one week. Buprenorphine was administered during the first 2 days post-surgery to manage pain.

The method in Section 3.2.2 was provided by Dr. Helen Collins; full procedure details can be found at the following link: https://www.protocols.io/view/intrastriatal-injections-of-ggrab5-ht3-0-virus-and-g5zcby72x.

3.2.3 $GRAB_{5\text{-}HT}$ imaging

For $GRAB_{5\text{-}HT}$ imaging experiments involving electrical stimulation, recordings were conducted as detailed in Chapter 2. The camera was set to an exposure time of 100 ms with 2×2 pixel binning. Excitation was provided by a continuously illuminated blue LED (470 nm) at an intensity of approximately 4 mW for a duration of 40 seconds for each recording, allowing the detection of each 5-HT release event. These acquisition parameters enabled the resolution of individual release events during train stimulations, depending on the off kinetics of the sensor. Data extraction and processing followed the methods described in Chapter 2.

In all experiments involving electrical stimulation, stimulation protocols were performed in duplicate, and the order of stimuli was randomized. Each experimental group included at least four animals ($N \geqslant 4$). Statistical significance was evaluated using two-way ANOVA, Student's t-test, and regression analysis in GraphPad Prism 10.

3.2.4 Immunochemistry and imaging

After completion of ex vivo slice experiments, 300 µm brain slices were fixed in 4% paraformaldehyde (PFA) in phosphate-buffered saline (PBS) for 2–3 days at 4 °C. Slices were then transferred to 30% sucrose in PBS for cryoprotection and storage. Lesioned and sham hemispheres were marked prior to fixation. To validate dopaminergic and serotonergic terminal loss and sensor expression, immunostaining was performed for tyrosine hydroxylase (TH), serotonin transporter (SERT), and green fluorescent protein (GFP, to enhance gGRAB5-HT3.0 signal). Slices were washed in PBS and PBS-T (0.3% Triton X-100, 0.05% sodium azide in PBS), then incubated overnight at room temperature with the following primary antibodies diluted 1:1000 in PBS-T with 1% normal donkey serum (NDS): anti-TH (Guinea pig, Synaptic Systems, #213 104), anti-SERT (Rabbit, Synaptic Systems, #340 003), anti-GFP (Chicken, Aves Labs, #GFP-1020). The next day, slices were washed again and incubated for 4 hours at room temperature in the dark with secondary antibodies (1:1000 in PBS-T + 1% NDS): Cy3

donkey anti-rabbit IgG (Jackson ImmunoResearch, #706-165-148), Cy5 donkey anti-guinea pig IgG (Jackson ImmunoResearch, #711-175-152), Alexa Fluor 488 donkey anti-chicken IgY (Jackson ImmunoResearch, #703-545-155). After final washes in PBS, slices were mounted onto labelled glass slides, dried briefly, and cover-slipped using VECTASHIELD® antifade mounting medium (Vector Laboratories, #H-1000). Slides were sealed with clear nail varnish and stored at 4 °C in the dark until imaging. Full procedural details can be found at the following link: https://www.protocols.io/view/immunohistochemical-validation-of-ggrab5-ht3-0-sen-g53sby8nf.

3.2.5 Drugs

Drugs were diluted in either dH_2O or DMSO (dymethl sulfoxide) to 1,000x stock aliquots and stored at -20 °C. Final drug concentrations were prepared in aCSF saturated with 95% O_2/ 5% CO_2 right before use.

Drug	Supplier	Action	Concentration	Solvent	References
Dihydro-β-erythroidine (DHβE) hydrobromide	Sigma-Aldrich	nAChR antagonist	1 µM	dH_2O	Threlfell et al. (2012); Roberts et al. (2020)
RS 23597-190	Tocris	5-HT_4R antagonist	100 µM	DMSO	Eglen et al. (1993) Deng et al. (2024)
Tetrodotoxin (TTX)	Bio-Techne	Na^+ channel blocker	1 µM	DMSO	Threlfell et al. (2012)
Cocaine hydrochloride	Sigma-Aldrich	DAT, SERT, NET	5 µM	dH_2O	Condon et al. (2020); Threlfell et al. (2021)
Citalopram hydrobromide	Sigma-Aldrich	SSRI	75 nM	DMSO	Stenfors et al. (2001)
Nomifensine maleate	Sigma-Aldrich	DAT inhibitor	2 µM	Hydrochloric acid (HCl)	Condon et al. (2019); Threlfell et al. (2021)
Sumatriptan succinate	Bio-Techne	5-$HT_{1B/1D}$R antagonist	1 µM	dH_2O	Pierce et al. (1996)

Oxotremorine-M	Tocris	mAChR agonist	5 µM	dH_2O	Threlfell et al. (2010)
(+)-Bicuculline	Abcam	$GABA_AR$ antagonist	10 µM	DMSO	Roberts et al. (2020); Stedehouder et al. (2024)
CGP 55845 hydrochloride	Abcam	$GABA_B$-R antagonist	4 µM	DMSO	Roberts et al. (2020); Stedehouder et al. (2024)

3.3 Results

3.3.1 Properties of the 5-HT signal measured with $GRAB_{5\text{-}HT}$ sensors in striatum

The structural similarity and anatomical overlap of DA and 5-HT can make it challenging to detect 5-HT, especially in DA-rich brain regions, without confounding detection of DA. Classic detection methods such as microdialysis and fast-scan cyclic voltammetry (FCV) can face challenges in separately detecting 5-HT from DA with either sufficient high spatiotemporal resolution, specificity or sensitivity. In the striatum, where DA is abundant, the regional varicosity density for 5-HT axons in rat striatum is documented as 2.8-10% of the density of DA varicosities (Descarries et al., 1990; Doucet et al., 1986; Mrini et al., 1995) and striatal tissue content of DA is 20-fold higher than 5-HT (De Deurwaerdère & Di Giovanni, 2017). We assume that the monoamine signal detected by FCV in the DLS has a negligible contribution from 5-HT. However, a newly developed florescent sensor $GRAB_{5\text{-}HT3.0}$ offers a potentially powerful method for monitoring 5-HT dynamics in real time. The $GRAB_{5\text{-}HT}$ sensor has excellent cell surface trafficking, high specificity, sensitivity, and spatiotemporal resolution, as well as rapid kinetics making it suitable for monitoring 5-HT dynamics *in vivo* (Deng et al., 2024). Evidence has shown that the GRAB5-$HT_{3.0}$ sensor has high specificity and sensitivity to 5-HT compared with DA and

other neurotransmitters tested in cultured rat cortical neurons (Deng et al., 2024). Based on this, I first explored the properties of $GRAB_{5\text{-}HT3.0}$ in striatum acute brain slices.

To verify the expression pattern of $GRAB_{5\text{-}HT3.0}$ sensors following viral injection into the DLS, immunofluorescence staining was performed on brain slices containing the DLS and SNr, as described in the Methods. Representative fluorescence images revealed robust GFP signal in the DLS, corresponding to GRAB expression that was detected via its GFP tag (Deng et al., 2024), and this signal co-localised with the 5-HT transporter (SERT) (**Fig. 3.1**). Notably, GFP signal was also detected in the substantia nigra pars reticulata (SNr) (**Fig. 3.1**), a non-injected region but one receiving dense 5-HT innervation from raphe (Corvaja et al., 1993; Van Der Kooy & Hattori, 1980; Wirtshafter & McWilliams, 1987) as well as striatonigral afferents from the injected regions of striatum. This expression is presumed to result from retrograde trafficking of the $GRAB_{5\text{-}HT}$ sensor from the DLS injection site. These findings confirmed detectable expression of $GRAB_{5\text{-}HT}$ sensors in the striatum.

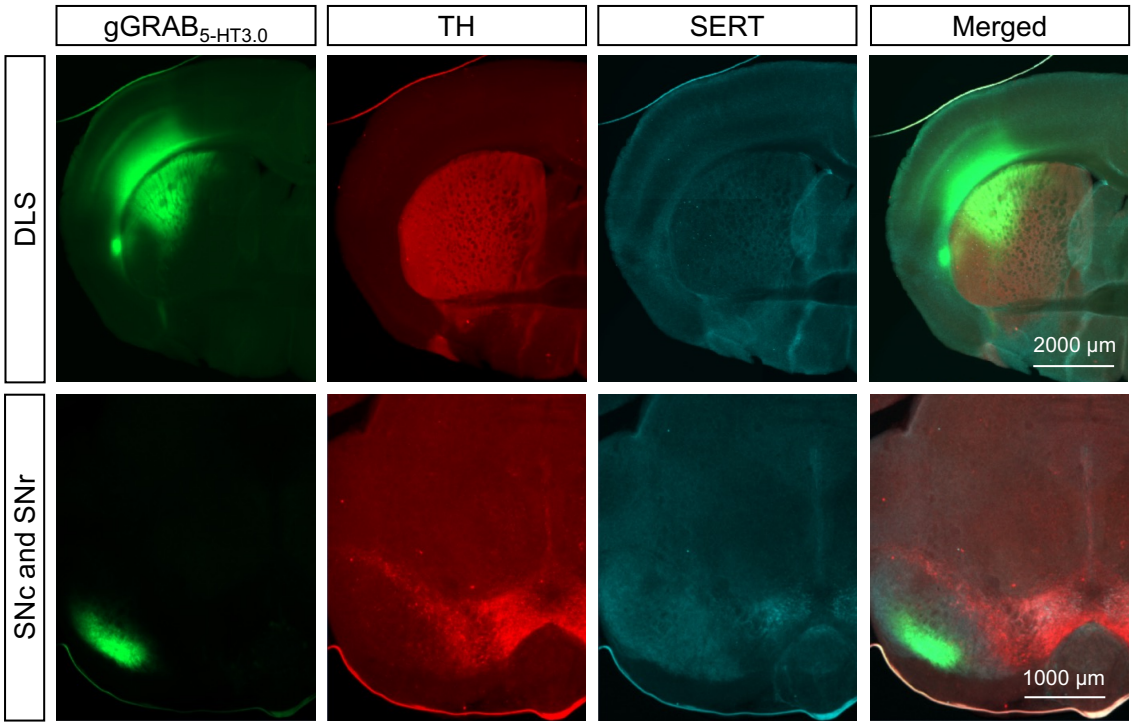

Figure 3.1. Expression of GRAB$_{5\text{-HT}}$ sensor following viral injection into the DLS. Representative fluorescence image showing GRAB$_{5\text{-HT}}$ expression (GFP, green) in the dorsal lateral striatum (DLS, top) and substantia nigra pars reticulata (SNr, bottom). Co-localised with tyrosine hydroxylase (TH, red) and the 5-HT transporter (SERT, cyan). Scale bar = 2000 µm (DLS), 1000 µm (SNr). Images were acquired by Dr. Helen Collins.

After confirming detectable expression of GRAB$_{5\text{-HT}}$ sensor in the striatum, I next evaluated their performance in acute brain slices. GRAB$_{5\text{-HT}}$ was bilaterally injected into either DLS or NAcC and following a three-week expression period, acute striatal slices were prepared, and electrical stimulation was delivered locally to evoke 5-HT release (**Fig. 3.2A**). The fluorescence change ($\Delta F/F_0$) upon each stimulation was recorded as the indicator of $[5\text{-HT}]_o$ dynamics.

First, signal stability of the sensor was assessed over a standard experimental time window (~40 min). Both the evoked peak amplitude ($\Delta F/F_0$) and baseline F_0 remained relatively stable, showing only a mild reduction of ~5% after 40 min (**Fig. 3.2B**). We speculate that the small

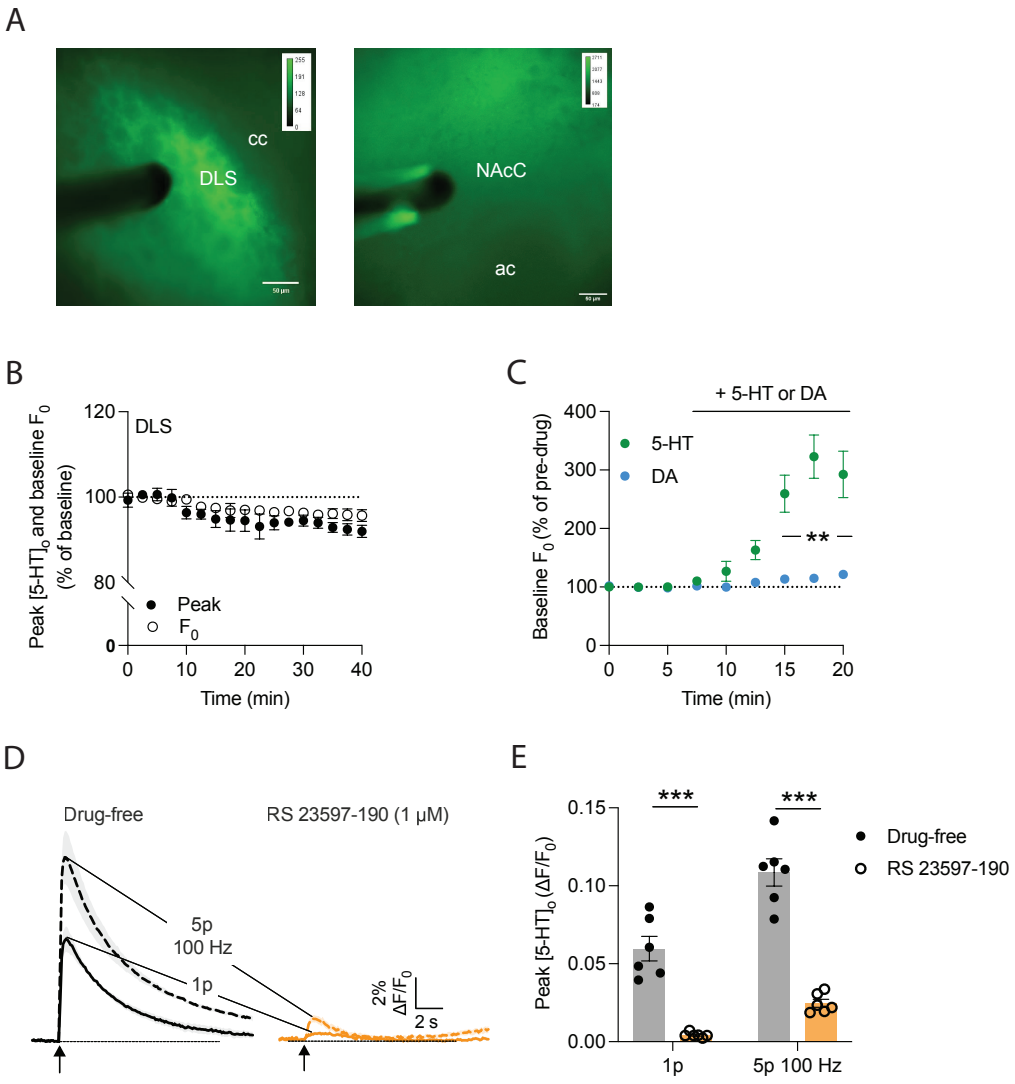

Figure 3.2. Striatal 5-HT signal measured with GRAB$_{5\text{-HT}}$ is not respond to DA and can be abolished by 5-HT$_4$R antagonist. (A) Fluorescence images showing GRAB$_{5\text{-HT}}$ expression (green) in DLS. Scale bar indicates 50 µm. **(B)** Normalized mean peak [5-HT]$_o$ and baseline fluorescence (F_0) ± SEM during consecutive 40 min recordings of 5-HT release evoked by 1p (*n* = 6 experiments/5 mice). **(C)** Normalized mean baseline fluorescence (F_0) ± SEM during the application of 10 µM 5-HT (green) or DA (blue) in DLS (*n* = 5 experiments/3 mice each). **(D)** Mean evoked 5-HT transients ± SEM, before (black) and after (orange) application of 100 µM RS 23597-190 in DLS (*n* = 6 experiments/3 mice). **(E)** Mean 1p and 5p 100 Hz [5-HT]$_o$ peak of drug-free conditions (black) and following RS 23597-190 application (orange) in DLS. 2-way ANOVA, Fisher's LSD post-*hoc* test, Student's unpaired t-test; $^{**}p < 0.005$, $^{***}p < 0.001$. Error bars are ± SEM.

decline in baseline F_0 was due to gradual photobleaching, while the reduction in evoked peak amplitude likely reflected a mild deterioration in vesicle pool, or slice health over time.

Next, the specificity of the $GRAB_{5\text{-}HT}$ sensor was examined by washing on either 10 μM 5-HT or 10 μM DA. As expected, bath application of 5-HT caused a robust elevation of baseline F_0, to ~300% of pre-drug levels, whereas DA had no detectable effect on fluorescence intensity (**Fig. 3.2C**; $t_{(8)} = 4.317$, $p = 0.0026$; Student's unpaired t-test). This result confirmed that the $GRAB_{5\text{-}HT}$ sensor responds selectively to extracellular 5-HT, with no cross-reactivity to DA, despite the high DA concentration in the striatum. However, we note that this does not fully rule out the possibility of sensitivity to endogenous DA, as applied DA will be rapidly cleared via the highly efficient DAT system. Therefore, further tests on the specificity of $GRAB_{5\text{-}HT}$ sensor are presented later in this chapter.

Since the $GRAB_{5\text{-}HT3.0}$ sensor was engineered based on the $5\text{-}HT_4$ receptor (Deng et al., 2024), its changes in fluorescence should be specific to activity at the $5\text{-}HT_4R$ and not artefacts due to other non-specific effects of stimulation. I therefore tested whether its signal could be blocked by a $5\text{-}HT_4R$ antagonist (Deng et al., 2024; Eglen et al., 1993), almost completely abolished the evoked 5-HT signal (**Fig. 3.2D-E**). This confirmed that the fluorescence signal is specifically mediated by binding to the $5\text{-}HT_4R$ of the sensor.

To further confirm that the $GRAB_{5\text{-}HT}$ signal is not an artefact, e.g. an evoked pH change, we used a mutated version of the sensor, $GRAB_{5\text{-}HT3.0mut}$, which has the same structure as $GRAB_{5\text{-}HT3.0}$ but lacks the ability to bind 5-HT (Deng et al., 2024). In the same way, I injected $GRAB_{5\text{-}HT3.0mut}$ sensor into the striatum as with $GRAB_{5\text{-}HT3.0}$. In acute slices prepared from these animals, I applied the same electrical stimulation protocols to evoke 5-HT release. No measurable evoked signal was detected in slices expressing the mutant sensor (**Fig. 3.3A-B**). Moreover, bath application of 10 μM 5-HT did not alter either the peak response or baseline F_0 in $GRAB_{5\text{-}HT3.0mut}$-expressing slices (**Fig. 3.3B-C**). These results confirm that the fluorescence signal observed with $GRAB_{5\text{-}HT3.0}$ is specifically dependent on ligand binding to the functional sensor, and not due to electrical stimulation artefacts or nonspecific changes in fluorescence.

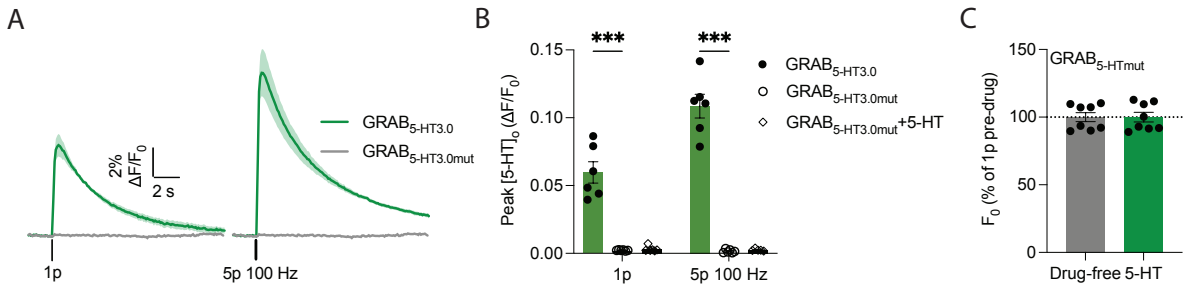

Figure 3.3. GAB5-HT$_{3.0mut}$ does not respond to electrical stimulations and external 5-HT. **(A)** Mean 1p and 5p 100 Hz evoked 5-HT transients ± SEM reported by GRAB$_{5\text{-}HT3.0}$ (green) or GRAB$_{5\text{-}HT3.0mut}$ (grey) in DLS (*n* = 4 experiments/3 mice). **(B)** Mean 1p and 5p at 100 Hz [5-HT]$_o$ peak reported by GRAB$_{5\text{-}HT3.0}$ (green) or GRAB5-HT$_{3.0mut}$ (grey) before and after the application of 10 µM 5-HT in DLS. **(C)** Normalized mean baseline fluorescence (F_0) ± SEM before (grey) and after (green) the application of 10 µM 5-HT in DLS (*n* = 8 experiments/3 mice). 2-way ANOVA, Fisher's LSD post-*hoc* test; ***$p < 0.001$. Error bars are ± SEM.

Together, these results demonstrate that GRAB$_{5\text{-}HT}$ is a reliable and selective tool for monitoring extracellular 5-HT dynamics in striatal slices, with minimal interference from DA.

Next, to determine whether the 5-HT signals detected by GRAB$_{5\text{-}HT3.0}$ sensors were action potential (AP)-dependent, I applied tetrodotoxin (TTX, 1 µM), a voltage-gated Na^+ channel blocker that abolishes AP generation. Application of TTX completely abolished electrically-evoked 5-HT release in DLS, indicating that the observed 5-HT transients were AP-dependent (**Fig. 3.4A-C**; $F_{(1,16)} = 36.86$, $p < 0.001$, RM ANOVA main effect of the drug; *n* = 5 slices from *N* = 3 mice). Baseline fluorescence (F_0) remained unchanged following TTX treatment (**Fig. 3.4A**), suggesting that GRAB$_{5\text{-}HT}$ expression and sensor stability were unaffected by blockade of Na^+ activity.

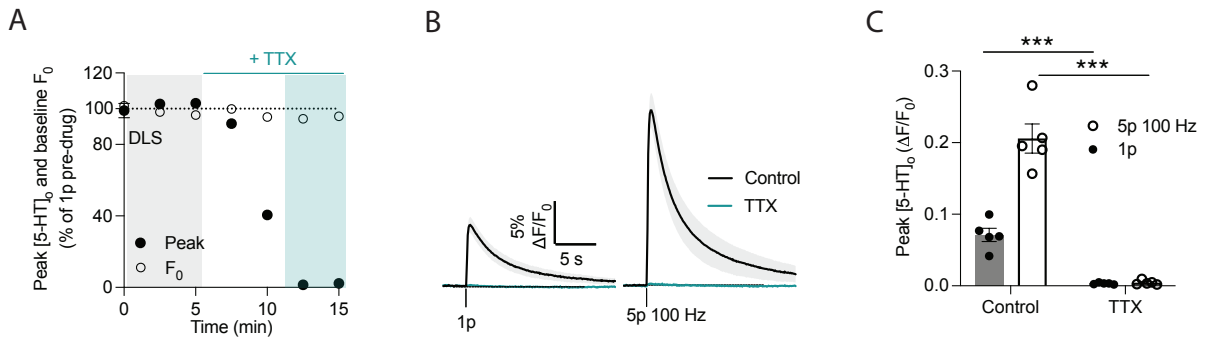

Figure 3.4. TTX abolished evoked 5-HT signal in DLS. (A) Normalized mean peak $[5\text{-HT}]_o$ and baseline fluorescence (F_0) ± SEM during consecutive 15 min recordings of 5-HT release evoked by 1p (*n* = 5 experiments/3 mice). **(B)** Mean evoked 5-HT transients ± SEM, before (black) and after (cyan) application of 1 µM TTX in DLS. Mean transients of $[5\text{-HT}]_o$ are derived from three timepoints prior to the application of TTX (grey shaded region) and last two timepoints (green shaded region). **(C)** Mean 1p and 5p 100 Hz $[5\text{-HT}]_o$ peak of control conditions and following TTX application in DLS (*n* = 5 experiments/3 mice). 2-way ANOVA, Fisher's LSD post-*hoc* test; ****p* < 0.001. Error bars are ± SEM.

3.3.2 Specificity of $GRAB_{5\text{-}HT}$ sensor in reporting 5-HT signals in a DA-dominated brain region – the striatum

As described above, it is crucial to confirm whether $GRAB_{5\text{-}HT3.0}$ can still maintain its high specificity to 5-HT in a DA-dominated brain region. Therefore, I employed a 6-hydroxydopamine (6-OHDA) lesion model to examine whether destruction of DA axons affects the $GRAB_{5\text{-}HT}$ signal. The underlying hypothesis was that if $GRAB_{5\text{-}HT}$ in the striatum predominantly reports 5-HT rather than DA, the $GRAB_{5\text{-}HT}$ signal should not be reduced by a DA lesion.

To achieve unilateral dopaminergic depletion, 6-OHDA was injected unilaterally into the SNc, while the contralateral SNc was injected with vehicle (ascorbic acid) as an internal control. In the same animals, 200 nL of the $GRAB_{5\text{-}HT}$ virus was also bilaterally injected into the DLS (**Fig. 3.5A**). After a three-week incubation period to allow for sufficient viral expression and lesion stabilization, acute striatal and midbrain slices were prepared. $GRAB_{5\text{-}HT}$ imaging was then

performed to monitor evoked 5-HT fluorescence responses on both sides, while FCV was used in parallel to verify changes in DA signals between the lesioned and non-lesioned sides.

We found that the 6-OHDA lesion resulted in a robust reduction of evoked extracellular DA concentrations ($[DA]_o$) in the lesioned hemisphere, with $[DA]_o$ reduced by ~70%, compared to the non-lesioned side (**Fig. 3.5B**). Specifically, $[DA]_o$ evoked by 1p or by a train of 5p at 100 Hz showed markedly attenuated peak amplitudes on the lesioned side, confirming a DA release deficit in the DLS (**Fig. 3.5D-E**). In contrast, $GRAB_{5\text{-}HT}$ fluorescence responses were preserved, with no significant difference in evoked signals between the lesioned and non-lesioned sides (**Fig. 3.5C**). 5-HT release and its short-term plasticity seemed unaffected by the loss of DA input (**Fig 3.5F-G**). Together, these findings suggest that the $GRAB_{5\text{-}HT}$ sensor predominantly reports 5-HT dynamics in DLS and is not substantially influenced by DA depletion.

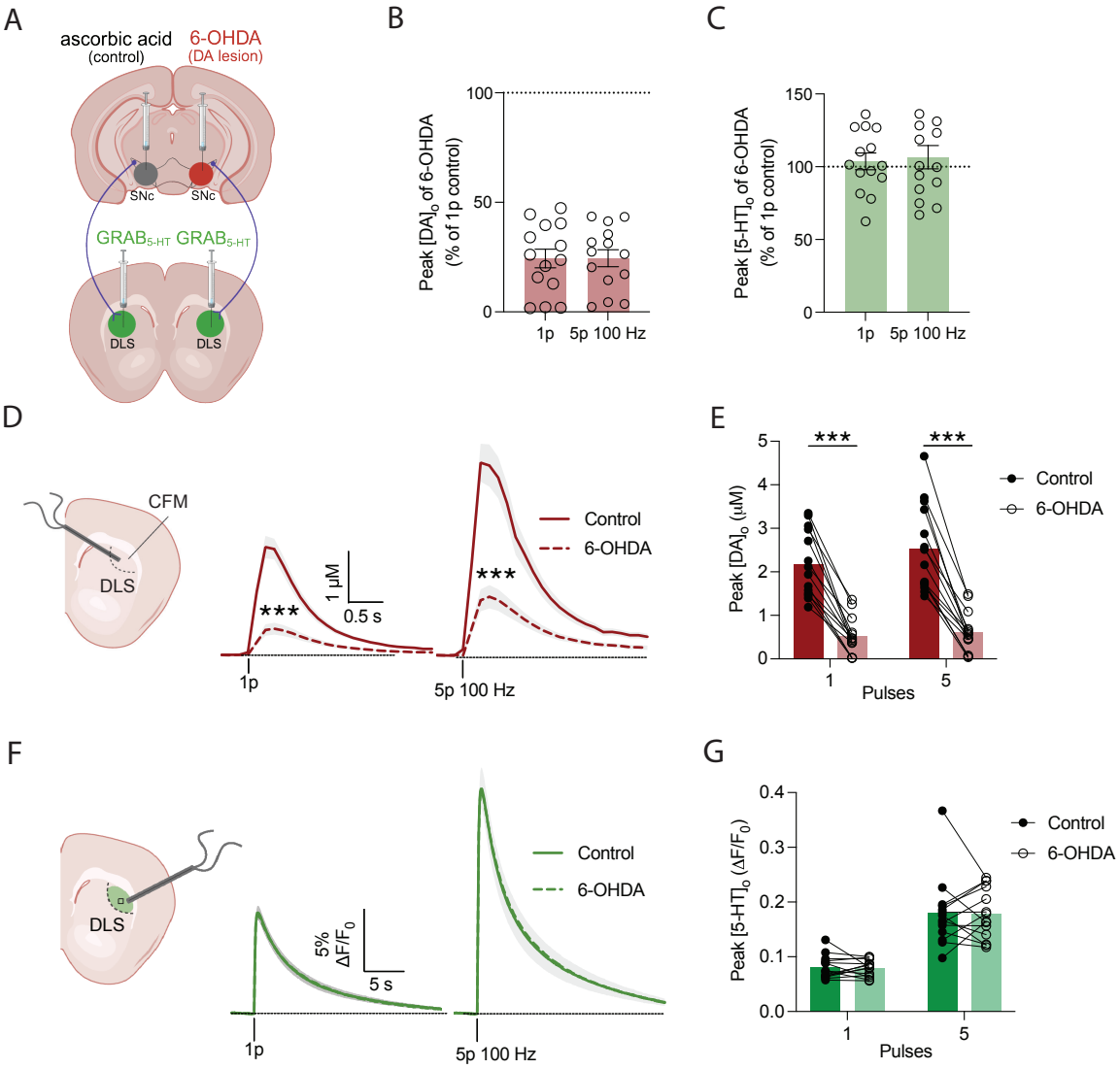

Figure 3.5. 6-OHDA induces unilateral DA depletion without affecting GRAB5-HT signalling. **(A)** Schematic of bilateral injection of $GRAB_{5\text{-}HT}$ into DLS, and unilateral injection of 6-OHDA or ascorbic acid (vehicle control) into SNc. **(B)** Normalized peak $[DA]_o$ evoked by 1p and 5p 100 Hz stimulation on the lesioned side, expressed as a percentage of the contralateral control side (set at 100%) in the DLS (*n* = 14 slices in 6 animals). **(C)** Normalized peak $[5\text{-HT}]_o$ evoked by 1p and 5p 100 Hz stimulation on the lesioned side, expressed as a percentage of the contralateral control side (set at 100%) in the DLS (*n* = 14 slices in 6 animals). **(D)** Schematic of the DA recording site and 1p and 5p 100 Hz evoked DA transients on the control (solid line) and lesioned (dashed line) sides (*n* = 14 slices in 6 animals). **(E)** Mean 1p and 5p 100Hz $[DA]_o$ peak ± SEM of the control side (solid dots) and the 6-OHDA lesion side (hollow dots) in DLS (*n* = 14 slices in 6 animals). **(F)** Schematic of GRAB5-HT recording site and mean 1p and 5p 100 Hz evoked 5-HT transients ± SEM, on the control (solid line) and lesion (dashed line) side. **(G)** Mean 1p and 5p 100Hz $[5\text{-HT}]_o$ peak ± SEM of the control side (solid dots) and the 6-OHDA lesion side (hollow dots) in DLS (*n* = 14 slices in 6 animals). 2-way ANOVA, Fisher's LSD post-hoc test; ***$p < 0.001$. Error bars are ± SEM.

To investigate potential local heterogeneity in lesion efficacy and monoamine dynamics, I quantified $[DA]_o$ and $[5\text{-}HT]_o$ of each recording site within the DLS, targeting three locations (sites a-c) spanning the medial-lateral axis (**Fig. 3.6A**). I measured evoked $[DA]_o$ and $[5\text{-}HT]_o$ at each site using FCV and $GRAB_{5\text{-}HT}$ imaging, respectively. The measurements of striatal DA and 5-HT were performed in random order, with recordings alternated between the lesion and control sides at sites a, b, and c within the same slice to minimize potential confounds from slice health or recording sequence.

Across all three sites, DA signals were significantly reduced on the lesioned side compared to the control hemisphere (**Fig. 3.6B,E,H**), confirming successful 6-OHDA-induced depletion. While evoked $[DA]_o$ at all sites decreased to approximately 30% of control levels, site b showed a slightly greater reduction, suggesting this region may have undergone a more extensive lesion (**Fig. 3.6E,G)**. Despite this variability in DA loss, 5-HT signals were comparable across all sites, with no significant difference observed between lesion and control sides (**Fig. 3.6C,F,I**). These findings indicate that ~70% loss of evoked $[DA]_o$, presumably due to DA denervation, across DLS subregions does not impact 5-HT release (**Fig. 3.6D,G,J**), further supporting the specificity of the $GRAB_{5\text{-}HT}$ sensor for reporting 5-HT dynamics in a DA-abundant brain region - the striatum.

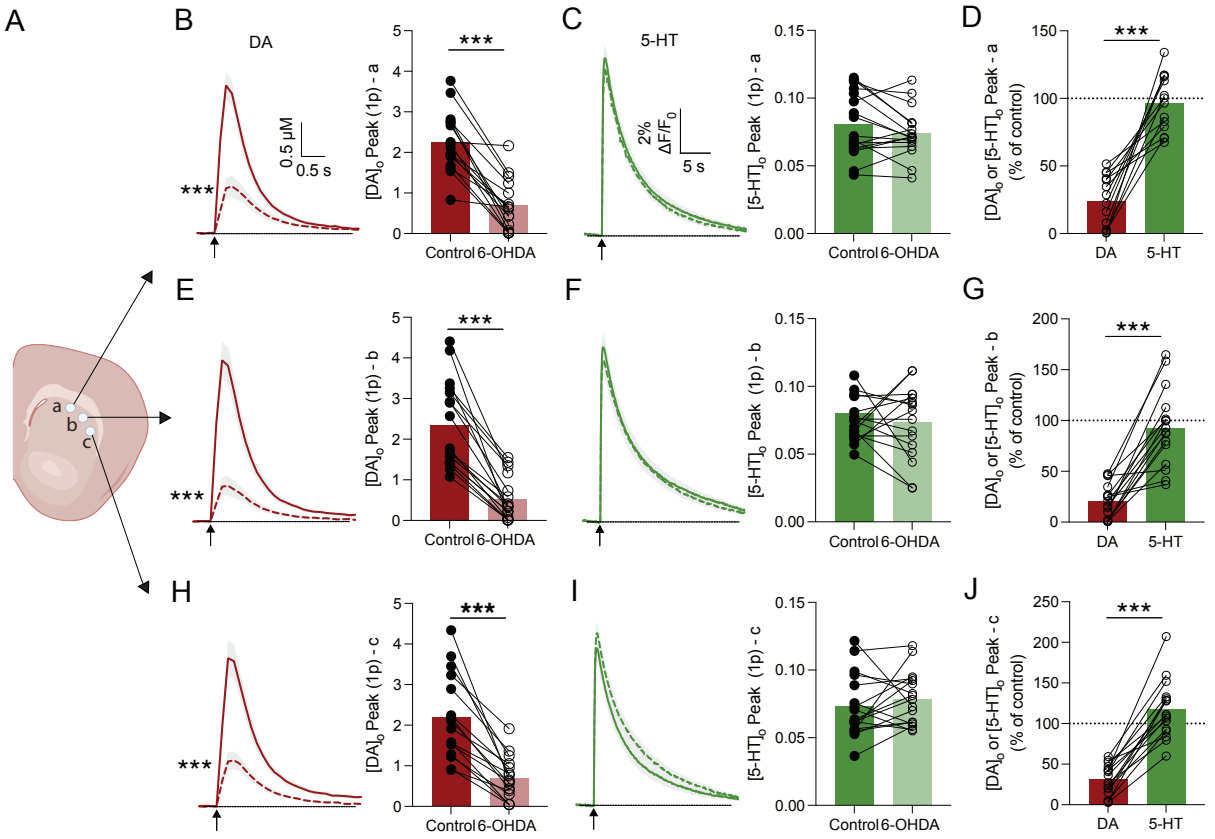

Figure 3.6. Multisite recording of $[DA]_o$ and $[5\text{-}HT]_o$ in the unilateral 6-OHDA animal model. **(A)** Schematic of three recording sites - a, b and c - across DLS. **(B,E,H)** Left: Mean 1p-evoked DA transients ± SEM from the control hemisphere (solid line) and 6-OHDA lesion hemisphere (dashed line) in DLS at recording sites a (B), b (E), and c (H). Right: Mean 1p-evoked peak of $[DA]_o$ ± SEM from the control hemisphere (solid dots) and 6-OHDA lesion hemisphere (hollow dots) in DLS at recording sites a (B), b (E), and c (H). **(C,F,I)** Left: Mean 1p-evoked 5-HT transients ± SEM from the control hemisphere (solid line) and 6-OHDA lesion hemisphere (dashed line) in DLS at recording sites a (C), b (F), and c (I). Right: Mean 1p-evoked peak of $[5\text{-}HT]_o$ ± SEM from the control hemisphere (solid dots) and 6-OHDA lesion hemisphere (hollow dots) in DLS at recording sites a (C), b (F), and c (I). **(D,G,J)** Normalised mean $[DA]_o$ (red) and $[5\text{-}HT]_o$ (green) peak ± SEM of its control hemisphere in DLS at recording sites a (D), b (G), and c (J). *n* = 14 slices in *N* = 6 animals. Student's paired t-test, ***$p < 0.001$. Error bars are ± SEM.

To confirm the DA lesion, we performed immunofluorescence staining after recording. Slices were fixed and labelled with antibodies against GFP (to visualize $GRAB_{5\text{-}HT}$ expression), tyrosine hydroxylase (TH, to mark DA axons), and the serotonin transporter (SERT, to identify 5-HT axons). In each slice, we observed a significant reduction in TH-immunoreactivity in the hemisphere corresponding to the 6-OHDA injection (**Fig. 3.7**; right hemisphere), confirming

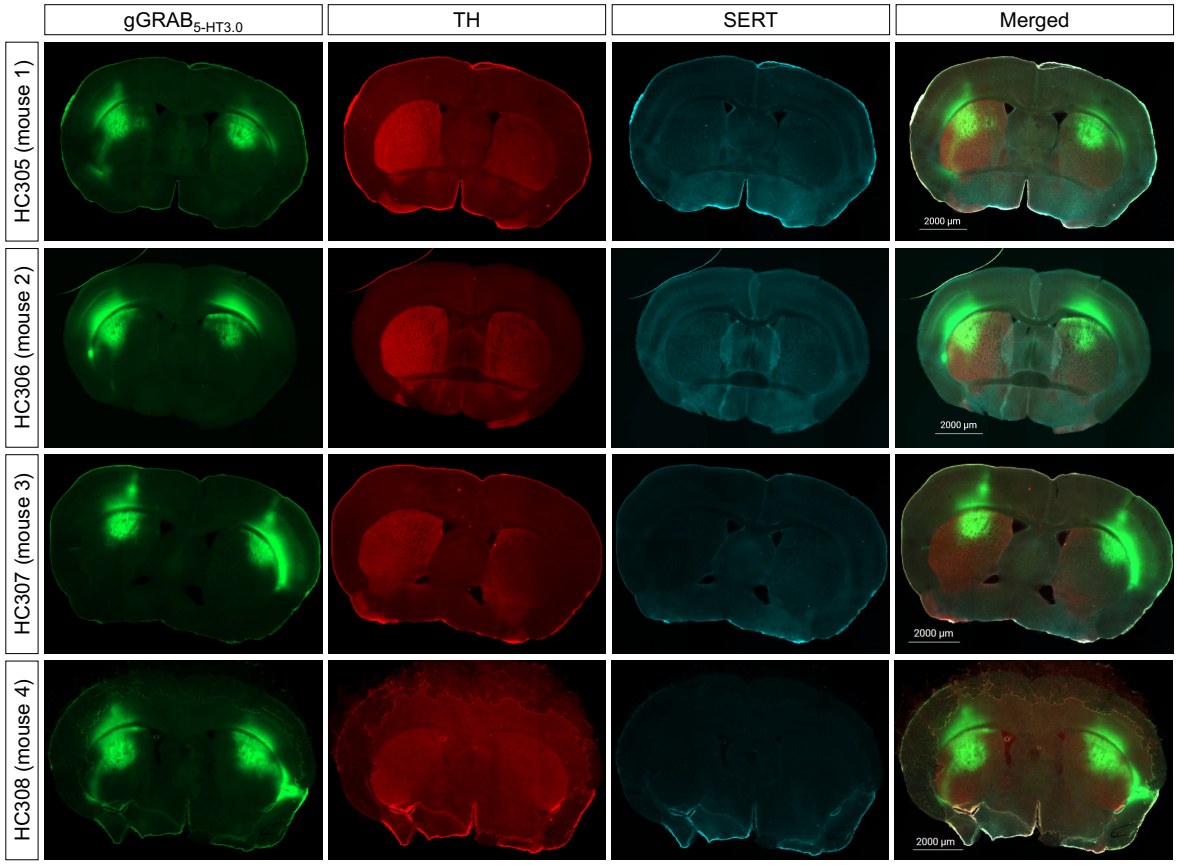

Figure 3.7. Immunostaining of GFP, TH, and SERT in striatal slices following unilateral 6-OHDA lesion. Coronal striatal sections from four mice (mouse 1-4) showing labelling of GFP (green), TH (red), and SERT (cyan). $GRAB_{5\text{-}HT3.0}$ was bilaterally injected into the DLS, and 6-OHDA was unilaterally injected into the SNc. The right hemisphere represents the 6-OHDA lesion side, while the left hemisphere was injected with ascorbic acid as control. Scale bar = 2000 µm. Immunostaining and image acquisition by Dr. Helen Collins.

effective DA axon loss. In contrast, the expression patterns of both $GRAB_{5\text{-}HT}$ (GFP) and SERT appeared comparable between hemispheres, with no obvious change following DA lesion (**Fig. 3.7**).

Together, these results indicate that the unilateral 6-OHDA lesion successfully depleted dopaminergic input in the DLS, without affecting 5-HT release or its anatomical distribution, further supporting the specificity of $GRAB_{5\text{-}HT}$ for monitoring striatal 5-HT dynamics.

Given our earlier observation that $GRAB_{5\text{-}HT3.0}$ expression injected into the DLS is trafficked to downstream projection areas, including the SNr, we next examined whether unilateral dopaminergic lesion affected 5-HT dynamics in the SNr as a further means to validate detected signals as 5-HT. Using $GRAB_{5\text{-}HT}$ imaging, we compared evoked 5-HT signals between the lesion and control hemispheres in the SNr (**Fig. 3.8A**). Consistent with our findings in the DLS, we observed no significant difference in peak or area under the curve (AUC) of 5-HT responses between hemispheres, regardless of stimulation paradigm - 1p or 5p at 100 Hz (**Fig. 3.8B-D**). 5-HT levels remained comparable across both sides, suggesting that 6-OHDA-induced dopaminergic depletion in the SNc does not impact serotonergic transmission in the SNr. These results further support the conclusion that $GRAB_{5\text{-}HT}$ selectively reports 5-HT dynamics and is not confounded by DA loss.

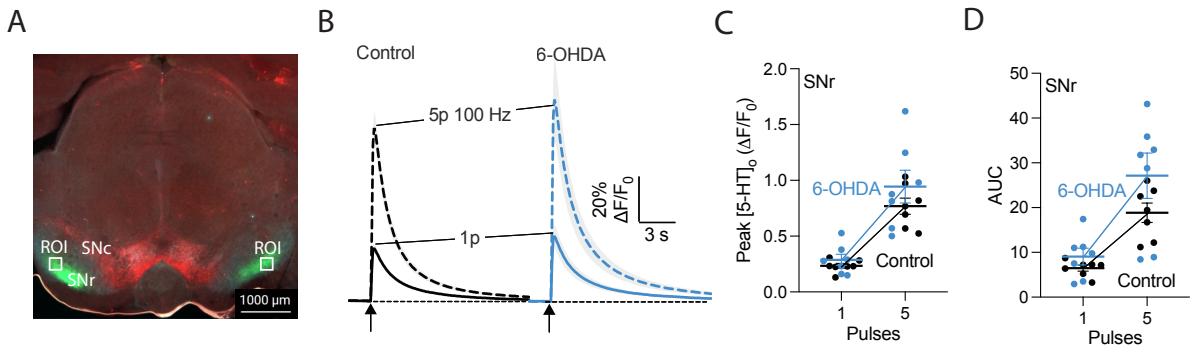

Figure 3.8. $[5\text{-HT}]_o$ release in SNr in an unilateral 6-OHDA animal model. (A) Recording sites (ROI) of 5-HT reported by $GRAB_{5\text{-}HT}$ in SNr. Scale bar = 1000 µM. **(B)** Mean evoked 5-HT transients ± SEM, of the control (black) and 6-OHDA lesion (blue) side in SNr (*n* = 7 experiments/4 mice). **(C)** Mean 1p and 5p 100 Hz $[5\text{-HT}]_o$ peak of the control (black) and 6-OHDA lesion (blue) side in SNr (*n* = 7 experiments/4 mice). **(D)** Mean 1p and 5p 100 Hz $[5\text{-HT}]_o$ AUC of the control (black) and 6-OHDA lesion (blue) side in SNr. 2-way ANOVA, Fisher's LSD post-*hoc* test. Error bars are ± SEM. Picture in (A) was taken by Dr. Helen Collins.

3.3.3 5-HT transmission comparison across DLS, NAcC and SNr

The development of the $GRAB_{5\text{-}HT}$ sensor enabled us to investigate striatal 5-HT transmission with higher temporal resolution compared to microdialysis. Building on my characterization of

the sensor as a reliable tool for detecting striatal 5-HT signals, I next compared the dynamics of 5-HT transmission between the dorsal and ventral striatum under drug-free conditions. As described in the Methods section, $GRAB_{5\text{-}HT}$ sensor was injected into the DLS and NAcC of mice. After a three-week incubation period, acute striatal brain slices were prepared. Using an identical stimulation protocol, we evoked 5-HT release and analyzed the resulting fluorescence transients. Several parameters were used to compare 5-HT dynamics across regions: peak amplitude, the 5p:1p ratio, AUC, and decay half-life.

First, we found that peak $[5\text{-HT}]_o$ in NAcC was consistently higher than in DLS following either 1p or 5p (100 Hz) stimulation (**Fig. 3.9A-B;** $F_{(1,52)} = 11.40$, $p = 0.001$, RM ANOVA main effect of the region; $n = 19$ slices in DLS and $n = 9$ slices from NAcC), indicating that 5-HT release in the ventral striatum is greater than that in the dorsal striatum regardless of stimulation strength. Next, we examined 5-HT reuptake dynamics. Interestingly, despite higher peak levels, the AUC in NAcC was significantly lower compared to the DLS (**Fig. 3.9C;** $t_{(24)} = 2.108$, $p = 0.0457$, Student's unpaired t-test), suggesting faster clearance of extracellular 5-HT in the ventral striatum. Consistent with this, a fit of the decay phase of each transient with a single-exponential curve to extract the decay half-life indicated a significantly shorter half-life in the NAcC than in the DLS (**Fig. 3.9D**; $F_{(1,52)} = 7.496$, $p = 0.008$, RM ANOVA main effect of the region). Next, we compared the 5p:1p ratio, which reflects aspects of local microcircuitry and short-term plasticity. We found that the 5p:1p ratio was much lower than 5 in both regions indicating significant short-term depression of release. This ratio was significantly lower in the DLS compared to the NAc (**Fig. 3.9E**; $t_{(20)} = 3.552$, $p = 0.0020$, Student's unpaired t-test), indicating that 5-HT release in the dorsal striatum is more strongly depressed during rapid pulse trains, likely partially due to greater nAChR-mediated inhibition.

To corroborate that evoked $[5\text{-HT}]_o$ signals reflect serotonergic innervation, we performed immunostaining on WT striatal slices using a 5-HT antibody (Immunostar anti-5-HT rabbit, AB

572263) to visualise and quantify the density of 5-HT-positive fibres (**Fig. 3.9F**). Fluorescence images of DLS and NAcC were captured under identical imaging conditions and quantified using a fixed threshold (200-255). Consistent with the release and re-uptake rate data, the 5-HT innervation density was significantly higher in NAcC than in the DLS (**Fig. 3.9G;** $t_{(17)} = 5.926$, $p < 0.001$, Student's paired *t*-test).

Overall, these results demonstrate that 5-HT release in ventral striatum reaches more elevated $[5\text{-HT}]_o$ in NAc than dorsal striatum. Specifically, 5-HT release in the NAcC is greater in magnitude and exhibits faster clearance kinetics compared to the DLS. These differences are consistent with our immunohistochemical findings showing there is higher 5-HT innervation in NAcC than in DLS.

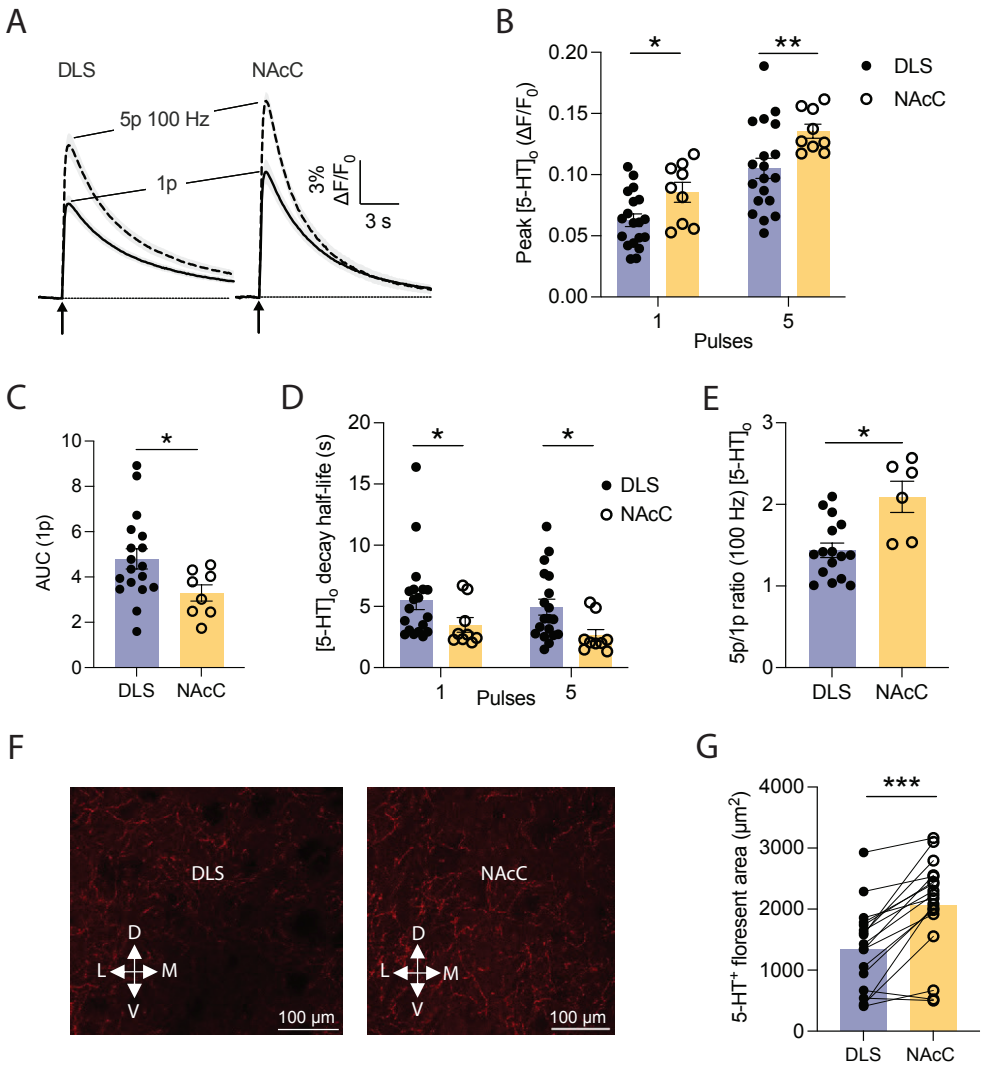

Figure 3.9. Comparison of 5-HT release in dorsal and ventral striatum. (A) Mean 1p (solid line) and 5p 100 Hz (dashed line) evoked 5-HT transients ± SEM in DLS (left) and NAcC (right) (DLS: *n* = 16 slices in 7 mice; NAcC: *n* = 6 slices in 3 mice). **(B)** Mean 1p and 5p at 100 Hz $[5\text{-HT}]_o$ peak in DLS (blue) and NAcC (yellow). **(C)** Mean 1p evoked $[5\text{-HT}]_o$ AUC in DLS (blue) and NAcC (yellow). **(D)** Ratios of peak $[5\text{-HT}]_o$ released by 5p 100 Hz versus 1p in DLS (blue) and NAcC (yellow). **(E)** Decay half-life of 1p and 5p 100 Hz evoked $[5\text{-HT}]_o$ in DLS (blue) and NAcC (yellow). **(F)** Immunofluorescence of labelling 5-HT in DLS (left) and NAcC (right). Scale bar indicates 100 µm. **(G)** Quantification of 5-HT innervation as indicated by 5-HT^+ florescent area (μm^2) in DLS (blue) and NAcC (yellow). Student's unpaired t-test, 2-way ANOVA, Fisher's LSD post-*hoc* test, $^*p < 0.05$, $^{**}p < 0.01$, $^{***}p < 0.0001$. Error bars are ± SEM. Images in (F) were taken by Wenhui Wu.

Following the comparison between dorsal and ventral striatum, we next examined how striatal 5-HT signals compare with those in SNr. As previously noted, the SNr receives some of the densest serotonergic innervation, with numerous 5-HT fibres projecting from the DRN (McDevitt et al., 2014). Therefore, we compared the 5-HT dynamics in the striatum with those observed in the SNr. As described in the Methods section, $GRAB_{5\text{-}HT}$ was injected into the DLS, and fluorescence were recorded following electrical stimulation in both striatum and SNr. I found that 5-HT signals detected in the SNr were markedly greater than in the striatum - approximately an order of magnitude higher (**Fig. 3.10A-B**; $F_{(1,78)} = 208.8$, $p < 0.001$, RM ANOVA main effect of the region). In particular, following 5p stimulation at 100 Hz, the evoked $\Delta F/F_0$ signal reached nearly 90% in the SNr, compared to only ~15% in DLS and NAcC on average. This difference was further corroborated by a significant region × pulse number interaction ($F_{(1,78)} = 68.42$, $p < 0.001$). We also compared the AUC values evoked by 1p stimulation. Consistent with the larger signal amplitudes in the SNr, the AUC in SNr were roughly three times greater than that averaged in DLS and NAcC (**Fig. 3.10C**; $t_{(39)} = 6.487$, $p = 0.001$, Student's unpaired t-test). Although the AUC of 5-HT signals in the SNr was markedly higher than averaged in DLS and NAcC, further analysis revealed that the decay half-life of the transient decay phase in SNr was significantly shorter than in the striatum (**Fig. 3.10D**; $F_{(1,82)} = 4.560$, $p = 0.04$, RM ANOVA main effect of the region). More rapid clearance of 5-HT in the SNr is consistent with the dense 5-HT innervation in this region and associated higher density of SERT, although other degradation mechanisms or other supporting cells facilitating 5-HT clearance might also participate. Furthermore, the 5p:1p ratio was significantly higher in the SNr compared to the average ratio in the DLS and NAcC (**Fig. 3.10E**; $t_{(31)} = 7.618$, $p < 0.001$, Student's unpaired *t*-test), indicating that short-term depression was less prominent in the SNr. Nonetheless, the ratio remained below 5, suggesting that some degree of depression was still present.

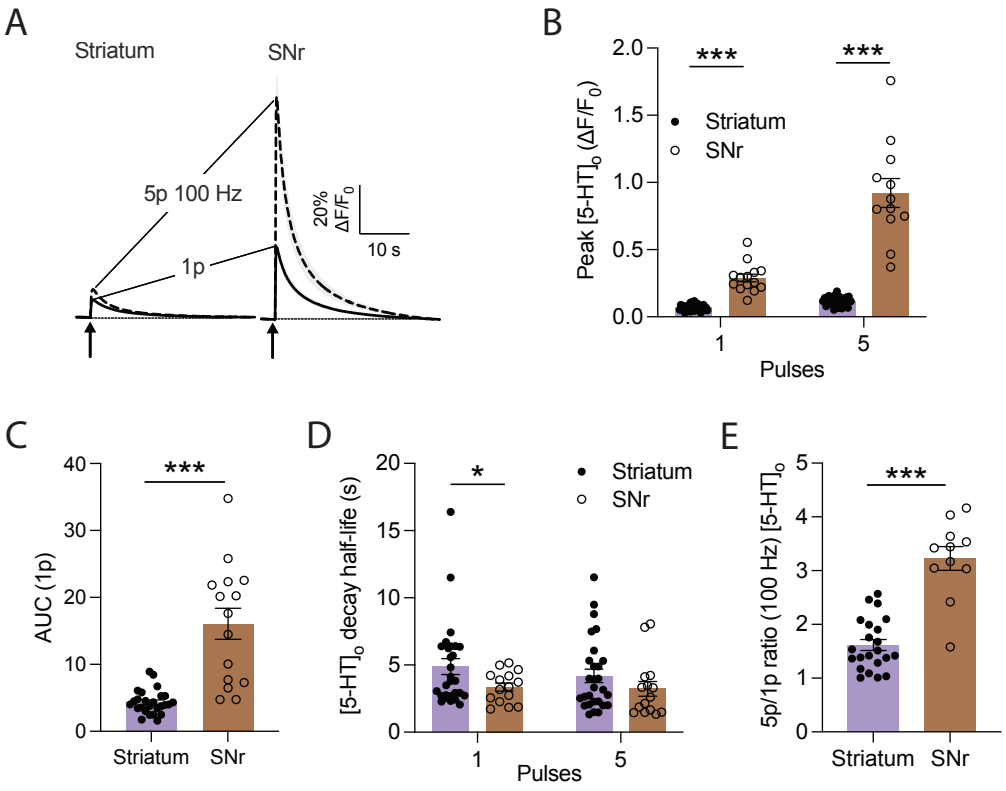

Figure 3.10. Comparison of the 5-HT transmission in striatum and SNr. (A) Mean 1p (solid line) and 5p 100 Hz (dashed line) evoked 5-HT transients ± SEM in striatum (left) and SNr (right) (Striatum: *n* = 28 slices in 13 mice; SNr: *n* = 12 slices in 6 mice). **(B)** Mean 1p and 5p at 100 Hz $[5\text{-HT}]_o$ peak in striatum (purple) and SNr (brown). **(C)** Mean 1p evoked $[5\text{-HT}]_o$ AUC in striatum (purple) and SNr (brown). **(D)** Ratios of peak $[5\text{-HT}]_o$ released by 5p 100 Hz versus 1p in striatum (purple) and SNr (brown) **(E)** Decay half-life of 1p and 5p 100 Hz evoked $[5\text{-HT}]_o$ in striatum (purple) and SNr (brown). Student's unpaired t-test, 2-way ANOVA, Fisher's LSD post-*hoc* test, **p* < 0.05, ****p* < 0.001. Error bars are ± SEM.

In summary, my data reveal regional differences in 5-HT transmission dynamics across the striatum. Further, compared to the striatum, the SNr exhibits significantly greater 5-HT release, faster clearance, and reduced short-term depression. These findings reflect the different serotonergic architecture of each region and highlight the value of high-resolution 5-HT sensors in dissecting region-specific neuromodulatory processes.

3.3.4 Striatal 5-HT clearance is mediated by both SERT and DAT

To better understand the clearance mechanisms of extracellular 5-HT in the striatum, I sought to investigate how striatal 5-HT is taken back up following release. Given the notably high

expression of DAT in the striatum, which is reported to be approximately 20-fold more dense than that of SERT (Bunin & Wightman, 1998), I hypothesized that 5-HT reuptake in the striatum is mediated not only by SERT, but also by DAT. Previous studies have provided evidence that 5-HT can be taken up by DA axons and co-released with DA (F.-M. Zhou et al., 2005), suggesting a complex interplay between the DA and 5-HT reuptake systems. Leveraging the temporal resolution of the $GRAB_{5\text{-}HT}$ sensor suited to exploring uptake kinetics, I assessed the contribution of each main monoamine uptake transporter on striatal 5-HT clearance. As described previously, I injected $GRAB_{5\text{-}HT}$ sensor into the DLS and prepared acute striatal brain slices after three weeks. In these experiment, all experiments were performed in the presence of DHßE, a selective nAChR antagonist (effects of DHBE to be discussed separately in Section 3.3.6).

As an initial step, I tested whether monoamine transporters mediate 5-HT reuptake by applying 5 µM cocaine, a non-selective DAT, SERT and NET inhibitor. Upon wash-on, I observed a biphasic change in evoked 5-HT peak amplitude over the 40 minutes of cocaine application: the peak amplitude of evoked $[5\text{-HT}]_o$ was initially increased by cocaine to approximately 120% of pre-drug values, followed by a gradual decline in these peak amplitudes to around 80% of the original pre-drug level (**Fig. 3.11A**). Thus, after 40-min wash-on of cocaine, the $[5\text{-HT}]_o$ peak amplitude was slightly less than prior to cocaine (**Fig. 3.11B-C**; $F_{(1,8)} = 3.392$, $p = 0.1028$, RM ANOVA main effect of the drug). Notably, the decrease appeared to be more pronounced under 5p stimulation compared with 1p stimulation (**Fig.3.11C**; $F_{(1,8)} = 9.792$, $p = 0.0140$, RM ANOVA main effect of the pulse number). In contrast, AUC showed a pronounced and sustained increase, reaching approximately 230% of the pre-drug level (**Fig. 3.11D-E;** $F_{(1,8)} = 37.92$, $p = 0.0003$, RM ANOVA main effect of the drug). This indicates that despite the reduced peak amplitude, the extracellular lifetime of released 5-HT was prolonged by cocaine demonstrating that striatal 5-HT reuptake is mediated by monoamine uptake transporters. Curve fitting of the

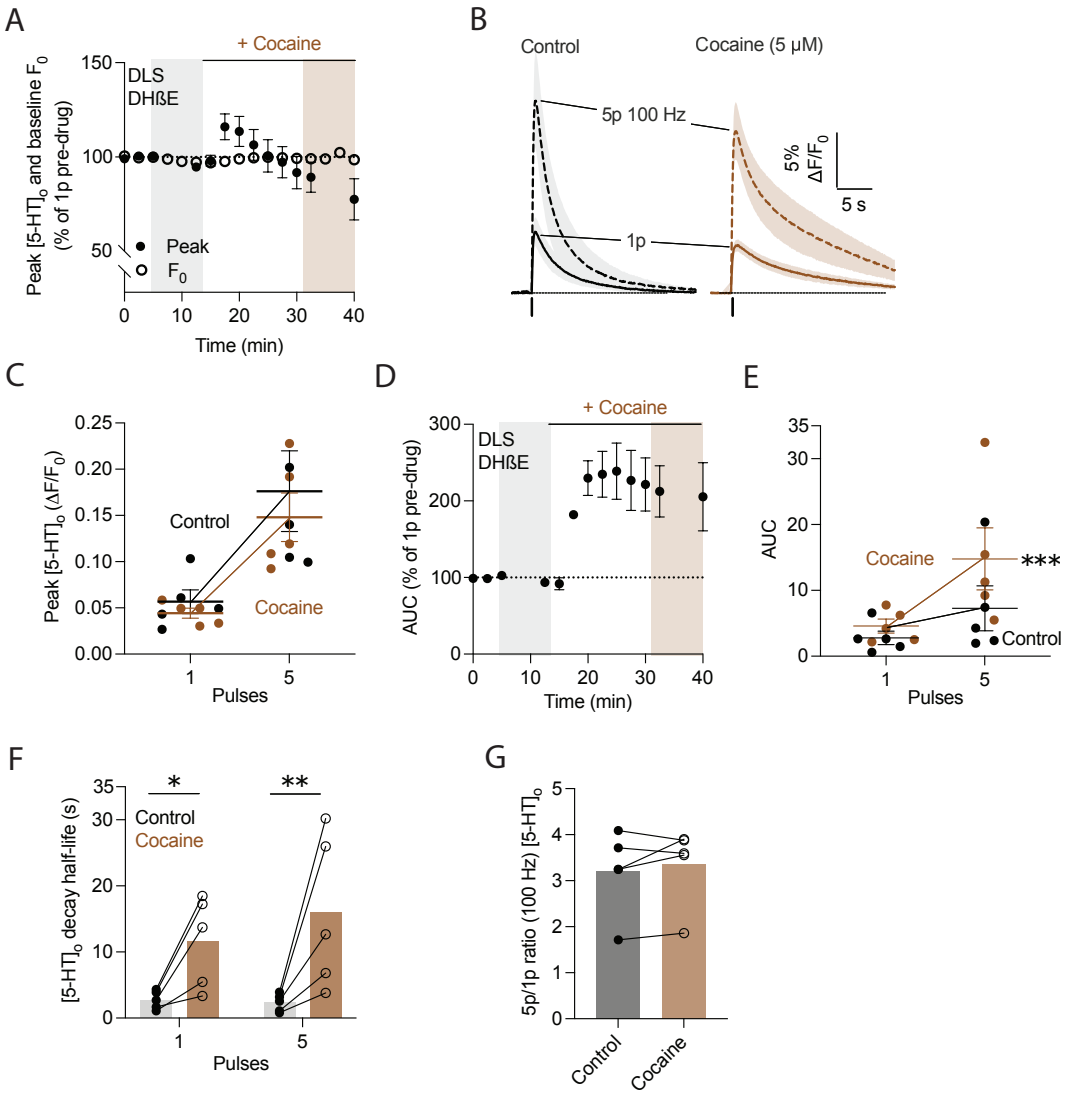

Figure 3.11. Striatal 5-HT reuptake is under control of the monoamine system. (A) Normalized mean peak $[5\text{-HT}]_o$ and baseline fluorescence (F_0) during consecutive recordings of 5-HT release evoked by 1p during the application of cocaine in the presence of DHßE in DLS (*n* = 5 experiments/3 mice). **(B)** Mean evoked 5-HT transients ± SEM, before (black) and after (brown) application of cocaine (in the presence of DHßE) in DLS. Mean transients of $[5\text{-HT}]_o$ are derived from two timepoints prior to the application of the drug (grey shaded region) and last two timepoints (brown shaded region). **(C)** Mean 1p, 5p 100 Hz $[5\text{-HT}]_o$ peak of control conditions (black) and following cocaine application (brown) in the presence of DHßE in DLS. **(D)** Normalized mean AUC $[5\text{-HT}]_o$ during consecutive recordings of 5-HT release evoked by 1p during the application of cocaine in the presence of DHßE in DLS. **(E)** Mean $[5\text{-HT}]_o$ AUC of control conditions (grey) and following drug application (brown) in the presence of DHßE in DLS. **(F)** Mean 1p and 5p 100 Hz decay half-life of $[5\text{-HT}]_o$ under control conditions (grey) and following drug application (brown) in the presence of DHßE in DLS. **(G)** Mean $[5\text{-HT}]_o$ of 5p at 100 Hz to 1p (5p/1p) in control (black) and in drug conditions (brown) in the presence of DHßE in DLS. 2-way ANOVA, Fisher's LSD post-*hoc* test. **p* < 0.05, ***p* < 0.01, ****p* < 0.001. Error bars are ± SEM.

decay phase of the transients also revealed a significant increase in decay half-life for both 1p- and 5p-evoked signals, reflecting a slowing of 5-HT clearance under cocaine (**Fig. 3.11F**; $F_{(1,8)}$ = 17.41, p = 0.0031, RM ANOVA main effect of the drug). No significant change of 5p:1p ratio was noted after cocaine application (**Fig. 3.11G**; $t_{(4)}$ = 0.9955, p = 0.3758, Student's paired t-test).

To further dissect the individual contributions of specific monoamine transporters, I next examined the role of SERT in striatal 5-HT reuptake. Since citalopram is a selective serotonin reuptake inhibitor (SSRI) with an IC_{50} of approximately 3 nM (Chen et al., 2005). A concentration of 75 nM was used in the following experiments. Wash-on of citalopram led to a significant increase in peak evoked $[5\text{-HT}]_o$, which rose to approximately 170% of the pre-drug level (**Fig. 3.12A-C**; $F_{(1,8)}$ = 29.49, p = 0.0006, RM ANOVA main effect of the drug). Similarly, citalopram produced a sustained increase in AUC, reaching around 250% of pre-drug level (**Fig. 3.12D-E**; $F_{(1,8)}$ = 0.0012, p = 0.0006, RM ANOVA main effect of the drug).

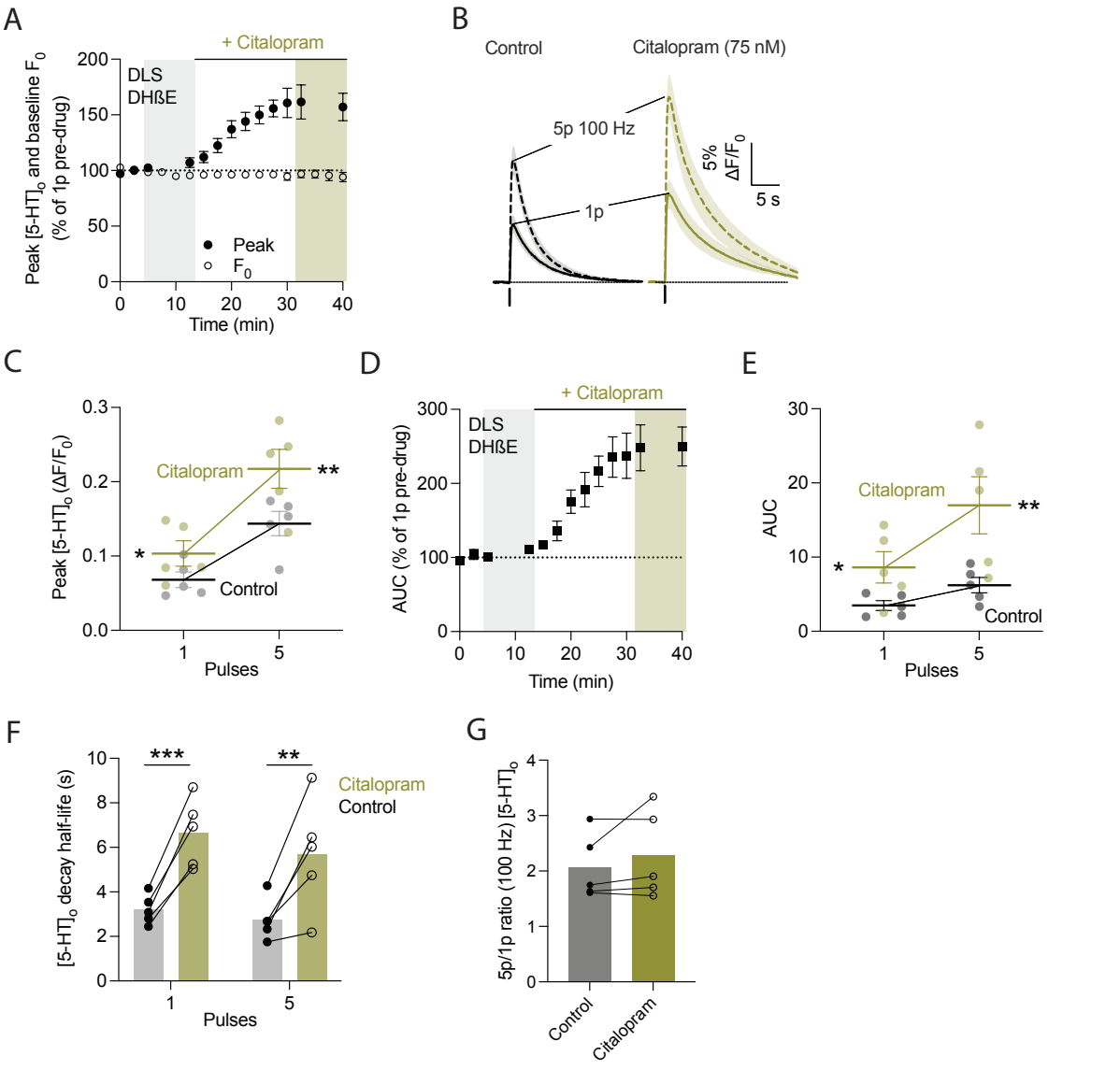

Figure 3.12. Citalopram prolonged and increased evoked 5-HT signal in DLS. (A) Normalized mean peak $[5\text{-HT}]_o$ and baseline fluorescence (F_0) during consecutive recordings of 5-HT release evoked by 1p during the application of citalopram in the presence of DHßE in DLS (n = 5 experiments/3 mice). **(B)** Mean evoked 5-HT transients ± SEM, before (black) and after (green) application of citalopram in the presence of DHßE in DLS. Mean transients of $[5\text{-HT}]_o$ are derived from two timepoints prior to the application of the drug (grey shaded region) and last two timepoints (green shaded region). **(C)** Mean 1p, 5p 100 Hz $[5\text{-HT}]_o$ peak of control conditions (black) and following citalopram application (green) in the presence of DHßE in DLS. **(D)** Normalized mean AUC $[5\text{-HT}]_o$ during consecutive recordings of 5-HT release evoked by 1p during the application of citalopram in the presence of DHßE in DLS. **(E)** Mean $[5\text{-HT}]_o$ AUC of control conditions (grey) and following drug application (green) in the presence of DHßE in DLS. **(F)** Mean 1p and 5p 100 Hz decay half-life of $[5\text{-HT}]_o$ under control conditions (grey) and following drug application (green) in the presence of DHßE in DLS. **(G)** Mean $[5\text{-HT}]_o$ of 5p at 100 Hz to 1p (5p/1p) in control (black) and in drug conditions (green) in the presence of DHßE in DLS. 2-way ANOVA, Fisher's LSD post-*hoc* test. *$p < 0.05$, **$p < 0.01$, ***$p < 0.001$. Error bars are ± SEM.

Consistent with the AUC results, curve fitting of the transient decay phase revealed a significant increase in decay half-life, again for both 1p- and 5p-evoked 5-HT responses (**Fig. 3.12F**; $F_{(1,8)}$ = 50.99, p < 0.0010, RM ANOVA main effect of the drug). The 5p:1p ratio remained unchanged after citalopram treatment (**Fig. 3.12G**; $t_{(4)}$ = 1.210, p = 0.2929, Student's paired t-test), indicating that short-term plasticity was not affected. Altogether, these results supports the conclusion that SERT plays a key role in mediating 5-HT reuptake. Furthermore, the specific and robust 5-HT signal enhancement observed with SSRI application validates that the $GRAB_{5\text{-}HT}$ sensor reliably reports extracellular 5-HT, rather than DA.

To determine whether the DAT contributes to striatal 5-HT reuptake, we next applied nomifensine (2 μM), a selective DAT blocker. Unlike the effects observed with cocaine or citalopram, nomifensine did not significantly alter peak $[5\text{-HT}]_o$ levels compared with the pre-drug condition (**Fig. 3.13A-C**; $F_{(1,8)}$ = 0.8048, p = 0.39, RM ANOVA main effect of the drug). However, the AUC of the $[5\text{-HT}]_o$ evoked by both 1p and 5p 100 Hz increased to approximately 160% of pre-drug values (**Fig. 3.13D-E**; $F_{(1,8)}$ = 24.91, p = 0.0011, RM ANOVA main effect of the drug), indicating a moderate prolongation of extracellular 5-HT lifetime. This effect was also validated by a significant drug × pulse number interaction ($F_{(1,8)}$ = 7.029, p = 0.0292). The decay half-life of $[5\text{-HT}]_o$ was also significantly increased following nomifensine application for both 1p- and 5p-evoked signals (**Fig. 3.13F**; $F_{(1,8)}$ = 31.50, p < 0.001, RM ANOVA main effect of the drug), suggesting that DAT participates in the clearance of 5-HT in striatum. Meanwhile, the 5p:1p ratio remained stable before and after nomifensine treatment (**Fig. 3.13G**; $t_{(4)}$ = 0.4343, p = 0.6864, Student's paired t-test), indicating that short-term plasticity was not affected.

Together, these results indicate that in addition to SERT, DAT also contributes to the reuptake of extracellular 5-HT in DLS. This highlights a dual-transporter mechanism underlying 5-HT clearance and further supports the existence of functional crosstalk between serotonergic and dopaminergic systems in striatum.

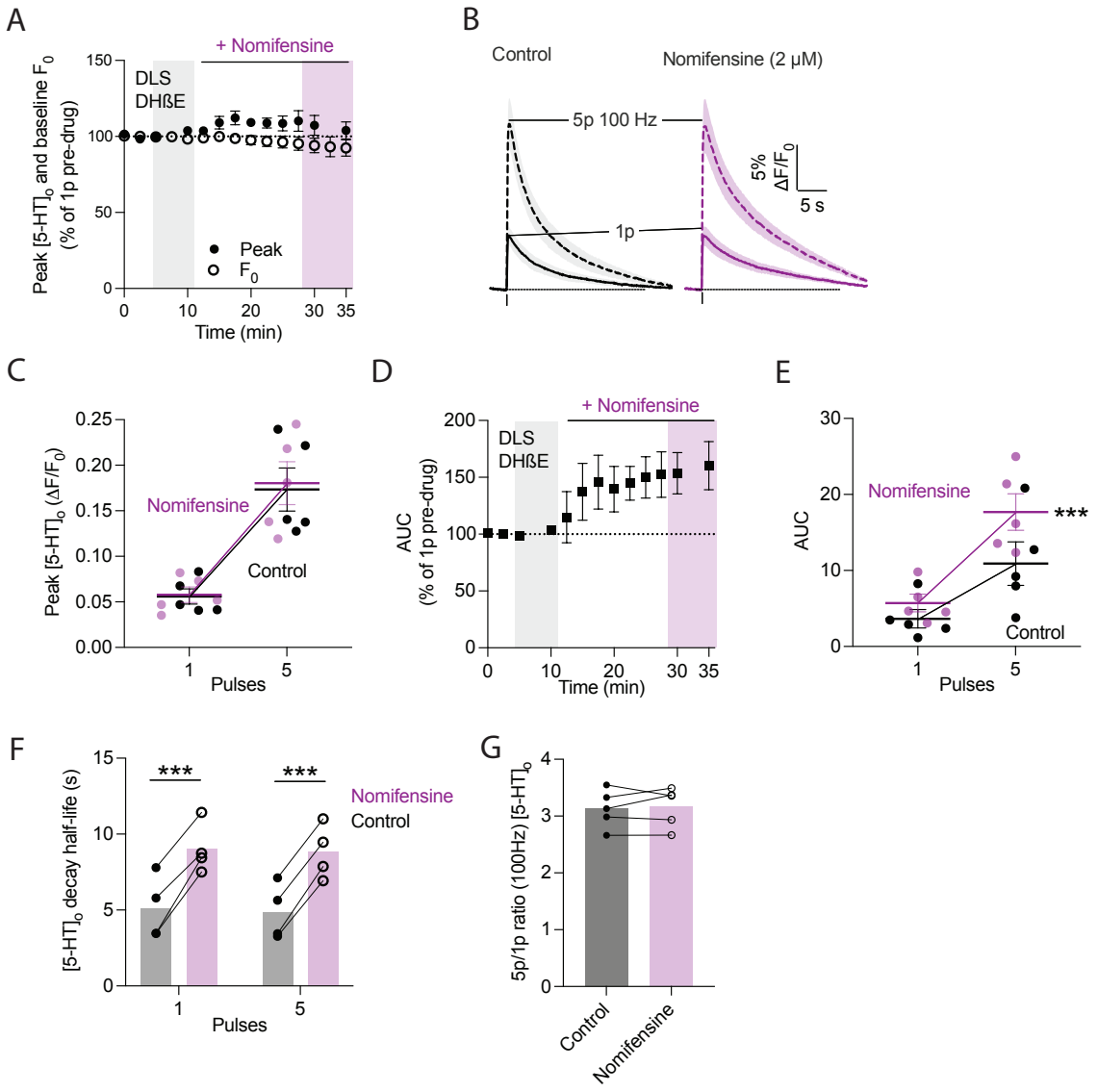

Figure 3.13. Nomifensine prolonged and increased evoked 5-HT signal in DLS. (A) Normalized mean peak $[5\text{-HT}]_o$ and baseline fluorescence (F_0) during consecutive recordings of 5-HT release evoked by 1p during the application of nomifensine in the presence of DHßE in DLS (*n* = 5 experiments/3 mice). **(B)** Mean evoked 5-HT transients ± SEM, before (black) and after (purple) application of nomifensine in the presence of DHßE in DLS. Mean transients of $[5\text{-HT}]_o$ are derived from two timepoints prior to the application of the drug (grey shaded region) and last two timepoints (purple shaded region). **(C)** Mean 1p, 5p 100 Hz $[5\text{-HT}]_o$ peak of control conditions (black) and following nomifensine application (purple) in the presence of DHßE in DLS. **(D)** Normalized mean AUC $[5\text{-HT}]_o$ during consecutive recordings of 5-HT release evoked by 1p during the application of nomifensine in the presence of DHßE in DLS. **(E)** Mean $[5\text{-HT}]_o$ AUC of control conditions (grey) and following drug application (purple) in the presence of DHßE in DLS. **(F)** Mean 1p and 5p 100 Hz decay half-life of $[5\text{-HT}]_o$ under control conditions (grey) and following drug application (purple) in the presence of DHßE in DLS. **(G)** Mean $[5\text{-HT}]_o$ of 5p at 100 Hz to 1p (5p/1p) in control (black) and in drug conditions (purple) in the presence of DHßE in DLS. 2-way ANOVA, Fisher's LSD post-*hoc* test. ***$p < 0.001$. Error bars are ± SEM.

3.3.5 Striatal 5-HT release is regulated by 5-HT auto-receptors

I investigated whether striatal 5-HT transmission is subject to regulation by serotonergic auto-receptors, focussing on a potential role of 5-$HT_{1B/1D}$ receptors, which are well-characterized presynaptic auto-receptors known to suppress 5-HT release (Göthert et al., 1995; Hagan et al., 2012). Thus, I used sumatriptan (1 µM), a selective 5-$HT_{1B/1D}$ agonist, and monitored its effects on evoked 5-HT signals.

Following wash-on of sumatriptan, I observed a progressive decrease in peak $[5\text{-HT}]_o$, which dropped to approximately 65% of the pre-drug level (**Fig. 3.14A-C;** $F_{(1,6)} = 77.46$, $p < 0.001$, RM ANOVA main effect of the drug). Both 1p- and 5p-evoked peaks were reduced, and this effect was validated by a significant drug × pulse number interaction (**Fig. 3.14C**; $F_{(1,6)} = 22.49$, $p = 0.003$), indicating that sumatriptan suppressed 5-HT release in an activity-dependent manner. Consistent with the decrease in signal amplitude, AUC was significantly reduced, reaching approximately 60% of pre-drug values after sumatriptan treatment (**Fig. 3.14D–E**; $F_{(1,6)} = 169.6$, $p < 0.001$, RM ANOVA main effect of the drug). A significant drug × pulse number interaction was also observed (**Fig. 3.14E**; interaction: $F_{(1,6)} = 25.00$, $p = 0.002$), with a reduction in the 5p:1p ratio following sumatriptan application (**Fig. 3.14F**; $t_{(3)} = 17.68$, $p = 0.0004$, Student's paired t-test), suggesting that 5-$HT_{1B/1D}$ receptor activation not only decreases release probability but also alters short-term dynamics.

In summary, activation of 5-$HT_{1B/1D}$ auto-receptors by sumatriptan significantly suppresses striatal 5-HT release and increases short-term inhibition, indicating that presynaptic auto-receptors offer an important modulatory mechanism for striatal 5-HT transmission.

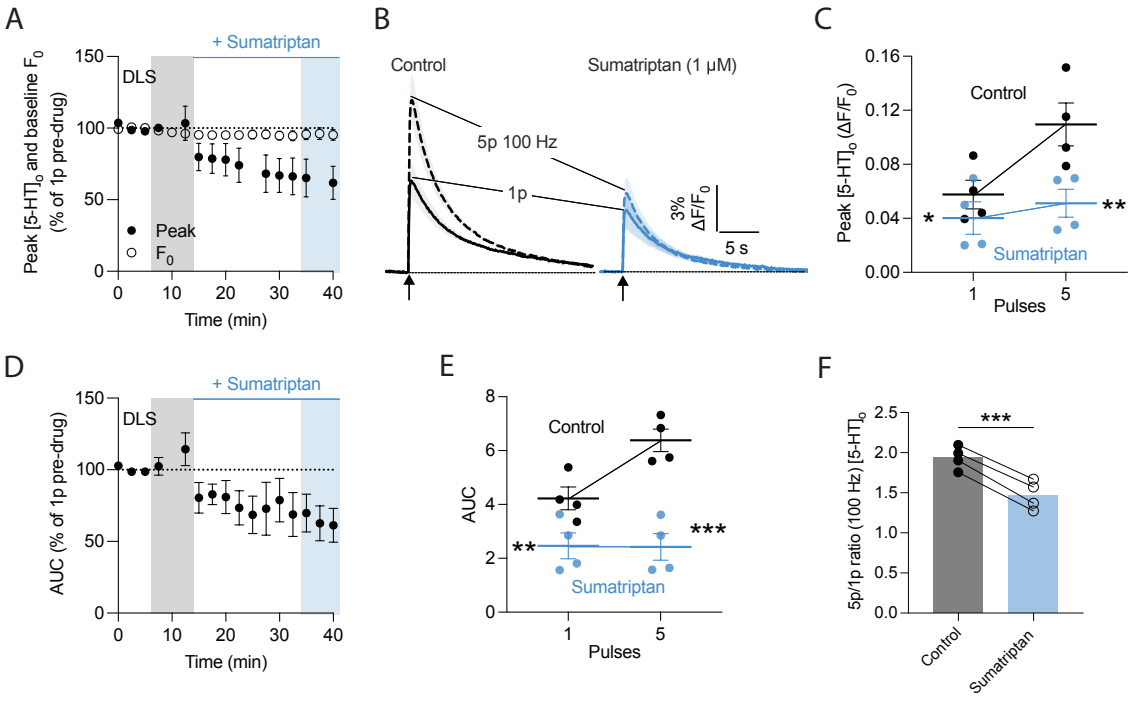

Figure 3.14. Sumatriptan supressed striatal 5-HT release. (A) Normalized mean peak $[5\text{-HT}]_o$ and baseline fluorescence (F_0) during consecutive recordings of 5-HT release evoked by 1p during the application of sumatriptan in DLS (*n* = 4 experiments/2 mice). **(B)** Mean evoked 5-HT transients ± SEM, before (black) and after (blue) application of sumatriptan in DLS. Mean transients of $[5\text{-HT}]_o$ are derived from two timepoints prior to the application of the drug (grey shaded region) and last two timepoints (blue shaded region). **(C)** Mean 1p, 5p 100 Hz $[5\text{-HT}]_o$ peak of control conditions (black) and following sumatriptan application (blue) in DLS. **(D)** Normalized mean AUC $[5\text{-HT}]_o$ during consecutive recordings of 5-HT release evoked by 1p during the application of sumatriptan in DLS. **(E)** Mean $[5\text{-HT}]_o$ AUC of control conditions (grey) and following drug application (blue) in DLS. **(F)** Mean $[5\text{-HT}]_o$ of 5p at 100 Hz to 1p (5p/1p) in control (black) and in drug conditions (blue) in DLS. 2-way ANOVA, Fisher's LSD post-*hoc* test. **p* < 0.05, ***p* < 0.01, ****p* < 0.001. Error bars are ± SEM.

3.3.6 Striatal 5-HT release is regulated by ACh via nAChRs in DLS and NAcC

Striatal ACh is known to modulate monoamine transmission through presynaptic nAChRs. Rice and Cragg (2004) demonstrated that ACh acts via nAChRs to support striatal DA release, minimising its pulse-number dependence, while in a later study, Threlfell showed that ACh released from striatal cholinergic interneurons can directly drive DA release from striatal axons through activation of presynaptic nAChRs (Threlfell et al., 2012). However, whether striatal 5-HT transmission is similarly regulated by ACh acting at nAChRs has been unknown.

To investigate this, DHβE (1 μM) was applied in acute striatal slices from mice injected with $GRAB_{5\text{-}HT}$ in either the DLS or NAcC. To assess the effect of DHβE on striatal 5-HT release under different stimulation frequencies (i.e., different pulse intervals), I recorded 5-HT transients evoked by 1p and 5p stimulation delivered at 2 Hz, 25 Hz, 50 Hz, and 100 Hz, both before and after DHβE wash-on. I analysed changes in peak amplitude, 5p:1p ratio at different stimulation frequencies and decay half-life to evaluate both the magnitude and short-term plasticity of 5-HT release under ACh modulation via nAChRs.

In the DLS, I found that DHβE wash-on selectively reduced 5-HT release evoked by 1p or low-frequency stimulation. Specifically, the peak $[5\text{-HT}]_o$ evoked by 1p stimulation decreased to approximately 60% of the pre-drug level (**Fig. 3.15A**). A similar reduction was observed for 5p stimulation at 2 Hz, particularly at the first pulse. The degree of inhibition gradually diminished with increasing pulse number within the 5p train. By the fifth pulse, the difference between pre- and post-DHβE conditions was minimal, suggesting a pulse-dependent loss of the inhibitory effect. In contrast, at higher stimulation frequencies, especially pulse interval less than 40 ms (5p at 25 Hz, 50 Hz, and 100 Hz) blocking nAChRs had little to no effect on the 5-HT peak

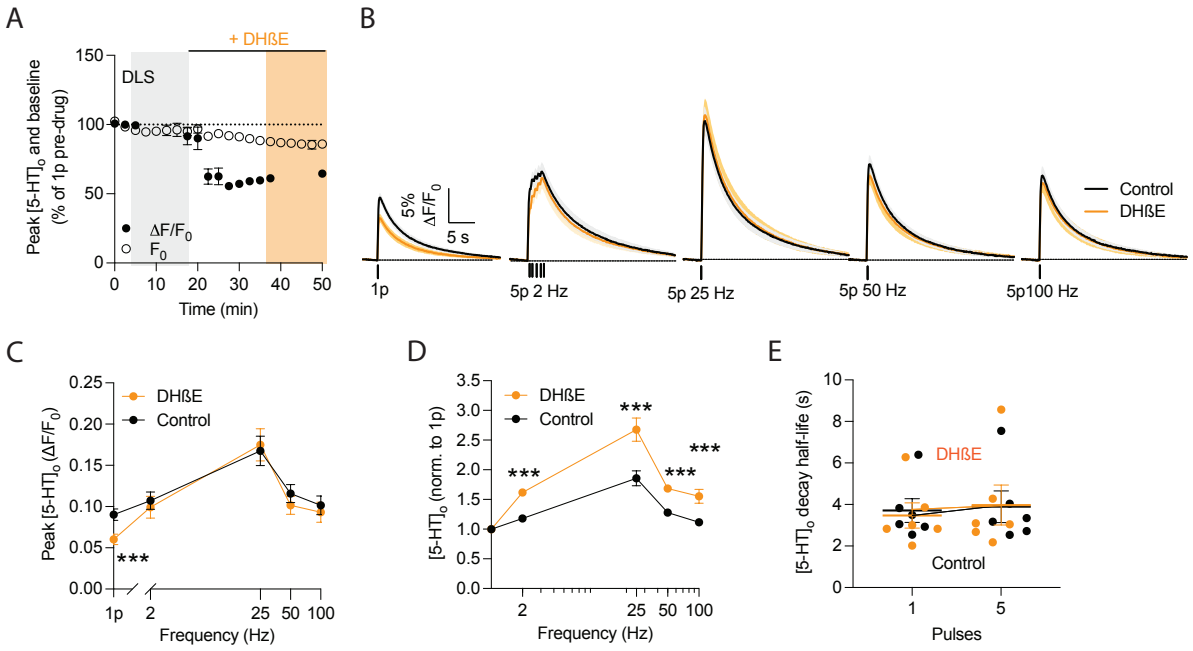

Figure 3.15. DHßE supressed evoked 5-HT release only by 1p in DLS. (A) Normalized mean peak $[5\text{-HT}]_o$ and baseline fluorescence (F_0) during consecutive recordings of 5-HT release evoked by 1p during the application of DHßE in DLS (n = 6 experiments/4 mice). **(B)** Mean evoked 5-HT transients ± SEM, before (black) and after (yellow) application of DHßE in DLS. Mean transients of $[5\text{-HT}]_o$ are derived from two timepoints prior to the application of the drug (grey shaded region) and last two timepoints (yellow shaded region). **(C)** Mean 1p, 5p at 2 Hz, 25 Hz, 50 Hz and 100 Hz $[5\text{-HT}]_o$ peak of control conditions (black) and following DHßE application (yellow) in DLS. **(D)** Normalized mean $[5\text{-HT}]_o$ of 5p at 2 Hz, 25 Hz, 50 Hz and 100 Hz to 1p (5p/1p) in control (black) and in drug conditions (yellow) in DLS. **(E)** Mean 1p and 5p 100 Hz decay half-life of $[5\text{-HT}]_o$ under control conditions (grey) and following drug application (yellow) in DLS. 2-way ANOVA, Fisher's LSD post-*hoc* test. ***$p < 0.001$. Error bars are ± SEM.

amplitude (**Fig. 3.15B-C**; $F_{(1,25)} = 23.20$, $p < 0.001$, RM ANOVA main effect of the drug). This was further validated by a significant frequency x drug interaction ($F_{(4,25)} = 7.410$, $p < 0.001$).

To further quantify changes of striatal 5-HT in short-term plasticity, I normalized the 5p-evoked responses to their corresponding 1p responses. I found that the 5p:1p ratio increased significantly across all frequencies (2, 25, 50, and 100 Hz) following DHβE treatment (**Fig. 3.15D**; $F_{(1,25)} = 46.99$, $p < 0.001$, RM ANOVA main effect of the drug). This was primarily due to the strong suppression of 1p-evoked release, while 5p-evoked release remained relatively intact. Additionally, I did not observe any significant change in decay half-life after DHβE

application, indicating that DHβE does not affect 5-HT clearance or reuptake kinetics (**Fig. 3.15E**; $F_{(1,10)}$ = 0.2017, p = 0.66, RM ANOVA main effect of the drug).

Together, these results suggest that in the DLS, nAChR blockade by DHβE suppresses low-frequency 5-HT release, particularly under 1p conditions, while leaving high-frequency release and 5-HT clearance unaffected. This supports a frequency-dependent regulatory role of nAChRs in modulating striatal 5-HT transmission.

Given the previously reported regional differences in cholinergic modulation across the striatum, I also examined the effect of nAChR blockade in the ventral striatum, specifically NAcC. This allowed us to directly compare how ACh regulates 5-HT transmission in distinct striatal subregions.

In the NAcC, I found that DHβE wash-on had no significant effect on 5-HT release evoked by either 1p or low-frequency stimulation. Specifically, the peak $[5\text{-HT}]_o$ evoked by 1p stimulation remained comparable to the pre-drug level (**Fig. 3.16A**). Similarly, 5p stimulation at 2 Hz did not show any notable change in peak amplitude following nAChR blockade. However, a distinct effect emerged at higher stimulation frequencies. When the inter-pulse interval dropped below 40 ms (5p at 25 Hz, 50 Hz, and 100 Hz) DHβE application significantly enhanced 5-HT release (**Fig. 3.16B-C**; $F_{(1,25)}$ = 10.45, p = 0.003, RM ANOVA main effect of the drug).

To further assess how nAChR blockade alters short-term plasticity of 5-HT transmission in the NAcC, I normalized 5p responses to their corresponding 1p responses. The 5p:1p ratio significantly increased across stimulation frequencies ≥ 25 Hz following DHβE treatment (**Fig. 3.16D**; $F_{(1,25)}$ = 39.84, p < 0.001, RM ANOVA main effect of the drug). These results suggest that nAChR inhibition preferentially facilitates high-frequency 5-HT release in the NAcC, in contrast to the suppressive effect observed in the DLS under low-frequency conditions. Consistent with the findings in the DLS, we did not observe any significant change in decay half-life before and

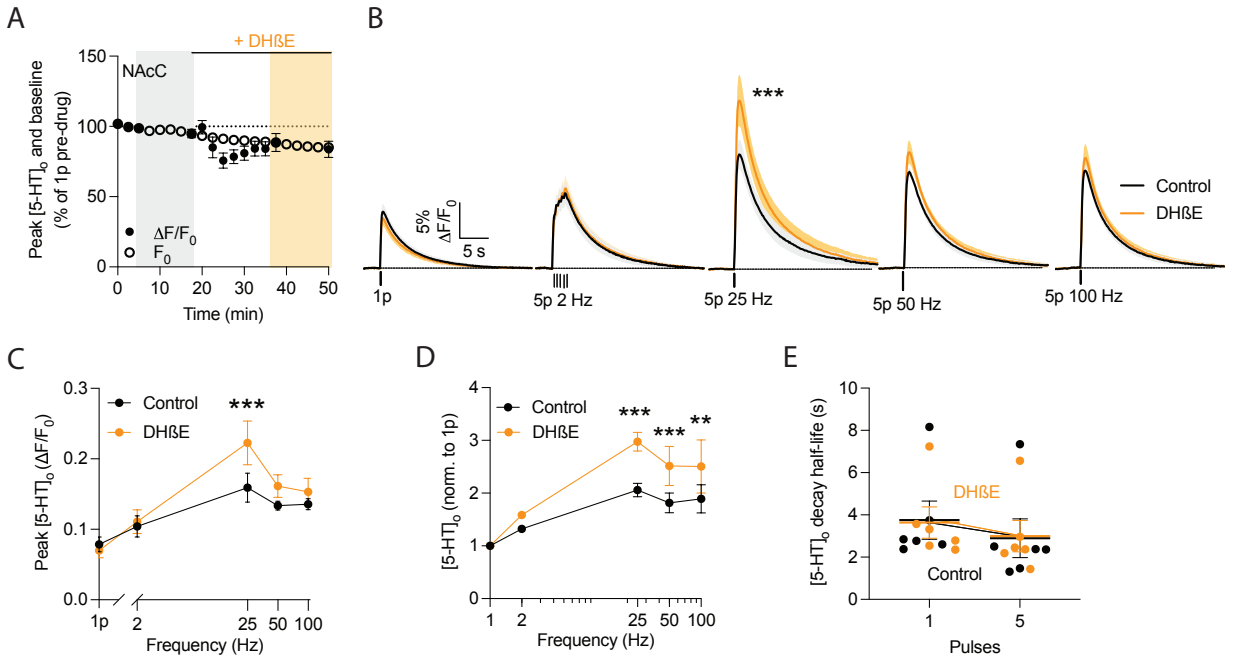

Figure 3.16. DHßE increased evoked 5-HT release at high stimulation frequency in NAcC. **(A)** Normalized mean peak $[5\text{-HT}]_o$ and baseline fluorescence (F_0) during consecutive recordings of 5-HT release evoked by 1p during the application of DHßE in NAcC (*n* = 6 experiments/3 mice). **(B)** Mean evoked 5-HT transients ± SEM, before (black) and after (yellow) application of DHßE in NAcC. Mean transients of $[5\text{-HT}]_o$ are derived from two timepoints prior to the application of the drug (grey shaded region) and last two timepoints (yellow shaded region). **(C)** Mean 1p, 5p at 2 Hz, 25 Hz, 50 Hz and 100 Hz $[5\text{-HT}]_o$ peak of control conditions (black) and following DHßE application (yellow) in NAcC. **(D)** Normalized mean $[5\text{-HT}]_o$ of 5p at 2 Hz, 25 Hz, 50 Hz and 100 Hz to 1p (5p/1p) in control (black) and in drug conditions (yellow) in NAcC. **(E)** Mean 1p and 5p 100 Hz decay half-life of $[5\text{-HT}]_o$ under control conditions (grey) and following drug application (yellow) in NAcC. 2-way ANOVA, Fisher's LSD post-*hoc* test. **p* < 0.05, ***p* < 0.01. Error bars are ± SEM.

after DHβE application in the NAcC, indicating that 5-HT clearance and reuptake dynamics were unaffected (**Fig. 3.16E**; $F_{(1,10)}$ = 0.0034, *p* = 0.95, RM ANOVA main effect of the drug).

Together, these results reveal a region-specific role of nAChRs in modulating striatal 5-HT transmission. While nAChR blockade in the DLS preferentially suppresses low-frequency release, it enhances high-frequency release in the NAcC, highlighting distinct cholinergic control mechanisms across dorsal and ventral striatal domains.

3.3.7 Striatal 5-HT release is regulated by ACh via mAChRs in DLS

Building on our findings regarding cholinergic modulation of 5-HT via nAChRs, I next investigated whether striatal 5-HT release is also regulated by muscarinic ACh receptors (mAChRs). Previous studies have shown that ACh can act on mAChRs to modulate striatal circuits, including DA transmission. For example, Threlfell et al. (2010) reported that activation of mAChR with oxotremorine-M (oxo-M) robustly suppressed 1p-evoked DA release, while having little effect (or even slightly enhancing) release evoked by high-frequency stimulation (4p at 100 Hz). These effects are lost when nAChRs are inhibited, indicating that that mAChRs regulate striatal DA release in a frequency-dependent manner by suppressing ACh release from cholinergic interneurons and thereby reducing nAChR-mediated modulation of neurotransmitter release (Threlfell et al., 2010).

To test whether mAChRs similarly regulate 5-HT transmission, I applied the same broad-spectrum mAChR agonists oxo-M (5 µM) to acute DLS slices from mice expressing $GRAB_{5\text{-}HT}$, using the same stimulation protocols as in previous experiments. 5-HT release was evoked by both 1p and 5p stimulation across a range of frequencies (2, 25 and 100 Hz), and I recorded fluorescence transients before and after oxo-M application.

I found that oxo-M strongly suppressed 5-HT release across all stimulation conditions (**Fig. 3.17A-C**; $F_{(1,20)} = 90.12$, $p < 0.001$, RM ANOVA main effect of the drug). The effect was most pronounced for 1p stimulation, where peak $[5\text{-HT}]_o$ decreased to approximately 40% of pre-drug levels. For 5p stimulation at 100 Hz, the suppression was less severe, with peak $[5\text{-HT}]_o$ reduced to about 70% of baseline. These results suggest that mAChR activation preferentially inhibits 5-HT release under low-activity conditions. To assess the impact of oxo-M on short-term plasticity, I calculated the 5p:1p ratio at different frequencies. A significant increase was observed in the 5p:1p ratio across stimulation conditions following oxo-M application, with the

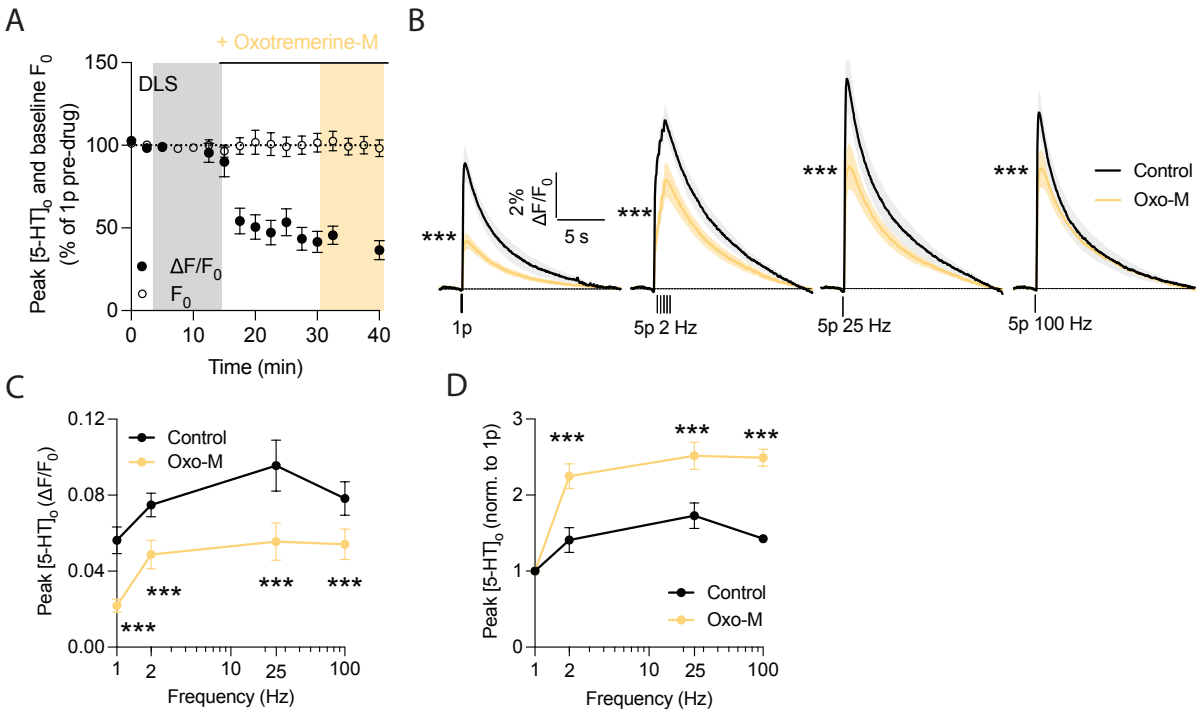

Figure 3.17. Activation of mAChR inhibited striatal 5-HT release in DLS. (A) Normalized mean peak $[5\text{-HT}]_o$ and baseline fluorescence (F_0) during consecutive recordings of 5-HT release evoked by 1p and 5p 100 Hz during application oxotremorine-M in DLS (n = 6 experiments/4 mice). **(B)** Mean evoked 5-HT transients ± SEM, before (black) and after (yellow) application of oxotremorine-M in DLS. Mean transients of $[5\text{-HT}]_o$ are derived from two timepoints prior to the application of the drug (grey shaded region) and last two timepoints (yellow shaded region). **(C)** Mean 1p, 5p at 2 Hz, 25 Hz and 100 Hz $[5\text{-HT}]_o$ peak of control conditions (black) and following drug application (yellow) in DLS. **(D)** Normalized mean $[5\text{-HT}]_o$ of 5p at 2 Hz, 25 Hz and 100 Hz to 1p (5p/1p) in control (black) and in drug conditions (yellow) in DLS. 2-way ANOVA, Fisher's LSD post-*hoc* test. ***p < 0.001. Error bars are ± SEM.

strongest effect at 100 Hz (**Fig. 3.17D**; $F_{(1,20)}$ = 79.42, p < 0.001, RM ANOVA main effect of the drug). This effect was further supported by a significant drug × frequency interaction (**Fig. 3.17D**; $F_{(3,20)}$ = 9.469, p = 0.0004, RM ANOVA interaction).

Together, these results demonstrate that activation of mAChRs by oxo-M potently suppresses striatal 5-HT release, particularly under low-frequency stimulation, and alters short-term release dynamics in a frequency-dependent manner.

Further, to determine whether the inhibitory effect of mAChR activation on 5-HT release is mediated via nAChR-dependent mechanisms, I repeated the oxo-M experiments under

continuous blockade of nAChRs. Specifically, DHβE (1 μM) was applied throughout the entire experiment to isolate mAChR effects from any nAChR-mediated cholinergic modulation.

Under these conditions, the inhibitory effect of oxo-M was completely abolished in the DLS. Peak $[5\text{-HT}]_o$ amplitudes remained unchanged after oxo-M application across all stimulation conditions (**Fig. 3.18A-C**; $F_{(1,12)} = 0.1836$, $p = 0.68$, RM ANOVA main effect of the drug). In addition, the 5p:1p ratio showed no significant change following oxo-M treatment in the presence of DHβE (**Fig. 3.18D**; $F_{(1,12)} = 0.0396$, $p = 0.85$, RM ANOVA main effect of the drug).

These findings suggest that the effect of mAChR activation on striatal 5-HT release is indirect and depends on functional nAChRs, likely through modulation of ACh release from cholinergic interneurons.

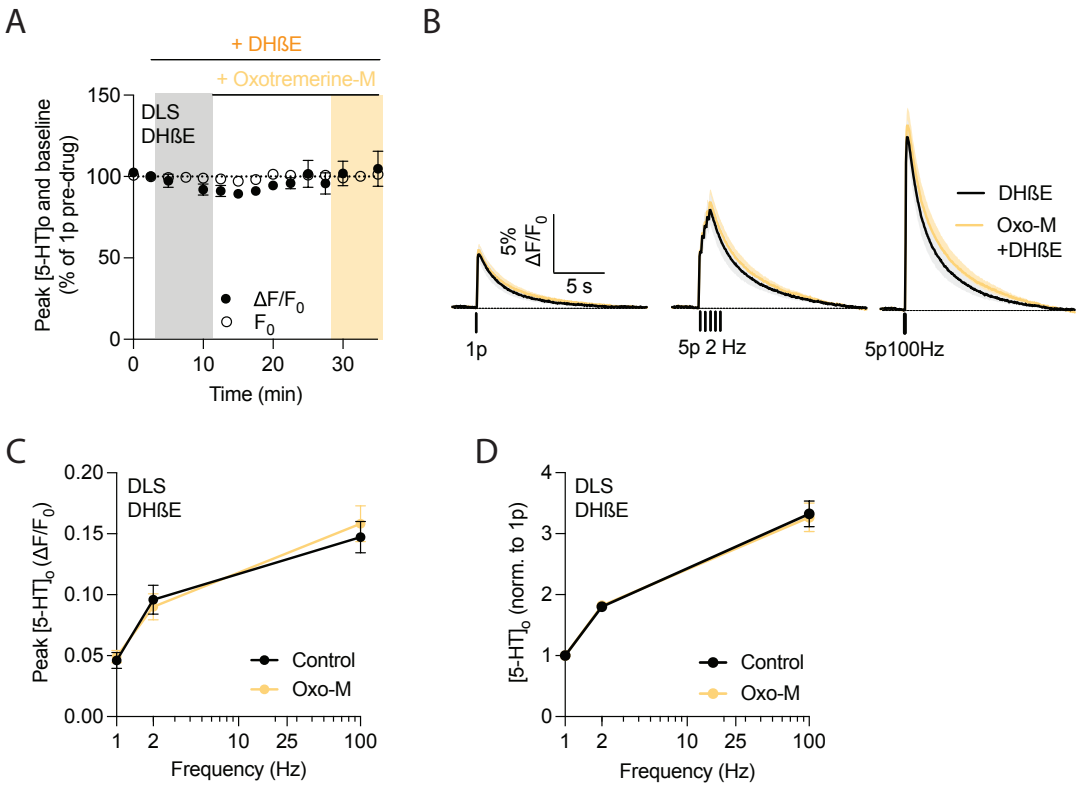

Figure 3.18. DHßE prevented the further inhibition of Oxotremorine-M on striatal 5-HT. (A) Normalized mean peak $[5\text{-HT}]_o$ and baseline fluorescence (F_0) during consecutive recordings of 5-HT release evoked by 1p during application oxotremorine-M in the presence of DHßE in DLS (*n* = 5 experiments/4 mice). **(B)** Mean evoked 5-HT transients ± SEM, before (black) and after (yellow) application of oxotremorine-M in the presence of DHßE in DLS. Mean transients of $[5\text{-HT}]_o$ are derived from two timepoints prior to the application of the drug (grey shaded region) and last two timepoints (yellow shaded region). **(C)** Mean 1p, 5p at 2 Hz and 100 Hz $[5\text{-HT}]_o$ peak of control conditions (black) and following drug application (yellow) in DLS in the presence of DHßE. **(D)** Normalized mean $[5\text{-HT}]_o$ of 5p at 2 Hz and 100 Hz to 1p (5p/1p) in control (black) and in drug conditions (yellow) in the presence of DHßE in DLS. 2-way ANOVA, Fisher's LSD post-*hoc* test. Error bars are ± SEM.

3.3.8 Antagonism of $GABA_{A\&B}$ receptors promoted striatal 5-HT release

GABAergic transmission plays a dominant role in striatal circuitry, and ambient GABA tone has been detected in both dorsal and ventral regions (Ade et al., 2008; Kirmse et al., 2009). Previous studies have shown that such tonic GABAergic signalling can inhibit striatal monoamine transmission, including DA release (Lopes et al., 2019; Roberts et al., 2020). Considering this, I sought to determine whether striatal 5-HT release is similarly regulated by

tonic GABAergic inhibition. Given the earlier finding that ACh can modulate 5-HT release via nAChRs, and to exclude indirect effects mediated by ACh, all experiments were conducted in the presence of the nAChR antagonist DHβE (1 μM).

To test the effect of GABAergic inhibition on 5-HT release, I applied a combination of $GABA_A$ and $GABA_B$ receptor antagonists: bicuculline (10 μM) and CGP 55845 (4 μM). Blockade of GABA receptors led to a robust increase in evoked 5-HT signals across all stimulation conditions. Specifically, 5-HT release was significantly enhanced following both 1p stimulation and 5p stimulation at 2, 25, and 100 Hz (**Fig. 3.19A-C**; $F_{(1,16)} = 31.05$, $p < 0.001$, RM ANOVA main effect of the drug). GABA receptor antagonism also significantly increased the AUC of 5-HT transients across stimulation frequencies (**Fig. 3.19D**; $F_{(1,16)} = 49.74$, $p < 0.001$, RM ANOVA main effect of the drug). No significant 5p:1p ratio changes were found at any stimulation frequency (**Fig. 3.19E**; $F_{(1,16)} = 3.983$, $p = 0.06$, RM ANOVA main effect of the drug), suggesting that the enhancement of 5-HT release by GABA receptor antagonism is not frequency-dependent.

In summary, these findings demonstrate that tonic GABAergic tone suppresses striatal 5-HT release, and that blocking $GABA_A$ and $GABA_B$ receptors facilitates 5-HT transmission independently of changes in cholinergic tone or short-term plasticity.

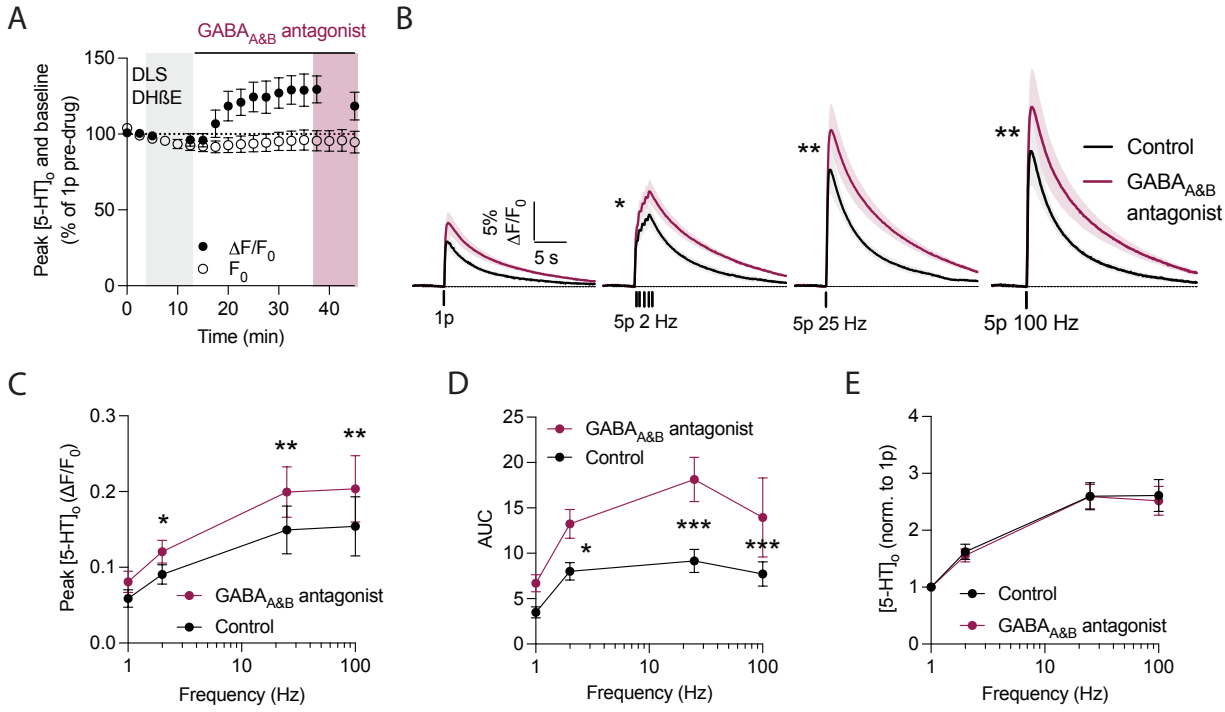

Figure 3.19. GABA$_{A\&B}$R antagonist increased striatal 5-HT release. (A) Normalized mean peak [5-HT]$_o$ and baseline fluorescence (F_0) during consecutive recordings of 5-HT release evoked by 1p during application of bicuculine (10 µM) and CGP55845 (4 µM) in the presence of DHßE in DLS (*n* = 5 experiments/3 mice). **(B)** Mean evoked 5-HT transients ± SEM, before (black) and after (purple) application of bicuculines and CGP55845 in the presence of DHßE in DLS. Mean transients of [5-HT]$_o$ are derived from two timepoints prior to the application of the drug (grey shaded region) and last two timepoints (purple shaded region). **(C)** Mean 1p, 5p at 2 Hz, 25 Hz and 100 Hz [5-HT]$_o$ peak of control conditions (black) and following drug application (purple) in DLS in the presence of DHßE. **(D)** Mean [5-HT]$_o$ AUC of control conditions (grey) and following drug application (purple) in DLS in the presence of DHßE. **(E)** Normalized mean [5-HT]$_o$ of 5p at 2 Hz, 25 Hz and 100 Hz to 1p (5p/1p) in control (black) and in drug conditions (purple) in the presence of DHßE in DLS. 2-way ANOVA, Fisher's LSD post-*hoc* test. *p < 0.05, **p < 0.01, ***p < 0.001. Error bars are ± SEM.

3.4 Discussion

In this chapter, I investigated the dynamics and regulation of striatal 5-HT release using the genetically encoded fluorescent sensor GRAB$_{5\text{-HT}}$. By combining real-time optical recordings in acute brain slices with pharmacological manipulations, I systematically characterized the basic

properties of evoked 5-HT signals and examined how they are modulated by uptake mechanisms, auto receptors, and local neurotransmitter systems including ACh and GABA.

My findings demonstrate that $GRAB_{5\text{-}HT}$ provides a reliable and selective readout of extracellular 5-HT in both DLS and NAcC. I validated the stability, specificity, and pharmacological sensitivity of this sensor under *ex vivo* conditions and further confirmed that it predominantly reports 5-HT rather than DA, even in the dopamine-rich striatal environment. Together, these results support the utility of $GRAB_{5\text{-}HT}$ for dissecting the mechanisms that shape serotonergic transmission in the striatum.

3.4.1 $GRAB_{5\text{-}HT3.0}$ to measure real-time 5-HT release in striatal slices

I first validated the fundamental properties of the new $GRAB_{5\text{-}HT}$ sensor under *ex vivo* conditions. Application of exogenous 5-HT induced strong fluorescence changes, whereas DA had no effect. The 5-HT_4R antagonist RS 23597-190 completely abolished electrically evoked signals, confirming that signal generation is 5-HT-dependent rather than an optical optical or other evoked artifact. Furthermore, a mutant version of the sensor ($GRAB_{5\text{-}HT3.0mut}$), incapable of binding 5-HT, showed no response to either stimulation or external 5-HT, further supporting that the evoked signal is not artifact. Although the lack of response from $GRAB_{5\text{-}HT3.0mut}$ provides strong evidence that the observed fluorescence signals are not artifacts, this control does not entirely exclude other confounding factors. It remains uncertain whether viral expression of the mutant sensor may have altered the physiological viability of the tissue. Although in our 6-OHDA experiment, the stable control hemisphere 5-HT signal indicate that $GRAB_{5\text{-}HT3.0}$ (expressed via AAV5) does not appear to compromise tissue health or the capacity for neurotransmitter release. However, the mutant sensor was delivered using a different viral serotype (AAV9), and differences in the expression efficiency, or potential cytotoxicity between AAV5 and AAV9 (especially at high viral titres) cannot be ruled out. To directly address this uncertainty, future

experiments incorporating FCV in the same slices following GRAB imaging would help confirm whether robust DA release can still be evoked. Such dual-modality validation would strengthen the interpretation of $GRAB_{5\text{-}HT3.0mut}$ as an appropriate negative control.

Beyond the striatum, I observed that $GRAB_{5\text{-}HT}$ fluorescence could also be detected in the midbrain SNr after striatal injections, resulting from trafficking of the sensor from striatum to midbrain. This is likely due to viral expression in striatal projection neurons, such as MSNs or GABAergic long-range interneurons, which transport the sensor in an anterograde fashion to their axons in the SNr. This anatomical observation highlights the potential for $GRAB_{5\text{-}HT}$ to label not only somatic compartments but also long-range projections.

Building on this anatomical expression pattern, I next focused on validating the chemical specificity of $GRAB_{5\text{-}HT}$ in the striatum, a region densely innervated by dopaminergic projections. While previous studies have demonstrated the specificity of $GRAB_{5\text{-}HT}$ in cultured cells and *in vivo* in the cortex (Deng et al., 2024), it remained unclear whether the sensor could reliably differentiate 5-HT from DA in DA-rich tissue like the striatum. Here, I systematically tested the specificity of the sensor under *ex vivo* conditions for the first time in this context. The strongest evidence for specificity comes from experiments using 6-OHDA lesions to selectively eliminate striatal DA. Despite ~70% loss of DA markers, evoked 5-HT signals measured by $GRAB_{5\text{-}HT}$ remained robust and unchanged, confirming that the sensor does not rely on DA input for its activation. Additionally, several properties of evoked 5-HT signal further support the detection of by $GRAB_{5\text{-}HT}$ of 5-HT over DA. For example, the 5p:1p ratio of evoked responses was higher for 5-HT (typically between 1.5-2) than the ratio for DA, which is often close to 1-1.3 due to nAChR-mediated suppression of DA release during following stimulations. This also suggests that 5-HT transmission in the striatum is subject to weaker inhibition compared to DA, resulting in a distinct dynamic signature.

Moreover, activation of 5-$HT_{1B/1D}$ autoreceptors using sumatriptan markedly suppressed $GRAB_{5\text{-}HT}$ signals, consistent with strong potential for these receptors to operate auto-inhibitory control of 5-HT release. In contrast, preliminary FCV data suggest that sumatriptan at the same concentration has no effect on DA release (data not shown), reinforcing the transmitter specificity of the $GRAB_{5\text{-}HT}$ sensor. Together, these findings strongly support the conclusion that $GRAB_{5\text{-}HT}$ predominantly reports striatal 5-HT release rather than DA.

Nonetheless, it is important to acknowledge that we cannot fully rule out the possibility of a small DA contribution to the recorded signal. Although minor DA involvement cannot be entirely excluded, this limitation does not substantially impair the utility of $GRAB_{5\text{-}HT}$ for investigating striatal 5-HT dynamics. Therefore, $GRAB_{5\text{-}HT}$ can be used as a reliable tool for reporting 5-HT transmission in the striatum under the conditions tested in my study.

3.4.2 Differences in evoked 5-HT release across dorsal, ventral striatum and SNr

After establishing the utility and specificity of $GRAB_{5\text{-}HT}$ for detecting real-time 5-HT release in striatal slices, I next sought to compare the characteristics of evoked 5-HT signals across key striatal subregions and midbrain, including DLS, NAcC, and SNr. These regions differ anatomically and functionally, and their serotonergic innervation density and local circuitry are also distinct. My aim was to determine whether these factors are reflected in measurable differences in 5-HT release dynamics.

As shown in **Fig. 3.9**, electrical stimulation evoked robust 5-HT transients in both DLS and NAcC. Notably, the peak amplitude was significantly higher in the NAcC compared to the DLS, indicating a greater initial release of 5-HT in the ventral striatum. However, this stronger release was accompanied by a smaller AUC and a shorter decay half-life, suggesting faster clearance of

5-HT in NAcC than in DLS. These differences likely reflect region-specific differences in 5-HT reuptake transporter expression or extracellular environment. Additionally, baseline fluorescence (F_0) remained comparable between DLS and NAcC, indicating that the observed signal differences are not due to variations in $GRAB_{5\text{-}HT}$ expression levels or tonic activation by ambient endogenous non-evoked 5-HT tone. Furthermore, when examining short-term plasticity by calculating the 5p:1p ratio, I found that NAcC displayed less depressed ratios than DLS across stimulation conditions**.** This suggests that ventral striatum experiences less short-term inhibitory modulation in NAcC. Taken together, these findings suggest that NAcC receives denser serotonergic input and exhibits less constrained 5-HT dynamics than DLS, consistent with previous anatomical studies (Jiménez-Sánchez et al., 2020).

To further explore regional distinctions, I next compared striatal 5-HT signals (DLS and NAcC combined) with those observed in SNr, a midbrain target that receives direct serotonergic projections from DRN (McDevitt et al., 2014). Compared to the striatum, the SNr showed a strikingly different profile of 5-HT release. Evoked peak amplitude in SNr was approximately an order of magnitude larger than in the striatum, and AUC was also substantially elevated, reflecting a very strong and prolonged 5-HT signal. However, decay half-life in SNr was shorter than in striatum, suggesting that despite its high amplitude, clearance rate is faster - possibly due to differences in extracellular space properties or higher SERT expression. Notably, the 5p:1p ratio in SNr was markedly higher than in striatum, indicating less short-term inhibition in SNr to suppress 5-HT subsequent release.

Collectively, these findings reveal region-specific profiles of 5-HT transmission across dorsal, ventral striatum and SNr. These distinctions likely arise from a combination of differential serotonergic innervation, transporter expression, and local circuit modulation, and underscore the importance of spatial context when interpreting 5-HT function in the basal ganglia.

3.4.3 Contribution of SERT and DAT to striatal 5-HT reuptake

Building on the observed regional dynamics of 5-HT release, I next examined how 5-HT clearance in the striatum is mediated by monoamine transporters, particularly SERT and DAT.

When SERT was blocked by the SSRI citalopram, evoked 5-HT signals became both larger in amplitude and slower to decay. This effect not only aligns with expectations for SERT inhibition but also further corroborates the specificity of the $GRAB_{5\text{-}HT}$ sensor for 5-HT. Notably, the increase in peak amplitude during 5p stimulation is likely influenced by the pharmacological inhibition of reuptake by citalopram, which prolongs extracellular 5-HT availability and enhances summation across pulses. It is therefore important to distinguish sensor limitations from the effects of citalopram on synaptic dynamics. Specifically, previous characterization has shown that $GRAB_{5\text{-}HT3.0}$ exhibits an on rate (τ_{on}) of approximately 0.25 s when locally puffing 10 μM 5-HT, and an off rate (τ_{off}) of about 1.66 seconds upon application of the $5\text{-}HT_4$ receptor antagonist RS 23597-190 (100 μM) in the continued presence of 5-HT (Deng et al., 2024). This relatively slow clearance of signal likely causes temporal summation of sensor activation during repeated stimulation, particularly under conditions where extracellular 5-HT clearance is pharmacologically impaired. Therefore, the increase in 5p peak amplitude under SSRI may not solely reflect enhanced release per se, but also the integration of lingering 5-HT signal due to delayed sensor deactivation. This further supports the conclusion that $GRAB_{5\text{-}HT}$ is a valid reporter of extracellular 5-HT and that its signal dynamics are closely tied to serotonergic uptake mechanisms.

Further, to probe the role of DAT in 5-HT reuptake, I applied a widely used DAT inhibitor nomifensine at a concentration of 2 μM (Condon et al., 2019). This dosage was chosen to achieve preferential DAT blockade, based on its reported K_i values of 26 nM for DAT and ~4000 nM for SERT, and IC_{50} values of 48 nM for DAT versus 830 nM for SERT in rat brain

synaptosomes (Katz et al., 2010; Tuomisto, 1977). Unlike SERT inhibition, DAT blockade had a selective effect: it prolonged decay half-life and increased AUC without significantly altering peak amplitude. One possible explanation is that blocking DAT increases extracellular DA after stimulation, which in turn activates D_2 receptors to indirectly suppress 5-HT release (more details in Chapter 4). This outcome is also consistent with previous evidence indicating that 5-HT can be taken up by DA axons and co-released with DA (F.-M. Zhou et al., 2005), further suggesting a functional interplay between serotonergic and dopaminergic clearance mechanisms.

Together, these findings indicate that both SERT and DAT contribute to striatal 5-HT reuptake. This dual-transporter mechanism may be particularly relevant in conditions such as drug addiction or depression, where transporter function is altered, and monoamine dynamics are disturbed. Understanding the relative contributions of these transporters helps inform pharmacological strategies targeting serotonergic systems in such disorders.

3.4.4 ACh acting at nAChRs to regulate 5-HT release is in a brain-region-dependent manner

I next investigated how local cholinergic signalling - particularly through nAChRs - modulates 5-HT release. My results using the nAChR antagonist DHβE revealed striking region-specific differences between DLS and NAcC. In DLS, DHβE significantly reduced 5-HT release evoked by 1p stimulation and the early pulses of 5p trains at low frequency (2 Hz) but had no significant effect on 5p-evoked responses at higher frequencies (25-100 Hz). This resulted in a pronounced increase in the 5p:1p ratio, suggesting that ACh acting at nAChRs may facilitate low-frequency 5-HT release in DLS, but this influence diminishes during high-frequency stimulation. By contrast, in the NAcC, DHβE had no significant effect on 1p-evoked release, but significantly increased 5p-evoked 5-HT signals starting from 25 Hz, likewise producing elevated 5p:1p ratios.

These data reveal an opposing frequency-dependent modulation pattern in NAcC, where nAChRs appear to constrain, rather than support, multi-pulse serotonergic responses.

Rather than indicating a strictly inhibitory or facilitatory role, these findings suggest that nAChR-mediated regulation of 5-HT release is both brain-region and frequency dependent. This mirrors prior observations in dopaminergic transmission: for instance, it has been reported that nAChRs facilitate low-frequency DA release in the dorsal striatum but inhibit high-frequency release, possibly via depolarization block or reduced axonal excitability (Rice & Cragg, 2004; Threlfell et al., 2012).Specifically, same paper showed that this frequency dependence is more pronounced in the DLS, whereas in the NAcC nicotinic regulation is less sensitive to high-frequency stimulation, reflecting differences in receptor subunit composition (Threlfell & Cragg, 2011).

Importantly, the observed effects may not solely reflect direct cholinergic modulation of serotonergic axons. Previous studies have shown that striatal DA release is also tightly regulated by nAChRs in a region- and frequency-specific manner (Brimblecombe et al., 2018; Rice & Cragg, 2004; Threlfell & Cragg, 2011). Given that DA itself can also modulate 5-HT transmission via D_1Rs and D_2Rs (see Chapter 4), the impact of DHβE likely reflects a combination of direct and indirect mechanisms. For example, in DLS, blocking nAChRs reduces 1p-evoked DA release, which may disinhibit 5-HT release via D_2Rs. Therefore, the effect of DHβE on 5-HT release described in this Chapter represents a composite of direct ACh modulation of 5-HT and indirect DA-mediated regulation. In future studies, to disentangle the pure impact of nAChRs on 5-HT axons, it will be essential to further isolate this pathway - for instance, by pharmacologically blocking DA receptors to eliminate DA's influence on 5-HT release.

Supporting the relevance of cholinergic regulation, recent work by Matityahu et al. (2024) demonstrated that synchronous activation of striatal ChIs induces local 5-HT release via volume

transmission (Matityahu et al., 2024). While this may reflect direct modulation of 5-HT axons, it is also plausible that ChI-driven activation of dopaminergic axons could lead to the release of 5-HT previously taken up into these axons. Previous study has reported that dopaminergic axons are known to accumulate and re-release 5-HT (F.-M. Zhou et al., 2005) with DA. At present, it remains unclear whether 5-HT axons within the striatum express functional nAChRs. This mechanism is enhanced in a hypercholinergic striatum in a mouse model of OCD-like behaviour, suggesting that ChIs critically shape serotonergic tone under both physiological and pathological conditions. These findings align with our own observations and further highlight that local ACh levels can modulate 5-HT output across striatal subregions, potentially in a behaviourally relevant manner.

3.4.5 Tonic GABAergic inhibition of 5-HT release

To investigate whether GABAergic signalling exerts tonic control over striatal 5-HT transmission, I examined the effects of bath-applied $GABA_A$ and $GABA_B$ receptor antagonists (bicuculline and CGP55845, respectively) on single-pulse release. Blocking GABA receptors significantly increased the peak amplitude and AUC of electrically evoked 5-HT signals in DLS, indicating that GABAergic inputs exert an inhibitory influence on striatal 5-HT release. However, the 5p:1p ratio remained unchanged, suggesting that the frequency dependence of 5-HT release is not altered, and that the tonic inhibition by GABA affects the overall magnitude rather than the short-term dynamics of release.

These findings are consistent with the idea of a tonic GABAergic inhibition of monoamine release in the striatum. A similar concept has been demonstrated for both DA and ACh transmission: previous studies showed that GABA receptor antagonism enhances ACh and DA levels in the striatum (DeBoer & Westerink, 1994; Lopes et al., 2019). Since the striatum is

densely GABAergic and contains ongoing ambient GABA tone, it is plausible that serotonergic axons or upstream regulatory neurons are similarly suppressed under basal conditions.

Multiple cellular pathways may underlie this GABAergic inhibition of striatal 5-HT I reported in this Chapter. On one hand, GABA may act directly on 5-HT axons, suppressing vesicular release via $GABA_A$ or $GABA_B$ receptors, as has been proposed for other monoaminergic systems. On the other hand, GABA may act indirectly through intermediary neurons that control serotonergic output, for example via ChIs or DA neurons that provide feedback to 5-HT axons. Since the potential contribution of ACh was already considered in this experiment by applying DHβE to block nAChRs, the indirect effect of GABA via ACh was minimized. However, the influence of GABA on DA release was not controlled in this context, leaving open the possibility that part of the effect on 5-HT was mediated via GABA–DA–5-HT interactions. In particular, dopaminergic axons are known to be under tonic GABAergic inhibition, and a previous study showed that GABA receptor antagonism increases DA levels in the striatum, which subsequently activate DA receptors and modulate downstream neurotransmission (Lopes et al., 2019). Given the established role of DA in modulating 5-HT release (see Chapter 4), it is conceivable that some of the GABAergic effects on 5-HT described here are mediated via disinhibition of DA. Therefore, the observed increase in 5-HT release following GABA receptor blockade likely reflects a composite effect, including direct disinhibition of 5-HT axons and indirect enhancement via GABA–DA–5-HT interactions.

To disentangle these pathways, future experiments could employ pharmacological or genetic tools to selectively block DA receptors (e.g., D_1R and D_2R antagonists) during GABA receptor manipulation, thereby isolating the direct GABAergic influence on serotonergic axons. Such work would be crucial for understanding how inhibitory microcircuits regulate striatal 5-HT levels, especially in disease contexts such as Parkinson’s disease and mood disorders, where GABA, DA, and 5-HT signalling are often disrupted.

Chapter 4.

Identifying the modulation of 5-HT release by DA receptors

4.1 Introduction

The striatum is a critical integrative hub within the basal ganglia, coordinating motor, cognitive, and reward-related processes. These functions are tightly regulated by neuromodulators, such as DA, ACh, GABA and 5-HT. While extensive research has delineated the role of DA in modulating striatal ACh transmission, the influence of DA on striatal 5-HT release remains relatively underexplored. Several earlier studies using techniques such as microdialysis, FCV and immunohistochemistry have reported that 5-HT levels or 5-HT receptor levels are regulated, at least in part, by dopaminergic signalling (Bang et al., 2020; Ferré et al., 1994; Laprade et al., 1996; Van Bockstaele & Pickel, 1993; F.-M. Zhou et al., 2005). However, despite these important insights, the experimental tools available at the time imposed significant limitations on temporal and spatial resolution.

To overcome these limitations and directly assess the modulation of 5-HT release by striatal DA, I used the genetically encoded 5-HT sensor - $GRAB_{5\text{-}HT3.0}$ (Deng et al., 2024) - in acute brain slices. This tool allows for real-time imaging of extracellular 5-HT release with high temporal and spatial resolution, enabling a more precise dissection of neuromodulatory mechanisms. Specifically, I investigated whether D_1R and D_2R individually influences 5-HT release in the DLS.

4.1.1 DA receptors and distribution in striatum

DA exerts its effects via two major classes of G protein-coupled receptors (GPCRs): the D_1-like receptors (D_1R and D_5R) and the D_2-like receptors (D_2R, D_3R, and D_4R) (Aghajanian et al., 1978; Beaulieu et al., 2015; Kebabian & Calne, 1979; Martel & Gatti McArthur, 2020). Receptors within each family share high sequence homology, which allows for reliable pharmacological discrimination between D_1-like and D_2-like receptors but makes it difficult to achieve selectivity between subtypes within the same family (Beaulieu & Gainetdinov, 2011; Vallone et al., 2000).

D_1-like receptors generally exhibit lower affinity for DA compared to D_2-like receptors - by approximately 10- to 100-fold - indicating that their recruitment is more prominent during periods of elevated extracellular DA levels, such as during phasic DA release (Martel & Gatti McArthur, 2020). Structurally, D_1-like receptors have seven transmembrane domains and signal via $G\alpha_{s/olf}$ proteins to stimulate adenylyl cyclase and elevate intracellular cAMP (Beaulieu et al., 2015; Beaulieu & Gainetdinov, 2011). The genes encoding D_1R and D_5R (DRD_1 and DRD_5) are intronless (Gingrich & Caron, 1993), and both subtypes are expressed post-synaptically. Among them, D_1R is more abundantly distributed, with high expression in the striatum, substantia nigra pars compacta (SNc), cortex, hippocampus, and amygdala (Beaulieu & Gainetdinov, 2011; Grandy et al., 1990; Vallone et al., 2000), while D_5R is found in the SNc, cortex, hippocampus, hypothalamus, and dentate gyrus.

D_2-like receptors also possess seven transmembrane domains, but they couple to $G\alpha_{i/o}$ proteins to inhibit adenylyl cyclase and reduce intracellular cAMP levels (Beaulieu et al., 2015; Beaulieu & Gainetdinov, 2011; Martel & Gatti McArthur, 2020). Unlike D_1Rs, D_2-like receptors are located both pre- and post-synaptically. In particular, D_2R functions as an autoreceptor on dopaminergic axons, regulating DA synthesis and release, and also acts post-synaptically on striatal neurons (Beaulieu & Gainetdinov, 2011), In rodents, the D_2R gene undergoes alternative splicing to generate two isoforms: D_2S (short), predominantly presynaptic, and D_2L (long), more common post-synaptically. Similarly, D_3R and D_4R exhibit splice and polymorphic variants in rodents and humans, respectively (Giros et al., 1991; Tol et al., 1992). Among the D_2-like receptors, D_2R has the highest expression in the brain, notably in the striatum, SNc, VTA, cortex, and hypothalamus (Beaulieu & Gainetdinov, 2011). D_3Rs are localized in the nucleus accumbens shell, hypothalamus, and cerebellum, while D_4Rs are found in the prefrontal cortex, hippocampus, and substantia nigra pars reticulata (Beaulieu & Gainetdinov, 2011; Vallone et al., 2000).

In addition to canonical signalling, DA receptors can form functional heterodimers. For example, D_1R can dimerize with D_2R, or with other neurotransmitter receptors such as adenosine A_1 or NMDA receptor subunits, forming D_1-A_1 or D_1-NR_1 complexes (Beaulieu et al., 2015; Perreault et al., 2014). These interactions add an additional layer of complexity and flexibility to dopaminergic signalling.

In the striatum, DA receptor-mediated modulation contributes critically to the control of neurotransmitter release, neuronal excitability and plasticity. D_1Rs are primarily expressed on direct-pathway medium spiny neurons (dMSNs), where their activation promotes excitability and output to basal ganglia motor circuits. Conversely, D_2Rs are enriched on indirect-pathway MSNs (iMSNs) and various interneurons, where they exert inhibitory control (Gerfen & Surmeier, 2011; Tritsch & Sabatini, 2012). The differential localization and intracellular coupling of D_1R and D_2R enable DA to exert bidirectional and circuit-specific effects.

While their role in modulating GABAergic and cholinergic transmission in the striatum has been extensively characterized, it remains largely unknown how D_1R and D_2R signalling influences serotonergic activity in this region. recent findings have demonstrated that DRN 5-HT neurons express both D_1 and D_2 dopamine receptors (Cai et al., 2022). Given the anatomical convergence of DA and 5-HT axons in the striatum and their reciprocal involvement in various neuropsychiatric disorders, understanding the DA receptor-specific regulation of striatal 5-HT release is of both mechanistic and therapeutic importance.

4.1.2 Dopaminergic regulation of ACh release: a benchmark model

A foundational example of the neuromodulatory capacity of DA is its ability to regulate striatal ACh release via D_2Rs. In the striatum, DA exerts inhibitory control over ChIs through D_2Rs expressed directly on these interneurons. Electrophysiological and optical recording studies

have demonstrated that D_2R activation reduces ChI firing and suppresses evoked ACh release (Alcantara et al., 2003; Lim et al., 2014; Maurice et al., 2004). For example, Lim et al. (2014) used optogenetics and microdialysis to show that D_2R agonists such as quinpirole reduced tonic ACh levels and phasic evoked responses in both dorsal and ventral striatum.

DA acting at D_2R downregulating ACh pathway has become a canonical model of neuromodulator interaction and provides an important conceptual foundation for examining whether DA might exert similar control over striatal 5-HT. Notably, the serotonergic innervation of the striatum, arising primarily from the DRN, is anatomically and functionally poised to interact with dopaminergic and cholinergic systems. However, the direct influence of DA on 5-HT release dynamics, particularly via D_1R and D_2R activation, remains to be fully characterized.

4.1.3 Rationale for investigating striatal DA modulation of 5-HT

Anatomically, 5-HT fibres from the dorsal raphe nucleus densely innervate the striatum and are positioned to interact with dopaminergic axons and their postsynaptic targets(Mori et al., 1985; Törk, 1990). Moreover, DA receptor expression is not restricted to dopaminergic neurons; previous studies suggest that D_1Rs and D_2Rs may be present on, or indirectly influence, 5-HT axons (Azmitia & Segal, 1978; De Deurwaerdère & Di Giovanni, 2017). These receptors could theoretically regulate 5-HT release via direct mechanisms - such as presynaptic receptor localization on serotonergic afferents - or through indirect pathways involving GABAergic or cholinergic interneurons. Functionally, both DA and 5-HT have been shown to regulate reward-related behaviour, motivation, and affect, often through complex and region-specific interactions (Daw et al., 2002; Di Giovanni et al., 2008). However, despite extensive study of DA - 5HT crosstalk in midbrain structures like the VTA and raphe, far less is known about how DA modulates 5-HT at the axonal level in striatum.

Therefore, in this chapter, I investigated how D_1R and D_2R activation or inhibition modulates striatal 5-HT release using a real-time detection of extracellular 5-HT sensor (Deng et al., 2024) - $GRAB_{5\text{-}HT}$ - in acute striatal slices. To determine whether DA receptor signalling modulates 5-HT release in a receptor-specific manner, I applied selective D_1R and D_2R agonists and antagonists while blocking nAChR-mediated cholinergic input with DHβE. This approach was designed to minimise cholinergic influences on dopaminergic axons, thereby allowing a clearer assessment of how D_1R and D_2R activation independently affect serotonergic transmission in the DLS.

4.2 Methods

4.2.1 Animals and slice preparation

Male and female wild-type C57BL/6J mice were culled by cervical dislocation and acute *ex vivo* brain slices were prepared as described in Chapter 2. All procedures were performed in accordance with institutional guidelines and the U.K. Animals (Scientific Procedures) Act, 1986.

4.2.2 Stereotaxic intracranial injections

Stereotaxic intracranial injections were performed to achieve viral transfection of an adeno-associated virus (AAV) containing the 5-HT3.0 genetically encoded fluorescent sensor (Deng et al., 2024). C57BL/6 wild type mice were anaesthetized with 4% isoflurane (IsoFlo, Zoetis) in 100% O_2, at a flow rate of ~2 L/min. Fur on the scalp was shaved, and mice were transferred to a stereotaxic frame (David Kopf Instruments). Isoflurane concentration was lowered to 1.5 – 2% for maintenance anesthesia. An incision was made along the scalp and stereotaxic coordinates were set relative to bregma, for injection in DLS (A/P: + 0.65, M/L: +/- 2.2, D/V: -2.7 to -2.5). Undiluted AAV2/5-hsyn-5-HT3.0 ($\geqslant$ 2.00 x 10^{12} genome copies per ml) (BrainVTA, China) was

infused bilaterally, with a Hamilton syringe and 32 gauge needle (Hamilton Company) at a rate of 200 nL/minute, for a total volume of 1000 nL per site. The needle was left *in situ* for 5 minutes post injection. The incision was closed using suture (Monocryl, Ethicon) and skin glue (Vetbond, 3M), and mice were transferred to a temperature-controlled cage to recover from anesthesia. Mice were culled for experiments 3-4 weeks post-surgery.

4.2.3 $GRAB_{5\text{-}HT}$ imaging

For $GRAB_{5\text{-}HT}$ imaging experiments involving electrical stimulation, recordings were conducted as detailed in Chapter 2. The camera was set to an exposure rate of 100 ms with 2×2 pixel binning. Excitation was provided by a continuously illuminated blue LED (470 nm) at an intensity of approximately 4 mW for a duration of 40 seconds for each recording, allowing the detection of each 5-HT release event. These acquisition parameters enabled the resolution of individual release events during train stimulations, depending on the off kinetics of the sensor. Data extraction and processing followed the methods described in Chapter 2.

In all experiments involving electrical stimulation, stimulation protocols were performed in duplicate, and the order of stimuli was randomized. Each experimental group included at least four animals ($N \geqslant 4$). Statistical significance was evaluated using two-way ANOVA, Student's t-test, and regression analysis in GraphPad Prism 10.

4.2.4 Drugs

Drugs were diluted in either dH_2O or DMSO (dymethil sulfoxide) to 1,000x stock aliquots and stored at -20 °C. Final drug concentrations were prepared in aCSF saturated with 95% O_2/ 5% CO_2 right before use.

Drug	Supplier	Action	Concentration	Solvent	References
Dihydro-β-erythroidine (DHβE) hydrobromide	Sigma-Aldrich	nAChR antagonist	1 μM	dH_2O	Threlfell et al. (2012); Roberts et al. (2020)
SKF81297 hydrobromide	MedChem Express (MCE)	D_1R agonist	1 μM	DMSO	Nesbit et al. (2022) Reavill et al. (1993)
SCH39166 hydrobromide	Tocris	D_1R antagonist	1 or 10 μM	DMSO	Zheng et al. (1999) Yang et al. (2020)
Quinpirole	Cambridge Bioscience	D_2R agonist	2 μM	DMSO	Brimblecombe et al. (2019)
L-741,626	Abcam	D_2R antagonist	1 or 2 μM	DMSO	Condon et al. (2019)

4.2.5 Data acquisition and analysis

GRAB sensor data were acquired and extracted by Image J and analyzed by locally written MATLAB script described in Section 2.3.5. Statistical tests were performed in GraphPad Prism 10.

4.3 Results

4.3.1 Striatal 5-HT is under regulation by DA via D_1Rs

4.3.1.1 Agonism of D_1R – SKF81297 augmented striatal 5-HT release

We first investigated the impact of D_1 receptor agonist SKF81297 on evoked 5-HT release in DLS in acute coronal slices of mouse striatum, using $GRAB_{5\text{-}HT3.0}$ to detect 5-HT released by electrical stimulus pulses delivered singly (1p) or in short trains of 5-pulses (5p) at 2 Hz and 100 Hz (**Fig. 4.1A**). To mimic physiologically relevant firing patterns of 5-HT neurons, we applied 5p stimulation at 2 Hz and 100 Hz, which approximate the tonic and burst firing frequencies, respectively, observed in serotonergic neurons *in vivo* (Mlinar et al., 2016). As we know from

Chapter 3 that striatal 5-HT is under control of ACh via nAChR in both DLS and NAcC, we excluded the indirect regulation from cholinergic circuits of DA/ACh on 5-HT by including nAChR antagonist DHßE throughout.

In DLS, the application of SKF81297 (1 μM) significantly increased $[5\text{-HT}]_o$ evoked by a single pulse and during five-pulse trains at both 2 Hz and 100 Hz, by approximately 125% of the pre-drug condition (**Fig. 4.1B-D**; $F_{(1,14)} = 18.93$, $p = 0.0007$, RM ANOVA main effect of the drug). SKF81297 significantly augmented the AUC of 5-HT transients, intriguingly prolonging the extracellular lifetime of 5-HT to ~160% of the pre-drug condition (**Fig. 4.1E**). Correspondingly, application of SKF81297 increased the decay half-life of $[5\text{-HT}]_o$ in DLS (**Fig. 4.1F**; $F_{(1,10)} = 18.75$, $p = 0.0015$, RM ANOVA main effect of the drug). In the presence of DHßE, the application of SKF81297 did not modify 5p:1p ratio of $[5\text{-HT}]_o$ in DLS (**Fig. 4.1G**; $F_{(1,28)} = 0.1715$, $p = 0.68$, RM ANOVA main effect of the drug). These findings indicated that the activation of D_1Rs by D_1R agonist SKF81297 increases 5-HT release probability, and this regulation is independent of ACh acting at nAChRs.

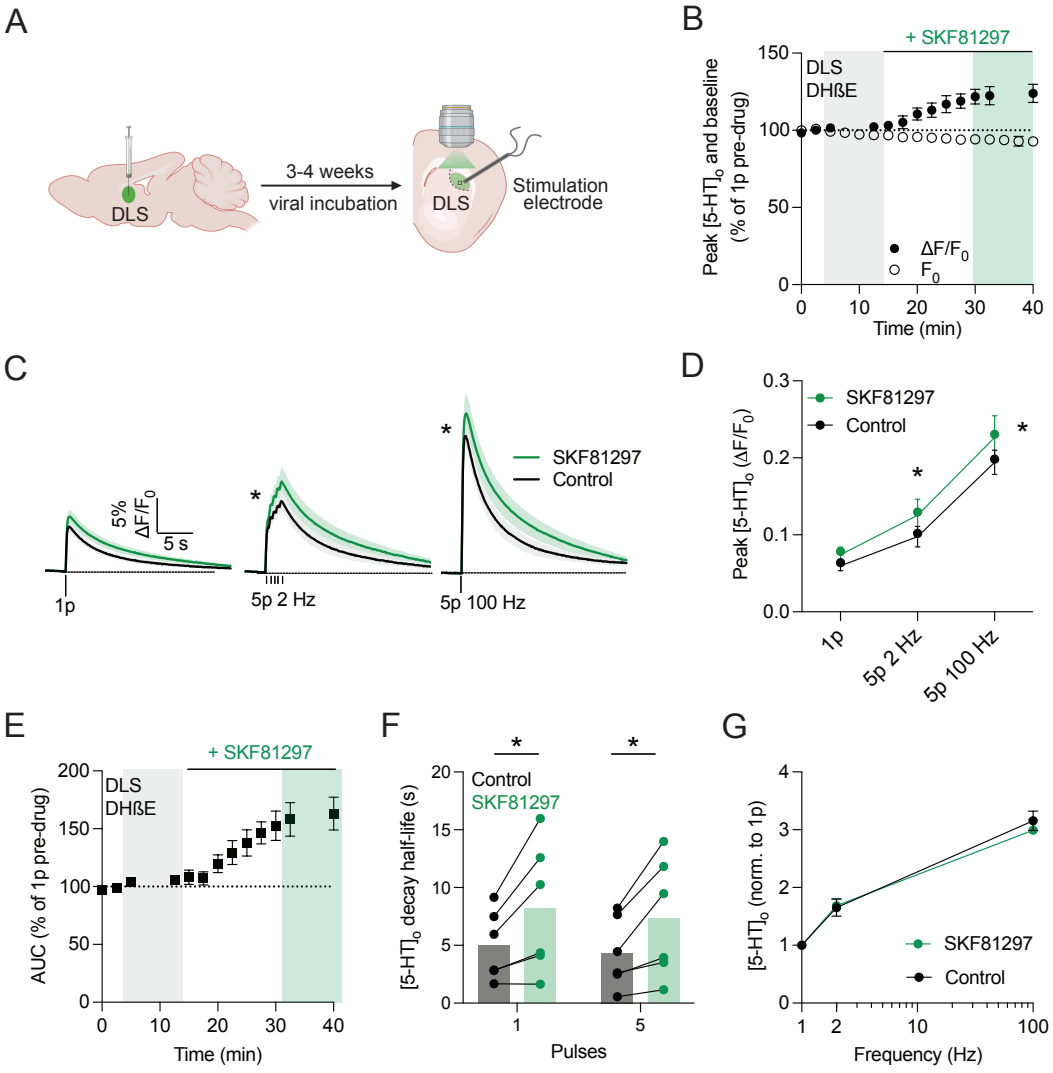

Figure 4.1. Agonism of D_1Rs facilitates striatal 5-HT release. (A) Viral delivery of $GRAB_{5\text{-}HT}$ to striatum for imaging extracellular 5-HT levels *ex vivo* and the schematic of stimulation and $GRAB_{5\text{-}HT}$ recording site. **(B)** Normalized mean peak $[5\text{-HT}]_o$ and baseline fluorescence (F_0) during consecutive recordings of 5-HT release evoked by 1p during application of SKF81297 in the presence of DHßE in DLS (*n* = 5 experiments/3 mice). **(C)** Mean evoked 5-HT transients ± SEM, before (black) and after (green) application of SKF81297 in the presence of DHßE in DLS. Mean transients of $[5\text{-HT}]_o$ are derived from three timepoints prior to the application of SKF81297 (grey shaded region) and last two timepoints (green shaded region). **(D)** Mean 1p, 5p 2 Hz and 5p 100 Hz $[5\text{-HT}]_o$ peak of control conditions (black) and following drug application (green) in DLS in the presence of DHßE. **(E)** Normalized mean AUC $[5\text{-HT}]_o$ during consecutive recordings of 5-HT release evoked by 1p during the application of SKF81297 in DLS. **(F)** Mean 1p and 5p 100 Hz decay half-life of $[5\text{-HT}]_o$ under control conditions (grey) and following drug application (green) in DLS. **(G)** Normalized mean $[5\text{-HT}]_o$ of 5p at 2 Hz and 100 Hz to 1p (5p/1p) in control (black) and in drug conditions (green) in the presence of DHßE in DLS. 2-way ANOVA, Fisher's LSD post-*hoc* test. **p* < 0.05. Error bars are ± SEM.

4.3.1.2 Antagonist of D_1R blocked the effect of D_1R agonist on 5-HT release

To corroborate the effect of SKF81297 on evoked $[5\text{-HT}]_o$ detected with $GRAB_{5\text{-HT}}$ is mediated by D_1Rs, we then used a competitive D_1R antagonist – SCH39166 (10 μM) to block the effect of SKF81297. The hypothesis is that if the high concentration of D_1R antagonist abolished the facilitatory effect that SKF81297 caused, then we can confirm this is a D_1R-mediated control on striatal 5-HT release. In the presence of SCH39166 (10 μM) and DHßE (1 μM), we found application of the same concentration of SKF81297 (1 μM) failed to cause any $[5\text{-HT}]_o$ peak change by either a single pulse or a five-pulse train at 100 Hz in DLS (**Fig. 4.2A-C**; $F_{(1,12)}$ = 0.001734, p = 0.97, RM ANOVA main effect of the drug). Correspondingly, the AUC of $[5\text{-HT}]_o$ did not increase when applying SKF81297 in the presence of SCH39166 (**Fig. 4.2D**). Similarly, with the presence of DHßE, the 5p:1p ratio of $[5\text{-HT}]_o$ remained at a similar level before and after washing on SKF81297 (**Fig. 4.2E**; $t_{(4)}$ = 1.383, p = 0.2607, Student's paired t-test). Altogether, these data suggest that the D_1R agonist SKF81297 - control of striatal 5-HT transmission is mediated by D_1Rs in DLS, which can be completely abolished by the D_1R antagonist. Additionally, this effect does not require the function of nAChRs in striatum.

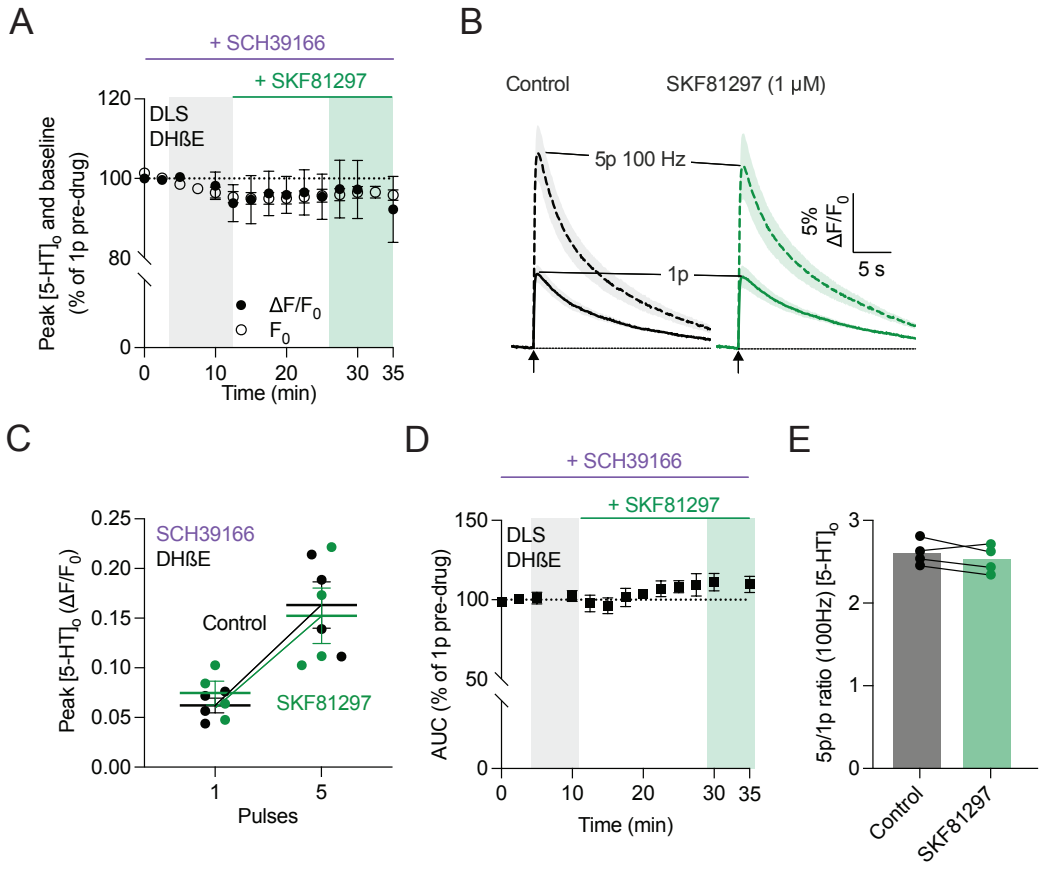

Figure 4.2. Antagonism of D_1R blocked the D_1R agonism-mediated facilitation of striatal 5-HT release. (A) Normalized mean peak $[5\text{-HT}]_o$ and baseline fluorescence (F_0) during consecutive recordings of 5-HT release evoked by 1p during application of SKF81297 in the presence of DHßE and SCH39166 in DLS ($n = 4$ experiments/3 mice). **(B)** Mean evoked 5-HT transients ± SEM, before (black) and after (green) application of SKF81297 in DLS in the presence of DHßE and SCH39166. Mean transients of $[5\text{-HT}]_o$ are derived from three timepoints prior to the application of SKF81297 (grey shaded region) and last two timepoints (green shaded region). **(C)** Mean 1p and 5p 100 Hz $[5\text{-HT}]_o$ peak of control conditions (black) and following drug application (green) in DLS in the presence of DHßE and SCH39166. **(D)** Mean $[5\text{-HT}]_o$ AUC of control conditions (grey) and following drug application (green) in the presence of DHßE and SCH39166 in DLS. **(E)** Ratios of peak $[5\text{-HT}]_o$ released by 5p versus 1p in DLS in the presence of DHßE and SCH39166. 2-way ANOVA, Fisher's LSD post-*hoc* test, Student's paired t-test. Error bars are ± SEM.

4.3.1.3 Effect of D_1R agonist CY208243 on striatal 5-HT release

To further corroborate that the effect SKF81297 was due to D_1R action, I performed the same experiment with an alternative D_1R agonist – CY208243. In DLS, application of the D_1R agonist CY20843 (10 µM) resulted in a significant reduction in extracellular 5-HT levels evoked by both

single-pulse and five-pulse stimulations delivered at 2 Hz and 100 Hz (**Fig. 4.3A-C**; $F_{(1,12)}$ = 22.26, $p < 0.001$, RM ANOVA main effect of the drug). Compared to pre-drug baseline, the peak response decreased to approximately 68% of the pre-drug level. Alongside this effect, CY20843 also modestly diminished the AUC of $[5\text{-HT}]_o$ evoked by 5p at 100 Hz, reducing the integrated extracellular presence of 5-HT especially to roughly 70% of control levels (**Fig. 4.3D**; $F_{(1,24)}$ = 1.780, $p = 0.19$, RM ANOVA main effect of the drug). However, the ratio of five-pulse to single-pulse responses remained unaffected by the drug in the presence of DHβE (**Fig. 4.3E**; $F_{(1,24)}$ = 3.52e-005, $p > 0.99$), indicating that CY20843 alters release magnitude without changing short-term dynamics. Together, these results suggest that D_1R activation by CY20843 suppresses 5-HT release in the DLS, independently of cholinergic modulation through nAChRs.

However, the outcome observed with 10 μM CY208243 appeared to contradict the effects previously seen with SKF81297, which robustly enhanced striatal 5-HT release via D_1R activation. In contrast, 10 μM CY208243 produced a suppressive effect on 5-HT transmission, raising the possibility that this concentration may have triggered off-target effects. In other words, this concentration may have exceeded the optimal window for specific D_1R activation, introducing pharmacological complexity. To address this concern, we repeated the same set of experiments using a lower concentration of CY208243 in 1 μM, aiming to assess whether a more selective activation of D_1Rs would replicate the facilitatory effect seen with SKF81297.

In DLS, application of the D_1 receptor agonist CY20843 at a lower concentration (1 μM) did not significantly alter $[5\text{-HT}]_o$ levels evoked by either single-pulse or five-pulse stimulations delivered at 2 Hz and 100 Hz (**Fig. 4.4A-C**; $F_{(1,12)}$ = 0.02316, $p = 0.88$, RM ANOVA main effect of the drug). Unlike the suppressive effect observed with 10 μM CY20843, the peak response following 1 μM CY208243 drug application remained at a similar level of the pre-drug condition, indicating no measurable change in evoked 5-HT amplitude. Consistently, CY20843 at 1 μM did

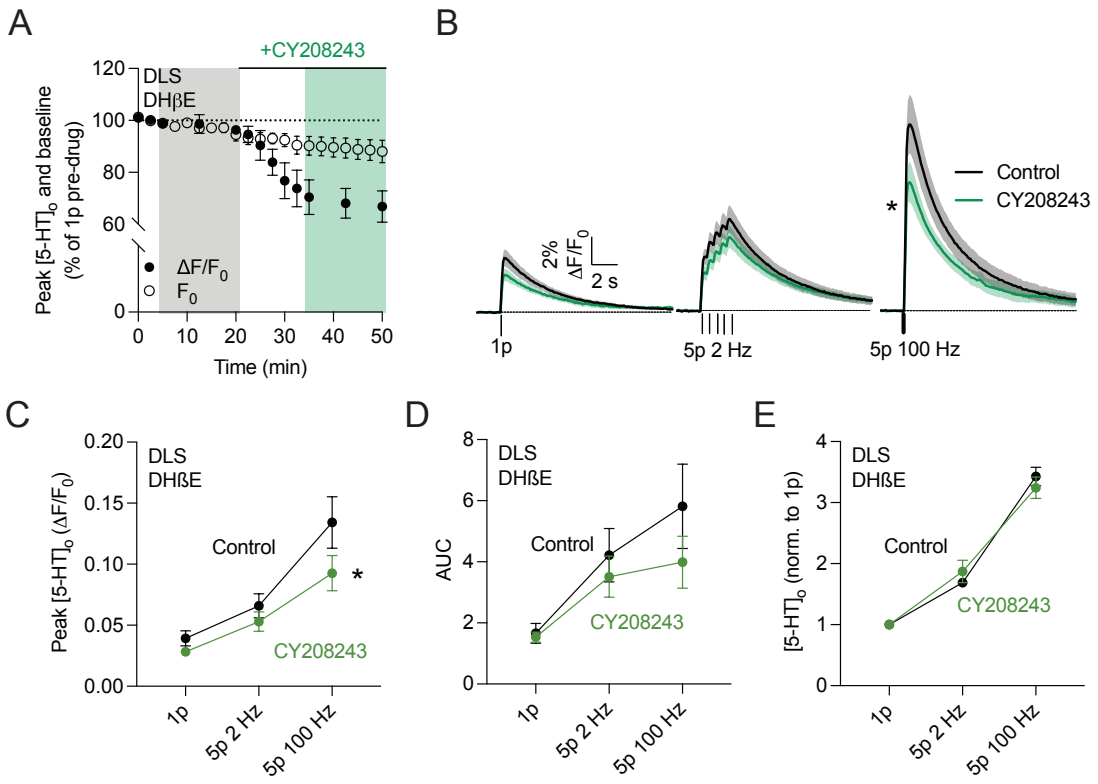

Figure 4.3. 10 µM CY208243 attenuated striatal 5-HT release. (A) Normalized mean peak $[5\text{-HT}]_o$ and baseline fluorescence (F_0) during consecutive recordings of 5-HT release evoked by 1p during application of 1 µM CY208243 in the presence of DHßE in DLS (n = 4 slices in 3 mice). **(B)** Mean evoked 5-HT transients ± SEM, before (black) and after (green) application of 1 µM CY208243 in DLS in the presence of DHßE. Mean transients of $[5\text{-HT}]_o$ are derived from three timepoints prior to the application of CY208243 (grey shaded region) and last two timepoints (green shaded region). **(C)** Mean 1p and 5p at 2 Hz and 100 Hz $[5\text{-HT}]_o$ peak of control conditions (black) and following drug application (green) in DLS in the presence of DHßE. **(D)** Mean $[5\text{-HT}]_o$ AUC of control conditions (grey) and following drug application (green) in the presence of DHßE in DLS. **(E)** Ratios of peak $[5\text{-HT}]_o$ released by 5p versus 1p in DLS before and after 1 µM CY208243 application in the presence of DHßE. 2-way ANOVA, Fisher's LSD post-*hoc* test, *p < 0.05, Error bars are ± SEM.

not affect the AUC of $[5\text{-HT}]_o$ evoked by 1p and 5p at 2 Hz or 100 Hz (**Fig. 4.4D**). The ratio of five-pulse to single-pulse responses (5p:1p) also showed no change when washing on CY208243 in the presence of DHβE (**Fig. 4.4E**; $F_{(1,12)}$ = 0.2198, p = 0.65), indicating that short-term facilitation dynamics were unaffected. These findings indicate that, at 1 µM, CY20843 does not modulate striatal 5-HT release in the DLS, in contrast to the concentration-dependent suppressive effects observed at 10 µM. This divergence suggests that CY208243 may engage different targets or downstream pathways at higher concentrations.

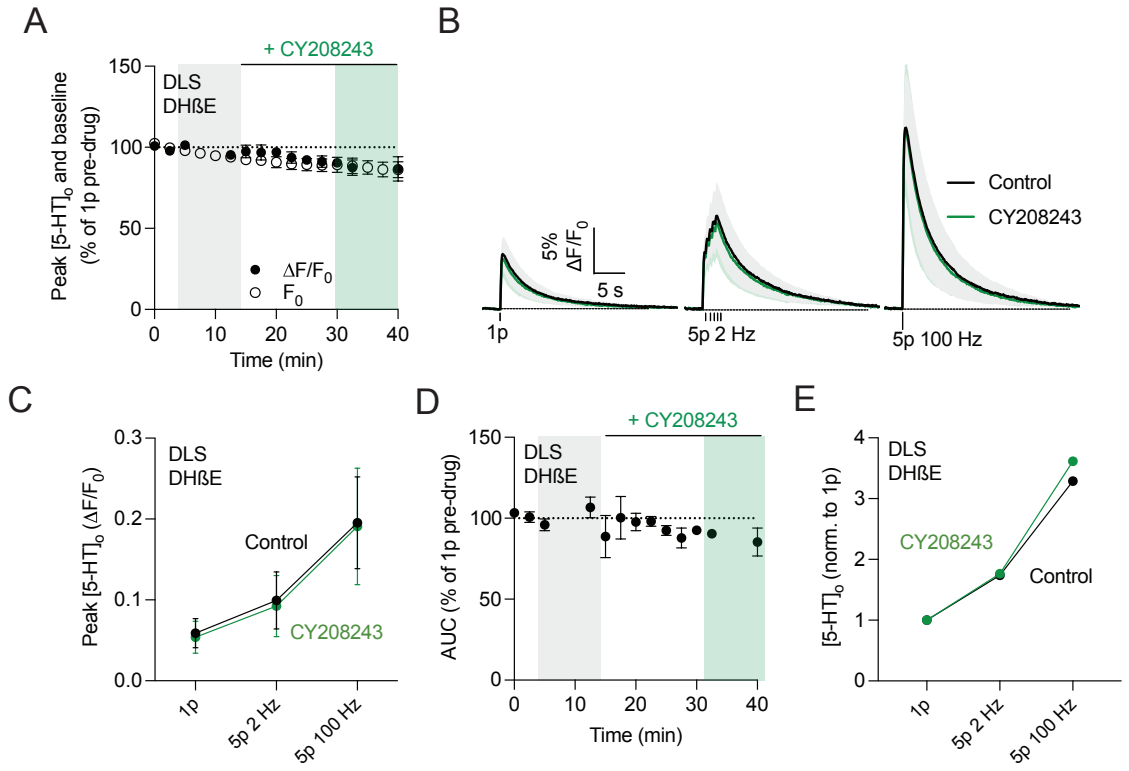

Figure 4.4. 1 µM of D_1R agonist CY208243 did not change striatal 5-HT release in DLS. **(A)** Normalized mean peak $[5\text{-HT}]_o$ and baseline fluorescence (F_0) during consecutive recordings of 5-HT release evoked by 1p during application of 1 µM CY208243 in the presence of DHßE in DLS (*n* = 3 experiments/2 mice). **(B)** Mean evoked 5-HT transients ± SEM, before (black) and after (green) application of 1 µM CY208243 in DLS in the presence of DHßE. Mean transients of $[5\text{-HT}]_o$ are derived from three timepoints prior to the application of CY208243 (grey shaded region) and last two timepoints (green shaded region). **(C)** Mean 1p and 5p at 2 Hz and 100 Hz $[5\text{-HT}]_o$ peak of control conditions (black) and following drug application (green) in DLS in the presence of DHßE. **(D)** Mean $[5\text{-HT}]_o$ AUC of control conditions (grey) and following drug application (green) in the presence of DHßE in DLS. **(E)** Ratios of peak $[5\text{-HT}]_o$ released by 5p versus 1p in DLS before and after 1 µM CY208243 application in the presence of DHßE. 2-way ANOVA, Fisher's LSD post-*hoc* test, Error bars are ± SEM.

4.3.1.4 D_1R antagonist did not change 5-HT release in DLS

We next sought to determine whether endogenous DA exerts a regulatory influence without externally activating D_1R. Specifically, we asked whether there is any dopaminergic tone, acting via D_1Rs, that contributes to the modulation of striatal 5-HT transmission. To address this, we applied a D_1R antagonist - SCH39166 - and examined whether blocking D_1R activity would

reduce 5-HT release, thereby revealing a role for endogenous DA in maintaining or facilitating serotonergic output. As previously discussed in Chapter 3, 5-HT release is modulated by ACh signalling via nAChRs. Therefore, to isolate the effect of DA receptor manipulation, all subsequent experiments were again conducted in the presence of DHβE to block nAChRs.

In DLS, application of the D_1 receptor antagonist SCH39166 at a concentration of 1 μM did not significantly alter $[5\text{-HT}]_o$ levels evoked by either single-pulse or five-pulse stimulations delivered at 2 Hz and 100 Hz (**Fig. 4.5A-C**; $F_{(1,24)} = 2.200$, $p = 0.15$, RM ANOVA main effect of the drug). Compared to the control condition, the peak amplitude of evoked 5-HT responses remained unchanged following SCH39166 application, indicating that blockade of D_1Rs under baseline conditions does not affect stimulus-evoked 5-HT release. Consistently, the AUC of $[5\text{-HT}]_o$ transients evoked by 1p also showed no significant difference before and after application of SCH39166 (**Fig. 4.5D**). Moreover, the ratio of five-pulse to single-pulse responses (5p:1p) remained unchanged when SCH39166 was washed on in the presence of DHβE (**Fig. 4.5E**; $F_{(1,24)} = 0.4081$, $p = 0.53$, RM ANOVA main effect of the drug), further confirming that short-term dynamics are not affected under these conditions.

Together, these results suggest that there is no detectable endogenous dopaminergic tone acting through D_1 receptors to regulate 5-HT release in DLS under these experimental conditions. Alternatively, it is also possible that blocking D_1Rs alone is insufficient to disrupt any existing dopaminergic influence on 5-HT transmission, implying that additional pathways or receptor subtypes may be involved.

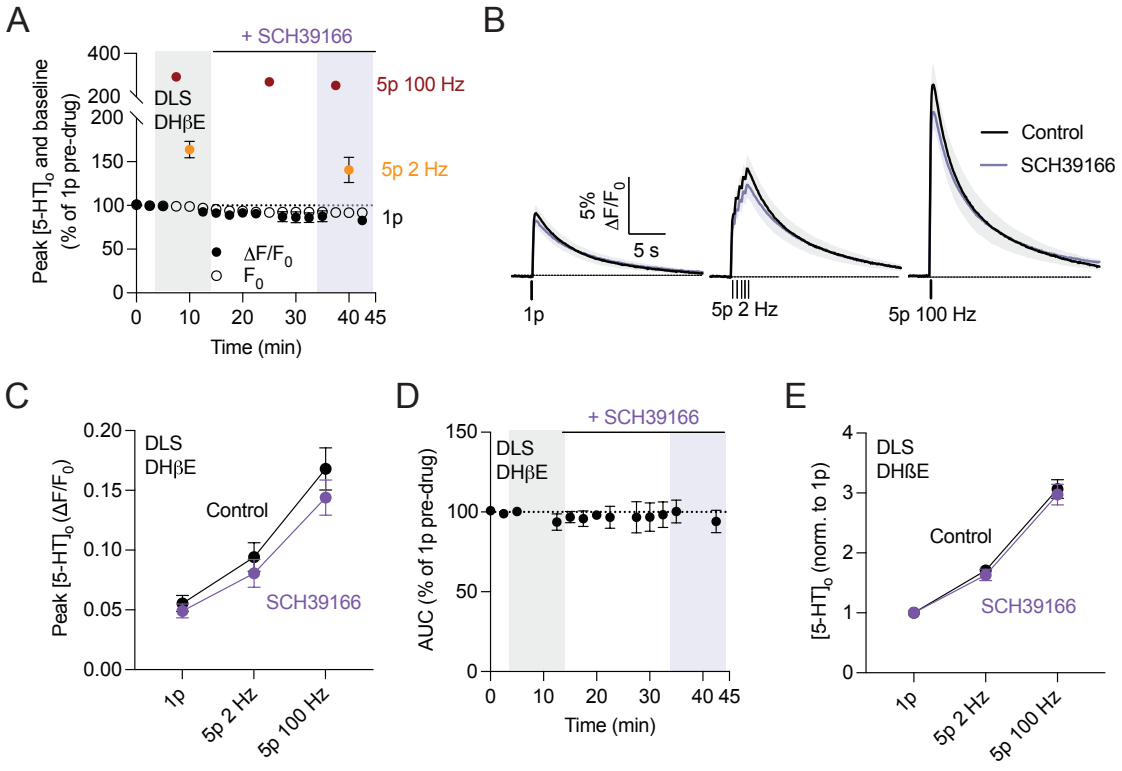

Figure 4.5. Antagonism of D_1R does not alter striatal 5-HT release. **(A)** Normalized mean peak $[5\text{-HT}]_o$ and baseline fluorescence (F_0) during consecutive recordings of 5-HT release evoked by 1p and 5p at 2 Hz and 100 Hz during application of SCH39166 in the presence of DHßE in DLS (*n* = 4 experiments/3 mice). **(B)** Mean evoked 5-HT transients ± SEM, before (black) and after (purple) application of SCH39166 in DLS in the presence of DHßE. Mean transients of $[5\text{-HT}]_o$ are derived from three timepoints prior to the application of SCH39166 (grey shaded region) and last two timepoints (purple shaded region). **(C)** Mean 1p, 5p 2 Hz and 5p 100 Hz $[5\text{-HT}]_o$ peak of control conditions (black) and following drug application (purple) in DLS in the presence of DHßE. **(D)** Mean $[5\text{-HT}]_o$ AUC of control conditions (grey) and following drug application (purple) in the presence of DHßE and SCH39166 in DLS. **(E)** Ratios of peak $[5\text{-HT}]_o$ released by 5p versus 1p at 2 Hz and 100 Hz in DLS in the presence of DHßE before (black) and after (purple) SCH39166 application. 2-way ANOVA, Fisher's LSD post-*hoc* test, Error bars are ± SEM.

4.3.2 Striatal 5-HT is under regulation by DA via D_2Rs

4.3.2.1 D_2R agonist quinpirole inhibited 5-HT release in DLS

In addition to D_1-like receptors, D_2-like receptors also play a critical role in dopaminergic modulation within the striatum. As the primary auto receptors for DA, D_2Rs regulate DA release and neuronal excitability, and are well-positioned to influence the interplay between the dopaminergic and serotonergic systems. Given their strategic localization and functional relevance, I next investigated whether activation of D_2Rs modulates 5-HT release in the striatum.

To assess whether D_2Rs regulate 5-HT release, I examined the effect of the D_2R agonist quinpirole (2 μM) on single-pulse (1p) and five-pulse at 2 Hz and 100 Hz evoked 5-HT release. As described previously, the 2 Hz and 100 Hz stimulation paradigm approximates the physiological tonic and burst firing frequency of 5-HT neurons (Mlinar et al., 2016), which aligns with the temporal window where D_2R-mediated effects are known to be prominent (Sulzer et al., 2016).

In DLS, application of the D_2 receptor agonist quinpirole (2 μM) led to a robust suppression of extracellular 5-HT levels evoked by both 1p and 5p stimulations at 2 Hz and 100 Hz (**Fig. 4.6A-B;** n = 5 slices in N = 4 animals). Compared to the pre-drug baseline, the peak 5-HT signal was reduced to approximately 40% of control levels (**Fig. 4.6C**; $F_{(1,12)} = 60.81$, $p < 0.001$, RM ANOVA main effect of the drug). This inhibitory effect was observed consistently across stimulation pulses and was further supported by a significant drug × stimulation pulse number interaction ($F_{(2,12)} = 4.830$, $p = 0.03$) and a main effect of stimulation pulses ($F_{(2,12)} = 13.96$, $p < 0.001$, RM ANOVA main effect of the pulses). In addition to the reduction in peak amplitude, quinpirole also significantly decreased the AUC of 5-HT transients, indicating a shortened duration of

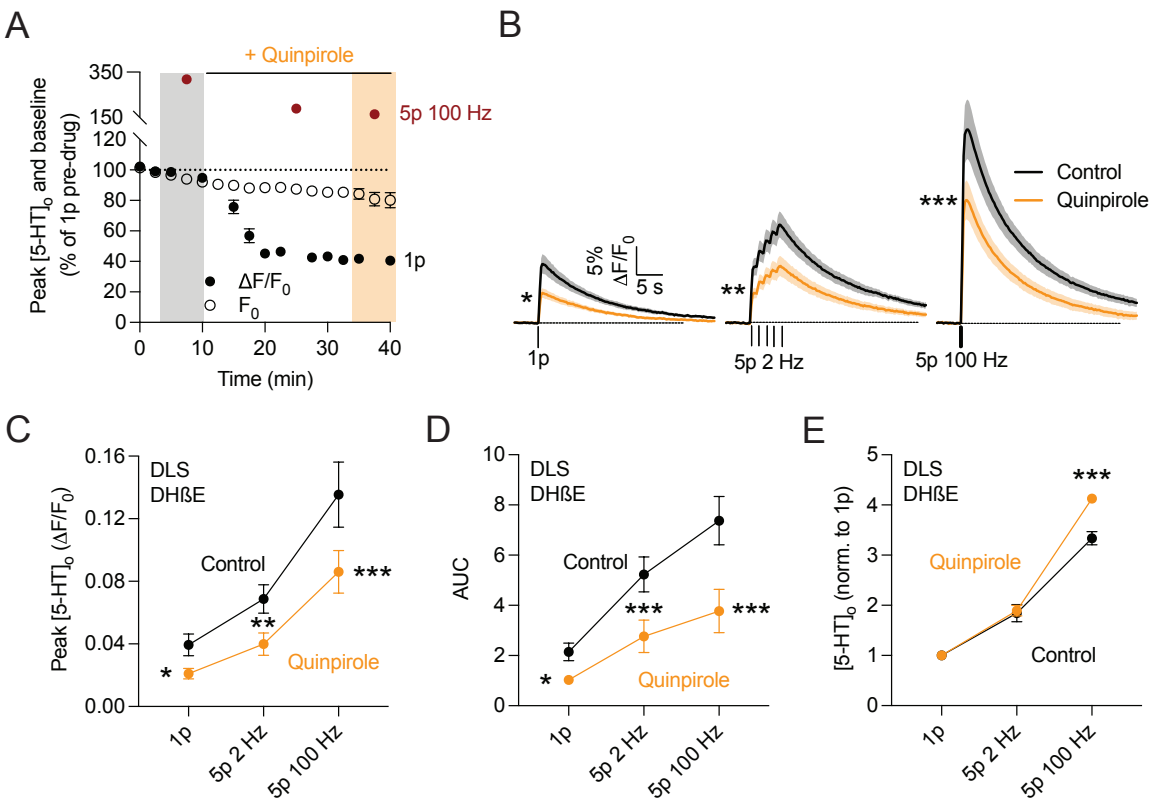

Figure 4.6. Quinpirole attenuated striatal 5-HT release in DLS. (A) Normalized mean peak $[5\text{-HT}]_o$ and baseline fluorescence (F_0) during consecutive recordings of 5-HT release evoked by 1p and 5p at 2 Hz and 100 Hz during application of quinpirole in the presence of DHßE in DLS (n = 5 experiments/3 mice). **(B)** Mean evoked 5-HT transients ± SEM, before (black) and after (orange) application of quinpirole in DLS in the presence of DHßE. Mean transients of $[5\text{-HT}]_o$ are derived from three timepoints prior to the application of quinpirole (grey shaded region) and last two timepoints (orange shaded region). **(C)** Mean 1p, 5p 2 Hz and 5p 100 Hz $[5\text{-HT}]_o$ peak of control conditions (black) and following drug application (orange) in DLS in the presence of DHßE. **(D)** Mean $[5\text{-HT}]_o$ AUC of control conditions (grey) and following drug application (orange) in the presence of DHßE in DLS. **(E)** Ratios of peak $[5\text{-HT}]_o$ released by 5p versus 1p at 2 Hz and 100 Hz in DLS in the presence of DHßE before (black) and after (orange) quinpirole application. 2-way ANOVA, Fisher's LSD post-*hoc* test, *$p < 0.05$, **$p < 0.01$, ***$p < 0.001$. Error bars are ± SEM.

extracellular 5-HT presence following stimulation (**Fig. 4.6D**; $F_{(1,12)}$=125.0, $p < 0.001$, RM ANOVA main effect of the pulses). Consistently, this decrease was robust across different stimulations by a drug × stimulation pulse number interaction ($F_{(2,12)}$ = 11.24, p = 0.002). Analysis of the 5p:1p ratio revealed that while this ratio remained unchanged at 2 Hz stimulation(**Fig. 4.6E**; p = 0.61, post-*hoc* uncorrected Fisher's LSD test), a modest increase

suggesting a frequency-dependent shift in short-term dynamics (**Fig. 4.6E**; $F_{(1,12)}$ = 28.03, p < 0.001, RM ANOVA main effect of the drugs; 5p 100 Hz: p < 0.001, post-*hoc* uncorrected Fisher's LSD test).

Together, these findings indicate that D_2R activation potently suppresses both the amplitude and duration of evoked 5-HT release in the DLS, with a minor alteration in short-term facilitation at high-frequency stimulation.

4.3.2.2 D_2R antagonist blocked 5-HT release inhibition induced by quinpirole

To verify whether the suppressive effect of the D_2R agonist quinpirole on evoked $[5\text{-HT}]_o$ is specifically mediated through D_2 receptors, we next applied the selective D_2R antagonist L-741,626 (1 µM) to determine whether it could block the action of quinpirole. Our working hypothesis was that if the presence of L-741,626 effectively prevented the reduction in 5-HT release induced by quinpirole, it would provide strong evidence that this modulation is indeed D_2R-dependent. In DLS, application of L-741,626 (1 µM) completely abolished the inhibitory effect of quinpirole (2 µM) on $[5\text{-HT}]_o$ peaks evoked by both 1p and 5p at 100 Hz stimulations in the presence of DHβE (1 µM) (**Fig. 4.7A–C**; $F_{(1,16)}$ = 0.0021, p = 0.96, RM ANOVA main effect of the drug).

Consistent with this, no difference was observed in the AUC of $[5\text{-HT}]_o$ transients following quinpirole application in the presence of L-741,626 and DHßE (**Fig. 4.7D**; $F_{(1,16)}$ = 1.133, p = 0.30, RM ANOVA main effect of the drug), further confirming the absence of D_2R-mediated suppression under these conditions. Moreover, the 5p:1p ratio remained stable before and after quinpirole application in slices treated with L-741,626 and DHβE (**Fig. 4.7E**; $t_{(4)}$ = 1.127, p = 0.3229, Student's paired t-test).

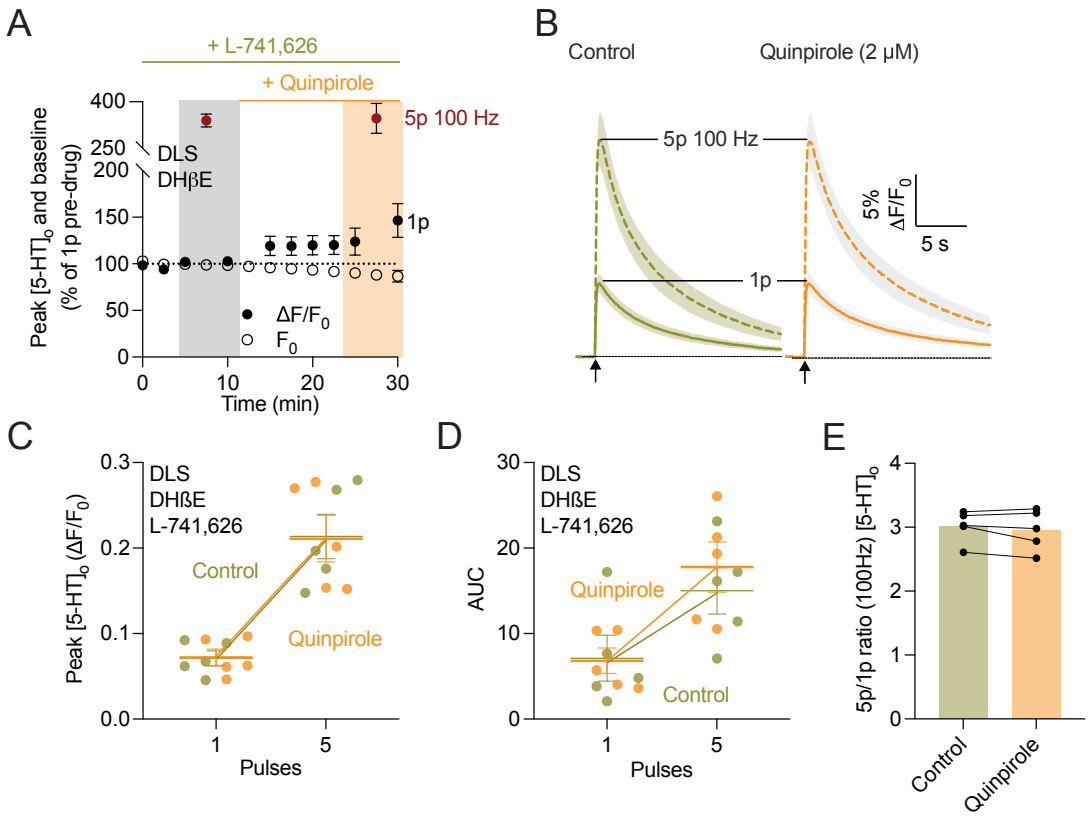

Figure 4.7. Antagonism of D_2R blocked the D_2R agonism-mediated inhibition of striatal 5-HT release. (A) Normalized mean peak $[5\text{-HT}]_o$ and baseline fluorescence (F_0) during consecutive recordings of 5-HT release evoked by 1p during application of quinpirole in the presence of DHßE and L-741,626 in DLS (*n* = 5 experiments/4 mice). **(B)** Mean evoked 5-HT transients ± SEM, before (green) and after (orange) application of SKF81297 in DLS in the presence of DHßE and L-741,626. Mean transients of $[5\text{-HT}]_o$ are derived from three timepoints prior to the application of SKF81297 (grey shaded region) and last two timepoints (orange shaded region). **(C)** Mean 1p and 5p 100 Hz $[5\text{-HT}]_o$ peak of control conditions (green) and following drug application (orange) in DLS in the presence of DHßE and L-741,626. **(D)** Mean $[5\text{-HT}]_o$ AUC of control conditions (green) and following drug application (orange) in the presence of DHßE and L-741,626 in DLS. **(E)** Ratios of peak $[5\text{-HT}]_o$ released by 5p versus 1p in DLS in the presence of DHßE and L-741,626. 2-way ANOVA, Fisher's LSD post-*hoc* test, Student's paired t-test. Error bars are ± SEM.

Taken together, these findings demonstrate that the inhibitory effect of quinpirole on 5-HT release in the DLS is dependent on D_2R activation and can be fully blocked by the D_2R antagonist L-741,626. This effect is independent of nAChR function, as DHβE was present throughout the experiment.

4.3.2.3 D_2R antagonist – L-741,626 – promoted striatal 5-HT release

To test whether 5-HT release is regulated by endogenous dopamine acting at D_2Rs, I examined the effect of the selective D_2R antagonist L-741,626 (1 μM) on 5-HT release evoked by single-pulse and five-pulse stimulation in the presence of DHßE. In DLS, D_2R antagonism significantly enhanced 5-HT release evoked by both 1p and 5p trains at 2 Hz and 100 Hz (**Fig. 4.8A-C**; $F_{(1,12)}$ = 53.59, p < 0.001, RM ANOVA main effect of the drugs; n = 5 slices from N = 5 mice). To determine whether this effect was due to endogenous activation of D_2Rs, I examined the impact of D_2R blockade on 5-HT release evoked specifically by the second and the following pulses individually in the 5p train. In DLS, the enhancement of 5-HT release observed specifically at the second pulse of the 2 Hz train (i.e., 500 ms after the first stimulus) is particularly notable and aligns well with the known kinetics of D_2R-mediated inhibition (**Fig. 4.8D**; $F_{(1,20)}$ = 87.30, p < 0.001, RM ANOVA main effect of the drugs). This has been further confirmed by a significant drug × pulse number interaction ($F_{(4,20)}$ = 4.234, p = 0.01).

In addition to the increased peak amplitude, surprisingly, the application of L-741,626 also resulted in a significant enhancement of the AUC of 5-HT transients evoked by both 1p and 5p (2 Hz and 100 Hz) stimulations, suggesting a prolonged presence of extracellular 5-HT following D_2R blockade (**Fig. 4.8E**; $F_{(1,12)}$ = 43.76, p < 0.001, RM ANOVA main effect of the drugs). Consistently, the decay half-life of 5-HT signals was significantly increased under D_2R antagonism in the DLS (**Fig. 4.8F**; $F_{(1,8)}$ = 37.30, p < 0.001, RM ANOVA main effect of the drugs). However, we did not expect that L-741,626 would influence 5-HT clearance. The underlying reasons for this unexpected effect will be discussed in **Section 4.4.2**. Despite these increases in signal amplitude and duration, the ratio of 5p to 1p responses remained unchanged in the presence of L-741,626 in the presence of DHßE (**Fig. 4.8G**; $F_{(1,24)}$ = 0.4260, p = 0.52, RM ANOVA main effect of the drugs), suggesting that D_2R blockade enhances overall 5-HT output without altering short-term facilitation dynamics. Overall, these data suggest that 5-HT release is under regulation by endogenous striatal DA acting at D_2Rs in DLS.

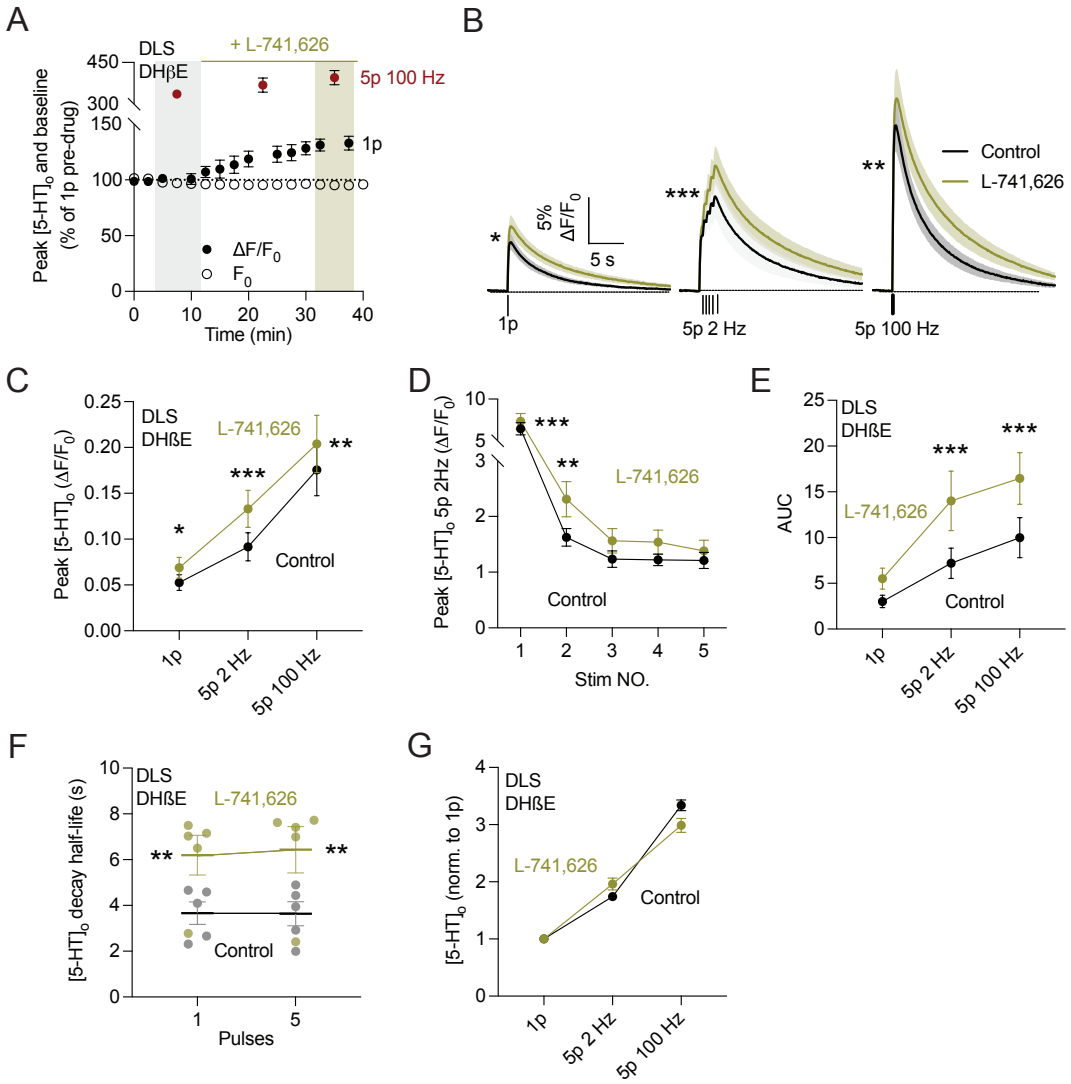

Figure 4.8. Antagonist of D_2R enhanced 5-HT release in DLS. (A) Normalized mean peak [5-HT]$_o$ and baseline fluorescence (F_0) during consecutive recordings of 5-HT release evoked by 1p and 5p at 100 Hz during application of L-741,626 in the presence of DHßE in DLS (n = 5 experiments/3 mice). **(B)** Mean evoked 5-HT transients ± SEM, before (black) and after (orange) application of L-741,626 in DLS in the presence of DHßE. Mean transients of [5-HT]$_o$ are derived from three timepoints prior to the application of quinpirole (grey shaded region) and last two timepoints (green shaded region). **(C)** Mean 1p, 5p 2 Hz and 5p 100 Hz [5-HT]$_o$ peak of control conditions (black) and following drug application (green) in DLS in the presence of DHßE. **(D)** Mean [5-HT]$_o$ peak of each pulse in 5p at 2 Hz in control conditions (black) and following drug application (green) in DLS in the presence of DHßE. **(E)** Mean [5-HT]$_o$ AUC of control conditions (grey) and following drug application (green) in the presence of DHßE in DLS. **(F)** Decay half-life of evoked [5-HT]$_o$ in control condition and in L-741,626 in DLS. **(G)** Ratios of peak [5-HT]$_o$ released by 5p versus 1p at 2 Hz and 100 Hz in DLS in the presence of DHßE before (black) and after (green) L-741,626 application. 2-way ANOVA, Fisher's LSD post-*hoc* test, *p < 0.05, **p < 0.01, ***p < 0.001. Error bars are ± SEM.

4.4 Discussion

4.4.1 D_1R control of striatal 5-HT release

My results demonstrate that activation of D_1 dopamine receptors enhances extracellular 5-HT levels in DLS. Specifically, application of the selective D_1R agonist SKF81297 significantly increased peak $[5\text{-HT}]_o$ in response to both single-pulse and five-pulse stimulation paradigms (2 Hz and 100 Hz). This increase was also reflected in the AUC of 5-HT transients and in prolonged decay kinetics, indicating a sustained elevation in 5-HT release and extracellular lifetime. Importantly, the 5p:1p ratio remained unchanged, suggesting that D_1R activation leads to a global enhancement of release probability without altering short-term plasticity. This facilitatory effect was fully abolished by co-application of the competitive D_1R antagonist SCH39166 (10 μM), confirming that the effect of SKF81297 is specifically mediated by D_1Rs.

Interestingly, the second D_1R agonist tested, CY208243, produced opposing effects depending on concentration. At 10 μM, CY208243 significantly suppressed 5-HT release, in contrast to SKF81297. However, this inhibitory effect could not be blocked by SCH39166 (not shown), raising concerns regarding off-target actions at high concentrations. Additionally, when tested at 1 μM, CY208243 showed no measurable effect on 5-HT release, further indicating dose-dependent variability in pharmacological specificity. The divergent effects of CY208243 highlight the critical importance of drug concentration and receptor selectivity. Previous studies have reported an *in vitro* Ki of 55 nM and EC_{50} of approximately 125 nM for CY208243 (Andersen & Jansen, 1990), suggesting that a concentration of 10 μM likely exceeds its optimal effective range. At this high dose, CY208243 may have lost its D_1R selectivity and instead activated other receptors, such as D_2Rs, which are known to inhibit 5-HT release. This is consistent with the inability of SCH39166 to reverse the suppressive effect, suggesting a non-D_1R mediated

mechanism. Moreover, the fact that 1 µM CY208243 had no effect supports either a lack of efficacy at that dose or that D_1Rs require more robust and selective activation to alter 5-HT output. In contrast, the SKF81297-mediated facilitation was robust and reproducible, and could be fully reversed by D_1R antagonism, making SKF81297 the more reliable tool for probing D_1R function in this context.

Administration of the D_1R antagonist alone in the presence of DHßE failed to alter 5-HT transmission, indicating that under basal slice conditions there is no evidence for endogenous D_1R-mediated DA control of 5-HT release.

These results suggest that D_1Rs exert a positive modulatory effect on serotonergic transmission in the striatum, but only when exogenously activated. The increase in AUC and decay half-life following SKF81297 application points to prolonged extracellular persistence of 5-HT, possibly reflecting enhanced vesicle fusion, reduced reuptake, or changes in diffusion dynamics.

When investigating the function of pharmacologically active receptors, it is crucial to account for the selectivity and pharmacodynamic profile of the drugs employed. In this study, we did not use genetic knockout models; rather, we relied on the application of receptor-targeting compounds to infer receptor function. This approach, while experimentally tractable, has important limitations. The strikingly opposite outcomes observed with two putative D_1R agonists (SKF81297 and CY208243) highlight the risk of overinterpreting results from a single compound. Each drug has its own pharmacological profile and may engage unintended targets, especially at higher concentrations. Absolute receptor selectivity is rarely achievable, and thus, the effect of one drug cannot be taken as a definitive representation of the receptor's endogenous role. To rigorously dissect receptor-specific mechanisms, it is important for the future studies to incorporate multiple pharmacological agents, ideally with differing selectivity profiles, alongside orthogonal validation strategies to minimize confounding indirect effects. This

principle will be essential for future efforts to accurately map receptor-specific modulation of 5-HT transmission.

4.4.2 D_2R control of striatal 5-HT release

In addition to D_1Rs, D_2 receptors - well-established as DA auto-receptors on dopaminergic neurons - also exert significant influence on striatal 5-HT dynamics. Pharmacological activation of D_2Rs with the agonist quinpirole robustly suppressed evoked 5-HT release in the DLS, reducing both the amplitude and AUC of 5-HT transients elicited by single pulses and five-pulse trains at 2 Hz and 100 Hz.

This inhibitory effect was abolished by co-application of the selective D_2R antagonist L-741,626, confirming that the action of quinpirole is mediated via D_2Rs. Moreover, application of L-741,626 alone significantly enhanced 5-HT release. Notably, this facilitation was strongest at the second stimulus of 5p at 2 Hz trains, consistent with the ~500 ms activation window for GPCR-mediated signalling, and suggestive of phasic DA engagement of D_2Rs (Sulzer et al., 2016). These findings strongly suggest that endogenous DA, though limited in slice preparations, is still capable of engaging D_2Rs to regulate 5-HT transmission under certain conditions. Importantly, while the exact cellular or synaptic locus of this effect remains unresolved, this represents clear pharmacological evidence for D_2R-mediated regulation of 5-HT in the DLS.

The finding that L-741,626 alone enhanced 1p-evoked 5-HT release - despite the absence of sustained DA tone - raises important considerations. Since it is generally accepted that DA tone is minimal in acute striatal slices due to the severing of midbrain dopaminergic afferents during tissue preparation (Sulzer et al., 2016), the observation that even these early or single pulses exhibit modest changes in response to D_2R antagonism nevertheless raises the possibility that additional mechanisms may be engaged. One interpretation is that short phasic DA release from

residual dopaminergic afferents may tonically suppress 5-HT via D_2Rs in a pulse-dependent manner, particularly under stimulation conditions that mimic physiological firing. Alternatively, it is possible that L-741,626 may exert additional pharmacological effects beyond D_2R blockade. Although L-741,626 is widely used as a selective D_2R antagonist, some reports have raised concerns that it may interact with components of the serotonergic system beyond DA receptors (Myslivecek, 2022). While there is no definitive evidence pinpointing its binding to a specific 5-HT receptor or transporter, its potential off-target effects suggest that it may influence serotonergic signalling and dynamics through unknown mechanisms. To test these possibilities, future studies should repeat these experiments using a chemically distinct D_2R antagonist such as sulpiride to confirm specificity. Additionally, monitoring DA release in real time alongside 5-HT would help determine whether phasic DA signals coincide with D_2R-dependent suppression of 5-HT. Further circuit-level analysis will also be necessary to determine the site of action for D_2Rs. These receptors may not be directly expressed on serotonergic axons; instead, they may influence local microcircuits such as GABAergic interneurons, which in turn gate 5-HT output. Combined optogenetic and pharmacogenetic approaches will be critical for mapping these mechanisms.

The D_2R-mediated enhancement of 5-HT release observed specifically at the second pulse of the 2 Hz train (500 ms after the first stimulus) is particularly notable and aligns well with the known kinetics of D_2R-mediated inhibition. Given that D_2Rs are G-protein-coupled receptors with relatively slow activation kinetics, the effect of phasically released DA is expected to peak approximately 500 ms following stimulation (Sulzer et al., 2016). Thus, the selective facilitation of 5-HT release at this time point in the presence of a D_2R antagonist likely reflects blockade of transient D_2R activation induced by the first pulse, supporting a model of phasic DA-dependent regulation of serotonergic transmission in the striatum.

4.4.3 Limitations and future directions

Despite providing new insights into the dopaminergic regulation of striatal 5-HT transmission, several limitations of this study should be acknowledged, which also guide directions for future work.

First, all experiments were conducted in acute striatal slices. While this preparation offers tight pharmacological control and precise temporal resolution, it lacks key components of the intact network, including long-range afferents and ongoing neuromodulatory tone. In particular, DA tone is thought to be minimal or absent in *ex vivo* slices (Sulzer et al., 2016), which limits our ability to investigate how physiological levels of endogenous DA regulate 5-HT release under more naturalistic conditions. Future *in vivo* experiments, such as those using fiber photometry may help address this limitation by enabling real-time monitoring of dopamine–serotonin interactions in behaving animals.

Second, although we pharmacologically blocked cholinergic influence on 5-HT transmission using DHβE to isolate dopaminergic effects, the striatum comprises a highly complex neuromodulatory network. Prior findings, including those in Chapter 3, demonstrate that GABAergic signalling plays a crucial role in modulating both DA and 5-HT transmission. Therefore, it remains possible that the dopaminergic effects observed here are partially shaped by unblocked GABAergic inputs or other local circuit mechanisms. Moreover, since our study relied solely on pharmacological manipulation of D_1Rs and D_2Rs, the precise cellular locus of action - whether on serotonergic axons directly or via indirect pathways involving interneurons or afferent projections - remains unresolved. Future studies that combine pharmacological blockade of both GABA and ACh receptors with genetic or circuit-level approaches - such as cell-type-specific knockout models or optogenetic stimulation of D_1R- or D_2R-expressing populations - will be essential to disentangle the direct versus indirect contributions of dopaminergic signalling. Additionally, anatomical mapping of D_1R and D_2R distribution on striatal 5-HT axons would provide crucial insight into whether dopaminergic modulation occurs via

terminal-autonomous mechanisms or is mediated through broader microcircuit interactions. Integrating pharmacology with targeted circuit-based tools will ultimately yield a more precise understanding of the mechanisms underlying DA-5-HT crosstalk in the striatum.

Lastly, all experiments were performed in the dorsolateral striatum, a region characterized by strong dopaminergic innervation and sparse serotonergic input. In contrast, ventral striatal regions such as the nucleus accumbens core receive denser serotonergic projections but comparatively weaker dopaminergic innervation. These regional differences may result in divergent receptor expression patterns and distinct modulatory mechanisms. Therefore, extending this work to other striatal subregions will be critical for determining whether dopaminergic regulation of 5-HT transmission is conserved or varies across the dorsal-ventral axis of the striatum.

Taken together, my findings support a model in which dopaminergic modulation of striatal 5-HT release occurs via both D_1R- and D_2R-dependent mechanisms, consistent with their canonical G_s- and $G_{i/o}$-coupled signalling pathways. Notably, D_2 receptors, with their higher affinity for DA, are likely engaged under tonic firing conditions and may exert a persistent inhibitory influence on serotonergic output. In contrast, D_1 receptors, which require higher DA concentrations for activation, may mediate transient facilitation of 5-HT release during phasic dopaminergic bursts. This dual regulation suggests a layered system in which the balance between tonic and phasic DA activity dynamically tunes serotonergic tone in the striatum.

Given the known interactions between DA and 5-HT systems in regulating mood, motivation, and motor behaviour, it would be highly informative to explore how these neuromodulatory influences unfold during behaviour. In particular, future experiments employing fibre photometry or voltammetry to simultaneously monitor striatal 5-HT and DA dynamics during defined behavioural tasks could provide key insights into how these systems coordinate in real time.

Such approaches could help clarify which dopaminergic pathway (D_1R-mediated facilitation or D_2R-mediated inhibition) dominates under specific behavioural conditions. Beyond establishing the dominant modulatory influence, a key future direction is to determine whether DA and 5-HT dynamics during behaviour are coordinated or antagonistic, and whether fluctuations in one system precede, follow, or mirror changes in the other. Dissecting the functional interplay between these two neuromodulatory systems within the same behavioural context could bring critical insights into how DA-5-HT crosstalk shapes striatal output and behaviour.

Chapter 5.

Assessing the effects of 5-HT_4R ligands on striatal DA release

5.1 Introduction

5.1.1 Diverse functional landscape of 5-HT receptor subtypes in the brain

The serotonergic system regulates a wide range of physiological and behavioural functions through its interaction with a diverse array of receptor subtypes. To date, at least 14 distinct 5-HT receptor subtypes have been identified, classified into seven families (5-HT$_1$ to 5-HT$_7$) (Barnes & Sharp, 1999; Hannon & Hoyer, 2008; Millan et al., 2008; Nichols & Nichols, 2008). With the exception of the ionotropic 5-HT$_3$ receptor, all 5-HT receptors are G-protein-coupled receptors (GPCRs), each linked to distinct intracellular signalling cascades. These include $G_{i/o}$-coupled 5-HT$_1$ and 5-HT$_5$ receptors, G_q-coupled 5-HT$_2$ receptors, and G_s-coupled 5-HT$_4$, 5-HT$_6$, and 5-HT$_7$ receptors (Bockaert et al., 2006; Hannon & Hoyer, 2008).

Phylogenetic analyses have revealed that the serotonin receptor families are remarkably conserved across vertebrate evolution, underscoring their fundamental role in neuromodulation (Nichols & Nichols, 2008; Peroutka & Howell, 1994). The seven-transmembrane domain structure typical of GPCRs is retained across species, and orthologues of nearly all human 5-HT receptor subtypes can be identified in rodents, with sequence homology frequently exceeding 80% (Peroutka & Howell, 1994).

Despite this molecular diversity, not all 5-HT receptor subtypes are equally distributed across brain regions. Many, including 5-HT$_{1a}$ and 5-HT$_{2a}$, are predominantly expressed in cortical and midbrain structures. In contrast, 5-HT$_4$ receptors (5-HT$_4$Rs) show marked enrichment in the basal ganglia, particularly in the striatum, across rodent, primate, and human brains (Compan et al., 1996; Vilaró et al., 2005). This specific anatomical localisation within the striatum - a key node in motor control, reinforcement learning, and dopamine signalling - raises important questions about the functional role of 5-HT$_4$Rs in regulating local circuit dynamics. Unlike other

5-HT receptor subtypes that may have diffuse or cortical-centric distributions, 5-HT$_4$Rs are uniquely positioned to influence striatal neurotransmission through both direct and indirect mechanisms. Therefore, the subsequent sections of this chapter will focus specifically on the detailed functional roles, modulatory mechanisms, and therapeutic potential of striatal 5-HT$_4$ receptors.

5.1.2 Function and therapeutic relevance of 5-HT$_4$ receptors

Serotonin subtype 4 receptors (5-HT$_4$Rs), a subtype of G_s-coupled receptors, are of interest as modulators of neural function due to their expression in limbic brain regions such as hippocampus and basal ganglia (Bonaventure et al., 2000; Compan et al., 1996; Gerald et al., 1995), and to the relatively advanced development and availability of their ligands. Ligands acting at 5-HT$_4$Rs are considered to have potential therapeutic utility in diverse neuropsychiatric, cognitive and psychomotor disturbances (Agrawal et al., 2020; Ballardin et al., 2024; Eglen et al., 1995; Ishii et al., 2019; Jansen et al., 2021; Lamirault & Simon, 2001; Ohno et al., 2015; Politis & Niccolini, 2015; Shen et al., 2011) through their ability to modulate circuits that shape mood, cognition, and motor function (Twarkowski et al., 2016; Ishii et al., 2019; Ballardin et al., 2024). For example, RS67333, a 5-HT$_4$R partial agonist, enhances memory performance in object recognition tasks and ameliorates stress-induced affective behaviours in rats (Lamirault & Simon, 2001; Orsetti et al., 2003), while in mouse models of PD, 5-HT$_4$R agonists RS67333 and prucalopride are reported to reduce L-DOPA-induced dyskinesias (Ballardin et al., 2024).

As a result, the anatomical distribution of 5-HT$_4$ receptors, combined with the extensive range of selective ligands, position the 5-HT$_4$ receptors as a highly attractive target for serotonergic research in both *in vivo* and *ex vivo* studies. The availability of various agonists, antagonists, and radioligands has facilitated detailed functional studies, enabling researchers to elucidate the precise roles of 5-HT$_4$Rs across different brain circuits. Given their influence on critical brain

functions and their emerging role in disease pathology, continued research on 5-HT$_4$ receptors is crucial for advancing our understanding of their mechanistic contributions and therapeutic potential, thereby aiding the development of novel pharmacological interventions for complex neuropsychiatric and neurodegenerative conditions.

5.1.3 Evidence for 5-HT$_4$R modulation of DA and ACh in the striatum

A growing body of evidence suggests that 5-HT$_4$Rs, their ligands in particular, have been suggested to modulate key neurotransmitters involved in cognitive and motor function such as acetylcholine (ACh) and dopamine (DA). *In vivo* and *ex vivo* studies have shown that 5-HT$_4$R agonists, including renzapride and (S)-zacopride, can increase extracellular DA levels in rat striatum (Bonhomme et al., 1995; De Deurwaerdère et al., 1997; Steward et al., 1996). 5-HT$_4$R mRNA and ligand-binding sites have been reported within the striatum, in rats, guinea pigs, and primates (Gerald et al., 1995; Vilaró et al., 2005) but there is a paucity of evidence regarding the expression of the 5-HT$_4$R *htr4* gene in midbrain DA neurons, consistent with a suggestion that any modulation of DA by 5-HT$_4$R ligands is indirect, via striatal circuits (De Deurwaerdère et al., 1997). Striatal 5-HT$_4$ receptors are thought to be localized on non-dopaminergic neurons, such as striatal cholinergic interneurons (ChIs) and D$_2$R-expressing striatal GABAergic projection neurons (Ballardin et al., 2024; Gerald et al., 1995; Lavoie & Parent, 1990; Patel et al., 1995). Both striatal ACh and GABA are known to modulate DA release (Lopes et al., 2019; Threlfell & Cragg, 2011) and to mediate the impact of other striatal modulators and circuits on DA signaling including opioids, glutamate, insulin and astrocytes (Britt & McGehee, 2008; Kosillo et al., 2016; Roberts et al., 2020; Stouffer et al., 2015) making them candidates for mediating an impact of 5-HT$_4$Rs on DA signalling. Several studies have explored striatal ACh regulation through serotonergic signalling. For instance, direct activation of 5-HT receptors using the broad-spectrum 5-HT receptor agonist quipazine has been shown to inhibit stimulation-induced ACh

overflow in both the rostral and caudal striatum (Jackson et al., 1988), suggesting a suppressive role of serotonergic input on cholinergic activity. However, evidence for specific involvement of 5-HT$_4$Rs remains mixed. One *in vivo* microdialysis study reported that administration of selective 5-HT$_4$R agonists - BIMU 1 and BIMU 8 - did not affect ACh release in the striatum, although it significantly enhanced ACh release in the prefrontal cortex (Consolo et al., 1994). These findings imply a region-specific role of 5-HT$_4$R activation in regulating cholinergic neurotransmission, possibly due to differential receptor distribution or circuit-level modulation.

5.1.4 Acetylcholine detection with GRAB$_{ACh}$

The genetically encoded GRAB$_{ACh}$ (GPCR-Activation-Based ACh) sensor represents a powerful tool for monitoring cholinergic transmission, offering the sensitivity, specificity and temporal resolution needed to probe ACh dynamics in complex brain circuits, such as the striatum (Jing et al., 2020). The optimized GRAB$_{ACh3.0}$ sensor is engineered by inserting a circularly permuted GFP into the third intracellular loop of the human M3 muscarinic receptor, enabling fluorescence changes upon ACh binding (Jing et al., 2020). It shows markedly enhanced fluorescence responses to physiologically relevant concentrations of ACh, making it well suited to detect changes in ACh release. Its rapid on/off kinetics allow detection of fast, transient ACh signals in response to stimuli, while its minimal coupling to downstream G-protein or β-arrestin signalling pathways helps preserve actual cholinergic activity (Jing et al., 2020). These properties make GRAB$_{ACh3.0}$ particularly advantageous for use in acute slice recordings, where resolving rapid and localized ACh dynamics is critical.

Striatal slice preparations have shown effective for visualizing stimulus-evoked ACh release using GRAB$_{ACh3.0}$, delivered via AAV-mediated expression. This approach enables the study of cholinergic signalling in defined circuits under both physiological and disease-relevant conditions. Notably, ACh dynamics can be assessed through changes in both fluorescence peak

amplitude and area under the curve, allowing reliable estimation of both the magnitude of ACh release and the efficiency of its clearance. These features make GRAB$_{ACh3.0}$ ideally suited for investigating how ACh release and reuptake dynamics are modulated in the striatum across different experimental conditions.

This strategy provides a critical experimental foundation for the subsequent sections of this chapter, which explore the modulatory influence of DA and 5-HT systems on striatal cholinergic activity, using GRAB$_{ACh3.0}$ as the primary readout tool.

5.1.5 Dual pharmacology of RS67333: 5-HT$_4$R agonism versus AChE inhibition

In addition to their primary actions at 5-HT$_4$Rs, some ligands possess pleiotropic properties that may complicate interpretation of their *in vivo* effects. RS67333, in particular, has structural similarities to the acetylcholinesterase (AChE) inhibitor donepezil and has been reported to inhibit AChE *in vitro* at submicromolar concentrations (Lecoutey et al., 2014). A pleiotropic profile of 5-HT$_4$R agonists as AChE inhibitors might complicate interpretation of their effects on neurotransmission in brain circuits involving ACh, but could also offer benefits as novel multitarget-directed ligands. AChE inhibition prolongs extracellular ACh availability, and can not only rescue ACh deficits in neurodegenerative cognitive deficits in cortical/hippocampal circuits, but also shapes how ACh activates striatal nicotinic ACh receptors (nAChRs) on DA axons to modulate DA release (Dajas-Bailador et al., 1996; F.-M. Zhou et al., 2001). It is highly plausible that 5-HT$_4$R ligands possessing efficacy as AChE inhibitors might thereby modify striatal ACh and, in turn, DA signalling.

Therefore, in this chapter, I explored the impact of RS67333, a purported dual 5-HT$_4$R agonist and AChE inhibitor, on striatal DA and ACh release dynamics. Specifically, we assessed

whether RS67333 modifies evoked striatal DA release detected directly with fast-scan cyclic voltammetry, and whether this effect was mediated via modulation of ACh input acting on striatal nAChRs. We addressed whether RS67333 modifies the sub-second clearance of extracellular ACh detected using sensor $GRAB_{ACh}$ consistent with AChE inhibition.

5.2 Methods

Experiments detailed in this chapter were carried out in accordance with the general methods described in Chapter 2. Variations and further details are reported below.

5.2.1 Animals and slice preparation

Male and female wild-type C57BL/6J mice were culled by cervical dislocation and acute *ex vivo* brain slices were prepared as described in Section 2.1.2. All procedures were performed in accordance with institutional guidelines and the U.K. Animals (Scientific Procedures) Act, 1986.

5.2.2 Fast-scan cyclic voltammetry

Fast-scan cyclic voltammetry was used to measure changes in $[DA]_o$, as described in Section 2.2. Each experiment was performed at a single recording site in either the DLS or NAcC. DA was evoked every 2.5 minutes by either single pulse (1p) or five-pulse train at 100 Hz (5p 100 Hz) electrical stimulation. Drug application was performed once signal stability was achieved: ≤ 10% variation across four consecutive recordings. Electrodes were calibrated at the end of the experimental day in 2 μM DA, prepared immediately beforehand in recording solutions. DA oxidation currents values were measured from background-subtracted voltammograms, converted to concentration using the electrode calibration factor. The drug RS67333 was found to be electroactive, reducing the sensitivity of the CFM to applied DA to an average sensitivity of

54 ± SEM % during calibration (29 electrodes, **Fig. 5.1A-B**). All $[DA]_o$ data collected with FCV in the presence of RS67333 were scaled for this loss of sensitivity with a coefficient of 100/54.

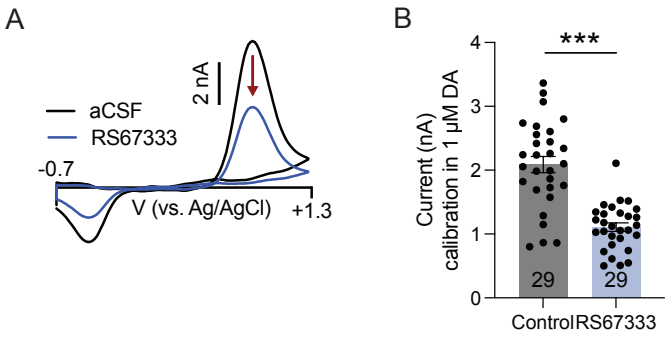

Figure 5.1. Calibration of 2 µM DA in aCSF and RS67333. (A) Representative voltammograms of 2 µM DA in aCSF (black) and in RS67333 (blue) for electric-evoked $[DA]_o$. **(B)** The oxidation current calibrated in 1 µM DA in aCSF and RS67333.

5.2.3 GRAB$_{DA}$ and GRAB$_{ACh}$ imaging

Green GRAB$_{DA3h}$ and GRAB$_{ACh3.0}$ were used in this Chapter of works (Jing et al., 2020; Zhuo et al., 2024). For GRAB$_{DA}$ and GRAB$_{ACh}$ imaging involving electrical stimulation, recordings were conducted following the procedures detailed in Chapter 2 section 2.3 and 2.4. In summary, the acute striatal brain slices were hemisected and transferred into a slice immersion recording chamber and superfused at ~2.5 ml/min with aCSF at 31-33 °C. A 10X water immersion objective was lowered into the superfusate and an LED (470 nm, 4 mW) was briefly switched on to allow for visualisation of green fluorescent protein (GFP) expression to confirm viral expression, and to place the stimulating electrode on top of slices. All images were recorded by a Prime BSI Express Scientific CMOS camera (field size: 665.6 µm x 665.6 µm). Sampling rate was 100 Hz, exposure time 10 ms, and pixels were binned 2x2. Images sequences were recorded for 5 s (for GRAB$_{ACh3.0}$) or 8 s (for GRAB$_{DA3h}$) with a 1 s pre-recording photo-bleaching time. These settings enabled detection of individual ACh and DA release events during

stimulation trains, depending on the off kinetics of the sensors. Electrical stimulations were delivered every 2.5 minutes. Fluorescence of GRAB$_{ACh}$ or GRAB$_{DA}$ was captured from the region of interest (ROI, 50 µm × 50 µm), at a distance of 50 µm from the stimulating electrode tip. Data are expressed as a change in fluorescence from baseline ($\Delta F/F_0$), where F_0 is the baseline signal prior to the stimulation. To evoked ACh or DA release, electrical stimulus pulses (1p or 5 pulses at 100 Hz; pulse duration, 200 µs; 0.6 mA) were given by a local bipolar concentric Pt/Ir electrode.

5.2.4 AChE chemiluminescent assays

AChE activity was measured using a commercially available colorimetric assay kit – Abcam, as described in Section 2.4. Dorsal and ventral striatal tissue punches (1.2 mm diameter) were collected from 300 µm-thick acute coronal striatal slices, prepared using a vibratome in ice-cold cutting solution as described Section 2.1.2. The test compounds (RS67333 or BIMU8 or ambenonium) were present in the reaction buffer throughout the entire assay process. Michaelis constant (K_m) and maximum reaction velocity (V_{max}) were determined by fitting the data to the Michaelis–Menten equation using non-linear regression.

5.2.5 Drugs

Stock solutions were prepared at 1,000x – 20,000x the final concentration and stored at -20°C. Final drug concentrations were prepared in aCSF on the day of the experiment.

Drug	Supplier	Action	Concentration	Solvent	References
Dihydro-β-erythroidine (DHβE) hydrobromide	Sigma-Aldrich	nAChR antagonist	1 µM	dH_2O	Threlfell et al. (2012); Roberts et al. (2020)
RS67333 hydrochloride	MedChem Express (MCE)	5-HT$_4$R agonist	1 or 10 µM	dH_2O	Cavaccini et al. (2018) Lecoutey et al. (2014)

BIMU8	Tocris	5-HT$_4$R agonist	1 µM	DMSO	Bickmeyer et al. (2002)
Ambenonium	Bio-Techne	AChE inhibitor	100 nM	dH_2O	Exley et al., (2008)

5.2.6 Data acquisition and analysis

FCV data were digitized and acquired using Axoscope 10.7 and extracted using locally written Python script. GRAB sensor data were extracted by Image J and analyzed by locally written MATLAB or Python script described in Section 2.3.5. Statistical tests were performed in GraphPad Prism 10.

5.3 Results

5.3.1 5-HT$_4$R ligand RS67333 attenuated DA release in DLS and NAcC

We first investigated the impact of 5-HT$_4$ receptor agonist RS67333 on evoked DA release in DLS and in NAcC in acute coronal slices of mouse striatum, using FCV at carbon-fibre microelectrodes to detect DA released by electrical stimulus pulses delivered singly (1p) or in short trains of 5-pulses (5p) at 100 Hz. The ratio of release evoked by these two protocols is useful as a tool for exposing dynamic changes in DA release probability, particularly those due to changes in the action of ACh acting at nAChRs (Rice & Cragg, 2004). In DLS, application of RS67333 (10 µM) significantly reduced $[DA]_o$ evoked by a single pulse, approximately halving peak $[DA]_o$ compared to pre-drug conditions (**Fig. 5.2A-B**; $F_{(1,10)} = 12.60$, $p = 0.0137$, RM ANOVA main effect of the drug). $[DA]_o$ evoked by 5p at 100 Hz was not reduced significantly from pre-drug levels in DLS (**Fig. 5.2A-B**; $p = 0.0690$, Fisher's LSD test), but correspondingly, the ratio of peak $[DA]_o$ evoked by 5p versus 1p (5p:1p ratio) was significantly increased by RS67333 from ~1.1 to ~2 (**Fig. 5.2C**; $t_{(5)} = 4.240$, $p = 0.0082$; Student's paired t-test). In NAcC,

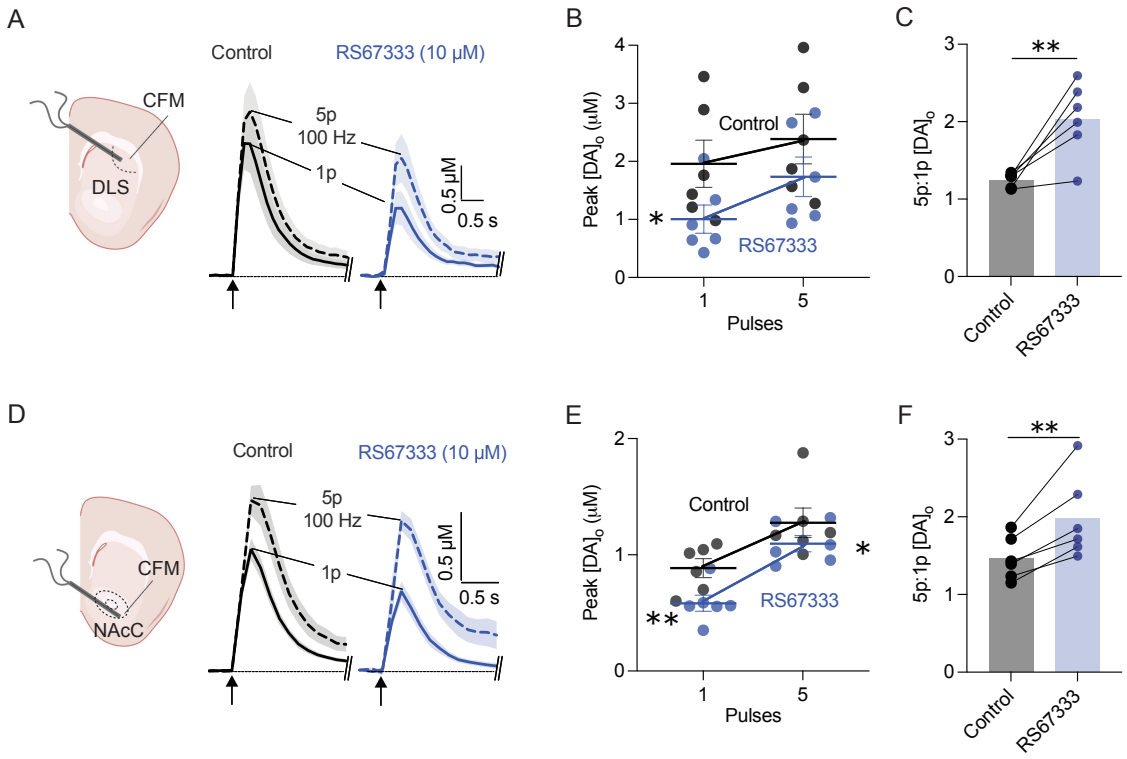

Figure 5.2. RS67333 modifies striatal DA release and short-term plasticity in DLS and NAcC reported by FCV. (A,D) Schematics of FCV stimulation and recording in (A) DLS or (D) NAcC, alongside mean $[DA]_o$ transients ± SEM evoked (at arrows) by single pulse (1p, solid line) and 5 pulses (100 Hz) (dashed line), before (black) and after (blue) application of RS67333 (n = 6 experiments in 5 mice). **(B,E)** Mean peak evoked $[DA]_o$ in control (grey) or with RS67333 (blue) in (B) DLS or (E) NAcC. **(C,F)** Ratios of peak $[DA]_o$ released by 5p versus 1p in (C) DLS or (F) NAcC. 2-way ANOVA, Fisher's LSD post-*hoc* test, Student's paired t-test. *$p < 0.05$, **$p < 0.01$. Error bars are ± SEM.

RS67333 significantly reduced $[DA]_o$ evoked by either 1p or 5p (100 Hz) (**Fig. 5.2D-E**; $F_{(1,10)} = 18.61$, $p = 0.0015$, RM ANOVA main effect of the drug) and also significantly increased 5p:1p ratio from ~1.4 to ~2 (**Fig. 5.2F**; $t_{(5)} = 4.375$, $p = 0.0072$; Student's paired t-test).

To corroborate the effects of RS67333 on evoked $[DA]_o$ detected with FCV, and control for any residual uncompensated electrochemical effects of changes to the detection of DA by the carbon-fibre microelectrode caused by the drug RS67333 (see 5.2.2), we also assessed the impact of RS67333 on $[DA]_o$ detected in DLS by imaging $GRAB_{DA}$ (Zhuo et al., 2024), a

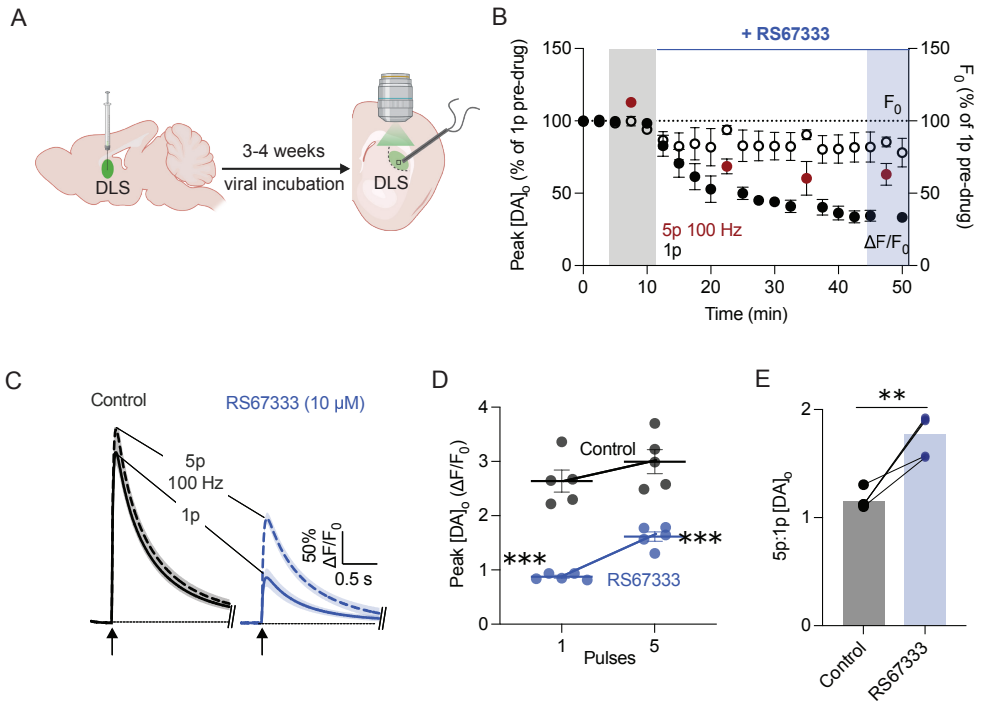

Figure 5.3. RS67333 modifies striatal DA release and short-term plasticity in DLS reported by GRAB$_{DA}$. (A) Viral delivery of GRABDA$_{3h}$ to striatum for imaging extracellular DA levels *ex vivo*. **(B)** Normalised mean peak $[DA]_o$ and baseline fluorescence (F_0) during consecutive recordings of DA release evoked by 1p (black) and 5p (100 Hz, red), during application of RS67333 in DLS (n = 5 experiments in 3 mice). **(C)** Mean evoked DA transients ± SEM, before (black) and after (blue) application of RS67333 (n = 5 experiments in 3 mice) in DLS. Mean transients of $[DA]_o$ are derived from three timepoints prior to the application of RS67333 (grey shaded region) and last three timepoints (blue shaded region). **(D)** Mean 1p and 5p 100 Hz $[DA]_o$ peak of control conditions (grey) and following drug application (blue) in DLS. **(E)** Ratio of peak $[DA]_o$ released by 5p versus 1p in control and drug conditions in DLS. 2-way ANOVA, Fisher's LSD post-*hoc* test, Student's paired t-test. *p < 0.05, ***p < 0.001. Error bars are ± SEM.

GPCR-activation-based-DA sensor expressed after intracranial delivery of viral vector (**Fig. 5.3A**). In broad agreement with observations using FCV, RS67333 significantly reduced $[DA]_o$ reported by dF/F after stimulation by 1p or 5p (100 Hz), and increased 5p:1p ratio (**Fig. 5.3B-E**; $F_{(1,8)}$ = 69.57, p < 0.0001, RM ANOVA main effect of the drug; 5p/1p: $t(4)$ = 5.675, p = 0.0048, Student's paired t-test). These observations with both DA detection techniques indicate that RS67333 decreases DA release probability and relieves a driver of short-term depression to modestly enhance the activity-dependence of DA release.

5.3.2 Modulation of DA release by RS67333 is mediated by ChIs

These effects of RS6733 are strongly reminiscent of the effects of changes to nAChR activity: either a reduction in ACh release or desensitisation of nAChRs has been shown to reduce $[DA]_o$ evoked by 1p and increase 5p:1p ratio (Rice & Cragg, 2004; H. Zhang & Sulzer, 2004). To test whether a change to nAChR activity is responsible for these effects of RS67333, we applied a competitive nAChR antagonist, DHβE, to prevent nAChR activation and subsequently assessed the impact of RS67333 on evoked $[DA]_o$, detected with FCV. In the presence of DHβE, in DLS and NAcC, the 5p:1p ratio was larger ($\geqslant$ 3) than seen in control conditions (compare **Fig 5.2**), as published previously (Rice & Cragg, 2004).

Furthermore, additional administration of RS67333 failed to reduce $[DA]_o$ evoked by 1p or 5p (100 Hz) in DLS (**Fig. 5.4A-B**; $F_{(1,10)}$ = 1.519, p = 0.2460, RM ANOVA main effect of the drug) and in NAcC (**Fig. 5.4D-E**; $F_{(1,8)}$ = 0.2762, p = 0.6134, RM ANOVA main effect of the drug). RS67333 did not modify 5p:1p ratio in both DLS (**Fig. 5.4C**; t(5) = 0.1848, p = 0.8606) and NAcC (**Fig.5.4F**; t(4) = 0.3974, p = 0.7113; Student's paired t-test). These findings indicate that RS67333 modulates striatal DA release via a mechanism involving changes to ACh acting on nAChRs.

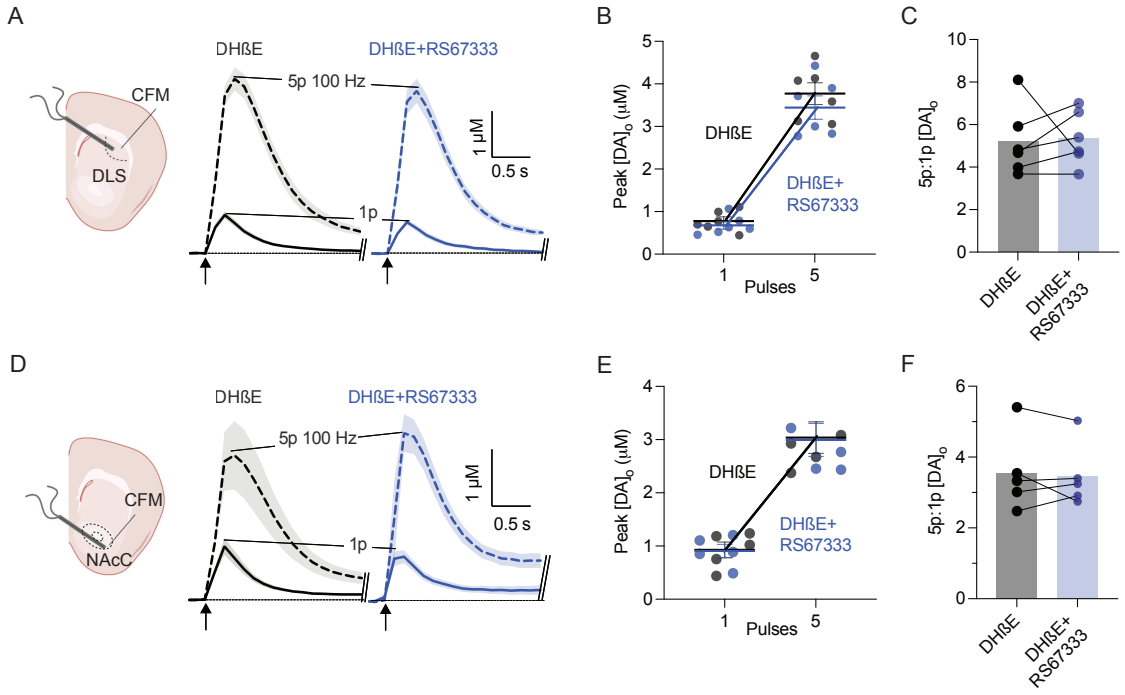

Figure 5.4. RS67333 does not modify evoked striatal DA release in the presence of nAChR antagonist DHβE. (A,D) Schematics of FCV stimulation and recording in (A) DLS or (D) NAcC, alongside mean $[DA]_o$ transients ± SEM evoked (at arrows) by single pulse (1p, solid line) and 5 pulses (100 Hz) (dashed line), before (black) and after (blue) application of RS67333, in the presence of DHßE (n = 6 experiments/5 mice in DLS; n = 5 experiments/4 mice in NAcC). **(B,E)** Mean peak evoked $[DA]_o$ in control (grey) or with RS67333 (blue) in (B) DLS or (E) NAcC, in the presence of DHßE. **(C,F)** Ratios of peak $[DA]_o$ released by 5p versus 1p in (C) DLS or (F) NAcC in the presence of DHßE. 2-way ANOVA, Fisher's LSD post-*hoc* test, Student's paired t-test. Error bars are ± SEM.

5.3.3 RS67333 changes ACh dynamics in DLS and NAcC

We therefore investigated directly whether RS67333 modifies extracellular ACh signals. We detected ACh levels in mouse striatal slice by imaging fluorescence of $GRAB_{ACh3.0}$ (Jing et al., 2020), a virally expressed genetic reporter, injected previously into striatum (**Fig. 5.5A**). In DLS, application of RS67333 did not significantly change peak dF/F evoked by 1p but slightly increased dF/F evoked by 5p (100 Hz) trains (**Fig. 5.5B-D**; $F_{(1,8)} = 0.1285$, $p_{(1p)} = 0.0609$, $p_{(5p)} = 0.0276$, RM ANOVA main effect of the drug, Fisher's LSD test). However notably, RS67333 approximately tripled the AUC of ACh transients, significantly prolonging the integrated

extracellular lifetime of ACh (**Fig. 5.5E-F**; $F_{(1,8)}$ = 49.26, p = 0.0001, RM ANOVA main effect of the drug). Single phase exponential decay curves fitted to $GRAB_{ACh}$ signals (**Fig. 5.5G**) indicated that RS67333 significantly extended the ACh extracellular half-lives for either 1p or 5p stimuli (**Fig. 5.5H**; $F_{(1,8)}$ = 7.527, p = 0.0253, RM ANOVA main effect of the drug). A similar effect was seen in the NAcC, where RS67333 did not modify the peak df/F of ACh transients but significantly augmented the AUC and decay half-life of $[ACh]_o$ (**Fig. 5.5I-K**; $F_{(1,10)}$ = 0.3993, p = 0.5416, RM ANOVA main effect of the drug; **Fig. 5.5L-M**, $F_{(1,10)}$ = 15.78, p = 0.0026, RM ANOVA main effect of the drug; **Fig. 5.5N**, $F_{(1,10)}$ = 44.33, p < 0.0001, RM ANOVA main effect of the drug). These data indicated that RS67333 significantly changed the dynamic, especially the clearance, of striatal ACh in both DLS and NAcC.

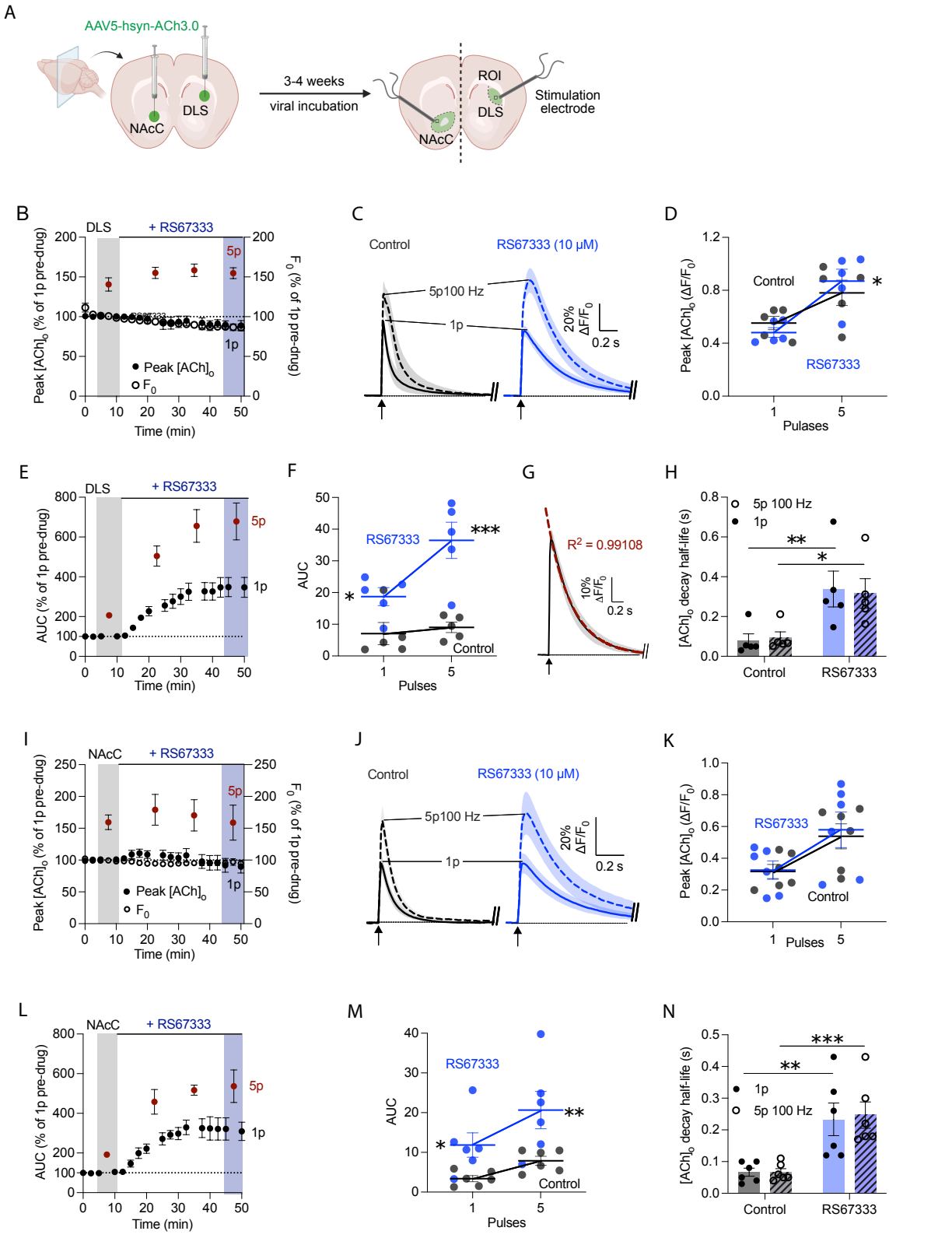
A
AAV5-hsyn-ACh3.0
NAcC
DLS
3-4 weeks
viral incubation
ROI
Stimulation electrode
B
DLS
+ RS67333
5p
1p
Peak [ACh]$_o$
F$_0$
Peak [ACh]$_o$ (% of 1p pre-drug)
F$_0$ (% of 1p pre-drug)
Time (min)
C
Control
RS67333 (10 µM)
5p100 Hz
1p
20% ΔF/F$_0$
0.2 s
D
Control
RS67333
Peak [ACh]$_o$ (ΔF/F$_0$)
Pulases
E
DLS
+ RS67333
AUC (% of 1p pre-drug)
Time (min)
F
RS67333
Control
AUC
Pulses
G
R^2 = 0.99108
10% ΔF/F$_0$
0.2 s
H
5p 100 Hz
1p
[ACh]$_o$ decay half-life (s)
Control
RS67333
I
NAcC
+ RS67333
Peak [ACh]$_o$
F$_0$
Peak [ACh]$_o$ (% of 1p pre-drug)
F$_0$ (% of 1p pre-drug)
Time (min)
J
Control
RS67333 (10 µM)
5p100 Hz
1p
20% ΔF/F$_0$
0.2 s
K
RS67333
Control
Peak [ACh]$_o$ (ΔF/F$_0$)
Pulses
L
NAcC
+ RS67333
AUC (% of 1p pre-drug)
Time (min)
M
RS67333
Control
AUC
Pulses
N
1p
5p 100 Hz
[ACh]$_o$ decay half-life (s)
Control
RS67333

Figure 5.5. RS67333 significantly prolongs striatal extracellular ACh dynamics in DLS and NAcC. (A) Viral delivery of GRAB$_{ACh}$ to striatum for imaging extracellular ACh levels *ex vivo*. **(B,I)** Schematic of stimulation and GRAB$_{ACh}$ recording site, alongside normalised mean peak [ACh]$_o$ and baseline fluorescence (F_0) during consecutive recordings of ACh release evoked by 1p (black) and 5p (100 Hz, red), during application of RS67333 in (B) DLS or (I) NAcC (n = 5 experiments/3 mice). **(C,J)** Mean evoked ACh transients ± SEM, before (black) and after (blue) application of RS67333 (n = 5 experiments in 3 mice) in (C) DLS or (J) NAcC. Mean transients of [ACh]$_o$ are derived from three timepoints prior to the application of RS67333 (grey shaded region) and last three timepoints (blue shaded region). **(D,K)** Mean 1p and 5p 100 Hz [ACh]$_o$ peak of control conditions (grey) and following drug application (blue) in (D) DLS or (K) NAcC. **(E,L)** Normalised mean AUC [ACh]$_o$ during consecutive recordings of ACh release evoked by 1p (black) and 5p (100 Hz, red), during application of RS67333 in (E) DLS or (L) NAcC (n = 5 experiments in 3 mice). **(F,M)** Mean 1p and 5p 100 Hz [ACh]$_o$ AUC of control conditions (grey) and following drug application (blue) in (F) DLS or (M) NAcC. **(G)** Example of nonlinear one phase decay fitting curve (red dash line), R^2 = 0.99108. **(H,N)** Mean 1p and 5p 100 Hz decay half-life of [ACh]$_o$ under control conditions (grey box) and following drug application (blue) in (H) DLS or (N) NAcC. 2-way ANOVA, Fisher's LSD post-*hoc* test, **p* < 0.05, ***p* < 0.01. Error bars are ± SEM.

5.3.4 RS67333 can act as an AChE inhibitor in striatum

The primary clearance mechanism for extracellular ACh is catabolism via AChE (Descarries et al., 1997) and therefore we tested whether RS67333 was an inhibitor of activity of AChE extracted from striatal tissue punches (**Fig. 5.6A**) using an AChE chemiluminescent assay. RS67333 (1 µM and 10 µM) concentration-dependently inhibited AChE activity (**Fig. 5.6B**; Drug-free: V_{max} = 4383, K_m = 137.1; 1 µM RS67333: V_{max} = 1538, K_m = 76.54; 10 µM RS67333: V_{max} = 303.9, K_m = 37.02; Nonlinear Michaelis-Menten fit). The inhibition of AChE with 10 µM RS67333 was comparable to the level seen after slice were treated with ambenonium (**Fig. 5.6B**; V_{max} = 145.0, K_m = 0.8631; Nonlinear Michaelis-Menten fit), a potent AChE inhibitor widely used in previous studies (Hodge et al., 1992; Yamamoto et al., 1991). These findings indicate that RS67333 is a potent inhibitor of striatal AChE, and so limits degradation of released ACh, extending ACh extracellular lifetime. Enhancements of striatal extracellular ACh readily cause nAChR desensitization and consequently change to downstream modulation of DA release by nAChRs across the striatum (Ochoa et al., 1989; F.-M. Zhou et al., 2001).

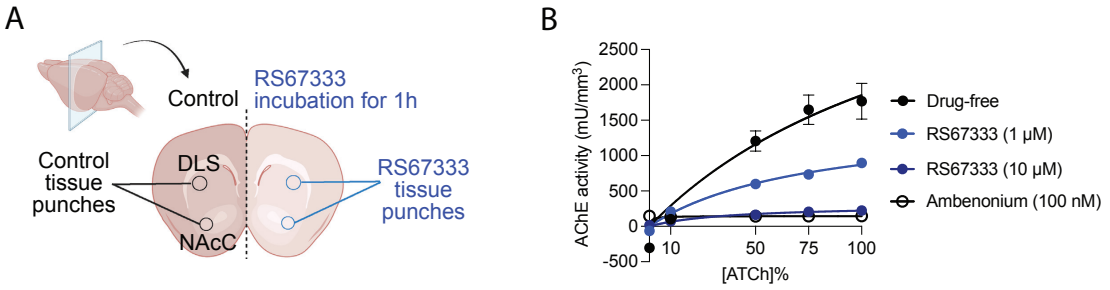

Figure 5.6. RS67333 inhibited AChE degradation in striatal slices. (A) Schematic of tissue punches from striatal slices with or without incubation in RS67333 (1 or 10 µM) for an hour (n = 4 slices in 4 animals). **(B)** Fitted Michaelis-Menten curves of AChE activity incubated with RS67333 (1 µM and 10 µM), ambenonium (100 nM) and drug-free condition.

5.3.5 5-HT$_4$R ligand BIMU8 does not inhibit AChE, or alter striatal ACh release

To investigate whether the effects of RS67333 on striatal ACh release (and in turn DA release) are solely due to an action as an AChE inhibitor, or whether agonism of 5-HT$_4$Rs can also contribute to modulation of ACh, we tested the effects of another 5-HT$_4$R ligand, BIMU8, on AChE activity, and in turn, ACh and DA release. First, we established that BIMU8 treatment (1 µM) of striatum did not detectably modify striatal AChE activity (**Fig. 5.7A-B**; Drug-free: V_{max} = 4383, K_m = 137.1; BIMU8: V_{max} = 4278, K_m = 129.7; Nonlinear Michaelis-Menten fit). Next, we tested whether BIMU8 (1 µM) could affect ACh release in DLS detected with GRAB$_{ACh}$. BIMU8 did not alter peak dF/F (**Fig. 5.7C-E**; $F_{(1,10)}$ = 0.1292, p = 0.7267, RM ANOVA main effect of the drug) or the AUC of ACh transients (**Fig. 5.7F-G**; $F_{(1,10)}$ = 0.1422, p = 0.7140, RM ANOVA main effect of the drug), or the decay half-life of ACh transients evoked by 1p or 5p (100 Hz) (**Fig. 5.7H**; $F_{(1,10)}$ = 0.3155, p = 0.5867, RM ANOVA main effect of the drug).

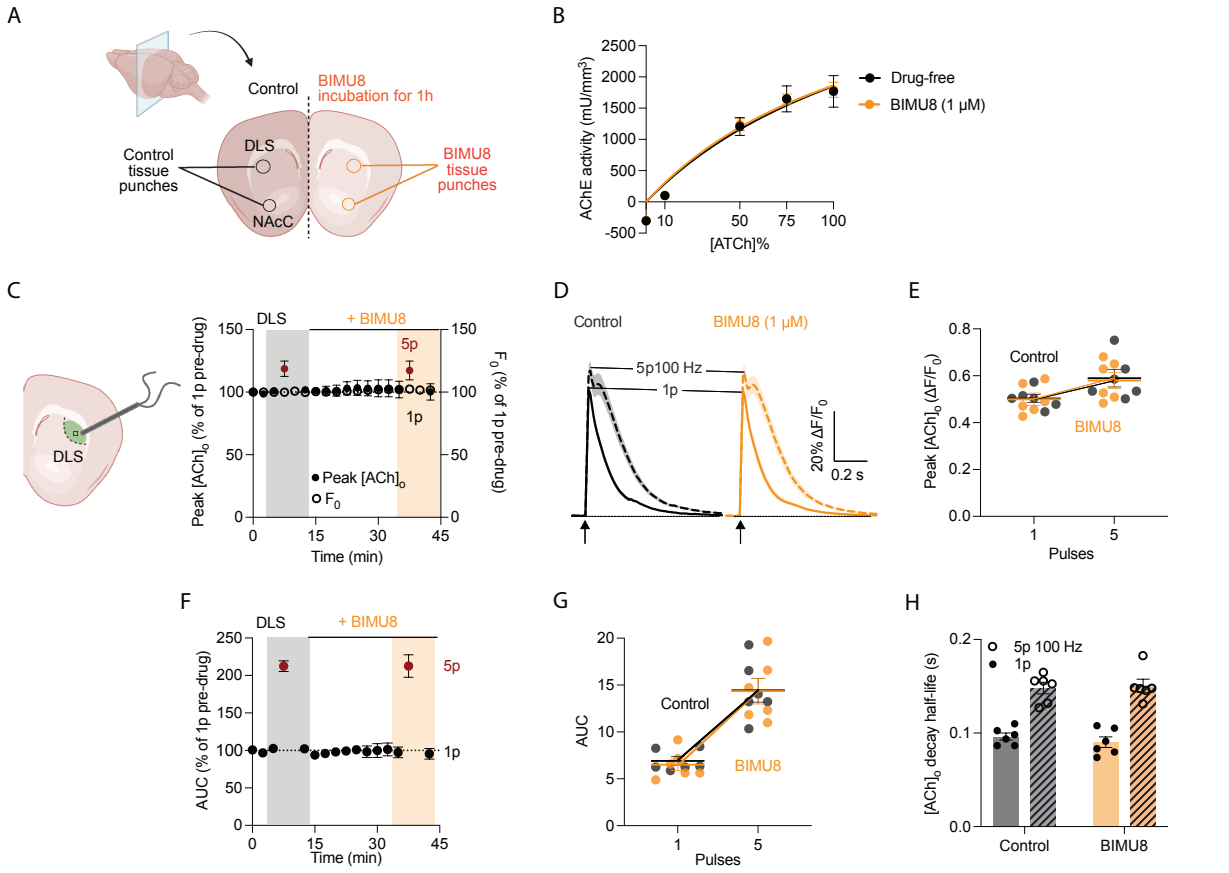

Figure 5.7. BIMU8 does not alter striatal AChE activity, or ACh dynamics in DLS. (A) Schematic of tissue punches from striatal slices with or without incubation in BIMU8 (1 µM) for an hour (n = 4 slices in 4 animals). **(B)** Fitted Michaelis-Menten curves of AChE activity incubated with BIMU8 (1 µM) and control condition. **(C)** Schematic of stimulation and GRAB$_{ACh}$ recording site, alongside normalised mean peak $[ACh]_o$ and baseline fluorescence (F_0) during consecutive recordings of ACh release evoked by 1p (black) and 5p (100 Hz, red), during application of BIMU8 in DLS (n = 6 experiments in 4 mice). **(D)** Mean evoked ACh transients ± SEM, before (black) and after (yellow) application of BIMU8 in DLS. Mean transients of $[ACh]_o$ is derived from three timepoints prior to the application of BIMU8 (grey shaded region) and last three timepoints (yellow shaded region). **(E)** Mean 1p and 5p 100 Hz $[ACh]_o$ peak of control conditions (grey) and following drug application (yellow) in DLS. **(F)** Normalised mean AUC $[ACh]_o$ during consecutive recordings of ACh release evoked by 1p (black) and 5p (100 Hz, red), during application of BIMU8 in DLS (n = 6 experiments in 4 mice). **(G)** Mean 1p and 5p 100 Hz $[ACh]_o$ AUC of control conditions (grey) and following drug application (yellow) in DLS. **(H)** Mean 1p and 5p 100 Hz decay half-life of $[ACh]_o$ under control conditions (grey box) and following drug application (yellow) in DLS. 2-way ANOVA, Fisher's LSD post-*hoc* test. Error bars are ± SEM.

Together, these findings indicate that BIMU8, unlike RS67333, does not inhibit AChE activity or influence striatal ACh release, suggesting that the modulatory effects of RS67333 on cholinergic transmission are unlikely to be mediated by 5-HT$_4$R activation alone.

5.3.6 5-HT$_4$R ligand BIMU8 does not alter striatal DA release

Finally, we assessed whether BIMU8 could alter DA release detected with FCV. BIMU8 failed to modify DA release evoked by either 1p or 5p (100 Hz) stimuli (**Fig. 5.8A-C**; $F_{(1,8)}$ = 2.036, p = 0.1915, RM ANOVA main effect of the drug). Consistent with this, the 5p/1p ratio of $[DA]_o$ in the presence of BIMU8 was not significantly different from the drug-free condition (**Fig. 5.8D**; $t(4)$ = 2.596, p = 0.0603; Student's paired t-test). These findings show that 5-HT$_4$R ligand BIMU8, does not exhibit signs of AChE inhibition at this concentration and correspondingly does not influence ACh or DA release dynamics in striatal slices, suggesting that 5-HT$_4$R activation alone is not responsible for striatal modulation of ACh or DA by 5-HT$_4$ ligands.

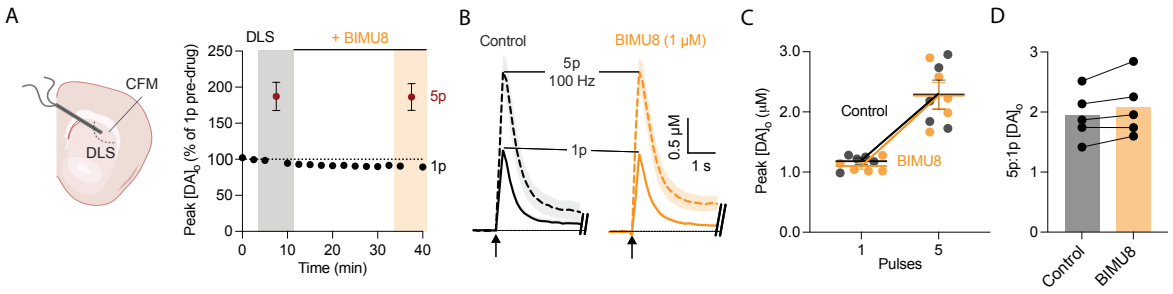

Figure 5.8. BIMU8 does not alter striatal DA dynamics in DLS. (A) Schematics of FCV stimulation and recording in DLS, alongside normalised mean peak $[DA]_o$ during consecutive recordings of DA release evoked by 1p (black) and 5p (100 Hz, red), during application of BIMU8. **(B)** mean $[DA]_o$ transients ± SEM evoked (at arrows) by single pulse (1p, solid line) and 5 pulses (100 Hz) (dashed line), before (black) and after (yellow) application of BIMU8 (n = 5 experiments in 4 mice). Mean transients of $[DA]_o$ are derived from three timepoints prior to the application of BIMU8 (grey shaded region) and last three timepoints (yellow shaded region). **(C)** Mean 1p and 5p 100 Hz $[DA]_o$ peak of control conditions (grey) and following drug application (yellow) in DLS. **(D)** Ratios of peak $[DA]_o$ released by 5p versus 1p in DLS. 2-way ANOVA, Fisher's LSD post-*hoc* test, Student's paired t-test. Error bars are ± SEM.

5.4 Discussion

In this study, we examined the actions of RS67333, a purported dual 5-HT$_4$ receptor agonist and AChE inhibitor, on striatal neurotransmission. We found that RS67333 reduces DA release in both dorsal and ventral striatum. This effect was mediated not via 5-HT4R activation, but via a prolongation of extracellular ACh signals, leading to desensitization of nAChRs on dopaminergic axons. This cholinergic mechanism was driven by potent inhibition of AChE enzymatic activity, confirmed using an AChE assay. In contrast, BIMU8, a 5-HT$_4$R ligand lacking AChE inhibitory activity, had no effect on either DA or ACh release. Together, these results establish that RS67333 acts as a functional AChE inhibitor in striatal circuits, altering ACh dynamics and thereby modulating DA transmission indirectly via nAChRs.

Importantly, to ensure that the observed reduction in DA signals was not an artefact of the detection method, we considered the potential influence of RS67333 on our measurement tools.

RS67333 was found to reduce the sensitivity of carbon fibre electrodes to DA during FCV, likely due to its electroactive structure. To correct for this, we calibrated each electrode individually and applied standardized correction coefficients as described in Methods. Moreover, to independently validate our findings, we employed a non-electrochemical approach using the genetically encoded fluorescent DA sensor $GRAB_{DA3h}$. Compared to FCV, $GRAB_{DA}$ provides superior spatial resolution and the ability to monitor DA dynamics over a broader time window, further strengthening the validity of these observations. These results together reinforce that RS67333 genuinely suppresses DA release via a biological mechanism, and not due to recording artefacts.

The modulation of DA release by ACh in the striatum is primarily mediated by nAChRs located on dopaminergic axons (Lopes et al., 2019; Threlfell & Cragg, 2011). These ligand-gated ion channels are activated by transient ACh release from ChIs, facilitating action potential–dependent DA release. However, nAChRs are highly sensitive to the temporal profile of ACh exposure. Short bursts of ACh promote receptor activation and DA release, whereas prolonged or excessive ACh presence leads to receptor desensitization - a conformational state in which the receptor remains bound by ligand but is functionally unresponsive (Ochoa et al., 1989; F.-M. Zhou et al., 2001). This desensitization, observed at α4β2 and α6-containing nAChRs that are presynaptically expressed on dopaminergic axons, serves as a protective mechanism against excitotoxicity but functionally suppresses dopaminergic output (Britt & McGehee, 2008; Ochoa et al., 1989). In our study, RS67333 significantly prolonged the extracellular ACh lifetime, as indicated by increased decay half-life and AUC of $GRAB_{ACh}$ signals. This likely resulted in sustained nAChR occupancy and receptor desensitization, thereby reducing the ability of ACh to gate DA release. Importantly, prior studies using AChE inhibitors such as donepezil and ambenonium have demonstrated that elevated ACh levels can desensitize nAChRs and reduce striatal DA output in rodent models, both *ex vivo* and *in vivo* (Hodge et al., 1992; Kramer et al.,

2022; Wang et al., 2014; F.-M. Zhou et al., 2001). Therefore, our findings are consistent with a model in which RS67333 suppresses DA release by potently inhibiting AChE, extending ACh availability, and inducing nAChR desensitization. This mechanistic cascade illustrates how modulation of ACh can dynamically influence DA transmission in the striatum and underscores the importance of cholinergic-dopaminergic interactions in interpreting the pharmacological effects of compounds like RS67333.

To further confirm that AChE is a direct and primary target of RS67333, future studies could examine whether RS67333 shares mechanistic properties with established AChE inhibitors, such as donepezil. For instance, assessing whether RS67333 produces additive effects when co-applied with known AChE blockers may help verify a shared target mechanism. Additionally, *in silico* docking approaches could provide structural evidence of the interaction of RS67333's interaction with the AChE active site (Akhoon et al., 2020; Kramer et al., 2022; Yu et al., 2022). These strategies would complement our enzymatic assay results and provide converging support that RS67333 acts through AChE inhibition to influence striatal ACh and DA transmission.

The ability of RS67333 to inhibit AChE may be structurally determined. RS67333 shares key pharmacophores with donepezil, a well-characterized AChE inhibitor, including a tertiary amine that engages the catalytic anionic site (CAS) of AChE, and aromatic moieties that interact with the active-site gorge via π–π stacking interactions (Lecoutey et al., 2014). These features have been functionally exploited in the design of donecopride - a compound incorporating structural elements of both RS67333 and donepezil - which retains dual activity as a 5-HT_4R agonist and AChE inhibitor and has been proposed as a therapeutic candidate for Alzheimer's disease (Lecoutey et al., 2014). Other 5-HT_4R agonists, such as RS67506, prucalopride, ML10302, CJ033466, have also been reported to weakly inhibit AChE, likely owing to similar structural characteristics (Lecoutey et al., 2014). However, this dual activity is not a general class effect.

For example, BIMU8, which we tested here, lacks AChE inhibitory function and did not affect ACh or DA transmission in our assays. Previous studies have shown that RS67333 inhibits human AChE with an IC_{50} of ~403 ± 86 nM (Lecoutey et al., 2014), therefore, in our experiments, RS67333 was applied at 10 µM in order to maximize its known off-target inhibition of AChE, which is a key focus of this study. Given that the EC_{50} of BIMU8 for wild type 5-HT_4R is ~ 7-18 nM (RM. Eglen et al., 1995; Pellissier et al., 2009; Schaus et al., 1998), BIMU8 was applied at 1 µM, a concentration widely used in the literature to selectively activate 5-HT_4Rs with minimal off-target effects (Uchiyama-Tsuyuki et al., 1996). To rule out concentration-dependent effects, we also tested BIMU8 at 10 µM and found no evidence of AChE inhibition, as supported by our $GRAB_{ACh}$ and AChE assay data (not shown). This reinforces the conclusion that not all 5-HT_4R ligands are AChE inhibitors, and that this is likely structure-dependent.

Our study is, to our knowledge, the first to demonstrate that RS67333 inhibits endogenous AChE activity in the striatum, expanding upon prior biochemical *in vitro* evidence that identified RS67333 as a sub-micromolar AChE inhibitor (Lecoutey et al., 2014). These findings also carry important implications for experimental studies that utilize RS67333 as a “selective” 5-HT_4R agonist. Previous reports have noted the impact of RS67333 on mood, neurogenesis, and memory, without accounting for AChE-mediated modulation of ACh and downstream targets (Faye et al., 2020; Freret et al., 2012; Lamirault & Simon, 2001; Mendez-David et al., 2014). Our data reveal that these effects may stem not solely from 5-HT_4R activation, but from potent cholinergic modulation via AChE inhibition. This adds a new layer of complexity to how RS67333 modulates brain circuits and provides a mechanistic foundation for its pleiotropic actions. Given the dual action of RS67333 on both 5-HT_4 receptors and AChE, it should not be considered a selective 5-HT_4R agonist in systems where cholinergic signalling contributes to circuit function. Our findings highlight the importance of accounting for cholinergic mechanisms -

particularly in regions where ACh and DA interact to shape neurotransmission, such as the striatum and hippocampusn - when interpreting the pharmacological or physiological effects.

Nonetheless, the identification of RS67333 as a dual-action ligand acting on both 5-HT_4 receptors and AChE offers new opportunities for therapeutic development. Although not clinically approved, its ability to simultaneously modulate serotonergic and cholinergic transmission, has made it a valuable research tool and a potential prototype for multi-target drug design. Given that both systems are dysregulated in neurodegenerative and neuropsychiatric disorders, such as AD, PD, and depression, RS67333's dual mechanism may offer therapeutic benefits in restoring neurotransmitter balance. Its effects on cognition, mood, and neuroprotection continue to warrant further investigation.

In summary, our studies have uncovered a pronounced function of RS67333 as an inhibitor of striatal AChE, which significantly shifts the understanding of the underlying circuits of how 5-HT_4R ligands regulating ACh and DA in striatum. Our study not only provides a new 5-HT_4R ligand pathway, but also emphasizes the importance of re-evaluating this compound's potential therapeutic applications, particularly in neurodegenerative and neuropsychiatric disorders where cholinergic and dopaminergic dysfunctions are central. These findings also highlight the importance of thoroughly evaluating off-target actions when using pharmacological tools to interpret circuit or behavioural functions.

Chapter 6.

Dysregulation of striatal 5-HT release in a mouse model of early Parkinson's disease

6.1 Introduction

6.1.1 Dysfunction of neurotransmission in PD

A hallmark of PD is the degeneration of nigrostriatal dopaminergic neurons, leading to a marked reduction of DA levels in the striatum (Bernheimer et al., 1973; Hornykiewicz, 2006). In the healthy brain, DA interacts with other neuromodulatory systems - including ACh and GABA - to regulate basal ganglia output and ensure normal motor control (Surmeier et al., 2014). Disruption of this finely tuned network in PD results in widespread synaptic dysfunction that extends beyond dopaminergic circuits. Today, levodopa (L-DOPA) remains the gold standard treatment for PD motor symptoms, but it does not correct underlying neurotransmitter imbalances and can induce long-term complications such as dyskinesia (Cenci, 2007).

Historically, PD has been described as a hypodopaminergic and hypercholinergic disorder (Barbeau, 1962). Animal model studies using neurophysiological and electrochemical approaches have demonstrated that dopaminergic depletion in the striatum leads to altered cholinergic interneuron (ChI) activity, often resulting in increased spontaneous firing rates and exaggerated ACh release in specific models, thereby disrupting the local DA-ACh balance that is critical for motor control (Maurice et al., 2015; Ztaou et al., 2016). However, these changes vary depending on the model and stage of pathology, and direct evidence from post-mortem human studies remains limited. Clinically, this imbalance was first addressed with anticholinergic drugs, which improved motor symptoms but were associated with cognitive and autonomic side effects (Lim et al., 2014; Paz et al., 2021).

In rodent models of PD, neurotransmitter alterations have been extensively characterized. DA depletion induced by 6-hydroxydopamine (6-OHDA) lesions leads to robust motor deficits and reductions in evoked DA release in the striatum (Zigmond et al., 1990). Alongside DA loss,

microdialysis studies in the 6-OHDA model have revealed elevated extracellular ACh levels in the striatum (Ikarashi et al., 1997; Tobón-Velasco et al., 2010). Although one study has reported reduced spontaneous firing of striatal ChIs following 6-OHDA lesions (Choi et al., 2020), the majority of electrophysiological evidence suggests that chronic dopaminergic depletion leads to ChI hyperexcitability. For instance, ChIs in 6-OHDA-lesioned mice exhibit increased tonic firing, depolarized membrane potentials, and enhanced excitatory synaptic input (Ding et al., 2010; Maurice et al., 2015). In addition to cholinergic changes, GABAergic transmission is also disrupted in a PD model. Expression of GABA transporters (GATs) is reduced, leading to enhanced tonic GABAergic inhibition of DA release, and DA axons co-release less GABA in the *SNCA*-OVX mouse model than in control mice (Roberts et al., 2020). Such GABAergic dysregulation may contribute to both motor impairments and compensatory changes in other neurotransmitter systems, including 5-HT.

Taken together, evidence from human studies and rodent models indicates that PD is not solely a dopaminergic disorder but involves complex maladaptation in multiple neurotransmitter systems. In early disease stages, before extensive neuronal loss occurs, these imbalances may already be present and could play a role in shaping disease progression and therapeutic responsiveness.

6.1.2 Striatal 5-HT dysfunction in PD

In addition to the well-characterized degeneration of nigrostriatal DA neurons, PD is also associated with marked alterations in the 5-HT system. Neuropathological studies indicate that brainstem raphe nuclei, including the DRN, are affected early in PD progression (Braak et al., 2003; Qamhawi et al., 2015), and post-mortem as well as *in vivo* PET imaging studies have revealed reduced striatal 5-HT transporter (SERT) availability and axonal terminal density, which correlate with non-motor symptoms such as depression, anxiety, sleep disturbances, and

fatigue (Bohnen & Albin, 2011; Politis et al., 2014; Politis & Loane, 2011). In the context of DA depletion and L-DOPA therapy, surviving 5-HT axons can abnormally convert exogenous L-DOPA into DA and release it in a dysregulated manner, lacking normal autoregulatory feedback, which has been proposed to contribute to the development of L-DOPA-induced dyskinesia (LID) (Carta et al., 2007; Rylander et al., 2010). In rodent PD models involving dopaminergic lesions (e.g., 6-OHDA or MPTP), studies have observed a significant increase in striatal serotonergic axon density, indicative of hyperinnervation (Muñoz et al., 2020; Rozas et al., 1998). This structural plasticity is accompanied by increased basal firing rates of serotonergic neurons, suggesting that the 5-HT system undergoes both anatomical and functional change in response to DA depletion. DA denervation also induces plastic changes in serotonergic axons that enhance L-DOPA-derived DA release, while pharmacological activation of $5\text{-HT}_{1A/1B}$ receptors or inhibition of 5-HT axon activity attenuates LID (Cenci, 2007; Huot & Fox, 2013). While these findings establish a role for 5-HT in PD pathophysiology, key gaps remain: it is unknown how 5-HT transmission is shaped during early onset of striatal dysfunction, whether its properties of release signalling, and whether its regulation by DA and GABA transmission that become dysfunctional also become dysregulated, and with what net outcome. The limited ability of established amine detection techniques like microdialysis or FCV to detect 5-HT over DA in striatum with either sufficient temporal or chemical sensitivity has hampered efforts to address potential dysregulation of 5-HT until now.

6.1.3 PD mouse models

A variety of animal models have been developed to study the pathogenesis of PD and to investigate potential therapeutic strategies. These include toxin-based models, such as the 6-OHDA lesion, which induces targeted degeneration of DA neurons, and genetic models, which

are generated by overexpressing or knocking out genes associated with PD, such as alpha-synuclein-overexpressing (*SNCA*-OVX) mice (Bové & Perier, 2012; Janezic et al., 2013).

Mutations and multiplications in the *SNCA* gene, which encodes the presynaptic protein α-synuclein, are linked to both familial and sporadic forms of PD (Singleton et al., 2003; Venda et al., 2010). Under physiological conditions, α-synuclein regulates synaptic vesicle mobilization and neurotransmitter release (Lautenschläger et al., 2018; Nemani et al., 2010), but in PD, it aggregates to form Lewy bodies - a pathological hallmark of neurodegeneration (Baba et al., 1998; Spillantini et al., 1998).

The *SNCA*-OVX mouse model overexpresses the entire human *SNCA* gene at disease-relevant levels while lacking endogenous mouse α-synuclein (Janezic et al., 2013). This genetic mutation allows the selective investigation of pathogenic mechanisms triggered by progressive human α-synuclein accumulation without interference from the native protein. *SNCA*-OVX mice show early striatal DA transmission impairments before neurodegeneration. Specifically, *ex vivo* recordings reveal that evoked DA release in DLS is reduced by approximately 30% in young adult *SNCA*-OVX mice (3-4 months old) compared to their *Snca*-/- littermates, with these deficits persisting across the lifespan (Janezic et al., 2013). Notably, these early release deficits occur prior to DA neuron loss and without alterations in SNc firing patterns or the release of other neurotransmitters such as 5-HT and NE (Janezic et al., 2013).

Alterations in GABAergic regulation of DA release are also evident from early adulthood. In the DLS of wild-type mice, DA release is subject to tonic GABAergic inhibition mediated by GABA transporters (GATs) (Lopes et al., 2019). In *SNCA*-OVX mice, GAT expression is downregulated, resulting in increased tonic GABAergic inhibition of DA release (Roberts et al., 2020). In addition, the DA release deficits in this model are also associated with concurrent

deficits in GABA co-release from DA axons, potentially further disrupting the spatiotemporal balance of inhibitory control within the striatum (Roberts et al., 2020).

These findings establish the *SNCA*-OVX line as a progressive and physiologically relevant model of early PD, characterised by selective α-synuclein overexpression, early-onset DA release deficits, and maladaptive changes in GABAergic regulation. While DA and GABAergic alterations have been documented, it remains unknown whether progressive α-synuclein accumulation in this model leads to early maladaptive changes in 5-HT transmission, a question addressed in the present work. Given the integrative role of 5-HT in modulating striatal function and its potential contribution to both motor and non-motor symptoms in PD, understanding how serotonergic signalling is altered during the early stages of the disease is essential. The *SNCA*-OVX model offers a unique opportunity to investigate these changes in the absence of widespread DA neuron loss, thereby isolating early synaptic alterations from downstream degenerative processes.

In this chapter, we used genetically encoded $GRAB_{5\text{-}HT}$ sensors to monitor evoked and tonic 5-HT release in DLS of *SNCA*-OVX mice and their *Snca*-/- controls. We further assess whether previously reported deficits in DA release (Janezic et al., 2013) and alterations in GABAergic regulation (Roberts et al., 2020) in *SNCA*-OVX mice influence serotonergic transmission. This approach aims to provide a comprehensive characterization of striatal 5-HT dysregulation in early PD and to identify potential mechanisms linking α-synuclein pathology to neurotransmitter imbalance.

6.2 Methods

Experiments detailed in this chapter were carried out in accordance with the general methods described in Chapter 2. Variations and further details are reported below.

6.2.1 Animal models

To investigate early-stage disruptions in striatal 5-HT transmission associated with α-synuclein overexpression, I employed a well-established transgenic mouse model that overexpresses human wild-type α-synuclein (*SNCA*-OVX) at levels relevant to PD (Janezic et al., 2013). Details of the generation and genotyping of this mouse line are provided in Chapter 2 (**Section 2.1.3**). Age- and sex-matched littermate mice lacking endogenous α-synuclein expression (*Snca* -/-) were used as controls throughout the experiments.

For *in situ* monitoring of 5-HT release, both *SNCA*-OVX and *Snca* -/- mice received stereotaxic injections of AAV2/5-hSyn-GRAB$_{5\text{-}HT3.0}$ targeted to the DLS, as described in **Section 2.3.1**. Three weeks post-injection, acute coronal brain slices containing the striatum were prepared for *ex vivo* imaging studies following the procedures outlined in Chapter 2 (**Section 2.2.4**).

All animals were between 3 and 4 months of age, a time window previously shown to capture early synaptic dysfunction in *SNCA*-OVX mice. At this developmental stage, striatal dopaminergic and GABAergic alternations have been consistently reported (Janezic et al., 2013; Roberts et al., 2020), making it suitable for examining potential serotonergic impairments. All recordings were conducted in DLS, a subregion where α-synuclein–dependent alterations in DA and GABAergic transmission have been previously characterized.

6.2.2 GRAB$_{5\text{-}HT}$ imaging

For experiments assessing electrically evoked 5-HT release, recordings were performed as outlined in Chapter 2 (**Sections 2.3.2**). Continuous blue light (470 nm) illumination at ~4-5 mW was used to excite the GRAB$_{5\text{-}HT}$ fluorophore. Electrical stimuli (0.6 mA, 200 µs) were delivered at intervals of 2.5 minutes, and stimulation protocols were performed in duplicate with random

presentation order. To exclude the effect of cholinergic system on striatal DA, GABA or 5-HT, the experiments were conducted in the presence of DHßE throughout.

In all experiments, a minimum of three animals (N ≥ 3) was used per condition. Slices from different genotypes were prepared on separate experimental days to avoid unnecessary photostimulation of non-imaged samples. This ensured that slices were only exposed to excitation light during active recording sessions, reducing potential phototoxic effects or sensor desensitisation across preparations.

Drug	Supplier	Action	Concentration	Solvent	References
Dihydro-β-erythroidine (DHβE) hydrobromide	Sigma-Aldrich	nAChR antagonist	1 µM	dH_2O	Threlfell et al. (2012); Roberts et al. (2020)
Citalopram	Sigma-Aldrich	SSRI	75 nM	DMSO	Stenfors et al. (2001)
(+)-Bicuculline	Abcam	$GABA_AR$ antagonist	10 µM	DMSO	Roberts et al. (2020); Stedehouder et al. (2024)
CGP 55845 hydrochloride	Abcam	$GABA_BR$ antagonist	4 µM	DMSO	Roberts et al. (2020); Stedehouder et al. (2024)
Quinpirole	Cambridge Bioscience	D_2R agonist	2 µM	DMSO	Brimblecombe et al. (2019)
L-741,626	Abcam	D_2R antagonist	1 µM	DMSO	Condon et al. (2019)

6.2.3 Drugs

Stock solutions were prepared at 1,000x – 20,000x the final concentration and stored at -20°C. Final drug concentrations were prepared in aCSF on the day of the experiment.

6.2.4 Data acquisition and analysis

FCV data were digitized and acquired using Axoscope 10.7 and extracted using locally written Python script. GRAB sensor data were extracted by Image J and analyzed by locally written MATLAB or Python script described in **Section 2.3.4**. Statistical tests were performed in GraphPad Prism 10.

6.3 Results

6.3.1 5-HT dynamics release in a mouse model of early PD

After establishing the fundamental properties and modulatory mechanisms of striatal 5-HT release in WT animals in Chapter 3, I assessed whether these dynamics are disrupted under early parkinsonian conditions. While previous studies have reported approximately 30% reduction of striatal DA release in this parkinsonian mouse model, the release of 5-HT when assessed in the SNr appears unaffected (Janezic et al., 2013). However, it remains unclear how 5-HT release in striatum is altered under early disease conditions. Therefore, I used mice overexpressing human α-synuclein (*SNCA*-OVX), a well-characterised mouse model of PD that exhibits functional alterations in DA and GABAergic transmission prior to cell loss (Janezic et al., 2013; Roberts et al., 2020). Littermate mice lacking endogenous α-synuclein (*Snca*-/-) were used as controls. Both groups were injected with the same $GRAB_{5\text{-}HT3.0}$ virus in DLS, and *ex vivo* slice recordings were performed 3-4 weeks later using electrical stimulation to evoke local 5-HT release.

Electrical stimulation of the DLS evoked robust 5-HT signals in both *Snca*-/- and *SNCA*-OVX animals. A marked enhancement in peak amplitude was observed in *SNCA*-OVX mice compared to that in *Snca*-/- mice under both 1p and 5p 100 Hz stimulation protocols (**Fig. 6.1A-C**; $F_{(2,184)}$ = 6.496, p = 0.002, RM ANOVA main effect of the genotype; WT: n = 45 slices/23 mice; *Snca*-/- and *SNCA*-OVX: n = 25 slices/8 pairs of mice). Notably, evoked $[5\text{-HT}]_o$ in *Snca*-/- mice

showed no significant deviation from WT animals in either condition. Additionally, the baseline (F_0) of evoked 5-HT signals in *SNCA*-OVX mice closely matched those recorded in *Snca*-/- and WT animals, suggesting that the removal of endogenous α-synuclein alone does not modify basal 5-HT dynamics. The augmented evoked 5-HT peaks observed in *SNCA*-OVX mice may indicate a compensatory upregulation of release mechanisms in the DLS.

To test whether there was a change in uptake, that might contribute to a change to the peak $[5\text{-HT}]_o$ detected, I examined the clearance kinetics of the evoked 5-HT signals. Exponential fitting of the decay phase revealed that *SNCA*-OVX mice exhibited significantly prolonged decay half-life compared with both *Snca*-/- and WT groups (**Fig. 6.1D-E**; $F_{(2,184)} = 17.66$, $p < 0.001$, RM ANOVA main effect of the genotype). These findings suggest impaired 5-HT reuptake or metabolism in *SNCA*-OVX animals. This impairment might contribute to the larger evoked $[5\text{-HT}]_o$ detected. The decay half-life of evoked 5-HT signals of *Snca*-/- mice again showed no significant difference from WT animals, supporting the notion that the slowed clearance is specific to the *SNCA*-OVX line.

To investigate whether these functional changes are accompanied by alterations in serotonergic innervation, we performed immunohistochemical staining of 5-HT fibres in both DLS and NAcC. As described in previous sections, tissue sections were labelled using a 5-HT antibody, and the bulk density of labelled fibres was quantified as an approximate measure of 5-HT innervation density. No significant differences were observed in 5-HT innervation density between *SNCA*-OVX, *Snca*-/-, and WT mice in either subregion (**Fig. 6.1F-G;** DLS: $F_{(2,51)} = 2.136$, $p = 0.0691$; NAcC: $F_{(2,51)} = 0.9719$, $p = 0.3852$; RM ANOVA main effect of the genotype; $n = 18$ slices/genotype). This suggests that the increased evoked $[5\text{-HT}]_o$ detected in *SNCA*-OVX mice is not due to a gross enrichment in serotonergic innervation.

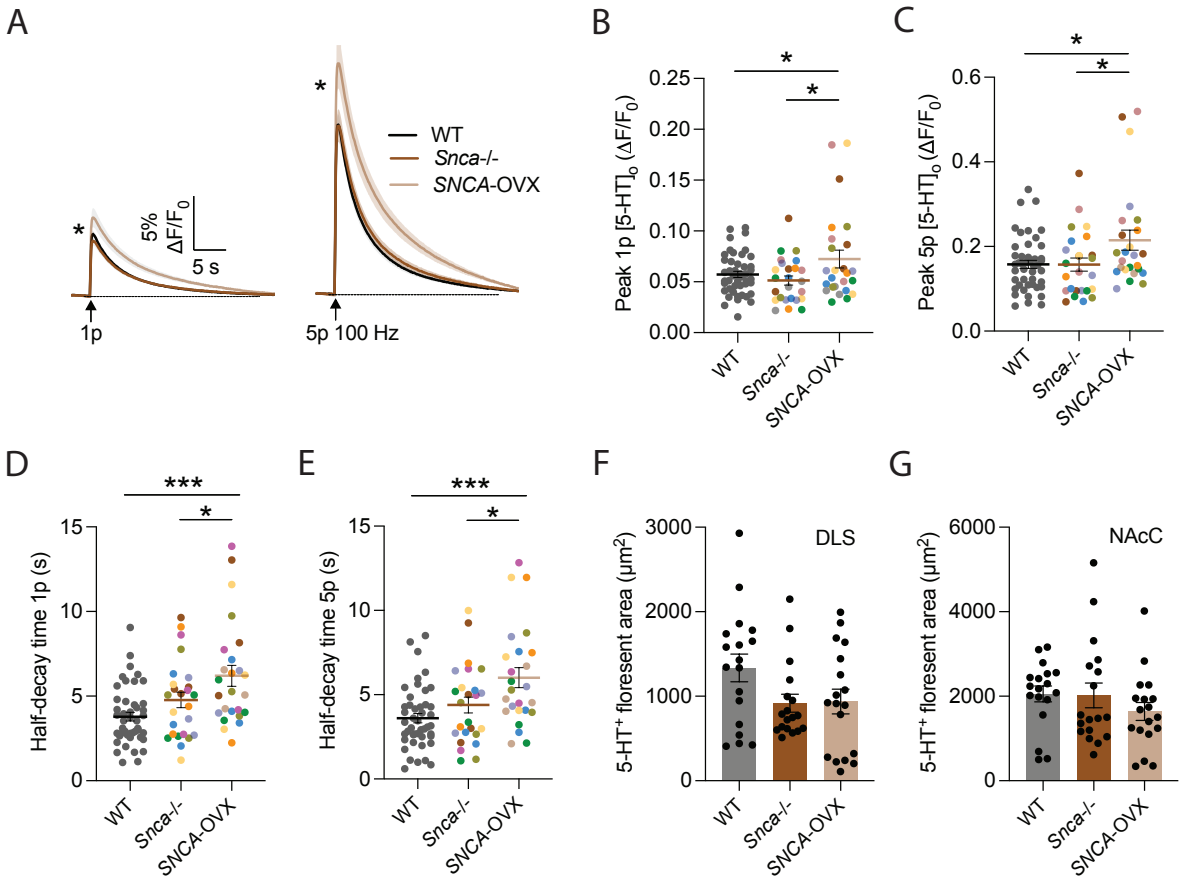

Figure 6.1. Striatal 5-HT signals in WT, *Snca*-/- and *SNCA*-OVX mice. (A) Mean evoked 5-HT transients ± SEM, in the presence of DHßE (1 μM) in DLS in WT, *Snca*-/- and *SNCA*-OVX mice (WT: *n* = 45 experiments/23 mice; *Snca*-/- and *SNCA*-OVX: *n* = 25 experiments/8 pairs of mice). **(B,C)** Mean 1p (B) and 5p 100 Hz (C) $[5\text{-HT}]_o$ peak in the presence of DHßE in DLS in WT, *Snca*-/- and *SNCA*-OVX mice. Each data point represents an individual slice. For *Snca*-/- and *SNCA*-OVX groups, slices originating from the same mouse are colour-coded identically. **(D,E)** Mean 1p (D) and 5p 100 Hz (E) decay half-life of $[5\text{-HT}]_o$ in the presence of DHßE (1 μM) in DLS in WT, *Snca*-/- and *SNCA*-OVX mice. Each data point represents an individual slice. For *Snca*-/- and *SNCA*-OVX groups, slices originating from the same mouse are colour-coded identically. **(F,G)** Quantification of 5-HT innervation as indicated by 5-HT^+ florescent area (μm^2) in DLS (F) and NAcC (G) from WT, *Snca*-/- and *SNCA*-OVX mice (*n* = 18 slices/6 mice). One-way ANOVA or 2-way ANOVA, Fisher's LSD post-*hoc* test, **p* < 0.05, ****p* < 0.001. Error bars are ± SEM.

Together, these findings indicate that striatal 5-HT transmission is dysregulated in *SNCA*-OVX mice, with enhanced stimulus-evoked release and impaired clearance, despite apparently normal 5-HT levels as assessed by 5-HT-immunoreactivity. These alterations may reflect compensatory mechanisms in response to α-synuclein-induced cellular stress, early synaptic dysfunction including down regulation of 5-HT uptake and might also involve a change to the

neuromodulator landscape. By contrast, *Snca*-/- mice display 5-HT dynamics indistinguishable from the WT control, reinforcing that the observed changes in 5-HT release are not due to the depletion of α-synuclein.

To determine whether dopaminergic mechanisms contribute to the altered 5-HT signals in *SNCA*-OVX mice, I assessed striatal 5-HT release in the presence of DA receptor antagonists. *SNCA*-OVX mice display an approximate 30% reduction in striatal DA release relative to controls (Janezic et al., 2013), raising the possibility that dysregulated DA-5-HT interactions could underlie the observed phenotype. To test this, I applied a combination of D_1 and D_2 receptor antagonists (SCH39166 and L-741,626, 1 μM each) to block dopaminergic influence on 5-HT axons and compared evoked 5-HT release in WT, *Snca*-/-, and *SNCA*-OVX mice.

In the presence of DA receptor antagonists, electrical stimulation of the DLS evoked 5-HT signals that were highly similar across all three genotypes. Peak amplitudes evoked by both 1p and 5p 100 Hz stimulation showed no significant differences between WT, *Snca*-/-, and *SNCA*-OVX mice (**Fig. 6.2A-B**; $F_{(2,58)} = 1.101$, $p = 0.34$, RM ANOVA main effect of the genotype; $n = 11$ experiments/6 pairs of mice). This contrasts with the enhanced evoked 5-HT signals observed in *SNCA*-OVX mice without DA receptor blockade (**Fig. 6.1**), suggesting that DA signalling plays a critical role in modulating 5-HT output in these animals.

Intriguingly, analysis of the decay kinetics revealed no significant differences in half-life values among the three genotypes when DA receptors were blocked (**Fig. 6.2C**; $F_{(2,58)} = 1.312$, $p = 0.28$, RM ANOVA main effect of the genotype). This impact of DA receptor inhibition is somewhat unexpected as DA receptors are not usually expected to change uptake transporter function particularly, raising the question of whether the decay kinetics of 5-HT signals detected by GRAB are a function of signal amplitude and not just uptake and sensor off-time.

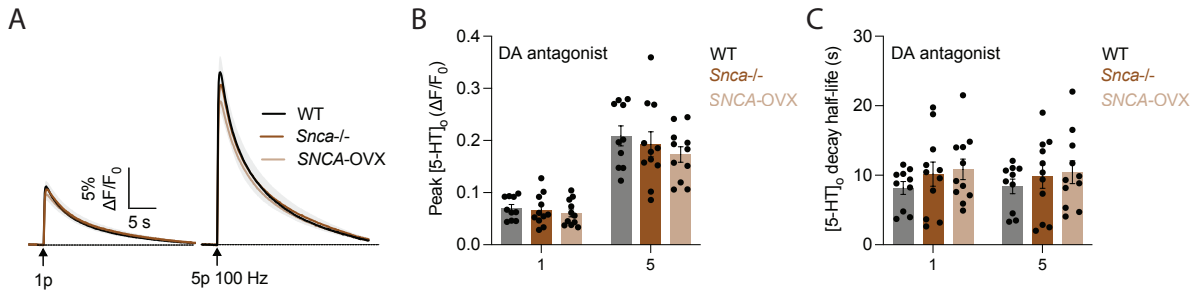

Figure 6.2. Striatal 5-HT dynamics in the presence of DA antagonist in WT, *Snca*-/- and *SNCA*-OVX mice. (A) Mean evoked 5-HT transients ± SEM, in the presence of SCH39166 (1 μM) and L-741,626 (1 μM) in DLS from WT, *Snca*-/- and *SNCA*-OVX mice (WT: *n* = 10 experiments/5 mice; *Snca*-/- and *SNCA*-OVX: *n* = 11 experiments/6 pairs of mice). **(B)** Mean 1p and 5p 100 Hz $[5\text{-HT}]_o$ peak in the presence of SCH39166 (1 μM) and L-741,626 (1 μM) in DLS from WT, *Snca*-/- and *SNCA*-OVX mice. **(C)** Mean 1p and 5p 100 Hz decay half-life of $[5\text{-HT}]_o$ in the presence of SCH39166 (1 μM) and L-741,626 (1 μM) in DLS from WT, *Snca*-/- and *SNCA*-OVX mice. 2-way ANOVA, Fisher's LSD post-*hoc* test. Error bars are ± SEM.

Together, these findings demonstrate that the dysregulated 5-HT transmission in *SNCA*-OVX mice is abolished by blocking DA receptor activity, highlighting a DA-dependent mechanism underlying the observed phenotype. In the absence of reduced DA acting at DA receptors, serotonergic dynamics across *SNCA*-OVX, *Snca*-/- and WT mice become indistinguishable, pointing to DA as a key modulator of 5-HT function in the striatum under disease-relevant conditions.

GABA also plays a critical role in striatal circuit function, and an enhanced GABAergic tone has been reported in the same *SNCA*-OVX mouse model of PD (Roberts et al., 2020). However, it remains unclear whether the effects of genotype on striatal 5-HT dynamics are modulated by the presence or absence of GABAergic input under these pathological conditions. To explore how 5-HT transmission behaves in the absence of GABAergic tone in *SNCA*-OVX mice, I next compared evoked $[5\text{-HT}]_o$ in the presence of $GABA_A$ and $GABA_B$ receptor antagonists – bicuculine (10 μM) and CGP55845 (4 μM) respectively. Under these conditions, *SNCA*-OVX mice again exhibited significantly elevated evoked $[5\text{-HT}]_o$ compared to both WT and *Snca*-/- mice (**Fig. 6.3A-B**; $F_{(2,24)} = 4.941$, $p = 0.02$, RM ANOVA main effect of the genotype; $n = 5$

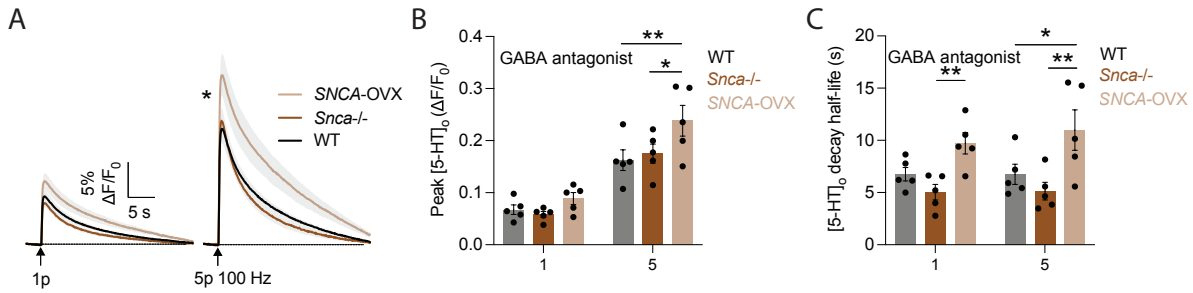

Figure 6.3. Striatal 5-HT dynamics in the presence of $GABA_{A\&B}R$ antagonist in WT, *Snca*-/- and *SNCA*-OVX mice. (A) Mean evoked 5-HT transients ± SEM, in the presence of bicuculine (10 μM) and CGP55845 (4 μM) in DLS from WT, *Snca*-/- and *SNCA*-OVX mice (WT: n = 5 experiments/4 pairs of mice). **(B)** Mean 1p and 5p 100 Hz $[5\text{-HT}]_o$ peak in the presence of bicuculine (10 μM) and CGP55845 (4 μM) in DLS from WT, *Snca*-/- and *SNCA*-OVX mice. **(C)** Mean 1p and 5p 100 Hz decay half-life of $[5\text{-HT}]_o$ in the presence of bicuculine (10 μM) and CGP55845 (4 μM) in DLS from WT, *Snca*-/- and *SNCA*-OVX mice. 2-way ANOVA, Fisher's LSD post-*hoc* test, *p < 0.05, **p < 0.01. Error bars are ± SEM.

experiments/3 pairs of mice). This enhancement was observed across both stimulation paradigms, resembling the pattern seen under baseline conditions (**Fig. 6.1**), and contrasting with the normalised response seen in the presence of DA receptor antagonists (**Fig. 6.2**).

Similarly, decay kinetics analysis showed prolonged half-life of 5-HT signals in *SNCA*-OVX mice compared with both *Snca*-/- and WT mice (**Fig. 6.3C**; $F_{(2,24)}$ = 11.72, p < 0.001, RM ANOVA main effect of the genotype). No significant differences in either peak amplitude or decay were found between WT and *Snca*-/- mice. These results demonstrate that, in the absence of GABAergic inhibition, the enhanced 5-HT release and impaired clearance observed in *SNCA*-OVX mice re-emerge.

To further examine whether dopaminergic and GABAergic influences exert opposing effects on striatal 5-HT dynamics in *SNCA*-OVX mice, I next assessed evoked 5-HT release under simultaneous blockade of DA and GABA receptors. This approach was designed to test whether removing both major modulatory inputs would counterbalance the effects of each other and thereby normalise the altered 5-HT transmission observed in this PD model. To this end, I applied both D_1/D_2R antagonists (SCH39166 and L-741,626, 1 μM each) and $GABA_{A/B}$ receptor

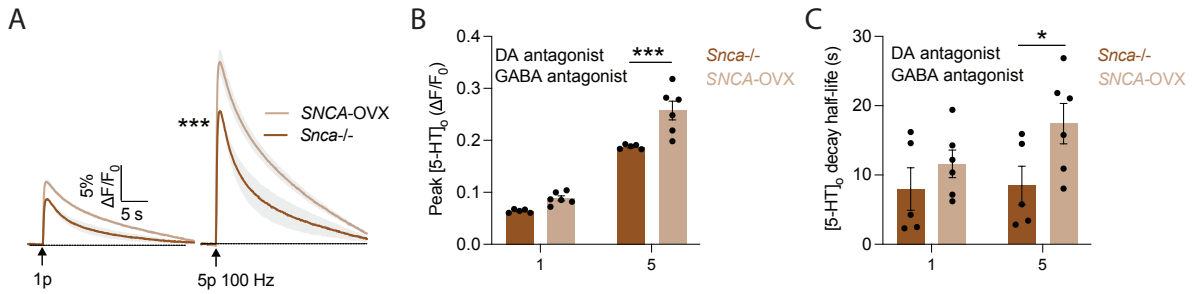

Figure 6.4. Striatal 5-HT dynamics in the presence of DA and $GABA_{A\&B}R$ antagonist in *Snca*-/- and *SNCA*-OVX mice. (A) Mean evoked 5-HT transients ± SEM, in the presence of bicuculine (10 µM), CGP55845 (4 µM), SCH39166 (1 µM), L-741,626 (1 µM) and DHßE (1 µM) in DLS from *Snca*-/- and *SNCA*-OVX mice (n = 6 experiments/4 pairs of mice). **(B)** Mean 1p and 5p 100 Hz $[5\text{-HT}]_o$ peak in the presence of bicuculine, CGP55845, SCH39166, L-741,626 and DHßE in DLS from *Snca*-/- and *SNCA*-OVX mice. **(C)** Mean 1p and 5p 100 Hz decay half-life of $[5\text{-HT}]_o$ in the presence of bicuculine, CGP55845, SCH39166, L-741,626 and DHßE in DLS from *Snca*-/- and *SNCA*-OVX mice. 2-way ANOVA, Fisher's LSD post-*hoc* test, *p < 0.05, ***p < 0.001. Error bars are ± SEM.

antagonists (bicuculline 10 µM and CGP55845 4 µM) during $GRAB_{5\text{-HT}}$ recordings in DLS slices from *Snca*-/- and *SNCA*-OVX mice.

In this condition, electrical stimulation evoked significantly larger 5-HT signals in *SNCA*-OVX mice compared to *Snca*-/- animals, particularly under 5p 100 Hz stimulation (**Fig. 6.4A-B**; $F_{(1,18)}$ = 20.41, p < 0.001, RM ANOVA main effect of the genotype; n = 5 experiments/3 pairs of mice). This enhancement was further reflected in the decay kinetics, where *SNCA*-OVX mice exhibited prolonged decay half-life compared with *Snca*-/- mice, again most notably under high-frequency stimulation (**Fig. 6.4C**; $F_{(1,18)}$ = 5.400, p = 0.003, RM ANOVA main effect of the genotype). Together, these results indicate that when both dopaminergic and GABAergic inputs are pharmacologically removed, striatal 5-HT release remains abnormally elevated in *SNCA*-OVX mice. These findings suggest that additional local or intrinsic mechanisms may contribute to the serotonergic compensation observed in this PD model.

6.3.2 SERT control of 5-HT release is diminished in PD mice

I next examined whether 5-HT reuptake via SERT is functionally altered. Previous reports have shown that DAT function is enhanced in *SNCA*-OVX mice (Threlfell et al., 2021), including evidence of greater impact of DAT blockers such as cocaine or nomifensine on evoked $[DA]_o$. Motivated by these findings, I applied the SERT blocker citalopram (75 nM) to assess whether 5-HT clearance mechanisms are similarly altered in the same PD mouse model.

SERT blockade with citalopram increased the peak amplitude of electrically evoked 5-HT release across all genotypes, but the effect was notably reduced in *SNCA*-OVX mice compared to both WT and *Snca*-/- animals (**Fig. 6.5A-C**). Under both 1p and 5p 100 Hz stimulation conditions, the increase in 5-HT peak amplitude following citalopram application was significantly smaller in *SNCA*-OVX mice than in controls (**Fig. 6.5C**; $F_{(2,24)} = 9.985$, $p < 0.001$, RM ANOVA main effect of the genotype; $n = 5$ experiments/3 pairs of mice). Similarly, the AUC of evoked $[5\text{-HT}]_o$ increased less in *SNCA*-OVX mice relative to WT and *Snca*-/- controls (**Fig. 6.5D-E**; $F_{(2,24)} = 10.70$, $p < 0.001$, RM ANOVA main effect of the genotype), indicating a diminished capacity of SERT blockade to prolong extracellular 5-HT levels in the PD model.

Additionally, in earlier experiments, I showed that the decay of 5-HT signals in *SNCA*-OVX mice has longer half-live than in WT and *Snca*-/- animals, consistent with impaired clearance. Following citalopram application, the $[5\text{-HT}]_o$ decay half-life remained slowest in *SNCA*-OVX mice despite the reduced peak and AUC response to SERT inhibition (**Fig. 6.5F**; $F_{(2,28)} = 15.58$, $p < 0.001$, RM ANOVA main effect of the genotype), potentially suggesting compromised function of an alternative transporter.

Together, these results demonstrate that SERT-mediated reuptake control is impaired in *SNCA*-OVX mice. The reduced sensitivity to pharmacological SERT blockade suggests a loss of functional SERT capacity, potentially contributing to the prolonged 5-HT signals observed under basal conditions in this early PD model. However, it is important to consider that 5-HT

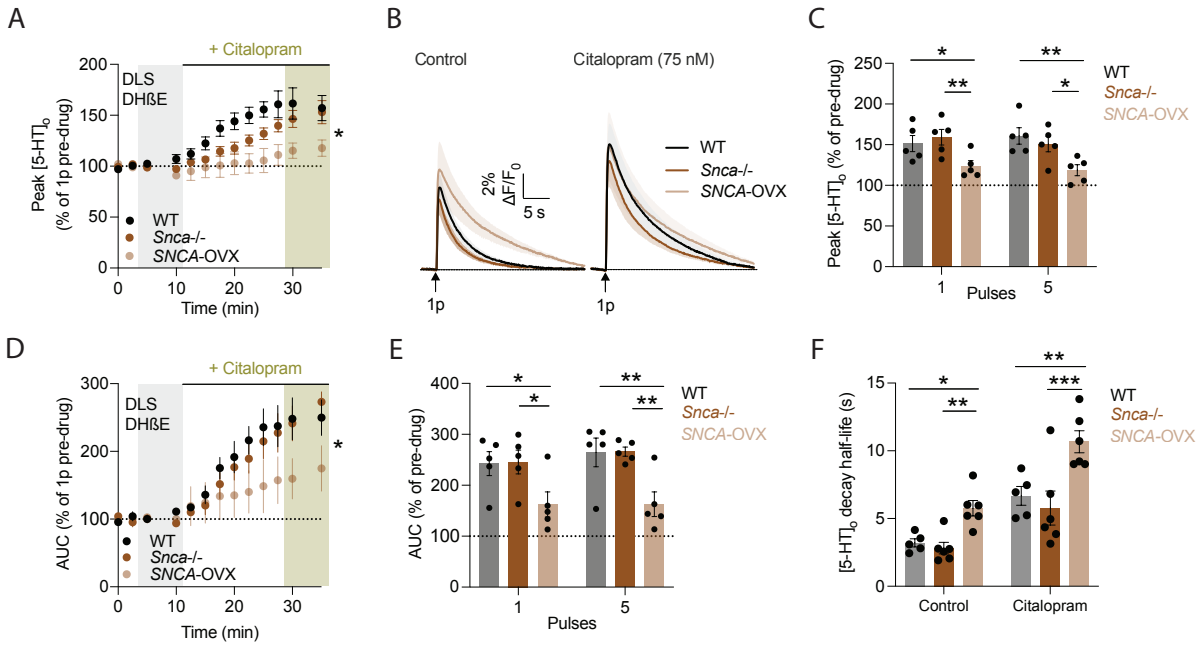

Figure 6.5. Citalopram prolonged and increased evoked 5-HT signal in WT, *Snca*-/- and *SNCA*-OVX mice. (A) Normalized mean peak $[5\text{-HT}]_o$ during consecutive recordings of 5-HT release evoked by 1p during the application of citalopram (75 nM) in the presence of DHβE in DLS in WT, *Snca*-/- and *SNCA*-OVX mice (n = 5 experiments/3 mice). **(B)** Mean 1p-evoked 5-HT transients ± SEM, before (left) and after (right) application of citalopram in the presence of DHβE in DLS in WT, *Snca*-/- and *SNCA*-OVX mice. Mean transients of $[5\text{-HT}]_o$ are derived from two timepoints prior to the application of the drug (grey shaded region) and last two timepoints (green shaded region). **(C)** Normalized 1p and 5p 100 Hz $[5\text{-HT}]_o$ peak after citalopram application in the presence of DHβE in DLS in WT, *Snca*-/- and *SNCA*-OVX mice. **(D)** Normalized mean AUC $[5\text{-HT}]_o$ during consecutive recordings of 5-HT release evoked by 1p during the application of citalopram (75 nM) in the presence of DHβE in DLS in WT, *Snca*-/- and *SNCA*-OVX mice. **(E)** Normalized 1p and 5p 100 Hz $[5\text{-HT}]_o$ AUC after citalopram application in the presence of DHβE in DLS in WT, *Snca*-/- and *SNCA*-OVX mice. **(F)** Mean 1p decay half-life of $[5\text{-HT}]_o$ under control conditions (grey) and following drug application (green) in the presence of DHβE in DLS in WT, *Snca*-/- and *SNCA*-OVX mice. 2-way ANOVA, Fisher's LSD post-*hoc* test. *$p < 0.05$, **$p < 0.01$, ***$p < 0.001$. Error bars are ± SEM.

clearance in the striatum is not relied solely on SERT. Previous studies and my earlier results indicate that DAT can also transport 5-HT. A critical unresolved issue is the relative contribution of SERT vs. DAT to 5-HT uptake in this context - we cannot currently determine which transporter plays the dominant role. Moreover, we do not yet have direct evidence to assess DAT-mediated 5-HT transport in *SNCA*-OVX mice, and further experiments would be needed to clarify this point.

6.3.3 D_2R-mediated inhibition of striatal 5-HT release is diminished in PD mice

I next directly investigated whether DA receptor-mediated modulation of 5-HT release is also affected. In WT animals, previous results in Chapter 4 demonstrated that dopaminergic signalling can regulate striatal 5-HT release through D_2 receptors. Given that DA release is reduced in *SNCA*-OVX mice, I hypothesised that endogenous activation of D_2 receptors might also be impaired, potentially altering D_2R-mediated modulation of 5-HT release. Therefore, I examined the effects of D_2 receptor activation in $GRAB_{5\text{-}HT}$-expressing slices from *SNCA*-OVX and *Snca*-/- animals. Quinpirole (2 μM) was bath-applied during *ex vivo* slice recordings and evoked 5-HT responses were measured in the DLS.

I found that quinpirole significantly suppressed $[5\text{-HT}]_o$ across all genotypes, reducing peak amplitude to approximately 50% of pre-drug levels (**Fig. 6.6A-C**). Importantly, the extent of suppression was comparable between *SNCA*-OVX and *Snca*-/- mice. I also compared the magnitude of quinpirole-induced suppression in the PD mouse model with the WT animals. Peak reduction following D_2 receptor activation was comparable among all three genotypes (**Fig. 6.6D**; $F_{(2,27)} = 2.422$, $p = 0.11$, RM ANOVA main effect of the genotype), suggesting in the PD mouse model, the ability of D_2 receptor activation to suppress 5-HT release is not functionally impaired.

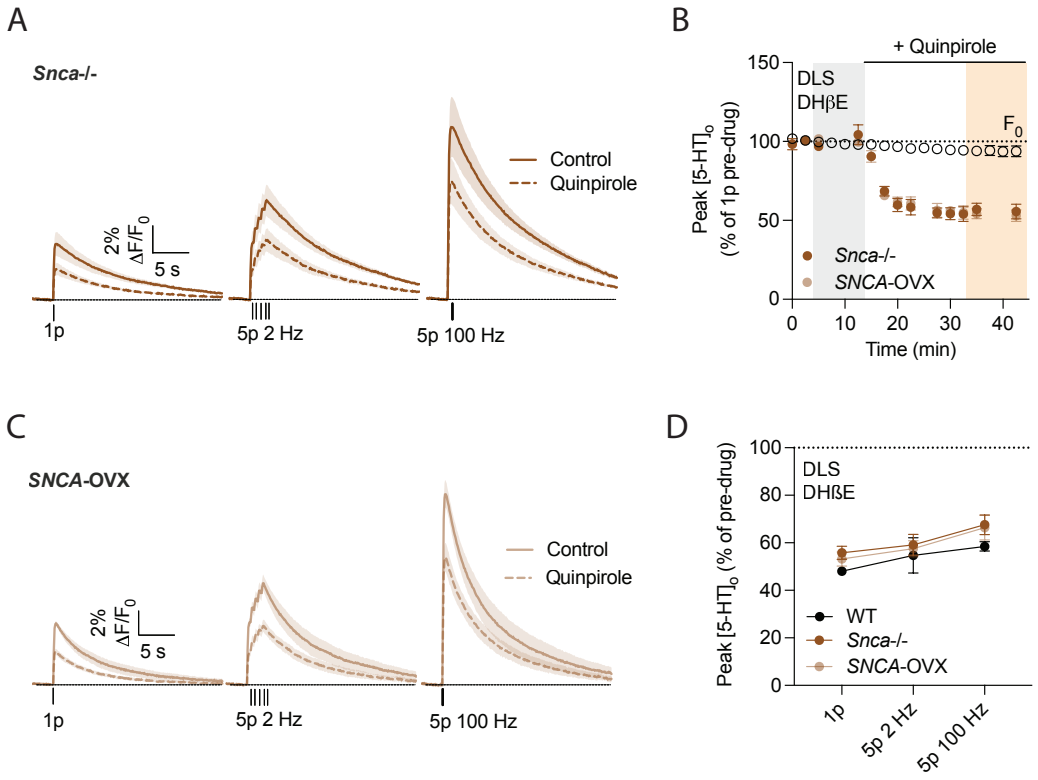

Figure 6.6. D_2R agonism-induced 5-HT inhibition showed no difference between *SNCA*-OVX and *Snca*-/- mice. (A,C) Mean evoked 5-HT transients ± SEM, before (solid line) and after (dash line) application of quinpirole (2 µM) in the presence of DHßE in DLS of *Snca*-/- (A) and *SNCA*-OVX (C) mice. Mean transients of $[5\text{-HT}]_o$ are derived from two timepoints prior to the application of the drug (grey shaded region) and last two timepoints (orange shaded region). **(B)** Normalized mean peak $[5\text{-HT}]_o$ and baseline fluorescence (F_0) during consecutive recordings of 5-HT release evoked by 1p during the application of quinpirole in the presence of DHßE in DLS in *Snca*-/- and *SNCA*-OVX mice. (*n* = 4 experiments/2 pairs of mice). **(D)** Normalized 1p, 5p 2 Hz and 5p 100 Hz $[5\text{-HT}]_o$ peak after quinpirole application in the presence of DHßE in DLS in WT, *Snca*-/- and *SNCA*-OVX mice. 2-way ANOVA, Fisher's LSD post-*hoc* test. Error bars are ± SEM.

If D_2R function is altered in the PD mouse model, such changes are likely to be mild. In this case, activating D_2Rs by externally applying an agonist may not be sensitive enough to detect these subtle dysfunctions in D_2R-mediated control of 5-HT release. Therefore, even though no differences were observed in D_2R agonist-induced modulation of 5-HT release between genotypes, I next used a complementary approach by pharmacologically blocking D_2Rs. In WT mice, as shown in Chapter 4, D_2R blockade reliably increases evoked 5-HT release in peak amplitude and AUC. Based on this observation, I similarly applied the selective D_2R antagonist

L-741,626 (1 μM) to $GRAB_{5\text{-}HT}$-expressing DLS slices from *Snca*-/-, and *SNCA*-OVX mice to determine whether D_2R control of 5-HT release is altered in the PD model. Blocking D_2R activity with L-741,626 increased evoked $[5\text{-HT}]_o$ to approximately 135% of pre-drug levels in both WT and *Snca*-/- animals, whereas the corresponding increase in *SNCA*-OVX mice was markedly attenuated, reaching only ~110% of pre-drug (**Fig. 6.7A,C-E**; $F_{(2,45)} = 12.91$, $p < 0.001$, RM ANOVA main effect of the genotype). This reduced facilitatory effect in *SNCA*-OVX animals was evident for both 1p and 5p 2 Hz and 100 Hz stimulations (**Fig. 6.7C-E**). Baseline fluorescence (F_0) values remained comparable across the three genotypes (**Fig. 6.7B**), indicating that the genotype differences reflect altered evoked release rather than baseline shifts. I further analysed each pulse-evoked 5-HT transient during a 5p 2 Hz stimulation train. Consistent with previous findings that DA receptor modulation of 5-HT release is maximal around 500 ms after the stimulus, the largest genotype difference was observed at the second pulse, where the increase in 5-HT release in *SNCA*-OVX mice was minimal compared to the robust facilitation seen in WT and *Snca*-/- animals (**Fig. 6.7F**; $F_{(2,70)} = 14.63$, $p < 0.001$, RM ANOVA main effect of the genotype).

Unlike peak amplitude, neither the AUC (**Fig. 6.7G**; $F_{(2,28)} = 1.429$, $p = 0.27$, RM ANOVA main effect of the genotype) nor the decay half-life (**Fig. 6.7H**; $F_{(2,28)} = 2.176$, $p = 0.13$, RM ANOVA main effect of the genotype) showed significant genotype-dependent differences following D_2R blockade.

Together, these findings demonstrate that while D_2Rs are stably coupled to the control of 5-HT release across genotypes, the D_2R-mediated inhibition of 5-HT release offered by endogenous DA is diminished in a mouse model of PD, as indicated by the diminished increase in evoked release after pharmacological D_2R blockade. This is consistent with the deficit in DA release in the model.

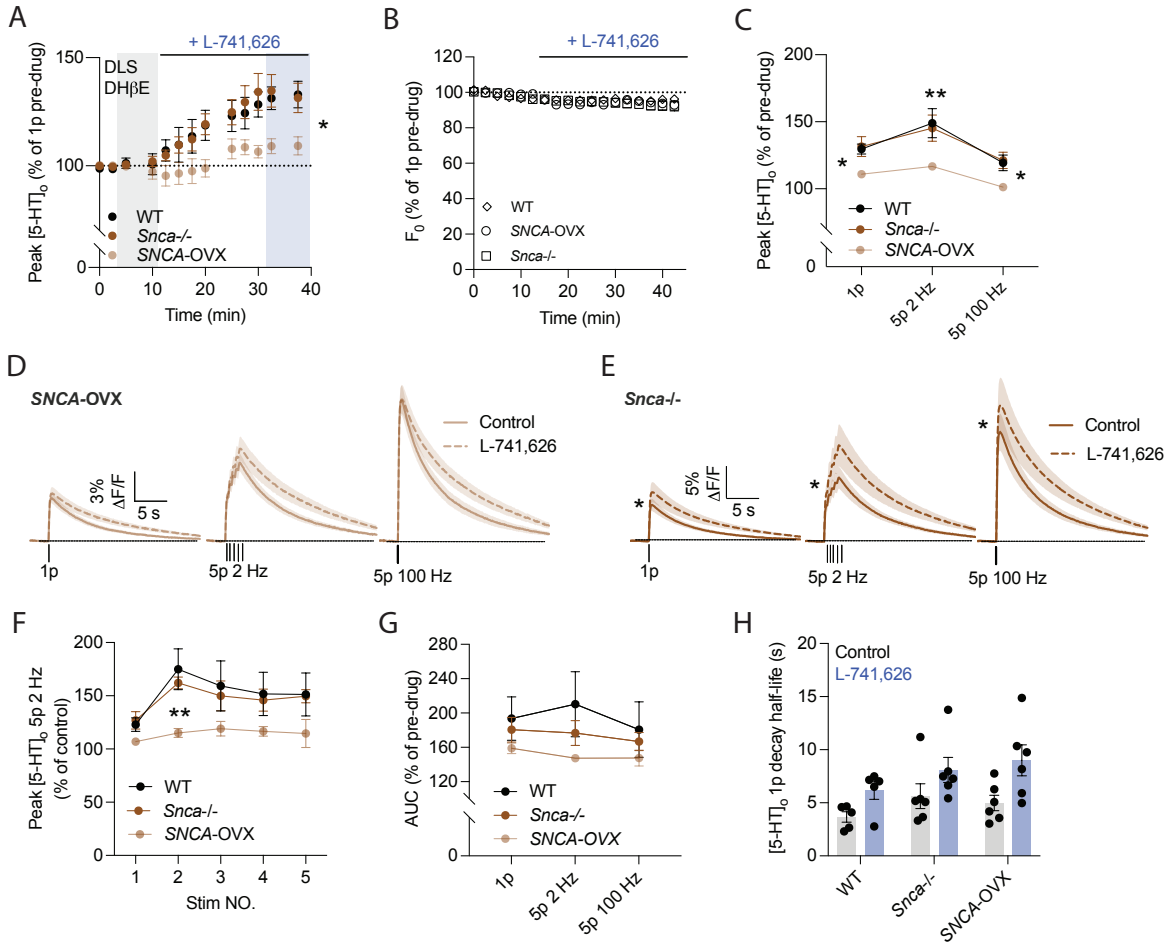

Figure 6.7. D_2R-mediated inhibition of striatal 5-HT release is diminished in *SNCA*-OVX mice compared with *Snca*-/- mice. (A) Normalized mean peak $[5\text{-HT}]_o$ during consecutive recordings of 5-HT release evoked by 1p during the application of L-741,626 (1 μM) in the presence of DHßE in DLS in WT, *Snca*-/- and *SNCA*-OVX mice. (*n* = 6 experiments/4 pairs of mice). **(B)** Normalized mean baseline fluorescence (F_0) during consecutive recordings of 5-HT release evoked by 1p during the application of L-741,626 (1 μM) in the presence of DHßE in DLS in WT, *Snca*-/- and *SNCA*-OVX mice. (*n* = 6 experiments/4 pairs of mice). **(C)** Normalized 1p, 5p 2 Hz and 5p 100 Hz $[5\text{-HT}]_o$ peak after L-741,626 application in the presence of DHßE in DLS in WT, *Snca*-/- and *SNCA*-OVX mice. **(D,E)** Mean evoked 5-HT transients ± SEM, before (solid line) and after (dash line) application of L-741,626 (1 μM) in the presence of DHßE in DLS of *SNCA*-OVX (D) and *Snca*-/- (E) mice. Mean transients of $[5\text{-HT}]_o$ are derived from two timepoints prior to the application of the drug (grey shaded region) and last two timepoints (blue shaded region). **(F)** Normalized each pulse of 5p 2 Hz $[5\text{-HT}]_o$ peak after L-741,626 application in the presence of DHßE in DLS in WT, *Snca*-/- and *SNCA*-OVX mice. **(G)** Normalized 1p, 5p 2 Hz and 5p 100 Hz $[5\text{-HT}]_o$ AUC after L-741,626 application in the presence of DHßE in DLS in WT, *Snca*-/- and *SNCA*-OVX mice. **(H)** Mean 1p decay half-life of $[5\text{-HT}]_o$ under control conditions (grey) and following drug application (blue) in the presence of DHßE in DLS in WT, *Snca*-/- and *SNCA*-OVX mice. 2-way ANOVA, Fisher's LSD post-*hoc* test. **p* < 0.05, ***p* < 0.01. Error bars are ± SEM.

To further validate whether the changes in D_2R control of 5-HT release observed in the chronic but mild *SNCA*-OVX model generalise to other Parkinsonian mouse models, we repeated the experiment in an acute PD mouse model generated by unilateral 6-OHDA injection into the SNc, as described in Chapter 3. This approach produces a rapid and profound loss (approximately 70% in our hands) of striatal DA release on the lesioned side, while the contralateral hemisphere serves as an internal control. $GRAB_{5\text{-}HT}$ was expressed bilaterally in the DLS and evoked 5-HT release was recorded *ex vivo* in both hemispheres before and after pharmacological D_2R blockade with L-741,626 (1 µM).

In contrast to the findings in *SNCA*-OVX mice, D_2R blockade increased evoked $[5\text{-HT}]_o$ to a similar extent in both lesioned and non-lesioned hemispheres under 1p and 5p at 2 Hz and 100 Hz stimulation (**Fig. 6.8A, D-F**; $F_{(1,12)} = 1.438$, $p = 0.25$, RM ANOVA main effect of the lesion). Moreover, absolute peak amplitudes also remained very similar between the two hemispheres, either before or after D_2R antagonist application (**Fig. 6.8B-C**; control: $F_{(1,24)} = 1.440$, $p = 0.24$; L-741,626: $F_{(1,24)} = 2.904$, $p = 0.10$, RM ANOVA main effect of the lesion). Consistent with the peak changes, the magnitude of AUC increase induced by D_2R blockade did not differ between lesioned and non-lesioned hemispheres (**Fig. 6.8G**; $F_{(1,24)} = 0.2673$, $p = 0.61$, RM ANOVA main effect of the lesion).

In contrast to the alterations observed in the *SNCA*-OVX model, D_2R-mediated regulation of 5-HT release remained unchanged in the acute unilateral 6-OHDA lesion model. This suggests that the diminished D_2R control observed in *SNCA*-OVX mice may reflect chronic, disease-related adaptations rather than an acute consequence of DA loss. Alternatively, it may result from broader changes in striatal neurochemistry or physiology that are absent from acute, targeted DA lesion models.

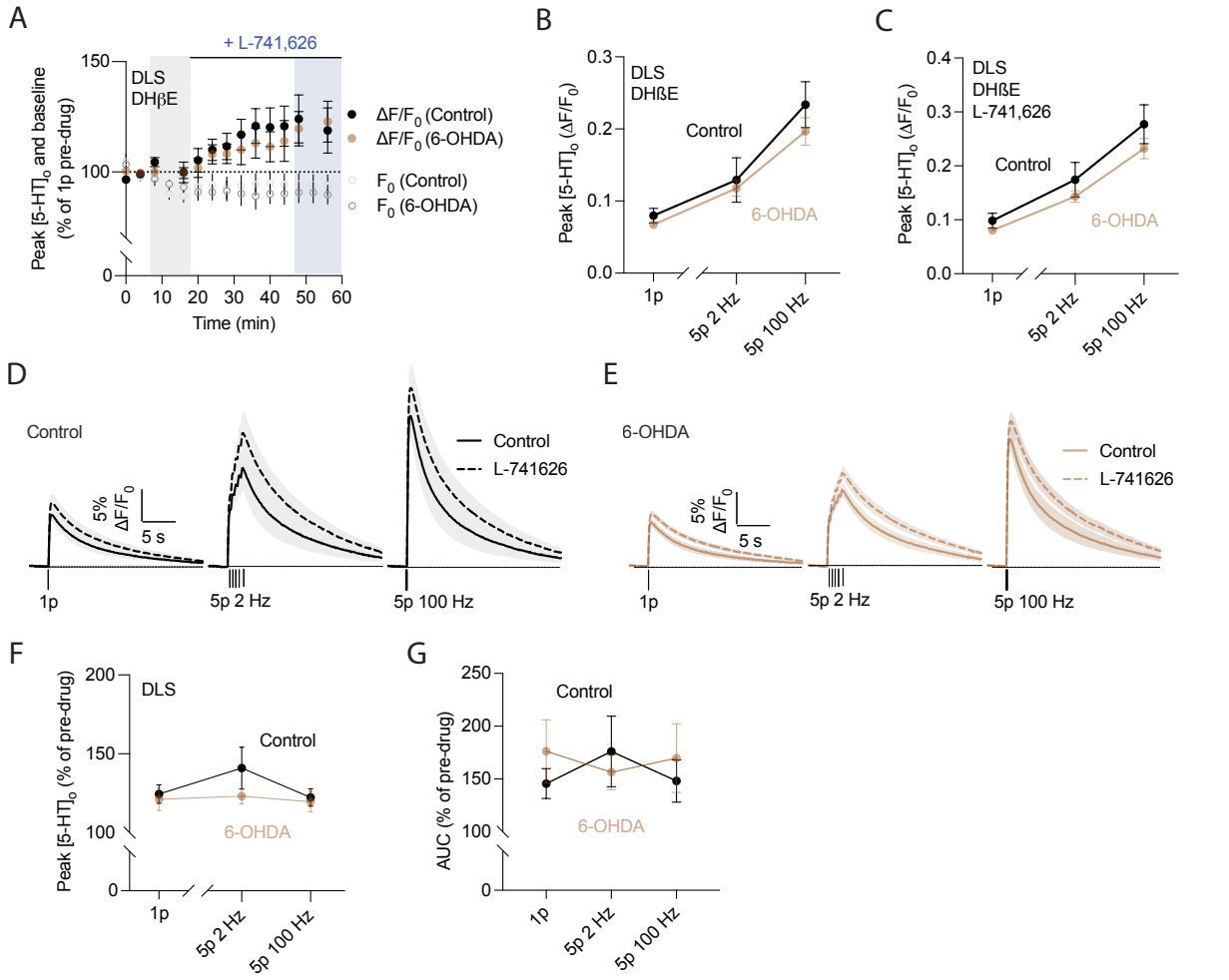

Figure 6.8. D_2R-mediated inhibition of striatal 5-HT release remains similar in a 6-OHDA acute PD mouse model. (A) Normalized mean peak $[5\text{-HT}]_o$ during consecutive recordings of 5-HT release evoked by 1p during the application of L-741,626 (1 µM) in the presence of DHßE in DLS in control and 6-OHDA mice. (*n* = 6 experiments/4 mice). **(B,C)** Mean 1p, 5p 2 Hz and 5p 100 Hz $[5\text{-HT}]_o$ peak before (B) and after (C) L-741,626 application in the presence of DHßE in DLS in control and 6-OHDA mice. **(D,E)** Mean evoked 5-HT transients ± SEM, before (solid line) and after (dash line) application of L-741,626 (1 µM) in the presence of DHßE in DLS in control (D) and 6-OHDA (E) mice. Mean transients of $[5\text{-HT}]_o$ are derived from two timepoints prior to the application of the drug (grey shaded region) and last two timepoints (blue shaded region). **(F)** Normalized 1p, 5p 2 Hz and 5p 100 Hz $[5\text{-HT}]_o$ peak after L-741,626 application in the presence of DHßE in DLS in control and 6-OHDA mice. **(G)** Normalized 1p, 5p 2 Hz and 5p 100 Hz $[5\text{-HT}]_o$ AUC after L-741,626 application in the presence of DHßE in DLS in control and 6-OHDA mice. 2-way ANOVA, Fisher's LSD post-*hoc* test. Error bars are ± SEM.

6.3.4 GABA-mediated facilitation on 5-HT release is enhanced in PD mice

To determine whether GABA-mediated facilitation of striatal 5-HT release is altered in the parkinsonian condition, I next assessed the effect of pharmacologically removing GABAergic tone in the *SNCA*-OVX mouse model. Previous studies have reported an enhanced GABA tone in PD mouse models (Roberts et al., 2020), prompting us to test whether such changes alter GABA-mediated facilitation of 5-HT release in the *SNCA*-OVX model. Similar to the previous section, both *SNCA*-OVX mice and their *Snca*-/- littermate controls were injected with $GRAB_{5\text{-}HT}$ in the DLS, and *ex vivo* slice recordings were performed 3-4 weeks later. Electrical stimulation was delivered to evoke local 5-HT release, and a combination of $GABA_A$ and $GABA_B$ receptor antagonists (bicuculline, 10 µM; CGP55845, 4 µM) were bath-applied to block inhibitory GABAergic tone.

Blockade of GABA receptors produced a robust facilitation of evoked 5-HT release in both genotypes, increasing peak amplitude to approximately 120% of pre-drug levels under both 1p and 5p 100 Hz stimulation (**Fig. 6.9A-C**). Baseline fluorescence (F_0) remained stable in all conditions, indicating that the drug effect was specific to stimulus-evoked responses (**Fig. 6.9A**). As previous mentioned, absolute peak amplitudes measured prior to GABA antagonist application were higher in *SNCA*-OVX mice compared to *Snca*-/- animals, and this difference persisted following blockade (**Fig. 6.9D**; $F_{(1,16)} = 15.46$, $p = 0.001$, RM ANOVA main effect of genotype). However, when expressed as a percentage of pre-drug values, the facilitation induced by GABA receptor antagonists was similar between *SNCA*-OVX and *Snca*-/- mice for both 1p and 5p stimulation protocols (**Fig. 6.9E**; $F_{(1,16)} = 3.245$, $p = 0.09$, RM ANOVA main effect of genotype). In line with this, the drug-induced increase in AUC was comparable between genotypes, with both groups reaching ~160% of pre-drug values (**Fig. 6.9F**; $F_{(1,16)} = 0.002$, $p = 0.99$, RM ANOVA main effect of genotype). These findings indicate that, despite the elevated

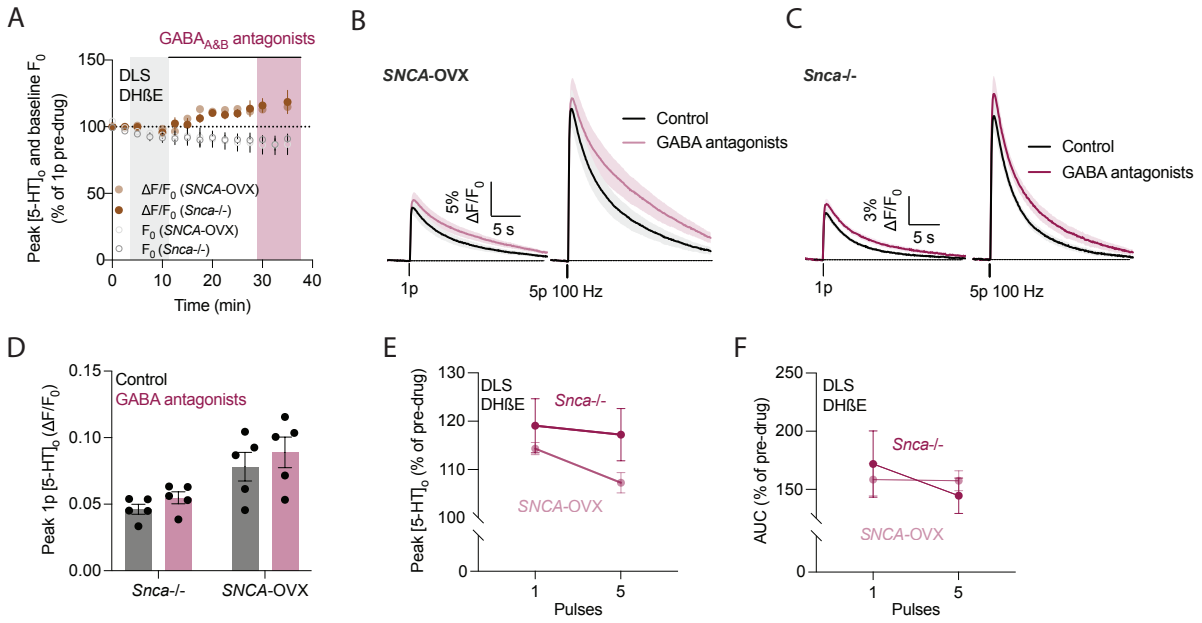

Figure 6.9. GABA-mediated facilitation on striatal 5-HT release shows no difference in *SNCA*-OVX mice. (A) Normalized mean peak [5-HT]$_o$ and baseline fluorescence (F_0) during consecutive recordings of 5-HT release evoked by 1p during application of bicuculines (10 µM) and CGP55845 (4 µM) in the presence of DHßE in DLS of *Snca*-/- and *SNCA*-OVX mice (n = 5 experiments/3 pairs of mice). **(B,C)** Mean evoked 5-HT transients ± SEM, before (black) and after (purple) application of bicuculines and CGP55845 in the presence of DHßE in DLS of *SNCA*-OVX (B) and *Snca*-/- (C) mice. Mean transients of [5-HT]$_o$ are derived from two timepoints prior to the application of the drug (grey shaded region) and last two timepoints (purple shaded region). **(D)** Mean 1p-evoked [5-HT]$_o$ peak of control conditions (black) and following drug application (purple) in DLS in the presence of DHßE of *Snca*-/- and *SNCA*-OVX mice. **(E)** Normalized 1p and 5p 100 Hz evoked [5-HT]$_o$ peak after the application of bicuculine and CGP55845 in DLS in the presence of DHßE of *Snca*-/- and *SNCA*-OVX mice. **(F)** Normalized 1p and 5p 100 Hz evoked [5-HT]$_o$ AUC after the application of bicuculine and CGP55845 in DLS in the presence of DHßE of *Snca*-/- and *SNCA*-OVX mice. 2-way ANOVA, Fisher's LSD post-*hoc* test. Error bars are ± SEM.

absolute [5-HT]$_o$ seen in *SNCA*-OVX mice, the magnitude of GABA-mediated facilitation is preserved relative to non-PD mouse controls.

DA and GABA both contribute to the regulation of striatal 5-HT release, and our earlier results indicated that D_2R-mediated dopaminergic control is diminished in *SNCA*-OVX mice. This raises the possibility that any concurrent change in GABA-mediated regulation might be masked under baseline conditions, as opposing effects from DA and GABA systems could cancel each other out. To further isolate GABAergic regulation on striatal 5-HT dynamic, we blocked DA signalling

at both D_1 and D_2 receptors using SCH39166 and L-741,626 (1 μM each) and then examined GABA-mediated control of 5-HT release. As in previous experiments, $GRAB_{5\text{-}HT}$ was expressed in the DLS, and recordings were performed on *ex vivo* DLS slices before and after application of the $GABA_A$ and $GABA_B$ receptor antagonists bicuculline (10 μM) and CGP55845 (4 μM).

Application of GABA receptor antagonists produced a larger increase in evoked 5-HT release in *SNCA*-OVX animals than in *Snca*-/- controls. In *SNCA*-OVX mice, peak amplitude increased to approximately 150% of pre-drug levels, whereas in *Snca*-/- mice the increase was limited to ~120% (**Fig. 6.10A-C**; $F_{(1,18)} = 25.20$, $p < 0.001$, RM ANOVA main effect of genotype). This genotype difference was evident in both 1p and 5p stimulation but was most pronounced for single-pulse stimulation (**Fig. 6.10D-E**; $F_{(1,16)} = 7.767$, $p = 0.0132$, RM ANOVA main effect of genotype). Consistent with these peak changes, AUC values increased to ~200% of pre-drug levels in *SNCA*-OVX mice compared with ~150% in *Snca*-/- animals (**Fig. 6.10F-H**; $F_{(1,16)} = 6.548$, $p = 0.02$, RM ANOVA main effect of genotype). Furthermore, the ratio of 5p/1p was decreased following GABA receptor blockade in both genotypes, but the magnitude of this reduction was substantially greater in *SNCA*-OVX mice (**Fig. 6.10I**; $F_{(1,16)} = 14.38$, $p = 0.002$, RM ANOVA main effect of the drug; $F_{(1,16)} = 4.728$, $p = 0.05$, interaction between drug × genotype).

Together, these results demonstrate that when dopaminergic influence is removed by DA receptor blockade, *SNCA*-OVX mice exhibit an enhanced GABA-mediated facilitation of evoked 5-HT release. This suggests that elevated GABA tone is present in the PD model and becomes functionally unmasked when DA–5-HT interactions are pharmacologically silenced.

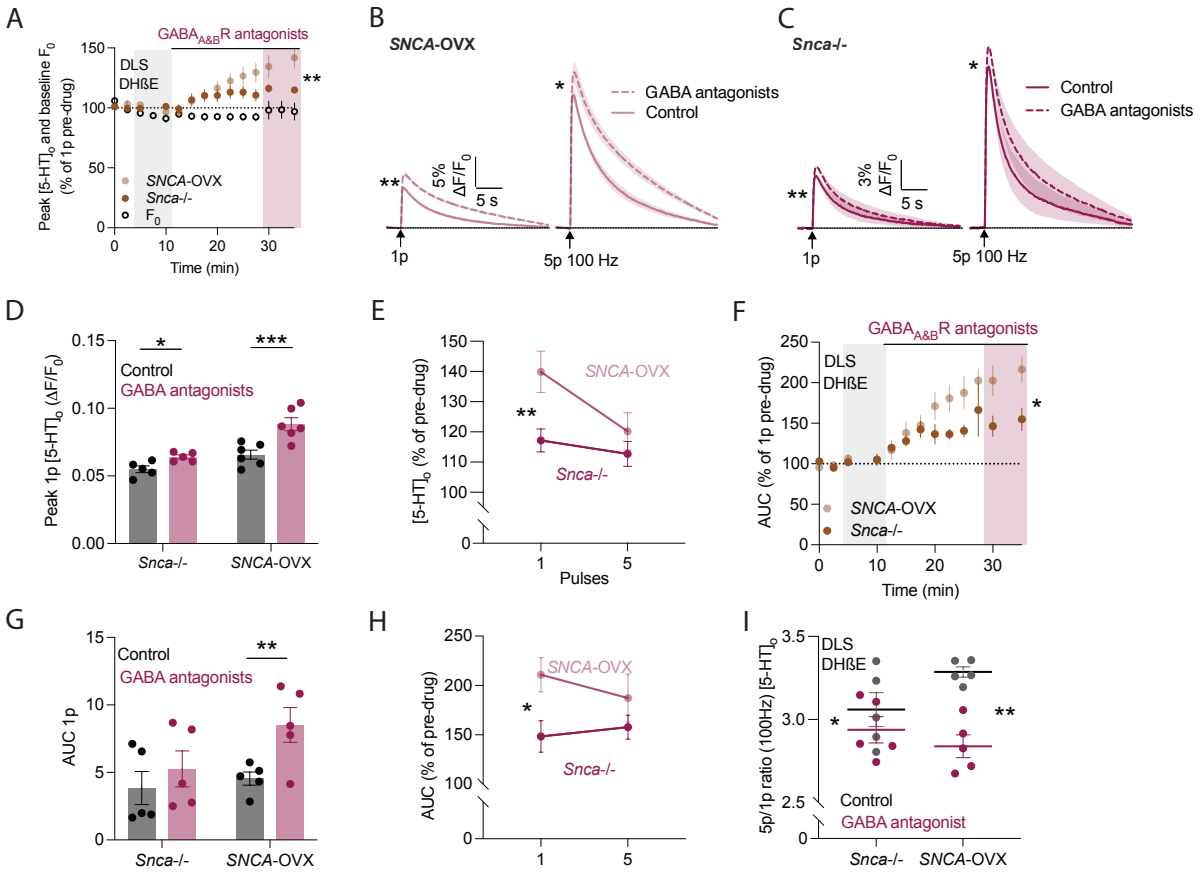

Figure 6.10. GABA-mediated facilitation on striatal 5-HT release is enhanced when blocking DA in *SNCA*-OVX mice. (A) Normalized mean peak $[5\text{-HT}]_o$ and baseline fluorescence (F_0) during consecutive recordings of 5-HT release evoked by 1p during application of bicuculines (10 µM) and CGP55845 (4 µM) in the presence of SCH39166 (1 µM), L-741,626 (1 µM) and DHßE in DLS of *Snca*-/- and *SNCA*-OVX mice (n = 5 experiments/3 pairs of mice). **(B,C)** Mean evoked 5-HT transients ± SEM, before (solid line) and after (dash line) application of bicuculines and CGP55845 in the presence of SCH39166, L-741,626 and DHßE in DLS of *SNCA*-OVX (B) and *Snca*-/- (C) mice. Mean transients of $[5\text{-HT}]_o$ are derived from two timepoints prior to the application of the drug (grey shaded region) and last two timepoints (purple shaded region). **(D)** Mean 1p-evoked $[5\text{-HT}]_o$ peak of control conditions (black) and following drug application (purple) in DLS in the presence of SCH39166, L-741,626 and DHßE of *Snca*-/- and *SNCA*-OVX mice. **(E)** Normalized 1p and 5p 100 Hz evoked $[5\text{-HT}]_o$ peak of after the application of bicuculine and CGP55845 in DLS in the presence of SCH39166, L-741,626 and DHßE of *Snca*-/- and *SNCA*-OVX mice. **(F)** Normalized mean AUC $[5\text{-HT}]_o$ during consecutive recordings of 5-HT release evoked by 1p during application of bicuculines and CGP55845 in the presence of SCH39166, L-741,626 and DHßE in DLS of *Snca*-/- and *SNCA*-OVX mice. **(G)** Mean 1p-evoked $[5\text{-HT}]_o$ AUC of control conditions (black) and following drug application (purple) in DLS in the presence of SCH39166, L-741,626 and DHßE of *Snca*-/- and *SNCA*-OVX mice. **(H)** Normalized 1p and 5p 100 Hz evoked $[5\text{-HT}]_o$ AUC of after the application of bicuculine and CGP55845 in DLS in the presence of SCH39166, L-741,626 and DHßE of *Snca*-/- and *SNCA*-OVX mice. **(I)** Normalized mean $[5\text{-HT}]_o$ of 5p 100 Hz to 1p (5p/1p) in control (black) and in bicuculine and CGP55845 conditions (purple) in the presence of SCH39166, L-741,626 and DHßE in DLS of *Snca*-/- and *SNCA*-OVX mice. 2-way ANOVA, Fisher's LSD post-*hoc* test. *$p < 0.05$, **$p < 0.01$. Error bars are ± SEM.

6.4 Discussion

6.4.1 Striatal 5-HT dynamics in a PD mouse model

In this section, we examined how 5-HT release is altered in *SNCA*-OVX mice under different background conditions. It is known that in this PD model, striatal DA release is reduced by ~30% and GABA tone is enhanced (Janezic et al., 2013; Roberts et al., 2020), while 5-HT is regulated by both DA and GABA (in Chapter 3), which in turn modulate each other. To disentangle these direct and indirect influences, we tested four conditions in which dopaminergic and/or GABAergic inputs were selectively preserved or blocked. To avoid the interplay between ACh and the other neurotransmitter systems, DHßE was presented throughout all experiments to block nAChRs in DLS slices.

In the first condition, both DA and GABA tone were preserved, meaning that no DA or GABA receptor antagonists were applied. Under these circumstances, we found that the evoked 5-HT release in *SNCA*-OVX mice exhibited a significantly higher peak amplitude compared with *Snca*-/- animals. The peak amplitude in *Snca*-/- mice was comparable to that observed in WT controls. In addition, the decay time of the evoked 5-HT signal in *SNCA*-OVX mice was longer than that in *Snca*-/- and WT mice. These results indicate that, when both dopaminergic and GABAergic modulation are intact, the baseline evoked 5-HT release in this PD mouse model is elevated relative to the non-PD control animals. However, it is important to note that these findings were obtained from single-site recordings. Multisite recordings as previously documented (Janezic et al., 2013) would be necessary to confirm whether this elevation in 5-HT release is consistent across sub-regions in DLS and as a known alteration in *SNCA*-OVX mice of this PD model. Nevertheless, the current data suggest that *SNCA*-OVX mice possess an intrinsically higher level of evoked 5-HT release under physiological modulatory conditions.

In the second condition, DA tone was preserved, but GABA tone was removed by applying $GABA_A$ and $GABA_B$ receptor antagonists. Under these circumstances, where DA remained intact, but GABA was blocked, the overall pattern of 5-HT release was similar to that observed in the baseline condition. Specifically, *SNCA*-OVX mice still exhibited a higher evoked 5-HT peak amplitude compared with *Snca*-/- animals, and the decay time followed the same pattern as in the baseline condition, with *SNCA*-OVX values exceeding those of *Snca*-/- mice. These results can be explained by considering both direct and indirect effects. Directly, in the absence of DA receptor antagonists, as described in this chapter, we did not observe any difference in GABA control on 5-HT release between genotypes, indicating that the facilitation of 5-HT release induced by GABA blockade was similar in *SNCA*-OVX and *Snca*-/- mice. Indirectly, however, the enhanced GABA-mediated inhibition of DA release in *SNCA*-OVX mice means that blocking GABA could result in greater DA availability (Roberts et al., 2020). This additional DA would then act on D_2 receptors to inhibit 5-HT release, as demonstrated in Chapter 3. Taken together, this indirect inhibitory pathway would be expected to slightly reduce 5-HT levels relative to the baseline condition. Nevertheless, under this GABA-blocked but DA-intact background, we still observed greater evoked 5-HT release in *SNCA*-OVX mice compared with *Snca*-/- animals.

In the third condition, DA action was blocked while GABA tone was preserved, achieved by applying D_1 and D_2 receptor antagonists. Under this circumstance, both the peak amplitude and decay half-life of evoked 5-HT release were similar across all three genotypes, with no clear elevation in *SNCA*-OVX animals compared with *Snca*-/- or WT controls. This outcome can be interpreted through both direct and indirect mechanisms. Directly, as shown in earlier experiments, D_2 receptor-mediated inhibition of 5-HT release is diminished in *SNCA*-OVX mice. Consequently, blocking DA receptors in these animals would be expected to have a smaller facilitatory effect on 5-HT release than in non-PD controls. Indirectly, DA can influence

GABAergic transmission, which in turn modulates 5-HT release. However, the regulation of striatal DA on GABA in this model is not yet established, making it difficult to predict the net contribution of this indirect pathway. Considering both mechanisms, it is plausible that the overall 5-HT level in this DA-blocked but GABA-intact background remains comparable across genotypes, consistent with our observations.

In the fourth condition, both DA and GABA tone were removed simultaneously by applying D_1, D_2, $GABA_A$, and $GABA_B$ receptor antagonists. In this background, *SNCA*-OVX mice once again exhibited a higher peak amplitude of evoked 5-HT release compared with *Snca*-/- animals. The decay half-life followed the same pattern, being longer in *SNCA*-OVX than in *Snca*-/-. The mechanistic interpretation in this case is relatively straightforward. Directly, blocking D_2 receptors would normally lead to an increase in 5-HT release by removing DA-mediated inhibition. However, because D_2 receptor-mediated inhibition of 5-HT release is already diminished in *SNCA*-OVX mice, the magnitude of this increase would be smaller compared with controls. At the same time, the enhanced GABAergic inhibition of 5-HT in *SNCA*-OVX mice means that blocking GABA receptors would produce a strong facilitatory effect on release. Indirectly, effects through DA-GABA interactions are absent in this condition, since both modulatory systems are pharmacologically blocked. Therefore, the net outcome in this condition is similar to the drug-free conditions, because the strong facilitatory effect from enhanced GABAergic inhibition of 5-HT release, once blocked, is counterbalanced by the smaller increase in 5-HT release resulting from diminished D_2 receptor-mediated inhibition in *SNCA*-OVX mice. As a result, the overall 5-HT levels remain comparable to those observed under drug-free conditions, in which *SNCA*-OVX animals exhibit higher evoked 5-HT release than non-PD controls.

Taken together, when both dopaminergic and GABAergic effects are intact, *SNCA*-OVX mice display higher evoked 5-HT release than controls. Strikingly, when all indirect influences are

eliminated by blocking both DA and GABA receptors, this elevation persists, which might initially suggest that no major dysfunction exists in these modulatory systems. However, this interpretation would be misleading. When either DA tone or GABA tone is blocked in isolation, the outcome changes: the two systems exert opposing influences on 5-HT release, such that alterations in one pathway can be masked by compensatory changes in the other. As a result, the observed elevation in 5-HT release is not a fixed feature across all backgrounds, but instead reflects a dynamic balance between dopaminergic and GABAergic regulation that shifts depending on which modulatory inputs remain active.

6.4.2 SERT-mediated 5-HT release in a PD mouse model

Next, we examined the regulation of 5-HT release by SERT in the PD model, focusing on possible dysregulation of SERT-mediated clearance. In the PD mouse model used in this chapter, it is already known that DAT function is enhanced, as blocking DAT with inhibitors such as cocaine or nomifensine produces a greater increase and prolongation of DA release in *SNCA*-OVX mice compared with *Snca*-/-. In contrast to this enhancement of DAT function, our results indicate that SERT function is diminished in *SNCA*-OVX animals. When SERT was blocked with the SSRI citalopram, the resulting increase and prolongation of 5-HT release were smallest in *SNCA*-OVX mice, relative to both control genotypes. Moreover, the decay half-life of the 5-HT signal in *SNCA*-OVX mice was already longer than in controls before drug application and remained longest after SERT blockade. These findings suggest that SERT-mediated clearance is less effective in *SNCA*-OVX animals, both under baseline conditions and when pharmacologically inhibited. Given that we previously showed in Chapter 3 that striatal 5-HT reuptake is jointly regulated by DAT and SERT, one plausible explanation is that the diminished SERT function represents a compensatory adaptation to the increased DAT activity. Such a mechanism could help maintain overall monoamine clearance balance in the striatum despite

elevated DAT-mediated DA uptake. We speculate that this SERT downregulation may be a localised phenomenon within the striatum, arising as a compensation for altered DAT and DA dynamics in this PD model.

6.4.3 D_2R-mediated inhibition of striatal 5-HT release

We next examined the regulation of 5-HT release by D_2 receptors in two PD mouse models, one genetic and one acute lesion. Interestingly, these two models produced divergent outcomes. In the genetic *SNCA*-OVX model, blocking D_2 receptors with the antagonist L-741,626 produced a smaller increase in evoked 5-HT release in *SNCA*-OVX mice compared with both control genotypes. This finding indicates that D_2 receptor-mediated inhibition of 5-HT release in DLS is diminished in *SNCA*-OVX animals. In contrast, in the acute unilateral 6-OHDA lesion model, blocking D_2 receptors increased 5-HT release to a similar extent in both the lesioned and non-lesioned hemispheres, and no significant difference in drug response was detected between the two sides.

This difference may come from the underlying DA pathology between the two PD mouse models. In the genetic *SNCA*-OVX model, mice are born with genetic deficits that affect striatal DA release. They have an approximately 30% reduction in DA release but show no dopaminergic neuron loss in the SNc at three months of age. Consequently, less DA is chronically available to act on D_2 receptors, making it plausible that D_2 receptor-mediated inhibition of 5-HT release is reduced. In contrast, the acute 6-OHDA lesion model produces a rapid and severe degeneration of dopaminergic neurons, leading to marked loss of DA innervation within only three weeks after injection. In this condition, different compensatory mechanisms may occur, or insufficient time may have elapsed for changes in D_2 receptor control of 5-HT release to emerge. This difference in the chronicity and nature of the DA deficit

likely explains why the two models show distinct patterns of D_2 receptor-mediated regulation of 5-HT release.

6.4.4 GABAR-mediated inhibition of striatal 5-HT release

Finally, we examined how GABA receptors regulate 5-HT release in the PD models. This regulation showed a strong dependence on whether DA was present in the background. When DA signalling was intact - without DA receptor blockade - we found no difference in GABA receptor control of 5-HT release between *SNCA*-OVX mice and controls. However, when we blocked DA signalling by applying D_1 and D_2 receptor antagonists, a clear difference appeared. In this case, blocking both $GABA_{A\&B}$ receptors caused a larger increase in evoked 5-HT release in *SNCA*-OVX mice than in controls, indicating that GABA tone was enhanced in the PD mouse model.

This pattern can be explained by our earlier finding that D_2 receptor control of 5-HT release is reduced in *SNCA*-OVX mice. When DA signalling is present, GABA receptor effects are combined with an already diminished D_2 receptor influence. Under these conditions, changes in GABA tone may be masked or counteracted by alterations in DA-mediated inhibition, so the overall GABA effect appears unchanged. When DA receptor activity is removed, these indirect interactions are eliminated, revealing the enhanced GABA tone in *SNCA*-OVX animals.

Overall, these results show that striatal DA and GABA systems interact in complex ways to shape striatal 5-HT release. In the PD model, reduced D_2 receptor control and increased GABA receptor control may work in opposite directions, partly cancelling each other out when both systems are active. This highlights the need to isolate specific pathways in experiments to detect changes that might otherwise be hidden by indirect effects.

6.4.5 General limitation

While these findings provide new insight into serotonergic dysregulation in PD models, several limitations should be acknowledged. First, most of our measurements were obtained from a restricted region within the DLS, which may not capture potential spatial heterogeneity across striatal subregions. Multisite recordings, or parallel assessment of the NAcC, could reveal region-specific regulatory differences. Second, our pharmacological manipulations isolate regulatory pathways in an artificial manner. Although this is necessary to dissect individual contributions, it may not fully reflect the *in vivo* situation where multiple modulatory systems interact dynamically. Third, the genetic and acute PD models differ in how the disease starts, how it develops, and how the brain adapts over time. These differences mean that results from one model cannot be directly applied to the other.

Despite these limitations, the present study demonstrates that serotonergic dysregulation in PD is not simply a unidirectional loss or gain of function, but rather the outcome of overlapping and sometimes opposing changes in multiple modulatory pathways. Understanding how these pathways interact, and under what conditions specific dysregulations become unmasked, will be essential for developing targeted therapeutic strategies aimed at restoring balanced 5-HT signalling in PD.

Chapter 7.

General discussion

The striatum is a major subcortical structure that integrates inputs from multiple neurotransmitter systems to regulate motor control, learning, and reward processing (Cataldi et al., 2022; Do et al., 2013; Nakano et al., 2000). 5-HT is an important neuromodulator in the striatum. It shapes local network activity through its actions on diverse receptor subtypes located on both projection neurons and interneurons (Bockaert et al., 2006; Cavaccini et al., 2018; Fuxe et al., 2012; Pommer et al., 2021). Dysregulation of striatal 5-HT signalling has been implicated in several neurological and psychiatric disorders, including PD, depression, and drug addiction (Marino et al., 2025; Miguelez et al., 2014; Muñoz et al., 2020). Despite its recognised importance, the precise mechanisms governing 5-HT release and its regulation within the striatum remain incompletely understood.

Previous studies on striatal 5-HT signalling have been limited by technical constraints. Conventional techniques such as microdialysis and FCV have restricted spatial and temporal resolution, making it difficult to measure sub-second changes in 5-HT release or to dissect circuit-specific modulation. Recent advances in genetically encoded sensors, such as $GRAB_{5\text{-}HT}$, now enable high-resolution measurements of extracellular 5-HT dynamics *in vivo* and *ex vivo*, providing new opportunities to investigate the cellular and synaptic mechanisms underlying serotonergic transmission.

This thesis uses $GRAB_{5\text{-}HT}$ to characterise the regulation of 5-HT release in the striatum in both health and PD conditions. Chapters 3 to 6 each address different aspects of striatal 5-HT regulation. In **Chapter 3**, I characterised the $GRAB_{5\text{-}HT}$ sensor, confirming its specificity and reliability for 5-HT detection, and then used it to investigate how other neurotransmitter, such as ACh and GABA, modulate 5-HT release in the striatum. **Chapter 4** focused on DA regulation of 5-HT, showing receptor-specific bidirectional effects through D_1R and D_2R. In **Chapter 5**, I examined, in turn, the influence of 5-HT_4R ligands on DA and ACh release, identifying a novel mechanism involving modulation of AChE activity. Finally, **Chapter 6** explored 5-HT signalling in

a PD mouse model, revealing multiple forms of dysregulation in release and receptor-mediated control. Together, these studies address important gaps in our understanding of how 5-HT release is controlled in the striatum and how this regulation is altered in PD.

In this chapter, I will discuss the main findings of this thesis and their implications for understanding striatal function in health and disease.

7.1 Measuring striatal 5-HT release with $GRAB_{5\text{-}HT}$

Previous methods for measuring 5-HT release in the striatum have been limited by insufficient spatial or temporal resolution, making it difficult to capture rapid and pathway-specific changes in serotonergic signalling. In this thesis, I used the genetically encoded sensor $GRAB_{5\text{-}HT}$ (Deng et al., 2024) to monitor extracellular 5-HT dynamics in acute striatal slices. This approach enabled direct detection of stimulus-evoked 5-HT release with sub-second resolution, providing a substantial advantage over traditional electrochemical and microdialysis techniques.

The first major benefit of using $GRAB_{5\text{-}HT}$ is its specificity for detecting 5-HT instead of DA, despite the structural similarity between the two monoamines and their overlapping anatomical projections even in a DA-rich region such as the striatum. In **Chapter 3**, I provided experimental evidence supporting the specificity of the sensor by showing that $GRAB_{5\text{-}HT}$ signals are unaffected by pharmacological depletion of DA. This provides strong evidence that the sensor is a reliable reporter of 5-HT release in the striatum and establishes the experimental foundation for all subsequent investigations into 5-HT regulation throughout this thesis.

Secondly, $GRAB_{5\text{-}HT}$ is sensitive enough to resolve *ex vivo* differences in 5-HT dynamics across brain regions and disease models. In the results presented in **Chapter 3**, I demonstrated that $GRAB_{5\text{-}HT}$ could detect distinct patterns of 5-HT release in DLS versus NAcC, and importantly, revealed altered 5-HT dynamics in a parkinsonian mouse model (*SNCA*-OVX) in **Chapter 6**.

These findings suggest that $GRAB_{5\text{-}HT}$ is not only suitable for detecting 5-HT presence but also can report regional and pathological differences in release probability, reuptake, and tonic signalling. This feature makes $GRAB_{5\text{-}HT}$ particularly valuable for studying the physiological and circuit-level mechanisms of serotonergic dysfunction in PD and other neuropsychiatric conditions.

Thirdly, unlike electrochemical methods such as FCV, $GRAB_{5\text{-}HT}$ is not limited by the electrochemical properties of the drugs or ligands used in the experiment. FCV recordings require careful consideration of whether the ligand or the agents are electroactive as described in **Chapter 5**, which may introduce interpretational difficulties or need for additional calibration. In contrast, $GRAB_{5\text{-}HT}$ relies on a genetically encoded GPCR-based sensor that turns ligand binding into a fluorescence signal (Deng et al., 2024). Therefore, most pharmacological ligands can be applied without interfering with signal readout - except those that directly target the 5-HT_4 receptor, which the sensor is based on. As long as this consideration is accounted for, $GRAB_{5\text{-}HT}$ provides a more flexible and interpretable tool for studying 5-HT release and modulation under diverse pharmacological conditions.

Despite its advantages, several limitations of GRAB5-HT should be acknowledged. First, because GRAB5-HT reports extracellular serotonin, the fluorescence signal inevitably reflects the net balance of release, diffusion, uptake, and the density of cells expressing the sensor in the local environment, rather than activity confined to a defined cell type. Although Cre-dependent viral constructs (e.g., in SERT-Cre mice) can restrict sensor expression, their main advantage is reducing variability in where and how much the sensor is expressed, rather than true cell-type specificity. More broadly, cell-type specific viral strategies have been applied to dissect serotonergic function *in vivo*. For example, Ogelman et al. (2024) employed a Cre-dependent inhibitory DREADD in SERT-Cre mice to selectively silence 5-HT neurons, and demonstrated that endogenous 5-HT promotes maturation and stabilization of excitatory

synapses in the prefrontal cortex via 5-HT_{2A} and 5-HT_7 receptor-mediated mechanisms (Ogelman et al., 2024). Such approaches highlight the value of combining genetic targeting with functional readouts to resolve the diverse contributions of 5-HT signalling.

Second, unlike FCV, $GRAB_{5\text{-}HT}$ cannot reflect the absolute concentrations of extracellular 5-HT. Instead, changes in fluorescence are reported as $\Delta F/F_0$ relative to a fitted baseline curve, which can vary depending on experimental conditions. While this is sufficient to detect relative changes in 5-HT release or reuptake, it limits the ability to quantify extracellular 5-HT in absolute concentration. Furthermore, the biological interpretation of the baseline fluorescence signal (F_0) remains unclear. Whether F_0 reflects tonic 5-HT levels or just a background of sensor expression or tissue environment or a combination of some/all is not yet fully resolved.

Third, the lower detection limit and dynamic range of $GRAB_{5\text{-}HT}$ in striatum tissue is not yet well defined. We do not currently know what the minimal detectable 5-HT change is under physiological conditions especially in striatal tissue, nor whether the sensor is saturated at higher concentrations of evoked 5-HT. This is an important area for future methodological work, particularly in calibrating fluorescence signals against known 5-HT concentrations *ex vivo* or even *in vivo*.

In conclusion, $GRAB_{5\text{-}HT}$ is a powerful tool for investigating serotonergic signalling in the brain. Its high temporal resolution, anatomical precision, and molecular specificity make it uniquely suited for studying 5-HT release and regulation in both health and disease contexts. While limitations exist, its advantages are particularly well suited to the aims of this thesis. Specifically, $GRAB_{5\text{-}HT}$ enabled detailed characterisation of the spatiotemporal properties of 5-HT dynamics in DLS and NAcC, and facilitated new insights into how these dynamics are altered in a parkinsonian mouse model. These findings highlight the utility of $GRAB_{5\text{-}HT}$ for understanding

the imbalances of serotonergic system in neurological disease, while also building the foundation for future work of sensor-based imaging approaches.

7.2 5-HT release in the striatum

The striatum is one of the brain regions exhibiting dense serotonergic innervation, primarily originating from the DRN (Nakano et al., 2000; Soghomonian et al., 1987; Waselus et al., 2006). Serotonergic axons arborise extensively across both the dorsal and ventral striatum and establish widespread extra synaptic release sites, contributing to a persistent extracellular presence of 5-HT (Bunin & Wightman, 1998; Pierret et al., 1998; Soghomonian et al., 1989). Despite this extensive innervation, the dynamics of striatal 5-HT release remain incompletely characterised, partially due to methodological challenges in isolating fast 5-HT transients and distinguishing them from closely related neuromodulators like DA in the striatum. This validation laid the foundation for subsequent experiments exploring region- and condition-specific 5-HT dynamics across dorsal and ventral striatal subregions.

7.2.1 Cholinergic modulation of 5-HT release

Striatal cholinergic interneurons (ChIs) are known to exert powerful modulation of local neurotransmission (Drenan et al., 2010; Jaunarajs et al., 2015; Exley & Cragg, 2008; Li et al., 2024; Lim et al., 2014). A recent study has revealed that synchronous activation of ChIs enhances the local range of 5-HT release in the striatum, via mechanisms similar to those influencing DA spread (Matityahu et al., 2024). This supports the concept that ACh signalling plays a direct regulatory role in serotonergic transmission. In turn, endogenous 5-HT also modulates striatal cholinergic signalling by acting on 5-HT receptors expressed on ChIs. For example, early studies demonstrated that 5-HT can inhibit striatal ACh release, with the extent of this modulation depending on the density of serotonergic innervation (D. Jackson et al.,

1988). More recent work has shown that 5-HT can profoundly excite striatal ChIs through 5-HT_{2c}, 5-HT_6 and 5-HT_7 receptors (Bonsi et al., 2007), highlighting the complexity of 5-HT-ACh interactions. Together, these findings underscore the importance of dissecting cholinergic regulation of 5-HT release in the striatum, particularly considering the complex receptor-mediated crosstalk between these two neuromodulatory systems.

In my experiments detailed in **Chapter 3**, I found that activation of nAChRs plays a significant role in modulating evoked 5-HT release in the striatum, in both frequency-dependent and region-specific manners. Specifically, in the DLS, blockade of nAChRs led to a notable reduction in 5-HT release when evoked by 1p and low-frequency stimulation, as shown in **Fig. 3.15**. This suggests that under low-frequency stimulation conditions, endogenous ACh provides basal activation of nAChRs, which facilitates 5-HT release. However, when the frequency of stimulation was increased to above 25 Hz, this effect was no longer observed. This indicates that cholinergic modulation of 5-HT release via nAChRs in the DLS is frequency-dependent, with nAChRs exerting a more prominent influence under low-activity conditions.

In contrast, in the NAcC, a strikingly different pattern of regulation emerged. As shown in **Fig. 3.16**, nAChR blockade did not significantly alter 5-HT release at single-pulse or low-frequency stimulation but led to a marked increase in release under high-frequency conditions. This indicates that nAChRs in the ventral striatum selectively constrain 5-HT release during burst-like activities. Taken together with the findings from the DLS, where nAChRs facilitate 5-HT release under low-frequency conditions, these results reveal a bidirectional role of nAChR signalling on serotonergic transmission in the striatum.

This bidirectional cholinergic modulation of 5-HT is similar to previously described patterns of frequency-dependent control of striatal DA release, where nAChRs are known to either enhance or suppress DA transmission depending on the frequency of the stimulus and local circuit

dynamics (Brimblecombe et al., 2018; Rice & Cragg, 2004; Threlfell & Cragg, 2011). However, a key distinction is that in dopaminergic systems, both facilitation and inhibition by nAChRs can be observed within a single subregion, such as the dorsal or ventral striatum. In contrast, my data suggest that for 5-HT, this bidirectional modulation is region-specific.

The mechanistic basis for this regional dissociation remains uncertain, but one plausible explanation lies in the potential multi-circuit modulation of 5-HT release by both direct and indirect cholinergic inputs. As demonstrated in **Chapter 4**, dopaminergic signalling also governs 5-HT release, and DA itself is subject to robust cholinergic modulation through both nAChRs and mAChRs. Thus, the observed effects of nAChR manipulation on 5-HT could reflect a combination of direct modulation (e.g., via nAChRs on serotonergic neurons) and indirect modulation (e.g., through ACh-driven changes in DA release, which in turn alters 5-HT output). Given that cholinergic regulation of DA is also frequency- and region-dependent, the 5-HT signal detected by $GRAB_{5\text{-}HT}$ sensors may represent an integrated output of multiple interacting neuromodulatory circuits.

This layered regulation complicates the interpretation of cholinergic influence on 5-HT transmission but also opens valuable opportunities for future work. Dissecting the relative contributions of direct and indirect effects, and how they vary across circuits and behavioural states, will be essential for understanding the true dynamics of serotonergic signalling in the striatum.

In contrast to the complexity readout observed with nAChR activation, I revealed that mAChR modulation of 5-HT release is indirect and solely nAChR-dependent (**Fig. 3.17** and **Fig. 3.18**). Activation of mAChRs has been shown to reduced tonic ACh release from ChIs, thereby decreasing basal nAChR activation which would ultimately inhibit evoked 5-HT release in the DLS. This aligns with previously reported dopaminergic regulation, in which mAChR-driven

modulation of ACh tone indirectly shapes dopaminergic output by regulating nAChR availability (Threlfell et al., 2010). My findings indicate that striatal 5-HT release is under the control of a universal cholinergic mechanism, in which tonic ACh maintains nAChR-mediated gating of 5-HT release, and this gating is further modulated by mAChRs. Such layered regulation may serve as a mechanism by which the striatum dynamically adopts serotonergic signalling in response to changes in network state or multiple behavioural contexts.

7.2.2 GABAergic inhibition of 5-HT release

GABAergic interneurons and projection neurons are abundant throughout the striatum and provide a powerful source of local inhibition, regulating multiple neurotransmitter systems including DA and ACh (DeBoer & Westerink, 1994; Lopes et al., 2019; Roberts et al., 2021). However, how GABAergic tone shapes serotonergic transmission in the striatum has remained far less understood.

In **Chapter 3** (**Section 3.3.8**), I examined the influence of GABAergic signalling on 5-HT release using pharmacological manipulations targeting both $GABA_A$ and $GABA_B$ receptors. My data showed that tonic GABAergic inhibition suppresses evoked 5-HT release, and that this suppression is partially relieved upon blocking GABA receptors.

While the results presented here demonstrate that blocking $GABA_A$ and $GABA_B$ receptors facilitates 5-HT release, they reflect the compound effect of dual-receptor antagonism. Previous studies have demonstrated that exogenous GABA can inhibit 5-HT release via presynaptic $GABA_B$ receptors in the rat striatum and PFC, suggesting a conserved mechanism of GABAergic suppression of serotonergic transmission across regions (Schlicker et al., 1984). Future studies should aim to identify the distinct roles of $GABA_A$ and $GABA_B$ receptors in modulating 5-HT release, which would be helpful to determine which subtype exerts dominant

influence under physiological conditions. In parallel, further work is needed to resolve whether GABAergic regulation of 5-HT arises from direct actions at serotonergic axons or reflects upstream circuit-level modulation. Moreover, as demonstrated in **Chapter 6**, GABAergic modulation of 5-HT release may occur via both direct inhibition at serotonergic axons and indirect mechanisms involving DA. In particular, my data showed that the presence or absence of DA receptor signalling influenced the final 5-HT output following GABA receptor manipulation, especially under conditions of DA imbalance. These findings suggest that the influence of GABA control on 5-HT release is at least partially mediated through its impact on DA signalling. To clarify the relative contributions of direct versus indirect regulation, future studies should include systematic DA receptor blockade in wild-type animals during GABAergic manipulation.

In summary, GABAergic signalling exerts a strong inhibitory effect on striatal 5-HT release, which is likely to be universal in striatum. While the exact mechanism remains unclear, the modulation likely involves both direct action at serotonergic axons and indirect pathways via DA. Future studies should dissect these components to clarify how GABA shapes 5-HT output under different physiological and pathological conditions.

7.2.3 Dopaminergic modulation of 5-HT release

DA has long been recognized as a critical modulator of striatal neurotransmission, and increasing evidence suggests that its regulatory influence extends to the serotonergic system (Ferré et al., 1994; Movassaghi et al., 2021; SŚmiałowski & Bijak, 1987). Multiple studies have shown that DA receptors can influence extracellular 5-HT levels in the striatum, using methods ranging from microdialysis to voltammetry and genetic approaches (Crespi et al., 1988; Ferré et al., 1994; John & Jones, 2007; Laprade et al., 1996). For instance, Laprade et al. (1996) demonstrated that dopaminergic drugs can significantly alter extracellular 5-HT concentrations, suggesting a receptor-level interaction between these two systems (Laprade et al., 1996).

In **Chapter 4**, I systematically investigated the effects of various DA receptor ligands on 5-HT release using the $GRAB_{5\text{-}HT}$ sensor. Although different DA receptor ligands showed variable effects on 5-HT release, the overall interpretation presented in **Chapter 4** supports a conclusion: activation of D_1 receptors tends to facilitate 5-HT release, whereas activation of D_2 receptors suppresses it. This distinction aligns with the functions of these receptor classes, where D_1 receptors are generally excitatory and D_2 receptors inhibitory (Clark & White, 1987; SŚmiałowski & Bijak, 1987). Although DHβE was included in all relevant experiments to exclude cholinergic contributions, this does not provide sufficient evidence to confirm a direct action of DA receptors on serotonergic axons. It is possible that DA receptor activation modulates local microcircuits, which in turn influence 5-HT release via indirect mechanisms. The observed effects may thus be a combination of direct modulation of 5-HT axons and indirect influences mediated by other neuronal populations.

Beyond receptor-level interactions, DA may also modulate serotonergic transmission through reuptake mechanisms. My data show that 5-HT can be taken up into dopaminergic axons via DAT, suggesting that DAT-mediated reuptake contributes to shaping extracellular 5-HT dynamics in the striatum. This observation is consistent with previous findings by Zhou et al. (2005), who demonstrated that 5-HT can enter DA axons through DAT and subsequently be co-released with DA, thereby implicating DA neurons in the regulation of serotonergic tone (F.-M. Zhou et al., 2005). This co-release mechanism of 5-HT via DA axons represents a distinct mechanism from well-established GABA co-release with DA, which relies on DA neurons expressing GABA transporters (GAT1) to actively accumulate GABA (Nelson et al., 2014; Tritsch et al., 2016). In contrast, 5-HT can be taken up into DA axons via DAT, likely due to the relatively broad substrate specificity and the high expression levels of DAT in the striatum. However, the relative proportion of 5-HT reuptake mediated by SERT versus DAT in the striatum remains unknown. This uncertainty complicates the interpretation of extracellular 5-HT signals and limits

our ability to simply use external application of DA or 5-HT to infer specific mechanisms. Because a high concentration of external 5-HT may be recycled through dopaminergic axons and subsequently re-released, the output signal detected by $GRAB_{5\text{-}HT}$ likely reflects an integrated outcome of both 5-HT and DA activity.

This interaction is particularly relevant in the context of PD, where patients are typically treated with L-DOPA to restore DA function. Clinical observations have shown that many PD patients concurrently take SSRIs to manage depression, introducing further complexity. SSRIs block SERT and increase extracellular 5-HT levels, which may promote 5-HT uptake into DA axons. As a result, each firing event may release less DA, potentially reducing the efficacy of L-DOPA treatment. This indicates a critical role of the 5-HT system in shaping dopaminergic output under pharmacological manipulation.

Nevertheless, interpretation of the decay kinetics in $GRAB_{5\text{-}HT}$ signals remains challenging. The decay phase of the $GRAB_{5\text{-}HT}$ fluorescence response is often used as an indicator for 5-HT clearance, but this measure does not purely reflect reuptake mechanisms. Instead, it is determined by several confounding factors, including the off kinetics of the sensor itself and the flow rate of the bath the slice is incubated in. According to the original characterisation of $GRAB_{5\text{-}HT}$ sensors, the sensor exhibits an off time (τ_{off}) of approximately 1.3 s *in vitro* (Deng et al., 2024). This relatively slow unbinding rate might be limiting the temporal resolution with which 5-HT clearance can be measured. As a result, the decay half-life observed in our imaging data likely reflects a combination of true 5-HT reuptake, sensor unbinding, and diffusion properties, and should be interpreted with caution when drawing mechanistic conclusions about serotonergic clearance dynamics.

Taken together, these findings suggest that dopaminergic modulation of 5-HT release is multi-layered, involving both receptor-driven control and transporter-mediated crosstalk between the

two systems. The net effect of DA on 5-HT transmission depends on the balance between these systems, which may shift across behavioural states or pathological conditions. Future studies will be essential to disentangle these contributions, using cell-type-specific tools and temporally resolved assays to determine the precise circuitry through which DA influences striatal serotonergic dynamics.

7.3 5-HT signalling in a mouse model of PD

Striatal 5-HT transmission has been increasingly recognised as a critical component in the pathophysiology of PD. Beyond the well-established DA neuron degeneration, evidence has revealed early and progressive disruptions to serotonergic systems in PD (Blesa et al., 2022; Huot & Fox, 2013; Qamhawi et al., 2015). Reduced striatal levels of key serotonergic markers - including 5-HT itself, its transporter (SERT), and the synthesising enzyme tryptophan hydroxylase - have been consistently reported in clinical and postmortem studies (Kerenyi et al., 2003; Kish et al., 2008). At the same time, enhanced striatal 5-HT innervation has been proposed as a compensatory mechanism for dopaminergic loss, with modest increases in SERT-expressing axonal varicosities observed in PD striatum (Bédard et al., 2011). However, this compensatory hypothesis remains debated, as other studies reported no significant change in striatal 5-HT fibre density or raphe neuron numbers (Jiménez-Sánchez et al., 2020). Thus, the exact dynamics of serotonergic adaptation in PD remain unresolved, particularly under differing models and stages of disease.

In **Chapter 6**, I explored striatal 5-HT signalling in two PD mouse models: *SNCA*-OVX animals, which exhibit a partial DA release deficit without overt DA neuron degeneration, and 6-OHDA-lesioned animals, representing acute and massive dopaminergic denervation. My findings revealed that 5-HT release was significantly enhanced in the *SNCA*-OVX model, suggesting a compensatory upregulation in response to moderate DA insufficiency. This aligns with previous

proposals of serotonergic compensation in early PD (Bédard et al., 2011). Surprisingly, however, this enhancement was not observed in the 6-OHDA model, despite the more severe DA depletion. This is in contrast with previous findings reporting increased striatal 5-HT levels following 6-OHDA lesions (Luthman et al., 1987). This inconsistency cannot be fully explained yet but may reflect differences in the temporal dynamics or underlying mechanisms of the two models. In the acute 6-OHDA paradigm, the duration of DA depletion may be insufficient to induce compensatory changes in the 5-HT system. Alternatively, the loss of DA neurons in this model may disrupt the pathways required to trigger serotonergic adaptation.

Analyses in **Chapter 6** revealed that the dynamics of 5-HT release in PD models depend heavily on background neuromodulation. In both conditions with intact or fully blocked DA and GABA signalling, *SNCA*-OVX animals showed elevated 5-HT release, suggesting a compensatory enhancement. However, when either DA or GABA signalling was selectively blocked - particularly when DA receptors were blocked alone - there was no genotype differences in 5-HT release. This indicates that the mechanisms regulating 5-HT release are altered in PD, and these changes only become apparent under certain circuit conditions. These results suggest that DA tone plays a critical role in shaping 5-HT output, and that its loss reveals hidden changes in serotonergic regulation that remain masked under intact neuromodulatory input.

Mechanistically, these shifts in regulation were reflected in altered receptor function. SERT-mediated reuptake was found to be impaired in PD animals, while GABA receptor-mediated inhibition was upregulated. Meanwhile, D_2 receptor-mediated inhibition of 5-HT release was attenuated in the PD mice. These opposing changes in dopaminergic and GABAergic control are consistent with previously reported alterations in dopaminergic and GABAergic tone in PD models (Janezic et al., 2013; Roberts et al., 2020), reflecting a shift in the balance of neuromodulatory regulation. Importantly, this also suggests that under certain conditions -

particularly without careful control of GABA and DA signalling - the net 5-HT output may appear unchanged, masking underlying circuit-level alterations.

My findings have implications for interpreting therapeutic treatment of PD. Drugs modulating dopaminergic or GABAergic tone may unintendedly alter serotonergic transmission. The serotonergic system itself has emerged as a potential therapeutic target in PD. Several studies have investigated whether modulating 5-HT signalling can ease motor or non-motor symptoms of PD. For instance, activation of 5-HT_{1A} receptors has been shown to reduce LID in both animal models and clinical trials (Kannari et al., 2001; Politis & Loane, 2011). This effect is thought to arise from presynaptic inhibition of 5-HT neuron activity, thereby reducing abnormal DA release from serotonergic axons. Additionally, preclinical studies have suggested that 5-HT_{2A} receptor antagonists might relieve motor difficulties and improve L-DOPA responsiveness (Hamadjida et al., 2018). Although these serotonergic targets are still being explored, they reflect growing recognition that 5-HT modulates the therapeutic efficacy and side-effect of DA-based treatments in PD.

Current evidence on 5-HT changes in PD remains inconsistent. While some studies report 5-HT axons hyperinnervation (Bédard et al., 2011; Li et al., 2013; Rozas et al., 1998), the prevailing view still supports a reduction or loss of serotonergic function in PD (Kerenyi et al., 2003; Nayyar et al., 2009; Schrag & Politis, 2016). In parallel, Garris and Wightman (1997) reported that striatal DA release *in vivo* remains largely unchanged even after significant DA depletion, with measurable release only dropping in very late-stage lesions. This suggests a compensatory capacity in dopaminergic axons to help maintain extracellular DA levels despite structural loss (Garris et al., 1997). This implies that functional neurotransmitter release can be maintained by compensatory mechanisms even when structural integrity is compromised. However, our data show that 5-HT release is already altered in early-stage PD models, suggesting that serotonergic axons may be more vulnerable or less capable of maintaining function compared

to DA axons. This could be due to differences in vesicle release properties, reuptake efficiency, or presynaptic control mechanisms between the two systems. It also raises the possibility that serotonergic dysfunction may emerge earlier than previously thought, potentially contributing to early circuit imbalance in PD.

In summary, my findings in **Chapter 6** show that striatal 5-HT signalling changes differently across PD models, shaped by both compensation and shifts in DA and GABA interactions, as summarized by **Fig. 7.1**. These changes may not appear under normal conditions but become clear when specific striatal circuits are blocked, highlighting the need to study 5-HT regulation in detail when multiple neurotransmitter system is affected.

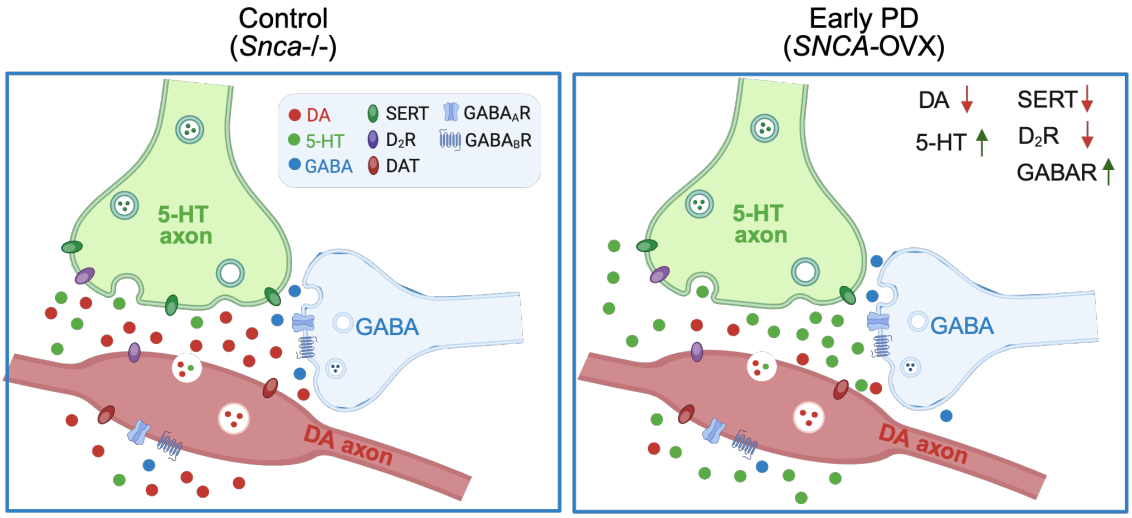

Figure 7.1. Dysfunction of 5-HT signalling in DLS in a mouse model of early PD. In early parkinsonian *SNCA*-OVX mice (3-4 months old), striatal 5-HT signalling is enhanced as a compensatory response to impaired DA release, accompanied by reduced D_2R-mediated inhibition and increased GABAergic suppression of 5-HT release. In addition, SERT-mediated control of 5-HT is diminished, further contributing to the altered serotonergic dynamics observed in this model.

7.4 Conclusion

In this thesis, I investigated the properties of striatal 5-HT transmission and characterised its release dynamics using a genetically encoded sensor. I demonstrated that 5-HT release is

jointly regulated by dopaminergic, cholinergic, and GABAergic inputs in the DLS. Furthermore, I revealed that each of these modulatory systems are disrupted to varying degrees in a mouse model of PD, leading to altered serotonergic transmission and a broader imbalance across striatal neuromodulatory networks. These findings provide new insights into how 5-HT signalling is integrated within basal ganglia circuits, and how this integration becomes dysregulated in the context of PD. My work contributes to a deeper understanding of neurotransmitter imbalance in neurodegenerative disease and may help guide future therapeutic strategies targeting serotonergic dysfunction.

Reference

Abg Abd Wahab, D. Y., Gau, C. H., Zakaria, R., Muthu Karuppan, M. K., A-rahbi, B. S., Abdullah, Z., Alrafiah, A., Abdullah, J. M., & Muthuraju, S. (2019). Review on Cross Talk between Neurotransmitters and Neuroinflammation in Striatum and Cerebellum in the Mediation of Motor Behaviour. *BioMed Research International*, *2019*, 1767203. https://doi.org/10.1155/2019/1767203

Ade, K. K., Janssen, M. J., Ortinski, P. I., & Vicini, S. (2008). Differential tonic GABA conductances in striatal medium spiny neurons. *The Journal of Neuroscience: The Official Journal of the Society for Neuroscience*, *28*(5), 1185–1197. https://doi.org/10.1523/JNEUROSCI.3908-07.2008

Aghajanian, G. K., Wang, R. Y., & Baraban, J. (1978). Serotonergic and non-serotonergic neurons of the dorsal raphe: Reciprocal changes in firing induced by peripheral nerve stimulation. *Brain Research*, *153*(1), 169–175. https://doi.org/10.1016/0006-8993(78)91140-X

Agrawal, L., Korkutata, M., Vimal, S. K., Yadav, M. K., Bhattacharyya, S., & Shiga, T. (2020). Therapeutic potential of serotonin 4 receptor for chronic depression and its associated comorbidity in the gut. *Neuropharmacology*, *166*, 107969–107987. https://doi.org/10.1016/j.neuropharm.2020.107969

Akhoon, B. A., Choudhary, S., Tiwari, H., Kumar, A., Barik, M. R., Rathor, L., Pandey, R., & Nargotra, A. (2020). Discovery of a New Donepezil-like Acetylcholinesterase Inhibitor for Targeting Alzheimer's Disease: Computational Studies with Biological Validation. *Journal of Chemical Information and Modeling*, *60*(10), 4717–4729. https://doi.org/10.1021/acs.jcim.0c00496

Albin, R. L., Young, A. B., & Penney, J. B. (1989). The functional anatomy of basal ganglia disorders. *Trends in Neurosciences*, *12*(10), 366–375. https://doi.org/10.1016/0166-2236(89)90074-x

Alcantara, A. A., Chen, V., Herring, B. E., Mendenhall, J. M., & Berlanga, M. L. (2003). Localization of dopamine D2 receptors on cholinergic interneurons of the dorsal striatum and nucleus accumbens of the rat. *Brain Research*, *986*(1–2), 22–29. https://doi.org/10.1016/s0006-8993(03)03165-2

Alex, K. D., Yavanian, G. J., McFarlane, H. G., Pluto, C. P., & Pehek, E. A. (2005). Modulation of dopamine release by striatal 5-HT2C receptors. *Synapse (New York, N.Y.)*, *55*(4), 242–251. https://doi.org/10.1002/syn.20109

Allen, N. J. (2014). Astrocyte Regulation of Synaptic Behavior. *Annual Review of Cell and Developmental Biology*, *30*(Volume 30, 2014), 439–463. https://doi.org/10.1146/annurev-cellbio-100913-013053

Andersen, P. H., & Jansen, J. A. (1990). Dopamine receptor agonists: Selectivity and dopamine D1 receptor efficacy. *European Journal of Pharmacology: Molecular Pharmacology*, *188*(6), 335–347. https://doi.org/10.1016/0922-4106(90)90194-3

Andrews, C. M., & Lucki, I. (2001). Effects of cocaine on extracellular dopamine and serotonin levels in the nucleus accumbens. *Psychopharmacology*, *155*(3), 221–229. https://doi.org/10.1007/s002130100704

Aransay, A., Rodríguez-López, C., García-Amado, M., Clascá, F., & Prensa, L. (2015). Long-range projection neurons of the mouse ventral tegmental area: A single-cell axon tracing analysis. *Frontiers in Neuroanatomy*, *9*. https://doi.org/10.3389/fnana.2015.00059

Araque, A. (2008). Astrocytes process synaptic information. *Neuron Glia Biology*, *4*(1), 3–10. https://doi.org/10.1017/S1740925X09000064

Ascherio, A., & Schwarzschild, M. A. (2016). The epidemiology of Parkinson's disease: Risk factors and prevention. *The Lancet. Neurology*, *15*(12), 1257–1272. https://doi.org/10.1016/S1474-4422(16)30230-7

Assous, M., Kaminer, J., Shah, F., Garg, A., Koós, T., & Tepper, J. M. (2017). Differential processing of thalamic information via distinct striatal interneuron circuits. *Nature Communications*, *8*(1), 15860. https://doi.org/10.1038/ncomms15860

Assous, M., & Tepper, J. M. (2019). Excitatory extrinsic afferents to striatal interneurons and interactions with striatal microcircuitry. *The European Journal of Neuroscience*, *49*(5), 593–603. https://doi.org/10.1111/ejn.13881

Avery, M. C., & Krichmar, J. L. (2017). Neuromodulatory Systems and Their Interactions: A Review of Models, Theories, and Experiments. *Frontiers in Neural Circuits*, *11*, 108. https://doi.org/10.3389/fncir.2017.00108

Avshalumov, M. V., Chen, B. T., Marshall, S. P., Peña, D. M., & Rice, M. E. (2003). Glutamate-Dependent Inhibition of Dopamine Release in Striatum Is Mediated by a New Diffusible Messenger, H2O2. *Journal of Neuroscience*, *23*(7), 2744–2750. https://doi.org/10.1523/JNEUROSCI.23-07-02744.2003

Azmitia, E. C., & Segal, M. (1978). An autoradiographic analysis of the differential ascending projections of the dorsal and median raphe nuclei in the rat. *The Journal of Comparative Neurology*, *179*(3), 641–667. https://doi.org/10.1002/cne.901790311

Baba, M., Nakajo, S., Tu, P. H., Tomita, T., Nakaya, K., Lee, V. M., Trojanowski, J. Q., & Iwatsubo, T. (1998). Aggregation of alpha-synuclein in Lewy bodies of sporadic Parkinson's disease and dementia with Lewy bodies. *The American Journal of Pathology*, *152*(4), 879–884.

Bacq, A., Balasse, L., Biala, G., Guiard, B., Gardier, A. M., Schinkel, A., Louis, F., Vialou, V., Martres, M.-P., Chevarin, C., Hamon, M., Giros, B., & Gautron, S. (2012). Organic cation transporter 2 controls brain norepinephrine and serotonin clearance and antidepressant response. *Molecular Psychiatry*, *17*(9), 926–939. https://doi.org/10.1038/mp.2011.87

Baganz, N. L., Horton, R. E., Calderon, A. S., Owens, W. A., Munn, J. L., Watts, L. T., Koldzic-Zivanovic, N., Jeske, N. A., Koek, W., Toney, G. M., & Daws, L. C. (2008). Organic cation transporter 3: Keeping the brake on extracellular serotonin in serotonin-transporter-deficient mice. *Proceedings of the National Academy of Sciences of the United States of America*, *105*(48), 18976–18981. https://doi.org/10.1073/pnas.0800466105

Baimel, C., Jang, E., Scudder, S. L., Manoocheri, K., & Carter, A. G. (2022). Hippocampal-evoked inhibition of cholinergic interneurons in the nucleus accumbens. *Cell Reports*, *40*(1), 111042. https://doi.org/10.1016/j.celrep.2022.111042

Ballardin, D., Makrini-Maleville, L., Seper, A., Valjent, E., & Rebholz, H. (2024). 5-HT4R agonism reduces L-DOPA-induced dyskinesia via striatopallidal neurons in unilaterally 6-OHDA lesioned mice. *Neurobiology of Disease*, *198*, 106559–106573. https://doi.org/10.1016/j.nbd.2024.106559

Balleine, B. W., & Ostlund, S. B. (2007). Still at the choice-point: Action selection and initiation in instrumental conditioning. In *Reward and decision making in corticobasal ganglia networks* (pp. 147–171). Blackwell Publishing.

Bamford, I. J., & Bamford, N. S. (2019). The Striatum's Role in Executing Rational and Irrational Economic Behaviors. *The Neuroscientist : A Review Journal Bringing Neurobiology, Neurology and Psychiatry*, *25*(5), 475–490. https://doi.org/10.1177/1073858418824256

Bang, D., Kishida, K. T., Lohrenz, T., White, J. P., Laxton, A. W., Tatter, S. B., Fleming, S. M., & Montague, P. R. (2020). Sub-second Dopamine and Serotonin Signaling in Human Striatum during Perceptual Decision-Making. *Neuron*, *108*(5), 999-1010.e6. https://doi.org/10.1016/j.neuron.2020.09.015

Barbeau, A. (1962). The pathogenesis of Parkinson's disease: A new hypothesis. *Canadian Medical Association Journal*, *87*(15), 802–807.

Barbeau, A. (1969). L-dopa therapy in Parkinson's disease: A critical review of nine years' experience. *Canadian Medical Association Journal*, *101*(13), 59–68.

Bari, A., Theobald, D. E., Caprioli, D., Mar, A. C., Aidoo-Micah, A., Dalley, J. W., & Robbins, T. W. (2010). Serotonin Modulates Sensitivity to Reward and Negative Feedback in a Probabilistic Reversal Learning Task in Rats. *Neuropsychopharmacology*, *35*(6), 1290–1301. https://doi.org/10.1038/npp.2009.233

Barnes, N. M., & Sharp, T. (1999). A review of central 5-HT receptors and their function. *Neuropharmacology*, *38*(8), 1083–1152. https://doi.org/10.1016/S0028-3908(99)00010-6

Beaulieu, J.-M., Espinoza, S., & Gainetdinov, R. R. (2015). Dopamine receptors—IUPHAR Review 13. *British Journal of Pharmacology*, *172*(1), 1–23. https://doi.org/10.1111/bph.12906

Beaulieu, J.-M., & Gainetdinov, R. R. (2011). The physiology, signaling, and pharmacology of dopamine receptors. *Pharmacological Reviews*, *63*(1), 182–217. https://doi.org/10.1124/pr.110.002642

Bédard, C., Wallman, M.-J., Pourcher, E., Gould, P. V., Parent, A., & Parent, M. (2011). Serotonin and dopamine striatal innervation in Parkinson's disease and Huntington's chorea. *Parkinsonism & Related Disorders*, *17*(8), 593–598. https://doi.org/10.1016/j.parkreldis.2011.05.012

Beery, A. K. (2018). Inclusion of females does not increase variability in rodent research studies. *Current Opinion in Behavioral Sciences*, *23*, 143–149. https://doi.org/10.1016/j.cobeha.2018.06.016

Bekris, L. M., Mata, I. F., & Zabetian, C. P. (2010). The Genetics of Parkinson Disease. *Journal of Geriatric Psychiatry and Neurology*, *23*(4), 228–242. https://doi.org/10.1177/0891988710383572

Benarroch, E. E. (2016). Astrocyte signaling and synaptic homeostasis. *Neurology*, *87*(3), 324–330. https://doi.org/10.1212/WNL.0000000000002875

Benloucif, S., & Galloway, M. P. (1991). Facilitation of dopamine release in vivo by serotonin agonists: Studies with microdialysis. *European Journal of Pharmacology*, *200*(1), 1–8. https://doi.org/10.1016/0014-2999(91)90658-d

Bennett, B. D., & Wilson, C. J. (1999). Spontaneous activity of neostriatal cholinergic interneurons in vitro. *The Journal of Neuroscience: The Official Journal of the Society for Neuroscience*, *19*(13), 5586–5596. https://doi.org/10.1523/JNEUROSCI.19-13-05586.1999

Berke, J. D., & Hyman, S. E. (2000). Addiction, dopamine, and the molecular mechanisms of memory. *Neuron*, *25*(3), 515–532. https://doi.org/10.1016/s0896-6273(00)81056-9

Bernheimer, H., Birkmayer, W., Hornykiewicz, O., Jellinger, K., & Seitelberger, F. (1973). Brain dopamine and the syndromes of Parkinson and Huntington Clinical, morphological and neurochemical correlations. *Journal of the Neurological Sciences*, *20*(4), 415–455. https://doi.org/10.1016/0022-510X(73)90175-5

Besson, M. J., Graybiel, A. M., & Nastuk, M. A. (1988). [3H]SCH 23390 binding to D1 dopamine receptors in the basal ganglia of the cat and primate: Delineation of striosomal compartments and pallidal and nigral subdivisions. *Neuroscience*, *26*(1), 101–119. https://doi.org/10.1016/0306-4522(88)90130-3

Björklund, A., & Dunnett, S. B. (2007). Dopamine neuron systems in the brain: An update. *Trends in Neurosciences*, *30*(5), 194–202. https://doi.org/10.1016/j.tins.2007.03.006

Blesa, J., Foffani, G., Dehay, B., Bezard, E., & Obeso, J. A. (2022). Motor and non-motor circuit disturbances in early Parkinson disease: Which happens first? *Nature Reviews Neuroscience*, *23*(2), 115–128. https://doi.org/10.1038/s41583-021-00542-9

Blomeley, C., & Bracci, E. (2005a). Excitatory effects of serotonin on rat striatal cholinergic interneurones. *The Journal of Physiology*, *569*(3), 715–721. https://doi.org/10.1113/jphysiol.2005.098269

Blomeley, C., & Bracci, E. (2005b). Excitatory effects of serotonin on rat striatal cholinergic interneurones. *The Journal of Physiology*, *569*(Pt 3), 715–721. https://doi.org/10.1113/jphysiol.2005.098269

Blomeley, C. P., & Bracci, E. (2009). Serotonin excites fast-spiking interneurons in the striatum. *The European Journal of Neuroscience*, *29*(8), 1604–1614. https://doi.org/10.1111/j.1460-9568.2009.06725.x

Bockaert, J., Claeysen, S., Bécamel, C., Dumuis, A., & Marin, P. (2006). Neuronal 5-HT metabotropic receptors: Fine-tuning of their structure, signaling, and roles in synaptic modulation. *Cell and Tissue Research*, *326*(2), 553–572. https://doi.org/10.1007/s00441-006-0286-1

Bohnen, N. I., & Albin, R. L. (2011). The cholinergic system and Parkinson disease. *Behavioural Brain Research*, *221*(2), 564–573. https://doi.org/10.1016/j.bbr.2009.12.048

Bolam, J. P., Hanley, J. J., Booth, P. A., & Bevan, M. D. (2000). Synaptic organisation of the basal ganglia. *Journal of Anatomy*, *196 (Pt 4)*(Pt 4), 527–542. https://doi.org/10.1046/j.1469-7580.2000.19640527.x

Bolam, J. P., & Pissadaki, E. K. (2012). Living on the edge with too many mouths to feed: Why dopamine neurons die. *Movement Disorders*, *27*(12), 1478–1483. https://doi.org/10.1002/mds.25135

Bolam, J. P., Wainer, B. H., & Smith, A. D. (1984). Characterization of cholinergic neurons in the rat neostriatum. A combination of choline acetyltransferase immunocytochemistry, Golgi-impregnation and electron microscopy. *Neuroscience*, *12*(3), 711–718. https://doi.org/10.1016/0306-4522(84)90165-9

Bonaventure, P., Hall, H., Gommeren, W., Cras, P., Langlois, X., Jurzak, M., & Leysen, J. E. (2000). Mapping of serotonin 5-HT(4) receptor mRNA and ligand binding sites in the post-mortem human brain. *Synapse (New York, N.Y.)*, *36*(1), 35–46. https://doi.org/10.1002/(SICI)1098-2396(200004)36:1<35::AID-SYN4>3.0.CO;2-Y

Bonaventure, P., Nepomuceno, D., Kwok, A., Chai, W., Langlois, X., Hen, R., Stark, K., Carruthers, N., & Lovenberg, T. W. (2002). Reconsideration of 5-Hydroxytryptamine (5-HT)7Receptor Distribution Using [3H]5-Carboxamidotryptamine and [3H]8-Hydroxy-2-(di-n-propylamino)tetraline: Analysis in Brain of 5-HT1A Knockout and 5-HT1A/1B Double-Knockout Mice. *The Journal of Pharmacology and Experimental Therapeutics*, *302*(1), 240–248. https://doi.org/10.1124/jpet.302.1.240

Bonhomme, N., De Deurwaèrdere, P., Le Moal, M., & Spampinato, U. (1995). Evidence for 5-HT4 receptor subtype involvement in the enhancement of striatal dopamine release induced by serotonin: A microdialysis study in the halothane-anesthetized rat. *Neuropharmacology*, *34*(3), 269–279. https://doi.org/10.1016/0028-3908(94)00145-i

Bonsi, P., Cuomo, D., Ding, J., Sciamanna, G., Ulrich, S., Tscherter, A., Bernardi, G., Surmeier, D. J., & Pisani, A. (2007). Endogenous Serotonin Excites Striatal Cholinergic Interneurons via the Activation of 5-HT 2C, 5-HT6, and 5-HT7 Serotonin Receptors: Implications for Extrapyramidal Side Effects of Serotonin Reuptake Inhibitors. *Neuropsychopharmacology*, *32*(8), Article 8. https://doi.org/10.1038/sj.npp.1301294

Bonsi, P., Cuomo, D., Martella, G., Madeo, G., Schirinzi, T., Puglisi, F., Ponterio, G., & Pisani, A. (2011). Centrality of Striatal Cholinergic Transmission in Basal Ganglia Function. *Frontiers in Neuroanatomy*, *5*, 6. https://doi.org/10.3389/fnana.2011.00006

Booth, H. D. E., Hirst, W. D., & Wade-Martins, R. (2017). The Role of Astrocyte Dysfunction in Parkinson's Disease Pathogenesis. *Trends in Neurosciences*, *40*(6), 358–370. https://doi.org/10.1016/j.tins.2017.04.001

Bové, J., & Perier, C. (2012). Neurotoxin-based models of Parkinson's disease. *Neuroscience*, *211*, 51–76. https://doi.org/10.1016/j.neuroscience.2011.10.057

Braak, H., Del Tredici, K., Rüb, U., de Vos, R. A. I., Jansen Steur, E. N. H., & Braak, E. (2003). Staging of brain pathology related to sporadic Parkinson's disease. *Neurobiology of Aging*, *24*(2), 197–211. https://doi.org/10.1016/s0197-4580(02)00065-9

Brandebura, A. N., Paumier, A., Onur, T. S., & Allen, N. J. (2023). Astrocyte contribution to dysfunction, risk and progression in neurodegenerative disorders. *Nature Reviews Neuroscience*, *24*(1), 23–39. https://doi.org/10.1038/s41583-022-00641-1

Brimblecombe, K. R., Connor-Robson, N., Bataille, C. J. R., Roberts, B. M., Gracie, C., O'Connor, B., te Water Naude, R., Karthik, G., Russell, A. J., Wade-Martins, R., & Cragg, S. J. (2024). Inhibition of striatal dopamine release by the L-type calcium channel inhibitor isradipine co-varies with risk factors for Parkinson's. *European Journal of Neuroscience*, *59*(6), 1242–1259. https://doi.org/10.1111/ejn.16180

Brimblecombe, K. R., & Cragg, S. J. (2015). Substance P Weights Striatal Dopamine Transmission Differently within the Striosome-Matrix Axis. *The Journal of Neuroscience: The Official Journal of the Society for Neuroscience*, *35*(24), 9017–9023. https://doi.org/10.1523/JNEUROSCI.0870-15.2015

Brimblecombe, K. R., & Cragg, S. J. (2017). The Striosome and Matrix Compartments of the Striatum: A Path through the Labyrinth from Neurochemistry toward Function. *ACS Chemical Neuroscience*, *8*(2), 235–242. https://doi.org/10.1021/acschemneuro.6b00333

Brimblecombe, K. R., Threlfell, S., Dautan, D., Kosillo, P., Mena-Segovia, J., & Cragg, S. J. (2018). Targeted Activation of Cholinergic Interneurons Accounts for the Modulation of Dopamine by Striatal Nicotinic Receptors. *eNeuro*, *5*(5). https://doi.org/10.1523/ENEURO.0397-17.2018

Britt, J. P., & McGehee, D. S. (2008). Presynaptic opioid and nicotinic receptor modulation of dopamine overflow in the nucleus accumbens. *The Journal of Neuroscience: The Official Journal of the Society for Neuroscience*, *28*(7), 1672–1681.

Brodnik, Z. D., Batra, A., Oleson, E. B., & España, R. A. (2019). Local GABAA Receptor-Mediated Suppression of Dopamine Release within the Nucleus Accumbens. *ACS Chemical Neuroscience*, *10*(4), 1978–1985. https://doi.org/10.1021/acschemneuro.8b00268

Brown, P., & Molliver, M. E. (2000). Dual Serotonin (5-HT) Projections to the Nucleus Accumbens Core and Shell: Relation of the 5-HT Transporter to Amphetamine-Induced

Neurotoxicity. *The Journal of Neuroscience*, *20*(5), 1952–1963. https://doi.org/10.1523/JNEUROSCI.20-05-01952.2000

Bunin, M. A., & Wightman, R. M. (1998). Quantitative Evaluation of 5-Hydroxytryptamine (Serotonin) Neuronal Release and Uptake: An Investigation of Extrasynaptic Transmission. *The Journal of Neuroscience*, *18*(13), 4854–4860. https://doi.org/10.1523/JNEUROSCI.18-13-04854.1998

Burré, J. (2015). The Synaptic Function of α-Synuclein. *Journal of Parkinson's Disease*, *5*(4), 699–713. https://doi.org/10.3233/JPD-150642

Burton, A. C., Nakamura, K., & Roesch, M. R. (2015). From ventral-medial to dorsal-lateral striatum: Neural correlates of reward-guided decision-making. *Neurobiology of Learning and Memory*, *0*, 51–59. https://doi.org/10.1016/j.nlm.2014.05.003

Cabin, D. E., Shimazu, K., Murphy, D., Cole, N. B., Gottschalk, W., McIlwain, K. L., Orrison, B., Chen, A., Ellis, C. E., Paylor, R., Lu, B., & Nussbaum, R. L. (2002). Synaptic vesicle depletion correlates with attenuated synaptic responses to prolonged repetitive stimulation in mice lacking alpha-synuclein. *The Journal of Neuroscience: The Official Journal of the Society for Neuroscience*, *22*(20), 8797–8807. https://doi.org/10.1523/JNEUROSCI.22-20-08797.2002

Cachope, R., Mateo, Y., Mathur, B. N., Irving, J., Wang, H.-L., Morales, M., Lovinger, D. M., & Cheer, J. F. (2012). Selective Activation of Cholinergic Interneurons Enhances Accumbal Phasic Dopamine Release: Setting the Tone for Reward Processing. *Cell Reports*, *2*(1), 33–41. https://doi.org/10.1016/j.celrep.2012.05.011

Cai, X., Liu, H., Feng, B., Yu, M., He, Y., Liu, H., Liang, C., Yang, Y., Tu, L., Zhang, N., Wang, L., Yin, N., Han, J., Yan, Z., Wang, C., Xu, P., Wu, Q., Tong, Q., He, Y., & Xu, Y. (2022). A D2 to D1 shift in dopaminergic inputs to midbrain 5-HT neurons causes anorexia in mice. *Nature Neuroscience*, *25*(5), 646–658. https://doi.org/10.1038/s41593-022-01062-0

Calabresi, P., Centonze, D., Pisani, A., Sancesario, G., Alan North, R., & Bernardi, G. (1998). Muscarinic IPSPs in rat striatal cholinergic interneurones. *The Journal of Physiology*, *510*(Pt 2), 421–427. https://doi.org/10.1111/j.1469-7793.1998.421bk.x

Carboni, E., Imperato, A., Perezzani, L., & Di Chiara, G. (1989). Amphetamine, cocaine, phencyclidine and nomifensine increase extracellular dopamine concentrations preferentially in the nucleus accumbens of freely moving rats. *Neuroscience*, *28*(3), 653–661. https://doi.org/10.1016/0306-4522(89)90012-2

Cardinal, R. N., Parkinson, J. A., Hall, J., & Everitt, B. J. (2002). Emotion and motivation: The role of the amygdala, ventral striatum, and prefrontal cortex. *Neuroscience and Biobehavioral Reviews*, *26*(3), 321–352. https://doi.org/10.1016/s0149-7634(02)00007-6

Carey, R. J., DePalma, G., & Damianopoulos, E. (2001). Cocaine and serotonin: A role for the 5-HT1A receptor site in the mediation of cocaine stimulant effects. *Behavioural Brain Research*, *126*(1), 127–133. https://doi.org/10.1016/S0166-4328(01)00253-4

Carli, M., & Invernizzi, R. W. (2014). Serotoninergic and dopaminergic modulation of cortico-striatal circuit in executive and attention deficits induced by NMDA receptor hypofunction

in the 5-choice serial reaction time task. *Frontiers in Neural Circuits*, *8*, 58. https://doi.org/10.3389/fncir.2014.00058

Carta, M., Carlsson, T., Kirik, D., & Björklund, A. (2007). Dopamine released from 5-HT terminals is the cause of l-DOPA-induced dyskinesia in parkinsonian rats. *Brain*, *130*(7), 1819–1833. https://doi.org/10.1093/brain/awm082

Cataldi, S., Stanley, A. T., Miniaci, M. C., & Sulzer, D. (2022). Interpreting the role of the striatum during multiple phases of motor learning. *The FEBS Journal*, *289*(8), 2263–2281. https://doi.org/10.1111/febs.15908

Cavaccini, A., Gritti, M., Giorgi, A., Locarno, A., Heck, N., Migliarini, S., Bertero, A., Mereu, M., Margiani, G., Trusel, M., Catelani, T., Marotta, R., De Luca, M. A., Caboche, J., Gozzi, A., Pasqualetti, M., & Tonini, R. (2018). Serotonergic Signaling Controls Input-Specific Synaptic Plasticity at Striatal Circuits. *Neuron*, *98*(4), 801-816.e7. https://doi.org/10.1016/j.neuron.2018.04.008

Cenci, M. A. (2007). Dopamine dysregulation of movement control in L-DOPA-induced dyskinesia. *Trends in Neurosciences*, *30*(5), 236–243. https://doi.org/10.1016/j.tins.2007.03.005

Chartier-Harlin, M.-C., Kachergus, J., Roumier, C., Mouroux, V., Douay, X., Lincoln, S., Levecque, C., Larvor, L., Andrieux, J., Hulihan, M., Waucquier, N., Defebvre, L., Amouyel, P., Farrer, M., & Destée, A. (2004). Alpha-synuclein locus duplication as a cause of familial Parkinson's disease. *Lancet (London, England)*, *364*(9440), 1167–1169. https://doi.org/10.1016/S0140-6736(04)17103-1

Chen, F., Larsen, M. B., Neubauer, H. A., Sánchez, C., Plenge, P., & Wiborg, O. (2005). Characterization of an allosteric citalopram-binding site at the serotonin transporter. *Journal of Neurochemistry*, *92*(1), 21–28.

Choi, S. J., Ma, T. C., Ding, Y., Cheung, T., Joshi, N., Sulzer, D., Mosharov, E. V., & Kang, U. J. (2020). Alterations in the intrinsic properties of striatal cholinergic interneurons after dopamine lesion and chronic L-DOPA. *eLife*, *9*, e56920. https://doi.org/10.7554/eLife.56920

Chung, W.-S., Allen, N. J., & Eroglu, C. (2015). Astrocytes Control Synapse Formation, Function, and Elimination. *Cold Spring Harbor Perspectives in Biology*, *7*(9), a020370. https://doi.org/10.1101/cshperspect.a020370

Clark, D., & White, F. J. (1987). Review: D1 dopamine receptor—the search for a function: A critical evaluation of the D1/D2 dopamine receptor classification and its functional implications. *Synapse*, *1*(4), 347–388. https://doi.org/10.1002/syn.890010408

Clayton, J. A. (2016). Studying both sexes: A guiding principle for biomedicine. *FASEB Journal: Official Publication of the Federation of American Societies for Experimental Biology*, *30*(2), 519–524. https://doi.org/10.1096/fj.15-279554

Coddington, L. T., & Dudman, J. T. (2019). Learning from Action: Reconsidering Movement Signaling in Midbrain Dopamine Neuron Activity. *Neuron*, *104*(1), 63–77. https://doi.org/10.1016/j.neuron.2019.08.036

Compan, V., Daszuta, A., Salin, P., Sebben, M., Bockaert, J., & Dumuis, A. (1996). Lesion Study of the Distribution of Serotonin 5-HT4 Receptors in Rat Basal Ganglia and Hippocampus. *European Journal of Neuroscience*, *8*(12), 2591–2598.

Condon, M. D., Platt, N. J., Zhang, Y.-F., Roberts, B. M., Clements, M. A., Vietti-Michelina, S., Tseu, M.-Y., Brimblecombe, K. R., Threlfell, S., Mann, E. O., & Cragg, S. J. (2019). Plasticity in striatal dopamine release is governed by release-independent depression and the dopamine transporter. *Nature Communications*, *10*(1), 4263. https://doi.org/10.1038/s41467-019-12264-9

Consolo, S., Arnaboldi, S., Giorgi, S., Russi, G., & Ladinsky, H. (1994). 5-HT4 receptor stimulation facilitates acetylcholine release in rat frontal cortex. *NeuroReport*, *5*(10), 1230–1242.

Cookson, M. R. (2012). Parkinsonism Due to Mutations in PINK1, Parkin, and DJ-1 and Oxidative Stress and Mitochondrial Pathways. *Cold Spring Harbor Perspectives in Medicine*, *2*(9), a009415. https://doi.org/10.1101/cshperspect.a009415

Corvaja, N., Doucet, G., & Bolam, J. P. (1993). Ultrastructure and synaptic targets of the raphe-nigral projection in the rat. *Neuroscience*, *55*(2), 417–427. https://doi.org/10.1016/0306-4522(93)90510-m

Cragg, S. J., & Rice, M. E. (2004). DAncing past the DAT at a DA synapse. *Trends in Neurosciences*, *27*(5), 270–277. https://doi.org/10.1016/j.tins.2004.03.011

Crespi, F., Martin, K. F., & Marsden, C. A. (1988). Simultaneous in vivo voltammetric measurement of striatal extracellular DOPAC and 5-HIAA levels: Effect of electrical stimulation of DA and 5-HT neuronal pathways. *Neuroscience Letters*, *90*(3), 285–291. https://doi.org/10.1016/0304-3940(88)90203-0

Crittenden, J. R., & Graybiel, A. M. (2011). Basal Ganglia Disorders Associated with Imbalances in the Striatal Striosome and Matrix Compartments. *Frontiers in Neuroanatomy*, *5*. https://doi.org/10.3389/fnana.2011.00059

Cui, G., Jun, S. B., Jin, X., Pham, M. D., Vogel, S. S., Lovinger, D. M., & Costa, R. M. (2013). Concurrent activation of striatal direct and indirect pathways during action initiation. *Nature*, *494*(7436), 238–242. https://doi.org/10.1038/nature11846

Dajas-Bailador, F., Costa, G., Emmett, S., Bonilla, C., & Dajas, F. (1996). Acetylcholinesterase inhibitors block acetylcholine-evoked release of dopamine in rat striatum, in vivo. *Brain Research*, *722*(1), 12–18. https://doi.org/10.1016/0006-8993(96)00133-3

Dankoski, E. C., Agster, K. L., Fox, M. E., Moy, S. S., & Wightman, R. M. (2014). Facilitation of Serotonin Signaling by SSRIs is Attenuated by Social Isolation. *Neuropsychopharmacology*, *39*(13), 2928–2937. https://doi.org/10.1038/npp.2014.162

Daw, N. D., Kakade, S., & Dayan, P. (2002). Opponent interactions between serotonin and dopamine. *Neural Networks: The Official Journal of the International Neural Network Society*, *15*(4–6), 603–616. https://doi.org/10.1016/s0893-6080(02)00052-7

Daws, L. C. (2021). Organic Cation Transporters in Psychiatric Disorders. *Handbook of Experimental Pharmacology*, *266*, 215–239. https://doi.org/10.1007/164_2021_473

Daws, L. C., Koek, W., & Mitchell, N. C. (2013). Revisiting serotonin reuptake inhibitors and the therapeutic potential of 'uptake-2' in psychiatric disorders. *ACS Chemical Neuroscience*, *4*(1), 16–21. https://doi.org/10.1021/cn3001872

De Ceglia, R., Ledonne, A., Litvin, D. G., Lind, B. L., Carriero, G., Latagliata, E. C., Bindocci, E., Di Castro, M. A., Savtchouk, I., Vitali, I., Ranjak, A., Congiu, M., Canonica, T., Wisden, W., Harris, K., Mameli, M., Mercuri, N., Telley, L., & Volterra, A. (2023). Specialized astrocytes mediate glutamatergic gliotransmission in the CNS. *Nature*, *622*(7981), 120–129. https://doi.org/10.1038/s41586-023-06502-w

De Deurwaerdère, P., & Di Giovanni, G. (2017). Serotonergic modulation of the activity of mesencephalic dopaminergic systems: Therapeutic implications. *Progress in Neurobiology*, *151*, 175–236. https://doi.org/10.1016/j.pneurobio.2016.03.004

De Deurwaerdère, P., L'hirondel, M., Bonhomme, N., Lucas, G., Cheramy, A., & Spampinato, U. (1997). Serotonin stimulation of 5-HT4 receptors indirectly enhances in vivo dopamine release in the rat striatum. *Journal of Neurochemistry*, *68*(1), 195–203. https://doi.org/10.1046/j.1471-4159.1997.68010195.x

De Deurwaerdère, P., Navailles, S., Berg, K. A., Clarke, W. P., & Spampinato, U. (2004). Constitutive Activity of the Serotonin2C Receptor Inhibits In Vivo Dopamine Release in the Rat Striatum and Nucleus Accumbens. *The Journal of Neuroscience*, *24*(13), 3235–3241. https://doi.org/10.1523/JNEUROSCI.0112-04.2004

De Pablo-Fernandez, E., Goldacre, R., Pakpoor, J., Noyce, A. J., & Warner, T. T. (2018). Association between diabetes and subsequent Parkinson disease: A record-linkage cohort study. *Neurology*, *91*(2), e139–e142. https://doi.org/10.1212/WNL.0000000000005771

DeBoer, P., & Westerink, B. H. (1994). GABAergic modulation of striatal cholinergic interneurons: An in vivo microdialysis study. *Journal of Neurochemistry*, *62*(1), 70–75. https://doi.org/10.1046/j.1471-4159.1994.62010070.x

DeLong, M. R. (1990). Primate models of movement disorders of basal ganglia origin. *Trends in Neurosciences*, *13*(7), 281–285. https://doi.org/10.1016/0166-2236(90)90110-v

DeLong, M. R., & Wichmann, T. (2007). Circuits and Circuit Disorders of the Basal Ganglia. *Archives of Neurology*, *64*(1), 20–24. https://doi.org/10.1001/archneur.64.1.20

Deng, F., Wan, J., Li, G., Dong, H., Xia, X., Wang, Y., Li, X., Zhuang, C., Zheng, Y., Liu, L., Yan, Y., Feng, J., Zhao, Y., Xie, H., & Li, Y. (2024). Improved green and red GRAB sensors for monitoring spatiotemporal serotonin release in vivo. *Nature Methods*, *21*(4), 692–702. https://doi.org/10.1038/s41592-024-02188-8

Descarries, L., Audet, M. A., Doucet, G., Garcia, S., Oleskevich, S., Séguéla, P., Soghomonian, J.-J., & Watkins, K. C. (1990). Morphology of Central Serotonin Neurons. *Annals of the New York Academy of Sciences*, *600*(1), 81–92. https://doi.org/10.1111/j.1749-6632.1990.tb16874.x

Descarries, L., Gisiger, V., & Steriade, M. (1997). Diffuse transmission by acetylcholine in the CNS. *Progress in Neurobiology*, *53*(5), 603–625. https://doi.org/10.1016/s0301-0082(97)00050-6

Descarries, L., Watkins, K. C., Garcia, S., Bosler, O., & Doucet, G. (1996). Dual character, asynaptic and synaptic, of the dopamine innervation in adult rat neostriatum: A quantitative autoradiographic and immunocytochemical analysis. *The Journal of Comparative Neurology*, *375*(2), 167–186.

Deurwaerdère, P. D., Stinus, L., & Spampinato, U. (1998). Opposite Change of In Vivo Dopamine Release in the Rat Nucleus Accumbens and Striatum That Follows Electrical Stimulation of Dorsal Raphe Nucleus: Role of 5-HT3 Receptors. *Journal of Neuroscience*, *18*(16), 6528–6538. https://doi.org/10.1523/JNEUROSCI.18-16-06528.1998

Dewey, S. L., Smith, G. S., Logan, J., Alexoff, D., Ding, Y. S., King, P., Pappas, N., Brodie, J. D., & Ashby, C. R. (1995). Serotonergic modulation of striatal dopamine measured with positron emission tomography (PET) and in vivo microdialysis. *The Journal of Neuroscience: The Official Journal of the Society for Neuroscience*, *15*(1 Pt 2), 821–829. https://doi.org/10.1523/JNEUROSCI.15-01-00821.1995

Di Giovanni, G., Di Matteo, V., Pierucci, M., & Esposito, E. (2008). Serotonin–dopamine interaction: Electrophysiological evidence. In G. Di Giovann, V. Di Matteo, & E. Esposito (Eds.), *Progress in Brain Research* (Vol. 172, pp. 45–71). Elsevier. https://doi.org/10.1016/S0079-6123(08)00903-5

Di Matteo, V., Di Giovanni, G., Pierucci, M., & Esposito, E. (2008). Serotonin control of central dopaminergic function: Focus on in vivo microdialysis studies. In G. Di Giovann, V. Di Matteo, & E. Esposito (Eds.), *Progress in Brain Research* (Vol. 172, pp. 7–44). Elsevier. https://doi.org/10.1016/S0079-6123(08)00902-3

DiFiglia, M., Aronin, N., & Leeman, S. E. (1982). Light microscopic and ultrastructural localization of immunoreactive substance P in the dorsal horn of monkey spinal cord. *Neuroscience*, *7*(5), 1127–1139. https://doi.org/10.1016/0306-4522(82)91120-4

Ding, J. B., Guzman, J. N., Peterson, J. D., Goldberg, J. A., & Surmeier, D. J. (2010). Thalamic Gating of Corticostriatal Signaling by Cholinergic Interneurons. *Neuron*, *67*(2), 294–307. https://doi.org/10.1016/j.neuron.2010.06.017

Do, J., Kim, J.-I., Bakes, J., Lee, K., & Kaang, B.-K. (2013). Functional roles of neurotransmitters and neuromodulators in the dorsal striatum. *Learning & Memory*, *20*(1), 21–28. https://doi.org/10.1101/lm.025015.111

Dodson, P. D., Dreyer, J. K., Jennings, K. A., Syed, E. C. J., Wade-Martins, R., Cragg, S. J., Bolam, J. P., & Magill, P. J. (2016). Representation of spontaneous movement by dopaminergic neurons is cell-type selective and disrupted in parkinsonism. *Proceedings of the National Academy of Sciences of the United States of America*, *113*(15), E2180-2188. https://doi.org/10.1073/pnas.1515941113

Dorocic, I. P., Fürth, D., Xuan, Y., Johansson, Y., Pozzi, L., Silberberg, G., Carlén, M., & Meletis, K. (2014). A Whole-Brain Atlas of Inputs to Serotonergic Neurons of the Dorsal and

Median Raphe Nuclei. *Neuron*, *83*(3), 663–678. https://doi.org/10.1016/j.neuron.2014.07.002

Dorsey, E. R., Elbaz, A., Nichols, E., Abbasi, N., Abd-Allah, F., Abdelalim, A., Adsuar, J. C., Ansha, M. G., Brayne, C., Choi, J.-Y. J., Collado-Mateo, D., Dahodwala, N., Do, H. P., Edessa, D., Endres, M., Fereshtehnejad, S.-M., Foreman, K. J., Gankpe, F. G., Gupta, R., … Murray, C. J. L. (2018). Global, regional, and national burden of Parkinson's disease, 1990–2016: A systematic analysis for the Global Burden of Disease Study 2016. *The Lancet Neurology*, *17*(11), 939–953. https://doi.org/10.1016/S1474-4422(18)30295-3

Dorst, M. C., Tokarska, A., Zhou, M., Lee, K., Stagkourakis, S., Broberger, C., Masmanidis, S., & Silberberg, G. (2020). Polysynaptic inhibition between striatal cholinergic interneurons shapes their network activity patterns in a dopamine-dependent manner. *Nature Communications*, *11*(1), 5113. https://doi.org/10.1038/s41467-020-18882-y

Doucet, G., Descarries, L., & Garcia, S. (1986). Quantification of the dopamine innervation in adult rat neostriatum. *Neuroscience*, *19*(2), 427–445. https://doi.org/10.1016/0306-4522(86)90272-1

Drenan, R. M., Grady, S. R., Steele, A. D., McKinney, S., Patzlaff, N. E., McIntosh, J. M., Marks, M. J., Miwa, J. M., & Lester, H. A. (2010). Cholinergic Modulation of Locomotion and Striatal Dopamine Release Is Mediated by α6α4* Nicotinic Acetylcholine Receptors. *Journal of Neuroscience*, *30*(29), 9877–9889. https://doi.org/10.1523/JNEUROSCI.2056-10.2010

Egerton, A., Ahmad, R., Hirani, E., & Grasby, P. M. (2008). Modulation of striatal dopamine release by 5-HT2A and 5-HT2C receptor antagonists: [11C]raclopride PET studies in the rat. *Psychopharmacology*, *200*(4), 487–496. https://doi.org/10.1007/s00213-008-1226-4

Eglen, R. M., Bley, K., Bonhaus, D. W., Clark, R. D., Hegde, S. S., Johnson, L. G., Leung, E., & Wong, E. H. (1993). RS 23597-190: A potent and selective 5-HT4 receptor antagonist. *British Journal of Pharmacology*, *110*(1), 119–126. https://doi.org/10.1111/j.1476-5381.1993.tb13780.x

Eglen, RM., Bonhaus, DW., Johnson, LG., Leung, E., & Clark, RD. (1995). Pharmacological characterization of two novel and potent 5-HT4 receptor agonists, RS 67333 and RS 67506, in vitro and in vivo. *British Journal of Pharmacology*, *115*(8), 1387–1392. https://doi.org/10.1111/j.1476-5381.1995.tb16628.x

Ehringer, H., & Hornykiewicz, O. (1960). [Distribution of noradrenaline and dopamine (3-hydroxytyramine) in the human brain and their behavior in diseases of the extrapyramidal system]. *Klinische Wochenschrift*, *38*, 1236–1239. https://doi.org/10.1007/BF01485901

Ekstrand, M. I., & Galter, D. (2009). The MitoPark Mouse—An animal model of Parkinson's disease with impaired respiratory chain function in dopamine neurons. *Parkinsonism & Related Disorders*, *15 Suppl 3*, S185-188. https://doi.org/10.1016/S1353-8020(09)70811-9

Eskenazi, D., Brodsky, M., & Neumaier, J. F. (2015). Deconstructing 5-HT6 receptor effects on striatal circuit function. *Neuroscience*, *299*, 97–106. https://doi.org/10.1016/j.neuroscience.2015.04.046

Eskow Jaunarajs, K. L., Bonsi, P., Chesselet, M. F., Standaert, D. G., & Pisani, A. (2015). Striatal cholinergic dysfunction as a unifying theme in the pathophysiology of dystonia. *Progress in Neurobiology*, *127–128*, 91–107. https://doi.org/10.1016/j.pneurobio.2015.02.002

Essman, W. D., Singh, A., & Lucki, I. (1994). Serotonergic properties of cocaine: Effects on a 5-HT2 receptor-mediated behavior and on extracellular concentrations of serotonin and dopamine. *Pharmacology, Biochemistry, and Behavior*, *49*(1), 107–113. https://doi.org/10.1016/0091-3057(94)90463-4

Exley, R., & Cragg, S. J. (2008). Presynaptic nicotinic receptors: A dynamic and diverse cholinergic filter of striatal dopamine neurotransmission. *British Journal of Pharmacology*, *153*(S1), S283–S297. https://doi.org/10.1038/sj.bjp.0707510

Faye, C., Hen, R., Guiard, B. P., Denny, C. A., Gardier, A. M., Mendez-David, I., & David, D. J. (2020). Rapid Anxiolytic Effects of RS67333, a Serotonin Type 4 Receptor Agonist, and Diazepam, a Benzodiazepine, Are Mediated by Projections From the Prefrontal Cortex to the Dorsal Raphe Nucleus. *Biological Psychiatry*, *87*(6), 514–525. https://doi.org/10.1016/j.biopsych.2019.08.009

Ferguson, S. M., Mitchell, E. S., & Neumaier, J. F. (2008). Increased Expression of 5-HT6 Receptors in the Nucleus Accumbens Blocks the Rewarding But Not Psychomotor Activating Properties of Cocaine. *Biological Psychiatry*, *63*(2), 207–213. https://doi.org/10.1016/j.biopsych.2007.02.018

Ferré, S., Cortés, R., & Artigas, F. (1994). Dopaminergic regulation of the serotonergic raphe-striatal pathway: Microdialysis studies in freely moving rats. *The Journal of Neuroscience: The Official Journal of the Society for Neuroscience*, *14*(8), 4839–4846. https://doi.org/10.1523/JNEUROSCI.14-08-04839.1994

Filippo, R. D., & Schmitz, D. (2024). Transcriptomic mapping of the 5-HT receptor landscape. *Patterns*, *5*(10). https://doi.org/10.1016/j.patter.2024.101048

Fischer, A. G., & Ullsperger, M. (2017). An Update on the Role of Serotonin and its Interplay with Dopamine for Reward. *Frontiers in Human Neuroscience*, *11*. https://www.frontiersin.org/articles/10.3389/fnhum.2017.00484

Foster, N. N., Barry, J., Korobkova, L., Garcia, L., Gao, L., Becerra, M., Sherafat, Y., Peng, B., Li, X., Choi, J.-H., Gou, L., Zingg, B., Azam, S., Lo, D., Khanjani, N., Zhang, B., Stanis, J., Bowman, I., Cotter, K., … Dong, H.-W. (2021). The mouse cortico–basal ganglia–thalamic network. *Nature*, *598*(7879), 188–194. https://doi.org/10.1038/s41586-021-03993-3

Freeman, J. a., Manis, P. b., Snipes, G. j., Mayes, B. n., Samson, P. c., Wikswo Jr., J. p., & Freeman, D. b. (1985). Steady growth cone currents revealed by a novel circularly vibrating probe: A possible mechanism underlying neurite growth. *Journal of Neuroscience Research*, *13*(1–2), 257–283. https://doi.org/10.1002/jnr.490130118

Freret, T., Bouet, V., Quiedeville, A., Nee, G., Dallemagne, P., Rochais, C., & Boulouard, M. (2012). Synergistic effect of acetylcholinesterase inhibition (donepezil) and 5-HT4 receptor activation (RS67333) on object recognition in mice. *Behavioural Brain Research*, *230*(1), 304–308. https://doi.org/10.1016/j.bbr.2012.02.012

Fuxe, K., Borroto-Escuela, D. O., Romero-Fernandez, W., Diaz Cabiale, Z., Rivera, A., Ferraro, L., Tanganelli, S., Tarakanov, A. O., Garriga, P., Narvaez, J. A., Ciruela, F., & Agnati, L. F. (2012). Extrasynaptic Neurotransmission in the Modulation of Brain Function. Focus on the Striatal Neuronal–Glial Networks. *Frontiers in Physiology*, *3*. https://doi.org/10.3389/fphys.2012.00136

Garris, P. A., Walker, Q. D., & Wightman, R. M. (1997). Dopamine release and uptake rates both decrease in the partially denervated striatum in proportion to the loss of dopamine terminals. *Brain Research*, *753*(2), 225–234. https://doi.org/10.1016/s0006-8993(97)00003-6

Garris, P. A., & Wightman, R. M. (1994). Different kinetics govern dopaminergic transmission in the amygdala, prefrontal cortex, and striatum: An in vivo voltammetric study. *The Journal of Neuroscience: The Official Journal of the Society for Neuroscience*, *14*(1), 442–450. https://doi.org/10.1523/JNEUROSCI.14-01-00442.1994

Gasser, P. J. (2019). Roles for the uptake2 transporter OCT3 in regulation of dopaminergic neurotransmission and behavior. *Neurochemistry International*, *123*, 46–49. https://doi.org/10.1016/j.neuint.2018.07.008

Gerald, C., Adham, N., Kao, H. T., Olsen, M. A., Laz, T. M., Schechter, L. E., Bard, J. A., Vaysse, P. J., Hartig, P. R., & Branchek, T. A. (1995). The 5-HT4 receptor: Molecular cloning and pharmacological characterization of two splice variants. *The EMBO Journal*, *14*(12), 2806–2815. https://doi.org/10.1002/j.1460-2075.1995.tb07280.x

Gerfen, C. R. (1985). The neostriatal mosaic. I. Compartmental organization of projections from the striatum to the substantia nigra in the rat. *The Journal of Comparative Neurology*, *236*(4), 454–476. https://doi.org/10.1002/cne.902360404

Gerfen, C. R., Herkenham, M., & Thibault, J. (1987). The neostriatal mosaic: II. Patch- and matrix-directed mesostriatal dopaminergic and non-dopaminergic systems. *The Journal of Neuroscience: The Official Journal of the Society for Neuroscience*, *7*(12), 3915–3934. https://doi.org/10.1523/JNEUROSCI.07-12-03915.1987

Gerfen, C. R., & Surmeier, D. J. (2011). Modulation of striatal projection systems by dopamine. *Annual Review of Neuroscience*, *34*, 441–466. https://doi.org/10.1146/annurev-neuro-061010-113641

Gingrich, J. A., & Caron, M. G. (1993). Recent advances in the molecular biology of dopamine receptors. *Annual Review of Neuroscience*, *16*, 299–321. https://doi.org/10.1146/annurev.ne.16.030193.001503

Giros, B., el Mestikawy, S., Bertrand, L., & Caron, M. G. (1991). Cloning and functional characterization of a cocaine-sensitive dopamine transporter. *FEBS Letters*, *295*(1–3), 149–154. https://doi.org/10.1016/0014-5793(91)81406-x

Gittis, A. H., & Kreitzer, A. C. (2012). Striatal microcircuitry and movement disorders. *Trends in Neurosciences*, *35*(9), 557–564. https://doi.org/10.1016/j.tins.2012.06.008

Gittis, A. H., Nelson, A. B., Thwin, M. T., Palop, J. J., & Kreitzer, A. C. (2010). Distinct roles of GABAergic interneurons in the regulation of striatal output pathways. *The Journal of Neuroscience: The Official Journal of the Society for Neuroscience*, *30*(6), 2223–2234. https://doi.org/10.1523/JNEUROSCI.4870-09.2010

Goldberg, J. A., & Wilson, C. J. (2016). Chapter 7—The Cholinergic Interneuron of the Striatum. In H. Steiner & K. Y. Tseng (Eds.), *Handbook of Behavioral Neuroscience* (Vol. 24, pp. 137–155). Elsevier. https://doi.org/10.1016/B978-0-12-802206-1.00007-6

Gonzalez-Rodriguez, P., Zampese, E., & Surmeier, D. J. (2020). Chapter 3—Selective neuronal vulnerability in Parkinson's disease. In A. Björklund & M. A. Cenci (Eds.), *Progress in Brain Research* (Vol. 252, pp. 61–89). Elsevier. https://doi.org/10.1016/bs.pbr.2020.02.005

Göthert, M. (1990). Presynaptic serotonin receptors in the central nervous system. *Annals of the New York Academy of Sciences*, *604*, 102–112. https://doi.org/10.1111/j.1749-6632.1990.tb31986.x

Göthert, M., Fink, K., Frölich, D., Likungu, J., Molderings, G., Schlicker, E., & Zentner, J. (1995). Presynaptic 5-HT auto- and heteroreceptors in the human central and peripheral nervous system. *Behavioural Brain Research*, *73*(1), 89–92. https://doi.org/10.1016/0166-4328(96)00076-9

Grace, A. A., & Bunney, B. S. (1983). Intracellular and extracellular electrophysiology of nigral dopaminergic neurons—1. Identification and characterization. *Neuroscience*, *10*(2), 301–315. https://doi.org/10.1016/0306-4522(83)90135-5

Grace, A. A., & Bunney, B. S. (1984). The control of firing pattern in nigral dopamine neurons: Burst firing. *The Journal of Neuroscience: The Official Journal of the Society for Neuroscience*, *4*(11), 2877–2890. https://doi.org/10.1523/JNEUROSCI.04-11-02877.1984

Grace, A. A., Floresco, S. B., Goto, Y., & Lodge, D. J. (2007). Regulation of firing of dopaminergic neurons and control of goal-directed behaviors. *Trends in Neurosciences*, *30*(5), 220–227. https://doi.org/10.1016/j.tins.2007.03.003

Grandy, D. K., Hanneman, E., Bunzow, J., Shih, M., Machida, C. A., Bidlack, J. M., & Civelli, O. (1990). Purification, Cloning, and Tissue Distribution of a 23-kDa Rat Protein Isolated by Morphine Affinity Chromatography. *Molecular Endocrinology*, *4*(9), 1370–1376. https://doi.org/10.1210/mend-4-9-1370

Graveland, G. A., & DiFiglia, M. (1985). The frequency and distribution of medium-sized neurons with indented nuclei in the primate and rodent neostriatum. *Brain Research*, *327*(1–2), 307–311. https://doi.org/10.1016/0006-8993(85)91524-0

Graybiel, A. M. (1998). The basal ganglia and chunking of action repertoires. *Neurobiology of Learning and Memory*, *70*(1–2), 119–136. https://doi.org/10.1006/nlme.1998.3843

Graybiel, A. M., & Ragsdale, C. W. (1978). Histochemically distinct compartments in the striatum of human, monkeys, and cat demonstrated by acetylthiocholinesterase staining. *Proceedings of the National Academy of Sciences of the United States of America*, *75*(11), 5723–5726. https://doi.org/10.1073/pnas.75.11.5723

Grimaldi, B., Bonnin, A., Fillion, M.-P., Ruat, M., Traiffort, E., & Fillion, G. (1998). Characterization of 5-ht6 receptor and expression of 5-ht6 mRNA in the rat brain during ontogenetic development. *Naunyn-Schmiedeberg's Archives of Pharmacology*, *357*(4), 393–400. https://doi.org/10.1007/PL00005184

Grosch, J., Winkler, J., & Kohl, Z. (2016). Early Degeneration of Both Dopaminergic and Serotonergic Axons – A Common Mechanism in Parkinson's Disease. *Frontiers in Cellular Neuroscience*, *10*. https://doi.org/10.3389/fncel.2016.00293

Guo, J.-D., & Rainnie, D. G. (2010). Presynaptic 5-HT1B receptor-mediated serotonergic inhibition of glutamate transmission in the bed nucleus of the stria terminalis. *Neuroscience*, *165*(4), 1390–1401. https://doi.org/10.1016/j.neuroscience.2009.11.071

Hagan, C. E., McDevitt, R. A., Liu, Y., Furay, A. R., & Neumaier, J. F. (2012). 5-HT1B autoreceptor regulation of serotonin transporter activity in synaptosomes. *Synapse (New York, N.Y.)*, *66*(12), 1024–1034. https://doi.org/10.1002/syn.21608

Hamadjida, A., Nuara, S. G., Bédard, D., Gaudette, F., Beaudry, F., Gourdon, J. C., & Huot, P. (2018). The highly selective 5-HT2A antagonist EMD-281,014 reduces dyskinesia and psychosis in the l-DOPA-treated parkinsonian marmoset. *Neuropharmacology*, *139*, 61–67. https://doi.org/10.1016/j.neuropharm.2018.06.038

Hannon, J., & Hoyer, D. (2008). Molecular biology of 5-HT receptors. *Behavioural Brain Research*, *195*(1), 198–213. https://doi.org/10.1016/j.bbr.2008.03.020

Hartung, H., Threlfell, S., & Cragg, S. J. (2011). Nitric Oxide Donors Enhance the Frequency Dependence of Dopamine Release in Nucleus Accumbens. *Neuropsychopharmacology*, *36*(9), 1811–1822. https://doi.org/10.1038/npp.2011.62

Hashemi, P., Dankoski, E. C., Lama, R., Wood, K. M., Takmakov, P., & Wightman, R. M. (2012). Brain dopamine and serotonin differ in regulation and its consequences. *Proceedings of the National Academy of Sciences of the United States of America*, *109*(29), 11510–11515. https://doi.org/10.1073/pnas.1201547109

Hashemi, P., Dankoski, E. C., Petrovic, J., Keithley, R. B., & Wightman, R. M. (2009). Voltammetric detection of 5-hydroxytryptamine release in the rat brain. *Analytical Chemistry*, *81*(22), 9462–9471. https://doi.org/10.1021/ac9018846

Hashemi, P., Dankoski, E. C., Wood, K. M., Ambrose, R. E., & Wightman, R. M. (2011). In vivo electrochemical evidence for simultaneous 5-HT and histamine release in the rat substantia nigra pars reticulata following medial forebrain bundle stimulation. *Journal of Neurochemistry*, *118*(5), 749–759. https://doi.org/10.1111/j.1471-4159.2011.07352.x

Hauser, S. R., Hedlund, P. B., Roberts, A. J., Sari, Y., Bell, R. L., & Engleman, E. A. (2015). The 5-HT7 receptor as a potential target for treating drug and alcohol abuse. *Frontiers in Neuroscience*, *8*. https://doi.org/10.3389/fnins.2014.00448

Haydon, P. G., & Carmignoto, G. (2006). Astrocyte Control of Synaptic Transmission and Neurovascular Coupling. *Physiological Reviews*, *86*(3), 1009–1031. https://doi.org/10.1152/physrev.00049.2005

Helboe, L., Egebjerg, J., & de Jong, I. E. M. (2015). Distribution of serotonin receptor 5-HT6 mRNA in rat neuronal subpopulations: A double in situ hybridization study. *Neuroscience*, *310*, 442–454. https://doi.org/10.1016/j.neuroscience.2015.09.064

Hersch, S. M., Yi, H., Heilman, C. J., Edwards, R. H., & Levey, A. I. (1997). Subcellular localization and molecular topology of the dopamine transporter in the striatum and substantia nigra. *Journal of Comparative Neurology*, *388*(2), 211–227. https://doi.org/10.1002/(SICI)1096-9861(19971117)388:2<211::AID-CNE3>3.0.CO;2-4

Hirrlinger, J., & Nimmerjahn, A. (2022). A perspective on astrocyte regulation of neural circuit function and animal behavior. *Glia*, *70*(8), 1554–1580. https://doi.org/10.1002/glia.24168

Hirst, W. D., Minton, J. A. L., Bromidge, S. M., Moss, S. F., Latter, A. J., Riley, G., Routledge, C., Middlemiss, D. N., & Price, G. W. (2000). Characterization of [125I]-SB-258585 binding to human recombinant and native 5-HT6 receptors in rat, pig and human brain tissue. *British Journal of Pharmacology*, *130*(7), 1597–1605. https://doi.org/10.1038/sj.bjp.0703458

Hjorth, S., Bengtsson, H. J., Kullberg, A., Carlzon, D., Peilot, H., & Auerbach, S. B. (2000). Serotonin autoreceptor function and antidepressant drug action. *Journal of Psychopharmacology*, *14*(2), 177–185. https://doi.org/10.1177/026988110001400208

Hodge, A., Humphrey, D., & Rosenberry, T. (1992). Ambenonium is a rapidly reversible noncovalent inhibitor of acetylcholinesterase, with one of the highest known affinities. *Molecular Pharmacology*, *41*, 937–942.

Hornykiewicz, O. (2006). The discovery of dopamine deficiency in the parkinsonian brain. *Journal of Neural Transmission. Supplementum*, *70*, 9–15. https://doi.org/10.1007/978-3-211-45295-0_3

Horton, R. E., Apple, D. M., Owens, W. A., Baganz, N. L., Cano, S., Mitchell, N. C., Vitela, M., Gould, G. G., Koek, W., & Daws, L. C. (2013). Decynium-22 Enhances SSRI-Induced Antidepressant-Like Effects in Mice: Uncovering Novel Targets to Treat Depression. *Journal of Neuroscience*, *33*(25), 10534–10543. https://doi.org/10.1523/JNEUROSCI.5687-11.2013

Huot, P., & Fox, S. H. (2013). The serotonergic system in motor and non-motor manifestations of Parkinson's disease. *Experimental Brain Research*, *230*(4), 463–476. https://doi.org/10.1007/s00221-013-3621-2

Hyland, B. I., Reynolds, J. N. J., Hay, J., Perk, C. G., & Miller, R. (2002). Firing modes of midbrain dopamine cells in the freely moving rat. *Neuroscience*, *114*(2), 475–492. https://doi.org/10.1016/s0306-4522(02)00267-1

Ibáñez-Sandoval, O., Tecuapetla, F., Unal, B., Shah, F., Koós, T., & Tepper, J. M. (2010). Electrophysiological and Morphological Characteristics and Synaptic Connectivity of

Tyrosine Hydroxylase-Expressing Neurons in Adult Mouse Striatum. *The Journal of Neuroscience*, *30*(20), 6999–7016. https://doi.org/10.1523/JNEUROSCI.5996-09.2010

Ibáñez-Sandoval, O., Tecuapetla, F., Unal, B., Shah, F., Koós, T., & Tepper, J. M. (2011). A Novel Functionally Distinct Subtype of Striatal Neuropeptide Y Interneuron. *Journal of Neuroscience*, *31*(46), 16757–16769. https://doi.org/10.1523/JNEUROSCI.2628-11.2011

Ibáñez-Sandoval, O., Xenias, H. S., Tepper, J. M., & Koós, T. (2015). Dopaminergic and Cholinergic Modulation of Striatal Tyrosine Hydroxylase Interneurons. *Neuropharmacology*, *95*, 468–476. https://doi.org/10.1016/j.neuropharm.2015.03.036

Ikarashi, Y., Takahashi, A., Ishimaru, H., Arai, T., & Maruyama, Y. (1997). Suppression of cholinergic activity via the dopamine D2 receptor in the rat striatum. *Neurochemistry International*, *30*(2), 191–197. https://doi.org/10.1016/S0197-0186(96)00024-1

Imperato, A., & Angelucci, L. (1989). 5-HT3 receptors control dopamine release in the nucleus accumbens of freely moving rats. *Neuroscience Letters*, *101*(2), 214–217. https://doi.org/10.1016/0304-3940(89)90533-8

Ishii, T., Kinoshita, K., & Muroi, Y. (2019). Serotonin 5-HT4 Receptor Agonists Improve Facilitation of Contextual Fear Extinction in an MPTP-Induced Mouse Model of Parkinson's Disease. *International Journal of Molecular Sciences*, *20*(21), 5340. https://doi.org/10.3390/ijms20215340

Jackson, B. P., Dietz, S. M., & Wightman, R. M. (1995). Fast-scan cyclic voltammetry of 5-hydroxytryptamine. *Analytical Chemistry*, *67*(6), 1115–1120. https://doi.org/10.1021/ac00102a015

Jackson, D., Stachowiak, M. K., Bruno, J. P., & Zigmond, M. J. (1988). Inhibition of striatal acetylcholine release by endogenous serotonin. *Brain Research*, *457*(2), 259–266. https://doi.org/10.1016/0006-8993(88)90694-4

Janezic, S., Threlfell, S., Dodson, P. D., Dowie, M. J., Taylor, T. N., Potgieter, D., Parkkinen, L., Senior, S. L., Anwar, S., Ryan, B., Deltheil, T., Kosillo, P., Cioroch, M., Wagner, K., Ansorge, O., Bannerman, D. M., Bolam, J. P., Magill, P. J., Cragg, S. J., & Wade-Martins, R. (2013). Deficits in dopaminergic transmission precede neuron loss and dysfunction in a new Parkinson model. *Proceedings of the National Academy of Sciences*, *110*(42). https://doi.org/10.1073/pnas.1309143110

Jankovic, J., & Tan, E. K. (2020). Parkinson's disease: Etiopathogenesis and treatment. *Journal of Neurology, Neurosurgery, and Psychiatry*, *91*(8), 795–808. https://doi.org/10.1136/jnnp-2019-322338

Jansen, C. U., Qvortrup, K. M., Jansen, C. U., & Qvortrup, K. M. (2021). Small Molecule Drugs for Treatment of Alzheimer's Diseases Developed on the Basis of Mechanistic Understanding of the Serotonin Receptors 4 and 6. In *Serotonin and the CNS - New Developments in Pharmacology and Therapeutics*. IntechOpen. https://doi.org/10.5772/intechopen.96381

Jiménez-Sánchez, L., Blesa, J., Del Rey, N. L., Monje, M. H. G., Obeso, J. A., & Cavada, C. (2020). Serotonergic innervation of the striatum in a nonhuman primate model of

Parkinson's disease. *Neuropharmacology*, *170*, 107806. https://doi.org/10.1016/j.neuropharm.2019.107806

Jing, M., Li, Y., Zeng, J., Huang, P., Skirzewski, M., Kljakic, O., Peng, W., Qian, T., Tan, K., Zou, J., Trinh, S., Wu, R., Zhang, S., Pan, S., Hires, S. A., Xu, M., Li, H., Saksida, L. M., Prado, V. F., … Li, Y. (2020). An optimized acetylcholine sensor for monitoring in vivo cholinergic activity. *Nature Methods*, *17*(11), 1139–1146.

John, C. E., & Jones, S. R. (2007). Voltammetric characterization of the effect of monoamine uptake inhibitors and releasers on dopamine and serotonin uptake in mouse caudate-putamen and substantia nigra slices. *Neuropharmacology*, *52*(8), 1596–1605. https://doi.org/10.1016/j.neuropharm.2007.03.004

Kalivas, P. W., & McFarland, K. (2003). Brain circuitry and the reinstatement of cocaine-seeking behavior. *Psychopharmacology*, *168*(1–2), 44–56. https://doi.org/10.1007/s00213-003-1393-2

Kannari, K., Yamato, H., Shen, H., Tomiyama, M., Suda, T., & Matsunaga, M. (2001). Activation of 5-HT1A but not 5-HT1B receptors attenuates an increase in extracellular dopamine derived from exogenously administered l-DOPA in the striatum with nigrostriatal denervation. *Journal of Neurochemistry*, *76*(5), 1346–1353. https://doi.org/10.1046/j.1471-4159.2001.00184.x

Katz, N. S., Guiard, B. P., El Mansari, M., & Blier, P. (2010). Effects of acute and sustained administration of the catecholamine reuptake inhibitor nomifensine on the firing activity of monoaminergic neurons. *Journal of Psychopharmacology (Oxford, England)*, *24*(8), 1223–1235. https://doi.org/10.1177/0269881109348178

Kawaguchi, Y. (1993). Physiological, morphological, and histochemical characterization of three classes of interneurons in rat neostriatum. *The Journal of Neuroscience: The Official Journal of the Society for Neuroscience*, *13*(11), 4908–4923. https://doi.org/10.1523/JNEUROSCI.13-11-04908.1993

Kawaguchi, Y., Wilson, C., & Emson, P. (1990). Projection subtypes of rat neostriatal matrix cells revealed by intracellular injection of biocytin. *The Journal of Neuroscience*, *10*(10), 3421–3438. https://doi.org/10.1523/JNEUROSCI.10-10-03421.1990

Kebabian, J. W., & Calne, D. B. (1979). Multiple receptors for dopamine. *Nature*, *277*(5692), 93–96. https://doi.org/10.1038/277093a0

Kelley, A. E. (2004). Ventral striatal control of appetitive motivation: Role in ingestive behavior and reward-related learning. *Neuroscience and Biobehavioral Reviews*, *27*(8), 765–776. https://doi.org/10.1016/j.neubiorev.2003.11.015

Kerenyi, L., Ricaurte, G. A., Schretlen, D. J., McCann, U., Varga, J., Mathews, W. B., Ravert, H. T., Dannals, R. F., Hilton, J., Wong, D. F., & Szabo, Z. (2003). Positron Emission Tomography of Striatal Serotonin Transporters in Parkinson Disease. *Archives of Neurology*, *60*(9), 1223–1229. https://doi.org/10.1001/archneur.60.9.1223

Kirmse, K., Kirischuk, S., & Grantyn, R. (2009). Role of GABA transporter 3 in GABAergic synaptic transmission at striatal output neurons. *Synapse*, *63*(10), 921–929. https://doi.org/10.1002/syn.20675

Kish, S. J., Shannak, K., & Hornykiewicz, O. (1988). Uneven Pattern of Dopamine Loss in the Striatum of Patients with Idiopathic Parkinson's Disease. *New England Journal of Medicine*, *318*(14), 876–880. https://doi.org/10.1056/NEJM198804073181402

Kish, S. J., Tong, J., Hornykiewicz, O., Rajput, A., Chang, L.-J., Guttman, M., & Furukawa, Y. (2008). Preferential loss of serotonin markers in caudate versus putamen in Parkinson's disease. *Brain*, *131*(1), 120–131. https://doi.org/10.1093/brain/awm239

Knowlton, B. J., Mangels, J. A., & Squire, L. R. (1996). A neostriatal habit learning system in humans. *Science (New York, N.Y.)*, *273*(5280), 1399–1402. https://doi.org/10.1126/science.273.5280.1399

Koch, J. C., Bitow, F., Haack, J., d'Hedouville, Z., Zhang, J.-N., Tönges, L., Michel, U., Oliveira, L. M. A., Jovin, T. M., Liman, J., Tatenhorst, L., Bähr, M., & Lingor, P. (2015). Alpha-Synuclein affects neurite morphology, autophagy, vesicle transport and axonal degeneration in CNS neurons. *Cell Death & Disease*, *6*(7), e1811–e1811. https://doi.org/10.1038/cddis.2015.169

Koe, B. K. (1976). Molecular geometry of inhibitors of the uptake of catecholamines and serotonin in synaptosomal preparations of rat brain. *The Journal of Pharmacology and Experimental Therapeutics*, *199*(3), 649–661.

Koeglsperger, T., Rumpf, S.-L., Schließer, P., Struebing, F. L., Brendel, M., Levin, J., Trenkwalder, C., Höglinger, G. U., & Herms, J. (2023). Neuropathology of incidental Lewy body & prodromal Parkinson's disease. *Molecular Neurodegeneration*, *18*(1), 32. https://doi.org/10.1186/s13024-023-00622-7

Koós, T., & Tepper, J. M. (1999). Inhibitory control of neostriatal projection neurons by GABAergic interneurons. *Nature Neuroscience*, *2*(5), 467–472. https://doi.org/10.1038/8138

Kosillo, P., Zhang, Y.-F., Threlfell, S., & Cragg, S. J. (2016). Cortical Control of Striatal Dopamine Transmission via Striatal Cholinergic Interneurons. *Cerebral Cortex*, *26*(11), 4160–4169. https://doi.org/10.1093/cercor/bhw252

Kosofsky, B. E., & Molliver, M. E. (1987). The serotoninergic innervation of cerebral cortex: Different classes of axon terminals arise from dorsal and median raphe nuclei. *Synapse*, *1*(2), 153–168. https://doi.org/10.1002/syn.890010204

Kramer, P. F., Brill-Weil, S. G., Cummins, A. C., Zhang, R., Camacho-Hernandez, G. A., Newman, A. H., Eldridge, M. A. G., Averbeck, B. B., & Khaliq, Z. M. (2022). Synaptic-like axo-axonal transmission from striatal cholinergic interneurons onto dopaminergic fibers. *Neuron*, *110*(18), 2949–2960. https://doi.org/10.1016/j.neuron.2022.07.011

Kügler, S., Kilic, E., & Bähr, M. (2003). Human synapsin 1 gene promoter confers highly neuron-specific long-term transgene expression from an adenoviral vector in the adult rat brain

depending on the transduced area. *Gene Therapy*, *10*(4), 337–347. https://doi.org/10.1038/sj.gt.3301905

Lamirault, L., & Simon, H. (2001). Enhancement of place and object recognition memory in young adult and old rats by RS 67333, a partial agonist of 5-HT4 receptors. *Neuropharmacology*, *41*(7), 844–853. https://doi.org/10.1016/S0028-3908(01)00123-X

Lanciego, J. L., Luquin, N., & Obeso, J. A. (2012). Functional neuroanatomy of the basal ganglia. *Cold Spring Harbor Perspectives in Medicine*, *2*(12), a009621. https://doi.org/10.1101/cshperspect.a009621

Laprade, N., Radja, F., Reader, T. A., & Soghomonian, J.-J. (1996). Dopamine Receptor Agonists Regulate Levels of the Serotonin 5-HT2A Receptor and its mRNA in a Subpopulation of Rat Striatal Neurons. *The Journal of Neuroscience*, *16*(11), 3727–3736. https://doi.org/10.1523/JNEUROSCI.16-11-03727.1996

Larsen, M. B., Sonders, M. S., Mortensen, O. V., Larson, G. A., Zahniser, N. R., & Amara, S. G. (2011). Dopamine transport by the serotonin transporter: A mechanistically distinct mode of substrate translocation. *The Journal of Neuroscience: The Official Journal of the Society for Neuroscience*, *31*(17), 6605–6615. https://doi.org/10.1523/JNEUROSCI.0576-11.2011

Lautenschläger, J., Stephens, A. D., Fusco, G., Ströhl, F., Curry, N., Zacharopoulou, M., Michel, C. H., Laine, R., Nespovitaya, N., Fantham, M., Pinotsi, D., Zago, W., Fraser, P., Tandon, A., St George-Hyslop, P., Rees, E., Phillips, J. J., De Simone, A., Kaminski, C. F., & Schierle, G. S. K. (2018). C-terminal calcium binding of α-synuclein modulates synaptic vesicle interaction. *Nature Communications*, *9*(1), 712. https://doi.org/10.1038/s41467-018-03111-4

Lavoie, B., & Parent, A. (1990). Immunohistochemical study of the serotoninergic innervation of the basal ganglia in the squirrel monkey. *Journal of Comparative Neurology*, *299*(1), 1–16. https://doi.org/10.1002/cne.902990102

Lecoutey, C., Hedou, D., Freret, T., Giannoni, P., Gaven, F., Since, M., Bouet, V., Ballandonne, C., Corvaisier, S., Malzert Fréon, A., Mignani, S., Cresteil, T., Boulouard, M., Claeysen, S., Rochais, C., & Dallemagne, P. (2014). Design of donecopride, a dual serotonin subtype 4 receptor agonist/acetylcholinesterase inhibitor with potential interest for Alzheimer's disease treatment. *Proceedings of the National Academy of Sciences of the United States of America*, *111*(36), E3825–E3830. https://doi.org/10.1073/pnas.1410315111

Lee, K., Dixon, A. K., Freeman, T. C., & Richardson, P. J. (1998). Identification of an ATP-sensitive potassium channel current in rat striatal cholinergic interneurones. *The Journal of Physiology*, *510 (Pt 2)*(Pt 2), 441–453. https://doi.org/10.1111/j.1469-7793.1998.441bk.x

Lesch, K.-P., & Waider, J. (2012). Serotonin in the Modulation of Neural Plasticity and Networks: Implications for Neurodevelopmental Disorders. *Neuron*, *76*(1), 175–191. https://doi.org/10.1016/j.neuron.2012.09.013

Li, H., Chen, Z., Tan, Y., Luo, H., Lu, C., Gao, C., Shen, X., Cai, F., Hu, J., & Chen, S. (2024). Enhancing striatal acetylcholine facilitates dopamine release and striatal output in parkinsonian mice. *Cell & Bioscience*, *14*(1), 146. https://doi.org/10.1186/s13578-024-01328-z

Li, L., Qiu, G., Ding, S., & Zhou, F.-M. (2013). Serotonin hyperinnervation and upregulated 5-HT2A receptor expression and motor-stimulating function in nigrostriatal dopamine-deficient Pitx3 mutant mice. *Brain Research*, *1491*, 236–250. https://doi.org/10.1016/j.brainres.2012.11.010

Li, M., Ye, X., Huang, Z., Ye, L., & Chen, C. (2025). Global burden of Parkinson's disease from 1990 to 2021: A population-based study. *BMJ Open*, *15*(4), e095610. https://doi.org/10.1136/bmjopen-2024-095610

Li, R. W., Yang, C., Kwan, Y.-W., Chan, S.-W., Lee, S. M.-Y., & Leung, G. P.-H. (2013). Involvement of Organic Cation Transporter-3 and Plasma Membrane Monoamine Transporter in Serotonin Uptake in Human Brain Vascular Smooth Muscle Cells. *Frontiers in Pharmacology*, *4*. https://doi.org/10.3389/fphar.2013.00014

Lim, S. A. O., Kang, U. J., & McGehee, D. S. (2014). Striatal cholinergic interneuron regulation and circuit effects. *Frontiers in Synaptic Neuroscience*, *6*. https://doi.org/10.3389/fnsyn.2014.00022

Liu, C., Cai, X., Ritzau-Jost, A., Kramer, P. F., Li, Y., Khaliq, Z. M., Hallermann, S., & Kaeser, P. S. (2022). An action potential initiation mechanism in distal axons for the control of dopamine release. *Science (New York, N.Y.)*, *375*(6587), 1378–1385. https://doi.org/10.1126/science.abn0532

Liu, X., Ying, J., Wang, X., Zheng, Q., Zhao, T., Yoon, S., Yu, W., Yang, D., Fang, Y., & Hua, F. (2021). Astrocytes in Neural Circuits: Key Factors in Synaptic Regulation and Potential Targets for Neurodevelopmental Disorders. *Frontiers in Molecular Neuroscience*, *14*, 729273. https://doi.org/10.3389/fnmol.2021.729273

Liu, Y., Traba, J. E., & Lüscher, C. (2025). Striatal Crosstalk Between Dopamine and Serotonin Systems. *eLife*, *14*. https://doi.org/10.7554/eLife.107252.1

Lopes, E. F., Roberts, B. M., Siddorn, R. E., Clements, M. A., & Cragg, S. J. (2019). Inhibition of Nigrostriatal Dopamine Release by Striatal GABAA and GABAB Receptors. *The Journal of Neuroscience: The Official Journal of the Society for Neuroscience*, *39*(6), 1058–1065. https://doi.org/10.1523/JNEUROSCI.2028-18.2018

Lopez, S. M., Gonzales, M. R., Alvarez, B. D., Amodeo, L. R., & Amodeo, D. A. (2025). Repeated 5-HT6 receptor activation facilitates flexible behavior in C57BL/6J mice. *Pharmacology Biochemistry and Behavior*, *255*, 174063. https://doi.org/10.1016/j.pbb.2025.174063

Luo, R., Partridge, J. G., & Vicini, S. (2013). Distinct roles of synaptic and extrasynaptic GABAAreceptors in striatal inhibition dynamics. *Frontiers in Neural Circuits*, *7*, 186. https://doi.org/10.3389/fncir.2013.00186

Luthman, J., Bolioli, B., Tsutsumi, T., Verhofstad, A., & Jonsson, G. (1987). Sprouting of striatal serotonin nerve terminals following selective lesions of nigro-striatal dopamine neurons in neonatal rat. *Brain Research Bulletin*, *19*(2), 269–274. https://doi.org/10.1016/0361-9230(87)90092-X

Marino, G., Campanelli, F., Natale, G., Carluccio, M. D., Servillo, F., Ghiglieri, V., & Calabresi, P. (2025). Synaptic Interactions Between Serotonergic and Dopaminergic Systems in Parkinson's Disease. *Current Neuropharmacology*, *23*(9), 1021–1035. https://doi.org/10.2174/011570159X336597241217062042

Martel, J. C., & Gatti McArthur, S. (2020). Dopamine Receptor Subtypes, Physiology and Pharmacology: New Ligands and Concepts in Schizophrenia. *Frontiers in Pharmacology*, *11*, 1003. https://doi.org/10.3389/fphar.2020.01003

Martín-Cora, F. J., & Pazos, A. (2004). Autoradiographic distribution of 5-HT7 receptors in the human brain using [3H]mesulergine: Comparison to other mammalian species. *British Journal of Pharmacology*, *141*(1), 92–104. https://doi.org/10.1038/sj.bjp.0705576

Mathur, B. N., Capik, N. A., Alvarez, V. A., & Lovinger, D. M. (2011). Serotonin Induces Long-Term Depression at Corticostriatal Synapses. *Journal of Neuroscience*, *31*(20), 7402–7411. https://doi.org/10.1523/JNEUROSCI.6250-10.2011

Matias, S., Lottem, E., Dugué, G. P., & Mainen, Z. F. (2017). Activity patterns of serotonin neurons underlying cognitive flexibility. *eLife*, *6*, e20552. https://doi.org/10.7554/eLife.20552

Matityahu, L., Hobel, Z. B., Berkowitz, N., Malgady, J. M., Gilin, N., Plotkin, J. L., & Goldberg, J. A. (2024). Synchronous activation of striatal cholinergic interneurons induces local serotonin release. *bioRxiv*, 2024.11.03.621726. https://doi.org/10.1101/2024.11.03.621726

Matsuda, W., Furuta, T., Nakamura, K. C., Hioki, H., Fujiyama, F., Arai, R., & Kaneko, T. (2009). Single nigrostriatal dopaminergic neurons form widely spread and highly dense axonal arborizations in the neostriatum. *The Journal of Neuroscience: The Official Journal of the Society for Neuroscience*, *29*(2), 444–453. https://doi.org/10.1523/JNEUROSCI.4029-08.2009

Maurice, N., Liberge, M., Jaouen, F., Ztaou, S., Hanini, M., Camon, J., Deisseroth, K., Amalric, M., Kerkerian-Le Goff, L., & Beurrier, C. (2015). Striatal Cholinergic Interneurons Control Motor Behavior and Basal Ganglia Function in Experimental Parkinsonism. *Cell Reports*, *13*(4), 657–666. https://doi.org/10.1016/j.celrep.2015.09.034

Maurice, N., Mercer, J., Chan, C. S., Hernandez-Lopez, S., Held, J., Tkatch, T., & Surmeier, D. J. (2004). D2 dopamine receptor-mediated modulation of voltage-dependent Na+ channels reduces autonomous activity in striatal cholinergic interneurons. *The Journal of Neuroscience: The Official Journal of the Society for Neuroscience*, *24*(46), 10289–10301. https://doi.org/10.1523/JNEUROSCI.2155-04.2004

McDevitt, R. A., Tiran-Cappello, A., Shen, H., Balderas, I., Britt, J. P., Marino, R. A. M., Chung, S. L., Richie, C. T., Harvey, B. K., & Bonci, A. (2014). Serotonergic versus

Nonserotonergic Dorsal Raphe Projection Neurons: Differential Participation in Reward Circuitry. *Cell Reports*, *8*(6), 1857–1869. https://doi.org/10.1016/j.celrep.2014.08.037

McGregor, M. M., & Nelson, A. B. (2019). Circuit Mechanisms of Parkinson's Disease. *Neuron*, *101*(6), 1042–1056. https://doi.org/10.1016/j.neuron.2019.03.004

Mendez-David, I., David, D. J., Darcet, F., Wu, M. V., Kerdine-Römer, S., Gardier, A. M., & Hen, R. (2014). Rapid Anxiolytic Effects of a 5-HT4 Receptor Agonist Are Mediated by a Neurogenesis-Independent Mechanism. *Neuropsychopharmacology*, *39*(6), 1366–1378. https://doi.org/10.1038/npp.2013.332

Michael, D. J., Joseph, J. D., Kilpatrick, M. R., Travis, E. R., & Wightman, R. M. (1999). Improving data acquisition for fast-scan cyclic voltammetry. *Analytical Chemistry*, *71*(18), 3941–3947. https://doi.org/10.1021/ac990491+

Miguelez, C., Morera-Herreras, T., Torrecilla, M., Ruiz-Ortega, J. A., & Ugedo, L. (2014). Interaction between the 5-HT system and the basal ganglia: Functional implication and therapeutic perspective in Parkinson's disease. *Frontiers in Neural Circuits*, *8*. https://doi.org/10.3389/fncir.2014.00021

Millan, M. J., Marin, P., Bockaert, J., & Cour, C. M. la. (2008). Signaling at G-protein-coupled serotonin receptors: Recent advances and future research directions. *Trends in Pharmacological Sciences*, *29*(9), 454–464. https://doi.org/10.1016/j.tips.2008.06.007

Millar, J., Stamford, J., Kruk, Z., & Wightman, M. (1985). Electrochemical, pharmacological and electrophysiological evidence of rapid dopamine release and removal in the rat caudate nucleus following electrical stimulation of the median forebrain bundle. *European Journal of Pharmacology*, *109*(3), 341–348. https://doi.org/10.1016/0014-2999(85)90394-2

Mirenowicz, J., & Schultz, W. (1996). Preferential activation of midbrain dopamine neurons by appetitive rather than aversive stimuli. *Nature*, *379*(6564), 449–451. https://doi.org/10.1038/379449a0

Mitchell, E. S., Sexton, T., & Neumaier, J. F. (2007). Increased Expression of 5-HT6 Receptors in the Rat Dorsomedial Striatum Impairs Instrumental Learning. *Neuropsychopharmacology*, *32*(7), 1520–1530. https://doi.org/10.1038/sj.npp.1301284

Miyazaki, K. W., Miyazaki, K., & Doya, K. (2012). Activation of Dorsal Raphe Serotonin Neurons Is Necessary for Waiting for Delayed Rewards. *Journal of Neuroscience*, *32*(31), 10451–10457. https://doi.org/10.1523/JNEUROSCI.0915-12.2012

Mlinar, B., Montalbano, A., Piszczek, L., Gross, C., & Corradetti, R. (2016). Firing Properties of Genetically Identified Dorsal Raphe Serotonergic Neurons in Brain Slices. *Frontiers in Cellular Neuroscience*, *10*, 195. https://doi.org/10.3389/fncel.2016.00195

Mogenson, G. J., Jones, D. L., & Yim, C. Y. (1980). From motivation to action: Functional interface between the limbic system and the motor system. *Progress in Neurobiology*, *14*(2), 69–97. https://doi.org/10.1016/0301-0082(80)90018-0

Molochnikov, I., & Cohen, D. (2014). Hemispheric differences in the mesostriatal dopaminergic system. *Frontiers in Systems Neuroscience*, *8*, 110. https://doi.org/10.3389/fnsys.2014.00110

Moret, C., & Briley, M. (2000). The possible role of 5-HT1B/D receptors in psychiatric disorders and their potential as a target for therapy. *European Journal of Pharmacology*, *404*(1), 1–12. https://doi.org/10.1016/S0014-2999(00)00581-1

Mori, S., Takino, T., Yamada, H., & Sano, Y. (1985). Immunohistochemical demonstration of serotonin nerve fibers in the subthalamic nucleus of the rat, cat and monkey. *Neuroscience Letters*, *62*(3), 305–309. https://doi.org/10.1016/0304-3940(85)90566-X

Movassaghi, C. S., Perrotta, K. A., Yang, H., Iyer, R., Cheng, X., Dagher, M., Fillol, M. A., & Andrews, A. M. (2021). Simultaneous serotonin and dopamine monitoring across timescales by rapid pulse voltammetry with partial least squares regression. *Analytical and Bioanalytical Chemistry*, *413*(27), 6747–6767. https://doi.org/10.1007/s00216-021-03665-1

Mrini, A., Soucy, J.-P., Lafaille, F., Lemoine, P., & Descarries, L. (1995). Quantification of the serotonin hyperinnervation in adult rat neostriatum after neonatal 6-hydroxydopamine lesion of nigral dopamine neurons. *Brain Research*, *669*(2), 303–308. https://doi.org/10.1016/0006-8993(94)01210-9

Muñoz, A., Lopez-Lopez, A., Labandeira, C. M., & Labandeira-Garcia, J. L. (2020). Interactions Between the Serotonergic and Other Neurotransmitter Systems in the Basal Ganglia: Role in Parkinson's Disease and Adverse Effects of L-DOPA. *Frontiers in Neuroanatomy*, *14*. https://doi.org/10.3389/fnana.2020.00026

Muzerelle, A., Scotto-Lomassese, S., Bernard, J. F., Soiza-Reilly, M., & Gaspar, P. (2016). Conditional anterograde tracing reveals distinct targeting of individual serotonin cell groups (B5–B9) to the forebrain and brainstem. *Brain Structure and Function*, *221*(1), 535–561. https://doi.org/10.1007/s00429-014-0924-4

Myslivecek, J. (2022). Dopamine and Dopamine-Related Ligands Can Bind Not Only to Dopamine Receptors. *Life*, *12*(5), Article 5. https://doi.org/10.3390/life12050606

Nair, S. G., Estabrook, M. M., & Neumaier, J. F. (2020). Chapter 18—Serotonin regulation of striatal function. In C. P. Müller & K. A. Cunningham (Eds.), *Handbook of Behavioral Neuroscience* (Vol. 31, pp. 321–335). Elsevier. https://doi.org/10.1016/B978-0-444-64125-0.00018-9

Nakano, K., Kayahara, T., Tsutsumi, T., & Ushiro, H. (2000). Neural circuits and functional organization of the striatum. *Journal of Neurology*, *247*(5), V1–V15. https://doi.org/10.1007/PL00007778

Navailles, S., & De Deurwaerdère, P. (2011). Presynaptic control of serotonin on striatal dopamine function. *Psychopharmacology*, *213*(2), 213–242. https://doi.org/10.1007/s00213-010-2029-y

Navailles, S., Moison, D., Ryczko, D., & Spampinato, U. (2006). Region-dependent regulation of mesoaccumbens dopamine neurons in vivo by the constitutive activity of central

serotonin2C receptors. *Journal of Neurochemistry*, *99*(4), 1311–1319. https://doi.org/10.1111/j.1471-4159.2006.04188.x

Nayyar, T., Bubser, M., Ferguson, M. C., Neely, M. D., Goodwin, J. S., Montine, T. J., Deutch, A. Y., & Ansah, T. A. (2009). Cortical serotonin and norepinephrine denervation in parkinsonism: Preferential loss of the beaded serotonin innervation. *The European Journal of Neuroscience*, *30*(2), 207–216. https://doi.org/10.1111/j.1460-9568.2009.06806.x

Nelson, A. B., Hammack, N., Yang, C. F., Shah, N. M., Seal, R. P., & Kreitzer, A. C. (2014). Striatal Cholinergic Interneurons Drive GABA Release from Dopamine Terminals. *Neuron*, *82*(1), 63–70. https://doi.org/10.1016/j.neuron.2014.01.023

Nemani, V. M., Lu, W., Berge, V., Nakamura, K., Onoa, B., Lee, M. K., Chaudhry, F. A., Nicoll, R. A., & Edwards, R. H. (2010). Increased expression of alpha-synuclein reduces neurotransmitter release by inhibiting synaptic vesicle reclustering after endocytosis. *Neuron*, *65*(1), 66–79. https://doi.org/10.1016/j.neuron.2009.12.023

Ng, N.-K., Lee, H.-S., & Wong, P. T.-H. (1999). Regulation of striatal dopamine release through 5-HT1 and 5-HT2 receptors. *Journal of Neuroscience Research*, *55*(5), 600–607. https://doi.org/10.1002/(SICI)1097-4547(19990301)55:5<600::AID-JNR7>3.0.CO;2-#

Nichols, D. E., & Nichols, C. D. (2008). Serotonin Receptors. *Chemical Reviews*, *108*(5), 1614–1641. https://doi.org/10.1021/cr078224o

Nirenberg, M. J., Chan, J., Liu, Y., Edwards, R. H., & Pickel, V. M. (1997). Vesicular monoamine transporter-2: Immunogold localization in striatal axons and terminals. *Synapse*, *26*(2), 194–198. https://doi.org/10.1002/(SICI)1098-2396(199706)26:2<194::AID-SYN10>3.0.CO;2-Y

Nishijo, T., Suzuki, E., & Momiyama, T. (2022). Serotonin 5-HT1A and 5-HT1B receptor-mediated inhibition of glutamatergic transmission onto rat basal forebrain cholinergic neurones. *The Journal of Physiology*, *600*(13), 3149–3167. https://doi.org/10.1113/JP282509

Nuytemans, K., Theuns, J., Cruts, M., & Van Broeckhoven, C. (2010). Genetic etiology of Parkinson disease associated with mutations in the SNCA, PARK2, PINK1, PARK7, and LRRK2 genes: A mutation update. *Human Mutation*, *31*(7), 763–780. https://doi.org/10.1002/humu.21277

Obeso, J. A., Rodriguez-Oroz, M. C., Stamelou, M., Bhatia, K. P., & Burn, D. J. (2014). The expanding universe of disorders of the basal ganglia. *Lancet (London, England)*, *384*(9942), 523–531. https://doi.org/10.1016/S0140-6736(13)62418-6

Obeso, J. A., Stamelou, M., Goetz, C. G., Poewe, W., Lang, A. E., Weintraub, D., Burn, D., Halliday, G. M., Bezard, E., Przedborski, S., Lehericy, S., Brooks, D. J., Rothwell, J. C., Hallett, M., DeLong, M. R., Marras, C., Tanner, C. M., Ross, G. W., Langston, J. W., … Stoessl, A. J. (2017). Past, present, and future of Parkinson's disease: A special essay on the 200th Anniversary of the Shaking Palsy. *Movement Disorders: Official Journal of the Movement Disorder Society*, *32*(9), 1264–1310. https://doi.org/10.1002/mds.27115

Ochoa, E. L. M., Chattopadhyay, A., & McNamee, M. G. (1989). Desensitization of the nicotinic acetylcholine receptor: Molecular mechanisms and effect of modulators. *Cellular and Molecular Neurobiology*, *9*(2), 141–178. https://doi.org/10.1007/BF00713026

Ogelman, R., Gomez Wulschner, L. E., Hoelscher, V. M., Hwang, I.-W., Chang, V. N., & Oh, W. C. (2024). Serotonin modulates excitatory synapse maturation in the developing prefrontal cortex. *Nature Communications*, *15*(1), 1368. https://doi.org/10.1038/s41467-024-45734-w

Ohno, Y., Shimizu, S., Tokudome, K., Kunisawa, N., & Sasa, M. (2015). New insight into the therapeutic role of the serotonergic system in Parkinson's disease. *Progress in Neurobiology*, *134*, 104–121. https://doi.org/10.1016/j.pneurobio.2015.09.005

Okaty, B. W., Freret, M. E., Rood, B. D., Brust, R. D., Hennessy, M. L., deBairos, D., Kim, J. C., Cook, M. N., & Dymecki, S. M. (2015). Multi-Scale Molecular Deconstruction of the Serotonin Neuron System. *Neuron*, *88*(4), 774–791. https://doi.org/10.1016/j.neuron.2015.10.007

Orsetti, M., Dellarole, A., Ferri, S., & Ghi, P. (2003). Acquisition, Retention, and Recall of Memory After Injection of RS67333, a 5-HT4 Receptor Agonist, Into the Nucleus Basalis Magnocellularis of the Rat. *Learning & Memory*, *10*(5), 420–426. https://doi.org/10.1101/lm.67303

Ota, Y., Zanetti, A. T., & Hallock, R. M. (2013). The Role of Astrocytes in the Regulation of Synaptic Plasticity and Memory Formation. *Neural Plasticity*, *2013*, 185463. https://doi.org/10.1155/2013/185463

Paixão, S., & Klein, R. (2010). Neuron–astrocyte communication and synaptic plasticity. *Current Opinion in Neurobiology*, *20*(4), 466–473. https://doi.org/10.1016/j.conb.2010.04.008

Parent, M., Wallman, M.-J., Gagnon, D., & Parent, A. (2011). Serotonin innervation of basal ganglia in monkeys and humans. *Journal of Chemical Neuroanatomy*, *41*(4), 256–265. https://doi.org/10.1016/j.jchemneu.2011.04.005

Patel, S., Roberts, J., Moorman, J., & Reavill, C. (1995). Localization of serotonin-4 receptors in the striatonigral pathway in rat brain. *Neuroscience*, *69*(4), 1159–1167. https://doi.org/10.1016/0306-4522(95)00314-9

Paz, R. M., Tubert, C., Stahl, A. M., Amarillo, Y., Rela, L., & Murer, M. G. (2021). Levodopa Causes Striatal Cholinergic Interneuron Burst-Pause Activity in Parkinsonian Mice. *Movement Disorders: Official Journal of the Movement Disorder Society*, *36*(7), 1578–1591. https://doi.org/10.1002/mds.28516

Pellissier, L. P., Sallander, J., Campillo, M., Gaven, F., Queffeulou, E., Pillot, M., Dumuis, A., Claeysen, S., Bockaert, J., & Pardo, L. (2009). Conformational toggle switches implicated in basal constitutive and agonist-induced activated states of 5-hydroxytryptamine-4 receptors. *Molecular Pharmacology*, *75*(4), 982–990. https://doi.org/10.1124/mol.108.053686

Peng, S., Liu, P., Wang, X., & Li, K. (2025). Global, regional and national burden of Parkinson's disease in people over 55 years of age: A systematic analysis of the global burden of

disease study, 1991–2021. *BMC Neurology*, *25*(1), 178. https://doi.org/10.1186/s12883-025-04191-8

Perese, D. A., Ulman, J., Viola, J., Ewing, S. E., & Bankiewicz, K. S. (1989). A 6-hydroxydopamine-induced selective parkinsonian rat model. *Brain Research*, *494*(2), 285–293. https://doi.org/10.1016/0006-8993(89)90597-0

Peroutka, S. J., & Howell, T. A. (1994). The molecular evolution of G protein-coupled receptors: Focus on 5-hydroxytryptamine receptors. *Neuropharmacology*, *33*(3–4), 319–324. https://doi.org/10.1016/0028-3908(94)90060-4

Perreault, M. L., Hasbi, A., O'Dowd, B. F., & George, S. R. (2014). Heteromeric Dopamine Receptor Signaling Complexes: Emerging Neurobiology and Disease Relevance. *Neuropsychopharmacology*, *39*(1), 156–168. https://doi.org/10.1038/npp.2013.148

Pert, C. B., Kuhar, M. J., & Snyder, S. H. (1976). Opiate receptor: Autoradiographic localization in rat brain. *Proceedings of the National Academy of Sciences*, *73*(10), 3729–3733. https://doi.org/10.1073/pnas.73.10.3729

Phelps, P. E., Houser, C. R., & Vaughn, J. E. (1985). *Immunocytochemical localization of choline acetyltransferase within the rat neostriatum: A correlated light and electron microscopic study of cholinergic neurons and synapses*. https://doi.org/10.1002/cne.902380305

Pierret, P., Vallée, A., Bosler, O., Dorais, M., Moukhles, H., Abbaszadeh, R., Lepage, Y., & Doucet, G. (1998). Serotonin Axons of the Neostriatum Show a Higher Affinity for Striatal Than for Ventral Mesencephalic Transplants: A Quantitative Study in Adult and Immature Recipient Rats. *Experimental Neurology*, *152*(1), 101–115. https://doi.org/10.1006/exnr.1998.6823

Pissadaki, E. K., & Bolam, J. P. (2013). The energy cost of action potential propagation in dopamine neurons: Clues to susceptibility in Parkinson's disease. *Frontiers in Computational Neuroscience*, *7*. https://doi.org/10.3389/fncom.2013.00013

Pithadia, A. B., & Jain, S. M. (2009). 5-Hydroxytryptamine Receptor Subtypes and their Modulators with Therapeutic Potentials. *Journal of Clinical Medicine Research*, *1*(2), 72–80. https://doi.org/10.4021/jocmr2009.05.1237

Pitman, K. A., Puil, E., & Borgland, S. L. (2014). GABA(B) modulation of dopamine release in the nucleus accumbens core. *The European Journal of Neuroscience*, *40*(10), 3472–3480. https://doi.org/10.1111/ejn.12733

Planert, H., Szydlowski, S. N., Hjorth, J. J. J., Grillner, S., & Silberberg, G. (2010). Dynamics of Synaptic Transmission between Fast-Spiking Interneurons and Striatal Projection Neurons of the Direct and Indirect Pathways. *Journal of Neuroscience*, *30*(9), 3499–3507. https://doi.org/10.1523/JNEUROSCI.5139-09.2010

Poewe, W., Seppi, K., Tanner, C. M., Halliday, G. M., Brundin, P., Volkmann, J., Schrag, A.-E., & Lang, A. E. (2017). Parkinson disease. *Nature Reviews. Disease Primers*, *3*, 17013. https://doi.org/10.1038/nrdp.2017.13

Poisson, C. L., Engel, L., & Saunders, B. T. (2021). Dopamine Circuit Mechanisms of Addiction-Like Behaviors. *Frontiers in Neural Circuits*, *15*. https://doi.org/10.3389/fncir.2021.752420

Politis, M., & Loane, C. (2011a). Serotonergic dysfunction in Parkinson's disease and its relevance to disability. *The Scientific World Journal*, *11*, 1726–1734. https://doi.org/10.1100/2011/172893

Politis, M., & Loane, C. (2011b). Serotonergic Dysfunction in Parkinson's Disease and Its Relevance to Disability. *The Scientific World Journal*, *11*, 1726–1734. https://doi.org/10.1100/2011/172893

Politis, M., & Niccolini, F. (2015). Serotonin in Parkinson's disease. *Behavioural Brain Research*, *277*, 136–145. https://doi.org/10.1016/j.bbr.2014.07.037

Politis, M., Wu, K., Loane, C., Brooks, D. J., Kiferle, L., Turkheimer, F. E., Bain, P., Molloy, S., & Piccini, P. (2014). Serotonergic mechanisms responsible for levodopa-induced dyskinesias in Parkinson's disease patients. *The Journal of Clinical Investigation*, *124*(3), 1340–1349. https://doi.org/10.1172/JCI71640

Pommer, S., Akamine, Y., Schiffmann, S. N., d'Exaerde, A. de K., & Wickens, J. R. (2021). The Effect of Serotonin Receptor 5-HT1B on Lateral Inhibition between Spiny Projection Neurons in the Mouse Striatum. *Journal of Neuroscience*, *41*(37), 7831–7847. https://doi.org/10.1523/JNEUROSCI.1037-20.2021

Porras, G., Di Matteo, V., Fracasso, C., Lucas, G., De Deurwaerdère, P., Caccia, S., Esposito, E., & Spampinato, U. (2002). 5-HT2A and 5-HT2C/2B Receptor Subtypes Modulate Dopamine Release Induced in Vivo by Amphetamine and Morphine in Both the Rat Nucleus Accumbens and Striatum. *Neuropsychopharmacology*, *26*(3), Article 3. https://doi.org/10.1016/S0893-133X(01)00333-5

Qamhawi, Z., Towey, D., Shah, B., Pagano, G., Seibyl, J., Marek, K., Borghammer, P., Brooks, D. J., & Pavese, N. (2015). Clinical correlates of raphe serotonergic dysfunction in early Parkinson's disease. *Brain*, *138*(10), 2964–2973. https://doi.org/10.1093/brain/awv215

Quinn, J. J., Pittenger, C., Lee, A. S., Pierson, J. L., & Taylor, J. R. (2013). Striatum-dependent habits are insensitive to both increases and decreases in reinforcer value in mice. *The European Journal of Neuroscience*, *37*(6), 1012–1021. https://doi.org/10.1111/ejn.12106

Rada, P. V., Mark, G. P., & Hoebel, B. G. (1993). In vivo modulation of acetylcholine in the nucleus accumbens of freely moving rats: I. Inhibition by serotonin. *Brain Research*, *619*(1), 98–104. https://doi.org/10.1016/0006-8993(93)91600-W

Ratna, D. D., & Francis, T. C. (2025). Extrinsic and intrinsic control of striatal cholinergic interneuron activity. *Frontiers in Molecular Neuroscience*, *18*, 1528419. https://doi.org/10.3389/fnmol.2025.1528419

Rice, M. E. (2000). Distinct regional differences in dopamine-mediated volume transmission. *Progress in Brain Research*, *125*, 277–290. https://doi.org/10.1016/S0079-6123(00)25017-6

Rice, M. E., & Cragg, S. J. (2004). Nicotine amplifies reward-related dopamine signals in striatum. *Nature Neuroscience*, *7*(6), 583–584. https://doi.org/10.1038/nn1244

Rice, M. E., & Cragg, S. J. (2008). Dopamine spillover after quantal release: Rethinking dopamine transmission in the nigrostriatal pathway. *Brain Research Reviews*, *58*(2), 303–313. https://doi.org/10.1016/j.brainresrev.2008.02.004

Rice, M. E., Patel, J. C., & Cragg, S. J. (2011). Dopamine release in the basal ganglia. *Neuroscience*, *198*, 112–137. https://doi.org/10.1016/j.neuroscience.2011.08.066

Riederer, P., & Müller, T. (2018). Monoamine oxidase-B inhibitors in the treatment of Parkinson's disease: Clinical–pharmacological aspects. *Journal of Neural Transmission*, *125*(11), 1751–1757. https://doi.org/10.1007/s00702-018-1876-2

Ring, H. A., & Serra-Mestres, J. (2002). Neuropsychiatry of the basal ganglia. *Journal of Neurology, Neurosurgery, and Psychiatry*, *72*(1), 12–21. https://doi.org/10.1136/jnnp.72.1.12

Roberts, B. M., Doig, N. M., Brimblecombe, K. R., Lopes, E. F., Siddorn, R. E., Threlfell, S., Connor-Robson, N., Bengoa-Vergniory, N., Pasternack, N., Wade-Martins, R., Magill, P. J., & Cragg, S. J. (2020). GABA uptake transporters support dopamine release in dorsal striatum with maladaptive downregulation in a parkinsonism model. *Nature Communications*, *11*(1), 4958–4975. https://doi.org/10.1038/s41467-020-18247-5

Roberts, B. M., Lambert, E., Livesey, J. A., Wu, Z., Li, Y., & Cragg, S. J. (2022). Dopamine Release in Nucleus Accumbens Is under Tonic Inhibition by Adenosine A1 Receptors Regulated by Astrocytic ENT1 and Dysregulated by Ethanol. *Journal of Neuroscience*, *42*(9), 1738–1751. https://doi.org/10.1523/JNEUROSCI.1548-21.2021

Roberts, B. M., Lopes, E. F., & Cragg, S. J. (2021). Axonal Modulation of Striatal Dopamine Release by Local γ-Aminobutyric Acid (GABA) Signalling. *Cells*, *10*(3). https://doi.org/10.3390/cells10030709

Roberts, J. C., Reavill, C., East, S. Z., Harrison, P. J., Patel, S., Routledge, C., & Leslie, R. A. (2002). The distribution of 5-HT6 receptors in rat brain: An autoradiographic binding study using the radiolabelled 5-HT6 receptor antagonist [125I]SB-258585. *Brain Research*, *934*(1), 49–57. https://doi.org/10.1016/S0006-8993(02)02360-0

Robinson, T. E., & Berridge, K. C. (1993). The neural basis of drug craving: An incentive-sensitization theory of addiction. *Brain Research. Brain Research Reviews*, *18*(3), 247–291. https://doi.org/10.1016/0165-0173(93)90013-p

Rocha, G. S., Freire, M. A. M., Britto, A. M., Paiva, K. M., Oliveira, R. F., Fonseca, I. A. T., Araújo, D. P., Oliveira, L. C., Guzen, F. P., Morais, P. L. A. G., & Cavalcanti, J. R. L. P. (2023). Basal ganglia for beginners: The basic concepts you need to know and their role in movement control. *Frontiers in Systems Neuroscience*, *17*, 1242929. https://doi.org/10.3389/fnsys.2023.1242929

Rossi, D., & Volterra, A. (2009). Astrocytic dysfunction: Insights on the role in neurodegeneration. *Brain Research Bulletin*, *80*(4), 224–232. https://doi.org/10.1016/j.brainresbull.2009.07.012

Rozas, G., Liste, I., Guerra, M. J., & Labandeira-Garcia, J. L. (1998). Sprouting of the serotonergic afferents into striatum after selective lesion of the dopaminergic system by MPTP in adult mice. *Neuroscience Letters*, *245*(3), 151–154. https://doi.org/10.1016/s0304-3940(98)00198-0

Ruat, M., Traiffort, E., Arrang, J. M., Tardivellacombe, J., Diaz, J., Leurs, R., & Schwartz, J. C. (1993). A Novel Rat Serotonin (5-HT6) Receptor: Molecular Cloning, Localization and Stimulation of cAMP Accumulation. *Biochemical and Biophysical Research Communications*, *193*(1), 268–276. https://doi.org/10.1006/bbrc.1993.1619

Ruat, M., Traiffort, E., Leurs, R., Tardivel-Lacombe, J., Diaz, J., Arrang, J. M., & Schwartz, J. C. (1993). Molecular cloning, characterization, and localization of a high-affinity serotonin receptor (5-HT7) activating cAMP formation. *Proceedings of the National Academy of Sciences of the United States of America*, *90*(18), 8547–8551. https://doi.org/10.1073/pnas.90.18.8547

Rylander, D., Parent, M., O'Sullivan, S. S., Dovero, S., Lees, A. J., Bezard, E., Descarries, L., & Cenci, M. A. (2010). Maladaptive plasticity of serotonin axon terminals in levodopa-induced dyskinesia. *Annals of Neurology*, *68*(5), 619–628. https://doi.org/10.1002/ana.22097

Salinas, A. G., Lee, J. O., Augustin, S. M., Zhang, S., Patriarchi, T., Tian, L., Morales, M., Mateo, Y., & Lovinger, D. M. (2023). Distinct sub-second dopamine signaling in dorsolateral striatum measured by a genetically-encoded fluorescent sensor. *Nature Communications*, *14*(1), 5915. https://doi.org/10.1038/s41467-023-41581-3

Salvan, P., Fonseca, M., Winkler, A. M., Beauchamp, A., Lerch, J. P., & Johansen-Berg, H. (2023). Serotonin regulation of behavior via large-scale neuromodulation of serotonin receptor networks. *Nature Neuroscience*, *26*(1), 53–63. https://doi.org/10.1038/s41593-022-01213-3

Santiago, J. A., & Potashkin, J. A. (2014). System-based approaches to decode the molecular links in Parkinson's disease and diabetes. *Neurobiology of Disease*, *72*, 84–91. https://doi.org/10.1016/j.nbd.2014.03.019

Santiago, M., Machado, A., & Cano, J. (1995). 5-HT3 receptor agonist induced carrier-mediated release of dopamine in rat striatum in vivo. *British Journal of Pharmacology*, *116*(1), 1545–1550. https://doi.org/10.1111/j.1476-5381.1995.tb16371.x

Sarkisyan, G., Roberts, A. J., & Hedlund, P. B. (2010). The 5-HT7 receptor as a mediator and modulator of antidepressant-like behavior. *Behavioural Brain Research*, *209*(1), 99–108. https://doi.org/10.1016/j.bbr.2010.01.022

Sauer, H., & Oertel, W. H. (1994). Progressive degeneration of nigrostriatal dopamine neurons following intrastriatal terminal lesions with 6-hydroxydopamine: A combined retrograde tracing and immunocytochemical study in the rat. *Neuroscience*, *59*(2), 401–415. https://doi.org/10.1016/0306-4522(94)90605-x

Saunders, A., Granger, A. J., & Sabatini, B. L. (2015). Corelease of acetylcholine and GABA from cholinergic forebrain neurons. *eLife*, *4*, e06412. https://doi.org/10.7554/eLife.06412

Schaeffer, E., & Berg, D. (2017). Dopaminergic Therapies for Non-motor Symptoms in Parkinson's Disease. *CNS Drugs*, *31*(7), 551–570. https://doi.org/10.1007/s40263-017-0450-z

Schapira, A. H. V. (2015). Glucocerebrosidase and Parkinson disease: Recent advances. *Molecular and Cellular Neurosciences*, *66*(Pt A), 37–42. https://doi.org/10.1016/j.mcn.2015.03.013

Schaus, J. M., Thompson, D. C., Bloomquist, W. E., Susemichel, A. D., Calligaro, D. O., & Cohen, M. L. (1998). Synthesis and structure-activity relationships of potent and orally active 5-HT4 receptor antagonists: Indazole and benzimidazolone derivatives. *Journal of Medicinal Chemistry*, *41*(11), 1943–1955. https://doi.org/10.1021/jm970857f

Schlicker, E., Classen, K., & Göthert, M. (1984). GABAB receptor-mediated inhibition of serotonin release in the rat brain. *Naunyn-Schmiedeberg's Archives of Pharmacology*, *326*(2), 99–105. https://doi.org/10.1007/BF00517304

Schrag, A., & Politis, M. (2016). Serotonergic loss underlying apathy in Parkinson's disease. *Brain*, *139*(9), 2338–2339. https://doi.org/10.1093/brain/aww190

Schultz, W. (1997). Dopamine neurons and their role in reward mechanisms. *Current Opinion in Neurobiology*, *7*(2), 191–197. https://doi.org/10.1016/S0959-4388(97)80007-4

Schultz, W. (2007). Multiple dopamine functions at different time courses. *Annual Review of Neuroscience*, *30*, 259–288. https://doi.org/10.1146/annurev.neuro.28.061604.135722

Schultz, W. (2013). Updating dopamine reward signals. *Current Opinion in Neurobiology*, *23*(2), 229–238. https://doi.org/10.1016/j.conb.2012.11.012

Schultz, W., Ruffieux, A., & Aebischer, P. (1983). The activity of pars compacta neurons of the monkey substantia nigra in relation to motor activation. *Experimental Brain Research*, *51*(3), 377–387. https://doi.org/10.1007/BF00237874

Schwarting, R. K. W., Thiel, C. M., Müller, C. P., & Huston, J. P. (1998). Relationship between anxiety and serotonin in the ventral striatum. *NeuroReport*, *9*(6), 1025.

Sershen, H., Hashim, A., & Lajtha, A. (2000). Serotonin-mediated striatal dopamine release involves the dopamine uptake site and the serotonin receptor. *Brain Research Bulletin*, *53*(3), 353–357. https://doi.org/10.1016/S0361-9230(00)00358-0

Sesack, S. R., Hawrylak, V. A., Guido, M. A., & Levey, A. I. (1997). Cellular and Subcellular Localization of the Dopamine Transporter in Rat Cortex. In D. S. Goldstein, G. Eisenhofer, & R. McCarty (Eds.), *Advances in Pharmacology* (Vol. 42, pp. 171–174). Academic Press. https://doi.org/10.1016/S1054-3589(08)60720-6

Sharp, T., & Foster, G. A. (1989). In vivo measurement using microdialysis of the release and metabolism of 5-hydroxytryptamine in raphe neurones grafted to the rat hippocampus. *Journal of Neurochemistry*, *53*(1), 303–306. https://doi.org/10.1111/j.1471-4159.1989.tb07329.x

Sharp, T., & Hjorth, S. (1990). Application of brain microdialysis to study the pharmacology of the 5-HT1A autoreceptor. *Journal of Neuroscience Methods*, *34*(1–3), 83–90. https://doi.org/10.1016/0165-0270(90)90045-h

Shen, F., Smith, J. A. M., Chang, R., Bourdet, D. L., Tsuruda, P. R., Obedencio, G. P., & Beattie, D. T. (2011). 5-HT4 receptor agonist mediated enhancement of cognitive function *in vivo* and amyloid precursor protein processing *in vitro*: A pharmacodynamic and pharmacokinetic assessment. *Neuropharmacology*, *61*(1), 69–79. https://doi.org/10.1016/j.neuropharm.2011.02.026

Shin, J. H., Adrover, M. F., & Alvarez, V. A. (2017). Distinctive Modulation of Dopamine Release in the Nucleus Accumbens Shell Mediated by Dopamine and Acetylcholine Receptors. *The Journal of Neuroscience*, *37*(46), 11166–11180. https://doi.org/10.1523/JNEUROSCI.0596-17.2017

Shin, J. H., Adrover, M. F., Wess, J., & Alvarez, V. A. (2015). Muscarinic regulation of dopamine and glutamate transmission in the nucleus accumbens. *Proceedings of the National Academy of Sciences*, *112*(26), 8124–8129. https://doi.org/10.1073/pnas.1508846112

Shukla, R., Watakabe, A., & Yamamori, T. (2014). mRNA expression profile of serotonin receptor subtypes and distribution of serotonergic terminations in marmoset brain. *Frontiers in Neural Circuits*, *8*, 52. https://doi.org/10.3389/fncir.2014.00052

Singleton, A. B., Farrer, M., Johnson, J., Singleton, A., Hague, S., Kachergus, J., Hulihan, M., Peuralinna, T., Dutra, A., Nussbaum, R., Lincoln, S., Crawley, A., Hanson, M., Maraganore, D., Adler, C., Cookson, M. R., Muenter, M., Baptista, M., Miller, D., … Gwinn-Hardy, K. (2003). Alpha-Synuclein locus triplication causes Parkinson's disease. *Science (New York, N.Y.)*, *302*(5646), 841. https://doi.org/10.1126/science.1090278

Ślifirski, G., Król, M., & Turło, J. (2021). 5-HT Receptors and the Development of New Antidepressants. *International Journal of Molecular Sciences*, *22*(16), 9015. https://doi.org/10.3390/ijms22169015

Smith, G. S., Dewey, S. L., Brodie, J. D., Logan, J., Vitkun, S. A., Simkowitz, P., Schloesser, R., Alexoff, D. A., Hurley, A., Cooper, T., & Volkow, N. D. (1997). Serotonergic modulation of dopamine measured with [11C]raclopride and PET in normal human subjects. *The American Journal of Psychiatry*, *154*(4), 490–496. https://doi.org/10.1176/ajp.154.4.490

Smith, Y., Bevan, M. D., Shink, E., & Bolam, J. P. (1998). Microcircuitry of the direct and indirect pathways of the basal ganglia. *Neuroscience*, *86*(2), 353–387. https://doi.org/10.1016/s0306-4522(98)00004-9

Soghomonian, J.-J., Descarries, L., & Watkins, K. C. (1989). Serotonin innervation in adult rat neostriatum. II. Ultrastructural features: A radioautographic and immunocytochemical study. *Brain Research*, *481*(1), 67–86. https://doi.org/10.1016/0006-8993(89)90486-1

Soghomonian, J.-J., Doucet, G., & Descarries, L. (1987). Serotonin innervation in adult rat neostriatum. I. Quantified regional distribution. *Brain Research*, *425*(1), 85–100. https://doi.org/10.1016/0006-8993(87)90486-0

Spillantini, M. G., Crowther, R. A., Jakes, R., Hasegawa, M., & Goedert, M. (1998). Alpha-Synuclein in filamentous inclusions of Lewy bodies from Parkinson's disease and dementia with lewy bodies. *Proceedings of the National Academy of Sciences of the United States of America*, *95*(11), 6469–6473. https://doi.org/10.1073/pnas.95.11.6469

Spring, M. G., & Nautiyal, K. M. (2024). Striatal Serotonin Release Signals Reward Value. *Journal of Neuroscience*, *44*(41). https://doi.org/10.1523/JNEUROSCI.0602-24.2024

SŚmiałowski, A., & Bijak, M. (1987). Excitatory and inhibitory action of dopamine on hippocampal neurons *in vitro*. Involvement of D2 and D1 receptors. *Neuroscience*, *23*(1), 95–101. https://doi.org/10.1016/0306-4522(87)90274-0

Stamford, J. A., Kruk, Z., & Millar, J. (1986). An in vivo voltammetric comparison of the effects of three psychomotor stimulants on electrically evoked neostriatal dopamine release. *Brain Research*, *366*(1–2), 350–353. https://doi.org/10.1016/0006-8993(86)91317-x

Stedehouder, J., Roberts, B. M., Raina, S., Bossi, S., Liu, A. K. L., Doig, N. M., McGerty, K., Magill, P. J., Parkkinen, L., & Cragg, S. J. (2024). Rapid modulation of striatal cholinergic interneurons and dopamine release by satellite astrocytes. *Nature Communications*, *15*(1), 10017. https://doi.org/10.1038/s41467-024-54253-7

Steinbusch, H. W. M. (1981). Distribution of serotonin-immunoreactivity in the central nervous system of the rat—Cell bodies and terminals. *Neuroscience*, *6*(4), 557–618. https://doi.org/10.1016/0306-4522(81)90146-9

Steward, L. J., Ge, J., Stowe, R. L., Brown, D. C., Bruton, R. K., Stokes, P. R., & Barnes, N. M. (1996). Ability of 5-HT4 receptor ligands to modulate rat striatal dopamine release in vitro and in vivo. *British Journal of Pharmacology*, *117*(1), 55–62.

Stouffer, M. A., Woods, C. A., Patel, J. C., Lee, C. R., Witkovsky, P., Bao, L., Machold, R. P., Jones, K. T., de Vaca, S. C., Reith, M. E. A., Carr, K. D., & Rice, M. E. (2015). Insulin enhances striatal dopamine release by activating cholinergic interneurons and thereby signals reward. *Nature Communications*, *6*(1), 8543–8555. https://doi.org/10.1038/ncomms9543

Sulzer, D., Cragg, S. J., & Rice, M. E. (2016). Striatal dopamine neurotransmission: Regulation of release and uptake. *Basal Ganglia*, *6*(3), 123–148. https://doi.org/10.1016/j.baga.2016.02.001

Surmeier, D. J., Ding, J., Day, M., Wang, Z., & Shen, W. (2007). D1 and D2 dopamine-receptor modulation of striatal glutamatergic signaling in striatal medium spiny neurons. *Trends in Neurosciences*, *30*(5), 228–235. https://doi.org/10.1016/j.tins.2007.03.008

Surmeier, D. J., Graves, S. M., & Shen, W. (2014). Dopaminergic modulation of striatal networks in health and Parkinson's disease. *Current Opinion in Neurobiology*, *29*, 109–117. https://doi.org/10.1016/j.conb.2014.07.008

Surmeier, D. J., Obeso, J. A., & Halliday, G. M. (2017). Selective neuronal vulnerability in Parkinson disease. *Nature Reviews. Neuroscience*, *18*(2), 101–113. https://doi.org/10.1038/nrn.2016.178

Suzuki, T., Miura, M., Nishimura, K., & Aosaki, T. (2001). Dopamine-Dependent Synaptic Plasticity in the Striatal Cholinergic Interneurons. *The Journal of Neuroscience*, *21*(17), 6492–6501. https://doi.org/10.1523/JNEUROSCI.21-17-06492.2001

Taschenberger, G., Garrido, M., Tereshchenko, Y., Bähr, M., Zweckstetter, M., & Kügler, S. (2012). Aggregation of αSynuclein promotes progressive in vivo neurotoxicity in adult rat dopaminergic neurons. *Acta Neuropathologica*, *123*(5), 671–683. https://doi.org/10.1007/s00401-011-0926-8

Tepper, J. M., Tecuapetla, F., Koós, T., & Ibáñez-Sandoval, O. (2010). Heterogeneity and Diversity of Striatal GABAergic Interneurons. *Frontiers in Neuroanatomy*, *4*, 150. https://doi.org/10.3389/fnana.2010.00150

Threlfell, S., Clements, M. A., Khodai, T., Pienaar, I. S., Exley, R., Wess, J., & Cragg, S. J. (2010). Striatal muscarinic receptors promote activity dependence of dopamine transmission via distinct receptor subtypes on cholinergic interneurons in ventral versus dorsal striatum. *The Journal of Neuroscience: The Official Journal of the Society for Neuroscience*, *30*(9), 3398–3408. https://doi.org/10.1523/JNEUROSCI.5620-09.2010

Threlfell, S., & Cragg, S. J. (2011). Dopamine signaling in dorsal versus ventral striatum: The dynamic role of cholinergic interneurons. *Frontiers in Systems Neuroscience*, *5*, 11–21. https://doi.org/10.3389/fnsys.2011.00011

Threlfell, S., Lalic, T., Platt, N. J., Jennings, K. A., Deisseroth, K., & Cragg, S. J. (2012). Striatal Dopamine Release Is Triggered by Synchronized Activity in Cholinergic Interneurons. *Neuron*, *75*(1), 58–64. https://doi.org/10.1016/j.neuron.2012.04.038

Threlfell, S., Mohammadi, A. S., Ryan, B. J., Connor-Robson, N., Platt, N. J., Anand, R., Serres, F., Sharp, T., Bengoa-Vergniory, N., Wade-Martins, R., Ewing, A., Cragg, S. J., & Brimblecombe, K. R. (2021). Striatal Dopamine Transporter Function Is Facilitated by Converging Biology of α-Synuclein and Cholesterol. *Frontiers in Cellular Neuroscience*, *15*. https://doi.org/10.3389/fncel.2021.658244

Tobón-Velasco, J. C., Silva-Adaya, D., Carmona-Aparicio, L., García, E., Galván-Arzate, S., & Santamaría, A. (2010). Early toxic effect of 6-hydroxydopamine on extracellular concentrations of neurotransmitters in the rat striatum: An *in vivo* microdialysis study. *NeuroToxicology*, *31*(6), 715–723. https://doi.org/10.1016/j.neuro.2010.07.003

Tol, H. H. M. V., Wu, C. M., Guan, H.-C., Ohara, K., Bunzow, J. R., Civelli, O., Kennedy, J., Seeman, P., Niznik, H. B., & Jovanovic, V. (1992). Multiple dopamine D4 receptor variants in the human population. *Nature*, *358*(6382), 149–152. https://doi.org/10.1038/358149a0

Törk, I. (1990). Anatomy of the serotonergic system. *Annals of the New York Academy of Sciences*, *600*, 9–34; discussion 34-35. https://doi.org/10.1111/j.1749-6632.1990.tb16870.x

Tran, J., Anastacio, H., & Bardy, C. (2020). Genetic predispositions of Parkinson's disease revealed in patient-derived brain cells. *Npj Parkinson's Disease*, *6*(1), 8. https://doi.org/10.1038/s41531-020-0110-8

Tritsch, N., & Sabatini, B. (2012). Dopaminergic modulation of synaptic transmission in cortex and striatum. *Neuron*, *76*(1). https://doi.org/10.1016/j.neuron.2012.09.023

Tritsch, N. X., Granger, A. J., & Sabatini, B. L. (2016). Mechanisms and functions of GABA co-release. *Nature Reviews Neuroscience*, *17*(3), 139–145. https://doi.org/10.1038/nrn.2015.21

Tuomisto, J. (1977). Nomifensine and its derivatives as possible tools for studying amine uptake. *European Journal of Pharmacology*, *42*(2), 101–106. https://doi.org/10.1016/0014-2999(77)90348-x

Twarkowski, H., Hagena, H., & Manahan-Vaughan, D. (2016). The 5-hydroxytryptamine4 receptor enables differentiation of informational content and encoding in the hippocampus. *Hippocampus*, *26*(7), 875–891. https://doi.org/10.1002/hipo.22569

Uchiyama-Tsuyuki, Y., Saitoh, M., & Muramatsu, M. (1996). Identification and characterization of the 5-HT4 receptor in the intestinal tract and striatum of the guinea pig. *Life Sciences*, *59*(25), 2129–2137. https://doi.org/10.1016/S0024-3205(96)00569-3

Vallone, D., Picetti, R., & Borrelli, E. (2000). Structure and function of dopamine receptors. *Neuroscience and Biobehavioral Reviews*, *24*(1), 125–132. https://doi.org/10.1016/s0149-7634(99)00063-9

Van Bockstaele, E. J., & Pickel, V. M. (1993). Ultrastructure of serotonin-immunoreactive terminals in the core and shell of the rat nucleus accumbens: Cellular substrates for interactions with catecholamine afferents. *Journal of Comparative Neurology*, *334*(4), 603–617. https://doi.org/10.1002/cne.903340408

Van Der Kooy, D., & Hattori, T. (1980). Single subthalamic nucleus neurons project to both the globus pallidus and substantia nigra in rat. *The Journal of Comparative Neurology*, *192*(4), 751–768. https://doi.org/10.1002/cne.901920409

Venda, L. L., Cragg, S. J., Buchman, V. L., & Wade-Martins, R. (2010). α-Synuclein and dopamine at the crossroads of Parkinson's disease. *Trends in Neurosciences*, *33*(12), 559–568. https://doi.org/10.1016/j.tins.2010.09.004

Venton, B. J., Michael, D. J., & Wightman, R. M. (2003). Correlation of local changes in extracellular oxygen and pH that accompany dopaminergic terminal activity in the rat caudate–putamen. *Journal of Neurochemistry*, *84*(2), 373–381. https://doi.org/10.1046/j.1471-4159.2003.01527.x

Venton, B. J., Seipel, A. T., Phillips, P. E. M., Wetsel, W. C., Gitler, D., Greengard, P., Augustine, G. J., & Wightman, R. M. (2006). Cocaine Increases Dopamine Release by Mobilization of a Synapsin-Dependent Reserve Pool. *Journal of Neuroscience*, *26*(12), 3206–3209. https://doi.org/10.1523/JNEUROSCI.4901-04.2006

Vertes, R. P., & Crane, A. M. (1997). Distribution, quantification, and morphological characteristics of serotonin-immunoreactive cells of the supralemniscal nucleus (B9) and pontomesencephalic reticular formation in the rat. *The Journal of Comparative Neurology*, *378*(3), 411–424.

Vilaró, M. T., Cortés, R., & Mengod, G. (2005). Serotonin 5-HT4 receptors and their mRNAs in rat and guinea pig brain: Distribution and effects of neurotoxic lesions. *The Journal of Comparative Neurology*, *484*(4), 418–439. https://doi.org/10.1002/cne.20447

Vilaró, M. T., Palacios, JoséM., & Mengod, G. (1990). Localization of m5 muscarinic receptor mRNA in rat brain examined by in situ hybridization histochemistry. *Neuroscience Letters*, *114*(2), 154–159. https://doi.org/10.1016/0304-3940(90)90064-G

Virk, M. S., Sagi, Y., Medrihan, L., Leung, J., Kaplitt, M. G., & Greengard, P. (2016). Opposing roles for serotonin in cholinergic neurons of the ventral and dorsal striatum. *Proceedings of the National Academy of Sciences of the United States of America*, *113*(3), 734–739. https://doi.org/10.1073/pnas.1524183113

Vollenweider, F. X., Vontobel, P., Hell, D., & Leenders, K. L. (1999). 5-HT Modulation of Dopamine Release in Basal Ganglia in Psilocybin-Induced Psychosis in Man—A PET Study with [11C]raclopride. *Neuropsychopharmacology*, *20*(5), 424–433. https://doi.org/10.1016/S0893-133X(98)00108-0

Volpicelli, F., Speranza, L., di Porzio, U., Crispino, M., & Perrone-Capano, C. (2014). The serotonin receptor 7 and the structural plasticity of brain circuits. *Frontiers in Behavioral Neuroscience*, *8*. https://doi.org/10.3389/fnbeh.2014.00318

Voorn, P., Vanderschuren, L. J. M. J., Groenewegen, H. J., Robbins, T. W., & Pennartz, C. M. A. (2004). Putting a spin on the dorsal–ventral divide of the striatum. *Trends in Neurosciences*, *27*(8), 468–474. https://doi.org/10.1016/j.tins.2004.06.006

Vuillet, J., Kerkerian, L., Kachidian, P., Bosler, O., & Nieoullon, A. (1989). Ultrastructural correlates of functional relationships between nigral dopaminergic or cortical afferent fibers and neuropeptide Y-containing neurons in the rat striatum. *Neuroscience Letters*, *100*(1–3), 99–104. https://doi.org/10.1016/0304-3940(89)90667-8

Wang, L., Shang, S., Kang, X., Teng, S., Zhu, F., Liu, B., Wu, Q., Li, M., Liu, W., Xu, H., Zhou, L., Jiao, R., Dou, H., Zuo, P., Zhang, X., Zheng, L., Wang, S., Wang, C., & Zhou, Z. (2014). Modulation of dopamine release in the striatum by physiologically relevant levels of nicotine. *Nature Communications*, *5*(1), 3925–3934. https://doi.org/10.1038/ncomms4925

Ward, R. P., & Dorsa, D. M. (1996). Colocalization of serotonin receptor subtypes 5-HT2A, 5-HT2C, and 5-HT6 with neuropeptides in rat striatum. *The Journal of Comparative Neurology*, *370*(3), 405–414.

Waselus, M., Galvez, J. P., Valentino, R. J., & Van Bockstaele, E. J. (2006). Differential projections of dorsal raphe nucleus neurons to the lateral septum and striatum. *Journal of Chemical Neuroanatomy*, *31*(4), 233–242. https://doi.org/10.1016/j.jchemneu.2006.01.007

Weiner, D. M., Levey, A. I., & Brann, M. R. (1990). Expression of muscarinic acetylcholine and dopamine receptor mRNAs in rat basal ganglia. *Proceedings of the National Academy of Sciences*, *87*(18), 7050–7054. https://doi.org/10.1073/pnas.87.18.7050

Wichmann, T., & Dostrovsky, J. O. (2011). Pathological basal ganglia activity in movement disorders. *Neuroscience*, *198*, 232–244. https://doi.org/10.1016/j.neuroscience.2011.06.048

Wightman, R. M., Amatore, C., Engstrom, R. C., Hale, P. D., Kristensen, E. W., Kuhr, W. G., & May, L. J. (1988). Real-time characterization of dopamine overflow and uptake in the rat striatum. *Neuroscience*, *25*(2), 513–523. https://doi.org/10.1016/0306-4522(88)90255-2

Wilson, C. J., Chang, H. T., & Kitai, S. T. (1990). Firing patterns and synaptic potentials of identified giant aspiny interneurons in the rat neostriatum. *The Journal of Neuroscience: The Official Journal of the Society for Neuroscience*, *10*(2), 508–519. https://doi.org/10.1523/JNEUROSCI.10-02-00508.1990

Winstanley, C. A., Dalley, J. W., Theobald, D. E. H., & Robbins, T. W. (2003). Global 5-HT depletion attenuates the ability of amphetamine to decrease impulsive choice on a delay-discounting task in rats. *Psychopharmacology*, *170*(3), 320–331. https://doi.org/10.1007/s00213-003-1546-3

Wirtshafter, D., & McWilliams, C. (1987). Suppression of locomotor activity produced by acute injections of kainic acid into the median raphe nucleus. *Brain Research*, *408*(1), 349–352. https://doi.org/10.1016/0006-8993(87)90403-3

Wise, R. A. (2004). Dopamine, learning and motivation. *Nature Reviews. Neuroscience*, *5*(6), 483–494. https://doi.org/10.1038/nrn1406

Xenias, H. S., Ibáñez-Sandoval, O., Koós, T., & Tepper, J. M. (2015). Are Striatal Tyrosine Hydroxylase Interneurons Dopaminergic? *The Journal of Neuroscience*, *35*(16), 6584–6599. https://doi.org/10.1523/JNEUROSCI.0195-15.2015

Yamamoto, K., Kohda, Y., Sawada, Y., & Iga, T. (1991). Pharmacokinetics of ambenonium, a reversible cholinesterase inhibitor, in rats. *Biopharmaceutics & Drug Disposition*, *12*(8), 613–625. https://doi.org/10.1002/bdd.2510120807

Yan, Z., & Surmeier, D. (1996). Muscarinic (m2/m4) receptors reduce N- and P-type Ca2+ currents in rat neostriatal cholinergic interneurons through a fast, membrane- delimited, G-protein pathway. *The Journal of Neuroscience*, *16*(8), 2592–2604. https://doi.org/10.1523/JNEUROSCI.16-08-02592.1996

Yang, H., Sampson, M. M., Senturk, D., & Andrews, A. M. (2015). Sex- and SERT-Mediated Differences in Stimulated Serotonin Revealed by Fast Microdialysis. *ACS Chemical Neuroscience*, *6*(8), 1487–1501. https://doi.org/10.1021/acschemneuro.5b00132

Yang, H., Thompson, A. B., McIntosh, B. J., Altieri, S. C., & Andrews, A. M. (2013). Physiologically Relevant Changes in Serotonin Resolved by Fast Microdialysis. *ACS Chemical Neuroscience*, *4*(5), 790–798. https://doi.org/10.1021/cn400072f

Yetnikoff, L., Lavezzi, H. N., Reichard, R. A., & Zahm, D. S. (2014). An update on the connections of the ventral mesencephalic dopaminergic complex. *Neuroscience*, *282*, 23–48. https://doi.org/10.1016/j.neuroscience.2014.04.010

Yin, H. H., Knowlton, B. J., & Balleine, B. W. (2004). Lesions of dorsolateral striatum preserve outcome expectancy but disrupt habit formation in instrumental learning. *The European Journal of Neuroscience*, *19*(1), 181–189. https://doi.org/10.1111/j.1460-9568.2004.03095.x

Yu, X., Zhang, Y., Zhang, M., Chen, Y., & Yang, W. (2022). Natural products as sources of acetylcholinesterase inhibitors: Synthesis, biological activities, and molecular docking studies of osthole-based ester derivatives. *Frontiers in Plant Science*, *13*. https://doi.org/10.3389/fpls.2022.1054650

Zahm, D. S. (1999). Functional-anatomical implications of the nucleus accumbens core and shell subterritories. *Annals of the New York Academy of Sciences*, *877*, 113–128. https://doi.org/10.1111/j.1749-6632.1999.tb09264.x

Zhang, H., & Sulzer, D. (2004). Frequency-dependent modulation of dopamine release by nicotine. *Nature Neuroscience*, *7*(6), 581–582. https://doi.org/10.1038/nn1243

Zhang, W., Yamada, M., Gomeza, J., Basile, A. S., & Wess, J. (2002). Multiple muscarinic acetylcholine receptor subtypes modulate striatal dopamine release, as studied with M1-M5 muscarinic receptor knock-out mice. *The Journal of Neuroscience: The Official Journal of the Society for Neuroscience*, *22*(15), 6347–6352. https://doi.org/10.1523/JNEUROSCI.22-15-06347.2002

Zhao, C., Cheung, K. M., Huang, I.-W., Yang, H., Nakatsuka, N., Liu, W., Cao, Y., Man, T., Weiss, P. S., Monbouquette, H. G., & Andrews, A. M. (2021). Implantable aptamer–field-effect transistor neuroprobes for in vivo neurotransmitter monitoring. *Science Advances*, *7*(48), eabj7422. https://doi.org/10.1126/sciadv.abj7422

Zhou, F. C., Lesch, K.-P., & Murphy, D. L. (2002). Serotonin uptake into dopamine neurons via dopamine transporters: A compensatory alternative. *Brain Research*, *942*(1–2), 109–119. https://doi.org/10.1016/S0006-8993(02)02709-9

Zhou, F.-M., Liang, Y., & Dani, J. A. (2001). Endogenous nicotinic cholinergic activity regulates dopamine release in the striatum. *Nature Neuroscience*, *4*(12), 1224–1229. https://doi.org/10.1038/nn769

Zhou, F.-M., Liang, Y., Salas, R., Zhang, L., De Biasi, M., & Dani, J. A. (2005). Corelease of dopamine and serotonin from striatal dopamine terminals. *Neuron*, *46*(1), 65–74. https://doi.org/10.1016/j.neuron.2005.02.010

Zhuo, Y., Luo, B., Yi, X., Dong, H., Miao, X., Wan, J., Williams, J. T., Campbell, M. G., Cai, R., Qian, T., Li, F., Weber, S. J., Wang, L., Li, B., Wei, Y., Li, G., Wang, H., Zheng, Y., Zhao, Y., … Li, Y. (2024). Improved green and red GRAB sensors for monitoring dopaminergic activity in vivo. *Nature Methods*, *21*(4), 680–691. https://doi.org/10.1038/s41592-023-02100-w

Zigmond, M. J., Abercrombie, E. D., Berger, T. W., Grace, A. A., & Stricker, E. M. (1990). Compensations after lesions of central dopaminergic neurons: Some clinical and basic implications. *Trends in Neurosciences*, *13*(7), 290–296. https://doi.org/10.1016/0166-2236(90)90112-n

Ztaou, S., Maurice, N., Camon, J., Guiraudie-Capraz, G., Goff, L. K.-L., Beurrier, C., Liberge, M., & Amalric, M. (2016). Involvement of Striatal Cholinergic Interneurons and M1 and M4 Muscarinic Receptors in Motor Symptoms of Parkinson's Disease. *Journal of Neuroscience*, *36*(35), 9161–9172. https://doi.org/10.1523/JNEUROSCI.0873-16.2016